The development of novel experimental strategies for elucidating the role of tryptophan metabolism in the neuropsychopathology of Human African Trypanosomiasis

Nadin A. Fathallah

Supervisors: Dr Neil Dawson and Dr Mick Urbaniak

2020

I declare that this thesis is my own work and has not been submitted in substantially the same form for a higher degree elsewhere.

Contents

List of figures

List of tables

Abstract

Trypanosoma brucei is an extracellular protozoan parasite that causes Human African Trypanosomiasis. Trypanosomes are found in the blood, lymphatic system, adipose tissue, and skin during the early stage infection, and additionally in the brain in the late stage infection. The late stage is characterised by neuropsychiatric symptoms and sleep disorder that occur through an undefined mechanism.

Trypanosomes cultured *in vitro* significantly deplete tryptophan from the media, using it in both protein synthesis and transamination reactions. In mammals, as well as forming an essential component of the kynurenine pathway, with both neurotoxic and neuroprotective branches, tryptophan is also the precursor of serotonin and melatonin, which are both implicated in sleep regulation. Research has also shown changes in brain tryptophan levels and increased 5-Hydroxytryptophan in stage II clinical samples.

In this thesis, I will investigate the connection between parasite localisation, tryptophan metabolism, and behaviour in a murine model of late stage HAT. *Ex vivo* imaging data using red-shifted luciferase expressing parasites reveals parasite localisation to many organs during early stage infection. HPLC-based analysis of brain tissue confirmed changes in *in vivo* tryptophan levels across the course of infection. Functional brain imaging found evidence for altered brain glucose metabolism and behavioural characterisation identified impaired locomotor, but not impaired learning and memory, in late stage HAT. Taken together this data suggests a correlation between parasite localisation, tryptophan metabolism and behavioural changes that may be clinically relevant. In addition, in the final chapter of this thesis I outline the development of genetically modified Trypanosomes that will allow future characterisation of the relationship between parasite tryptophan metabolism and the changes seen in host brain function and behaviour.

Acknowledgments

Firstly, I would like to express my sincere gratitude to my supervisors Dr Neil Dawson and Dr Mick Urbaniak for their continuous support throughout my PhD studies. I would like to thank Neil for always going above and beyond, providing me with the positivity and enthusiasm I so very much needed at my (very many!) low points, and for always making me laugh. Neil, you were a great life mentor, always teaching me to look at the bright side of life using your dark sense of humour. I would like to thank Mick who consistently encouraged and challenged me to become a better research scientist. You both complemented each other like ying and yang, and for that I immeasurably thank you both.

This work would not have materialized without the immense support from the rest of the lab team, who picked me up when times were tough and helped me along the way. Dr Becky Hughes, Dr Jayde Whittingham-Dowd, Dr Greg Bristow and Dr Corinna Benz thank you all for the help along the way, with experiments, advice or even just for cups of tea and a gossip break with Alex Hardgrave. Becky and Jayde you were, and still are, my role models for women in research, showing me that with great juggling and the frequent use of profanities, you can have it all! Last, but in no way least, I would like to thank my family for their unwavering support throughout my entire academic endeavour. Soraya, Taleb and Kariman- you guys are my life and I'm sorry your big sister has been away for so long. Dad, this is for you. You have been my mum and dad since day one, pushing me to achieve the best in life and I could never thank you enough. I'm sorry I was away through your sickness and chemo, but I did this all for you. Jonny you are my partner, my better half, my best friend, and I can't wait to become your wife. Thank you for always making me laugh until my stomach hurts and tears roll down my eyes.

Abbreviations

^{14}C-2-DG	^{14}C-2-Deoxyglucose
5-HT	Serotonin, 5-Hydroxytryptamine
AHC	Anterior
APOL-1	Apolipoprotein L1
aPRL	Anterior Prelimbic Cortex
BBB	Blood-Brain Barrier
BLA	Basolateral Amygdala
CB	Cerebellum
CeA	Central Amygdala
Cg1	Cingulate Area 1
CNS	Central Nervous System
CP	Cysteine Protease
CSF	Cerebrospinal Fluid
CVO's	Circumventricular organs
DHCA1	Dorsal Hippocampus 1
DHCA2	Dorsal Hippocampus 2
DHDG	
DHML	
DLO	Dorsolateral Orbital
DLST	Dorsolateral Striatum
DM	Dorsomedial
DMST	Dorsomedial Striatum
DR	Dorsal Raphé
DRN	Dorsal Raphe Nucleus
GABA	gamma-Aminobutyric acid
GP	Globus Pallidus

Hab	Habenula
HAT	Human African Trypanosomiasis
HDB	Horizontal Limb of the Diagonal Band of Broca
HPLC	High Pressure Liquid Chromatography
IDO	Indoleamine 2,3-dioxygenase
IFN-γ	Interferon gamma
IL	Infralimbic
Ins	Insular
KAT II	Kynurenine aminotransferase II
KMO	Kynurenine-3-monooxygenase
KP	Kynurenine Pathway
KYN	Kynurenine
KYNA	Kynurenic Acid
Lent	Lateral Entorhinal Cortex
LH	Lateral
LO	Lateral Orbital
LPO	Lateral Preoptic
LS	Lateral Septal Nucleus
M2	Motor Cortex
MD	Medial Dorsal
MeA	Medial Amygdala
MG	Medial Geniculate
MO	Medial Orbital
MPOM	Medial Preoptic
mPRL	Medial Prelimbic
MR	Median Raphé
MS	Medial Septal Nucleus

MT1	Melatonin Receptor 1
MT2	Melatonin Receptor 2
NaC	Nucleus Accumbens
NaS	Nucleus Accumbens Septi
NMDA	*N-methyl-D-aspartate*
NMDAr	*N-methyl-D-aspartate* receptor
NORT	Novel Object Recognition
NREM	Non-rapid eye movement
OF	Open field
PAG	Periaqueductal Grey
Pir	Piriform
Prh	Perirhinal Cortex
PTRE	Post-treatment reactive encephalopathy
PVN	Paraventricular
QA	Quinolinic Acid
Re	Reticular Thalamus
REM	Rapid eye movement
RI	Recognition Index
RSG	Retrosplenial Cortex
S1BF	Somatosensory Cortex Barrel Fie
SCN	Suprachiasmatic nucleus
SNC	Substantia Nigra Pars Compacta
SNR	Substantia Nigra Pars Reticulata
SWS	Slow Wave Sleep
Sz	Schizophrenia
T. b. brucei	*Trypanosoma brucei brucei*

T. b. gambiense *Trypanosoma brucei gambiense*

T. b. rhodesiense *Trypanosoma brucei rhodesiense*

T. gondii	*Toxoplasma gondii*
TDO	Tryptophan 2,3-dioxygenase
TFL-1	Trypanosome Lytic Factor 1
TFL-2	Trypanosome Lytic Factor 2
TNFα	Tumor necrosis factor alpha
V1	Visual Cortex
VDB	Vertical Limb of the Diagonal Band of Broca
VHCA1	Ventral Hippocampus 1
VHCA2	Ventral Hippocampus 2
VHCA3	Ventral Hippocampus 3
VHML	
VHsub	Ventral Subiculum Hippocampus
VLPO	Ventrolateral preoptic nucleus
VLST	Ventrolateral Striatum
VMST	Ventromedial Striatum
VPM	Ventromedial
VSG	Variant Surface Glycoprotein
VTA	Ventral Tegmental Area
W	Tryptophan
WBC	White Blood Cell

Chapter 1.0 Introduction

1.1 Human African Trypanosomiasis (HAT)

The protozoan parasite *Trypanosoma brucei* is the etiological agent responsible for Human African Trypanosomiasis (HAT), more commonly known as sleeping sickness (1). Infection with *Trypanosoma brucei gambiense* (*T. b. gambiense*) or *Trypanosoma brucei rhodesiense* (*T. b. rhodesiense*), causing West African and East African sleeping sickness respectively, both result in systemic and neurological disability throughout Sub-Saharan Africa (2). If left untreated, both forms of the disease are invariably fatal (3). *Trypanosoma brucei brucei* is another subspecies, which only infects domestic and wild animals but not humans (4). African trypanosomiasis is found only in sub-Saharan Africa (Figure 1.1), where the climate and habitats are suitable for its insect vector, the tsetse fly, to survive (5). The disease mainly affects remote underdeveloped rural regions, with disease transmission occurring in humans mostly during activities such as farming, washing clothes or fishing (4).

There has been a global scientific effort to develop new drugs, diagnostic tools and non-pharmaceutical interventions for the parasitic disease (4). Since the early 2000's, the number of HAT cases have dropped dramatically (Figure 1.2), with less than 4,000 cases reported in 2014 (6). Indeed, included in the 2012 London Declaration, HAT is one of the five neglected tropical diseases which the World Health Organisation hopes to successfully eliminate as a public health problem by 2030 (7–9).

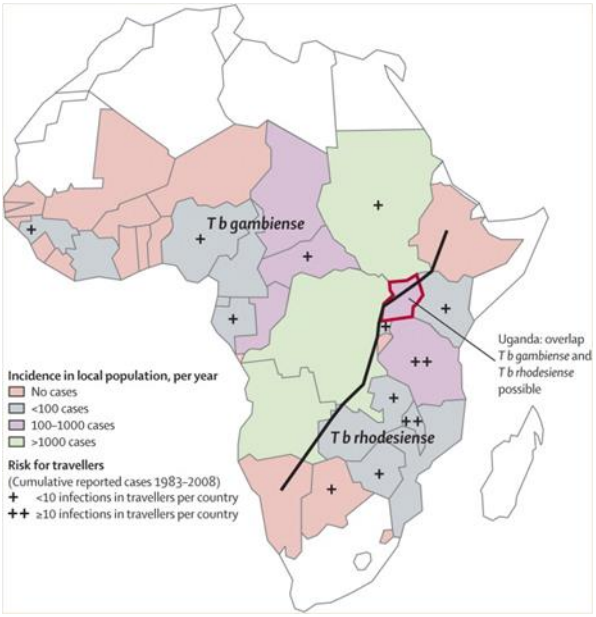

Figure 1.1 Distribution of Human African Trypanosomiasis (HAT) in Africa

Distribution, incidence and risk for travellers of HAT in Africa. The black line geographically dividing the areas in which the two sub-species *Trypanosoma brucei gambiense* and *Trypanosoma brucei rhodesiense* are found in Africa.

Figure taken from Brun *et al*, 2010 (4)

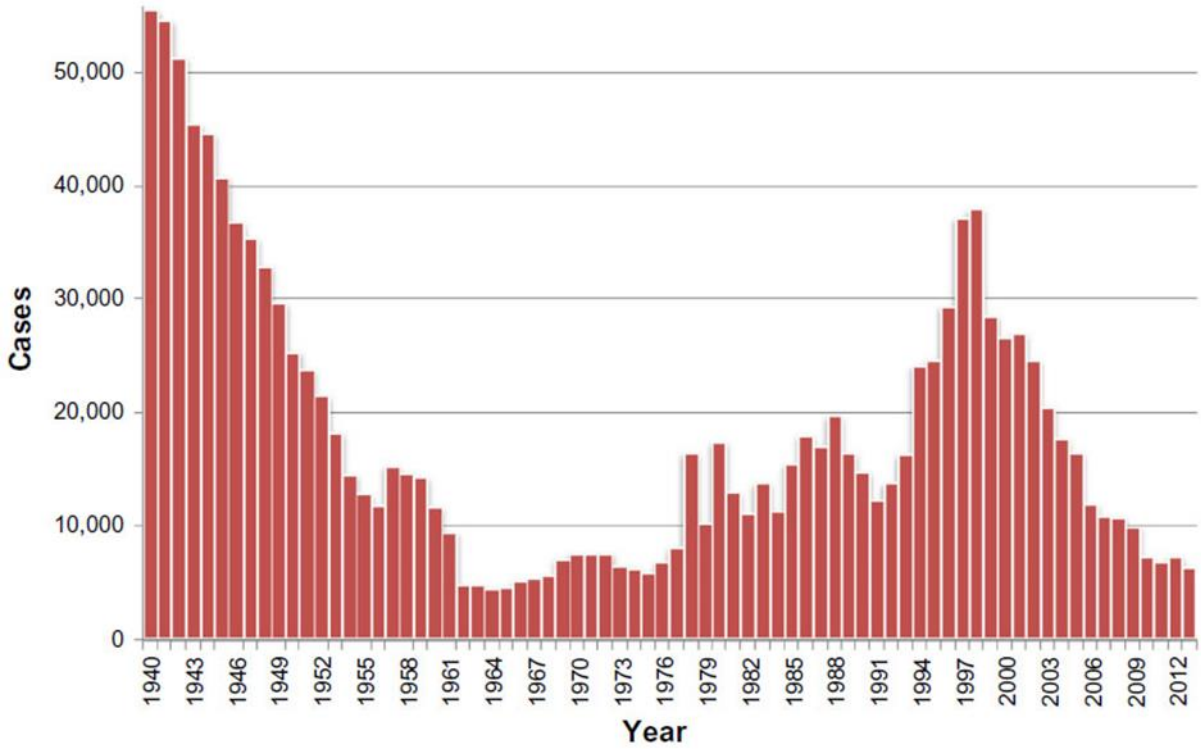

Figure 1.2 Total number of human African Trypanosomiasis cases reported to the World Health Organisation, 1940-2013

Figure adapted from Franco *et al*, 2014 (10)

1.1.1 Insect Vector

Transmission of Trypanosomes is by the blood-sucking tsetse fly of the *Glossina* species, and the parasite cycles between the mammalian bloodstream and the tsetse fly (11). It takes approximately 21 days after feeding on an infected animal host for the flies to become infected, with the fly remaining infective for life (12).

As demonstrated by Figure 3, in the mammalian bloodstream African trypanosomes show a polymorphism as part of their life cycle, with dividing slender forms, intermediate forms, and the final stumpy form (13,14). In the fly vector, the mammalian bloodstream form changes to the midgut form, transforming to the migration epimastigote form, which then develops in the salivary glands to the final metacyclic form (11,15). The procyclic and epimastigote forms found in the tsetse fly undergo cell multiplication, as does the long slender bloodstream form of the African trypanosome found in the mammalian host (4,16). However, in the final developmental stage, the infective metacyclic form found in the tsetse fly salivary glands, and the short stumpy form in the mammalian bloodstream do not undergo cell multiplication (15,17). In humans a primary lesion at the site of the bite, commonly known as a trypanosomal chancre, typically develops 10 days later, after which the parasites enter the bloodstream and lymph nodes (11,18).

In a recent study by Caljon et al, 2016 (19) the authors describe the retention of actively proliferating intradermal trypanosome populations at the site of the insect bite. Scanning electron microscopy was used to document interactions between adipocytes and parasites at the site of the insect bite, highlighting the potential role of retained

parasites in the re-infection of other tsetse flies that feed at the bite soon after initial inoculation of mammalian host.

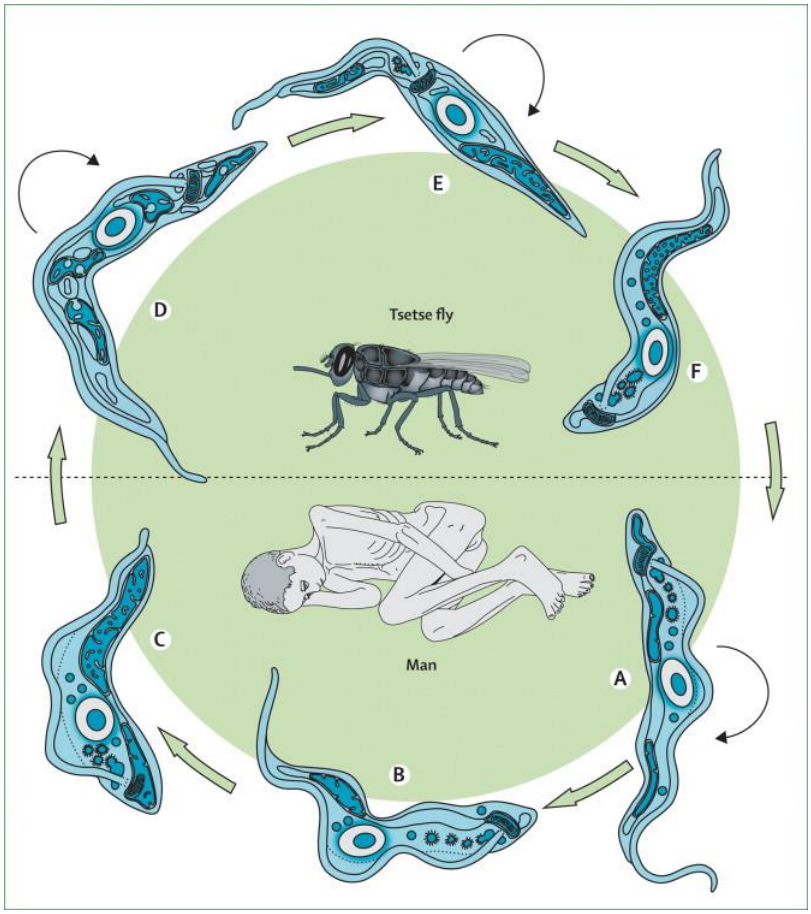

Figure 1.3 Life Cycle of African Trypanosomes

Bloodstream forms of Trypanosomes show a polymorphism with (A) dividing slender forms, (B) intermediate forms, and (C) stumpy forms. In the tsetse fly vector, bloodstream forms transform to (D) dividing midgut forms, then to (E) the migrating epimastigote forms, which develop in the salivary glands to (F) the infective metacyclic forms, which are injected during the next blood meal into the mammalian host.

Figure taken from Brun *et al*, 2010 (4)

1.1.2 Tissue Tropism

Tissue tropism refers to the ability of a pathogenic organism, such as Trypanosomes, to infect a specific organ or sets of organs in the host, thereby establishing an infection niche (20). An improved understanding of host-microorganism interactions relies on untangling the complex relationship between tropism and pathogenesis (21). In the case of *T. b. brucei*, technological advances have allowed for better characterisation of known and newly reported tissue tropisms (22). Histological evidence for the accumulation of the parasites in the spleen, liver, muscle, heart, lymph nodes, kidney, lung and brain has been well documented for many years (23,24). More recently, the skin (25,26) and adipose tissue (27) have also been reported as significant reservoirs for the pathogen. The presence of parasites in the dermis represents an important role in transmission, perhaps explaining active foci of infection despite eradication of disease and also alludes to the potential role of asymptomatic carriers in perpetuating disease transmission (28). Interestingly, the adipose tissue represents a new reservoir recently identified in experimental infections of *T. b. brucei* in rodents. However, there are currently no reports stating the detection of parasites in adipose depots in infected humans (22). Further investigation is warranted, to more clearly establish the potential clinical relevance of the adipose tissue reservoir in humans, which may have limited relevance given that most Sub-Saharan African individuals in rural areas prone to the disease suffer malnourishment and very low levels of body fat (29,30).

In any case, the reasons underlying tissue distribution of Trypanosomes in the mammalian host remains poorly understood, as does the role of each tissue niche in disease transmission (22). For instance, in the case of central nervous system (CNS) invasion, parasites are no longer accessible to the bite of a tsetse fly once in the brain

and therefore are no longer transmissible (31–33), which seems counter-intuitive. However, there may be selective advantages for the parasites residing in the CNS, including immune evasion and relative protection from treatment, thus allowing for increased trypanosome numbers and enhanced transmission (34). Residing in the CNS may also reduce virulence, that aids in the establishment of a more chronic infection (35).

1.1.3 Clinical Features

There are two distinct stages of HAT disease; the early haemolymphatic stage when the parasites are found in the blood and lymph nodes, and the later encephalitic stage where the parasites crossed the blood-brain barrier (BBB) and become established within the CNS (36). Late-stage HAT disease includes characteristic neurological features such as sleep disorder, neuropsychiatric symptoms, motor and sensory disturbances, progressive cerebral oedema and eventually coma leading to death (11).

Infection with *T. b. gambiense* is described as having a chronic progressive course, with the estimated duration of infection being 3 years, divided between the first and second stage of the disease (37). On the other hand, *T. b. rhodesiense* disease is acute and rapidly develops, and if left untreated death occurs within weeks or months (38). Differences in the clinical symptoms induced by the two sub-species is summarised in Table 1.1

Table 1.1 Clinical Presentation of HAT in *T.b. gambiense* and *T.b. rhodesiense*

Characteristic	T.b. gambiense	T.b. rhodesiense
Disease Progression	Slow	Rapid
Stage I Symptoms	Fever, headache, malaise	Fever, enlarged lymph nodes, itching
Time of CNS Invasion	1-2 years	4-5 weeks
Stage II Symptoms	Daytime somnolence, paralysis, coma	Psychiatric disturbances
Time to death if untreated	Years	Months

Table 1 reconstructed from Ponte-Sucre, 2016 (36)

1.1.4 Disease Staging and Biomarkers for Diagnosis

Accurate and rapid diagnosis of HAT is extremely important as both diagnosis and treatment are highly dependent on disease stage (6). Current diagnosis for the disease includes a serological blood test (for gambiense disease only), followed by blood microscopy, and microscopy of the cerebrospinal fluid (CSF) to check for presence of parasites (Figure 1.4) (6). If no parasites are observed in the CSF, but stage 2 disease is suspected, a white blood cell (WBC) count is conducted (6). Often, a WBC count above an arbitrary threshold, usually 5 WBC/μL, is used for staging. However, lumbar puncture is required for the collection of CSF and as this invasive, painful procedure requires trained personnel it is not always conducted (39). The challenge of lumbar puncture requirement is compounded by the issue of poor sensitivity, making accurate staging difficult to perform (40).

As the number of recorded HAT cases has dramatically reduced since the early 2000s, it has highlighted the need for a final push to develop new diagnostic techniques and tools to eradicate HAT completely (30). In recent years, neopterin, a CSF metabolite has been found to be one of the most sensitive molecular biomarkers for HAT disease staging (41,42). Analysis of the levels of neopterin in the CSF before, during and after treatment highlighted the significance of the compound as a biomarker, as well as a marker indicative of treatment outcome following chemotherapy (43). However, there are certain drawbacks concerning the use of neopterin as biomarker of disease stage (6). CSF collection through lumbar puncture is still required, and the associated specificity of the test is still low (43). For example, elevated CSF neopterin has also been identified in other neurological infections, such as malaria, tuberculosis and HIV, limiting its specificity. Moreover, the situation is further complicated by the fact that malaria, HIV

and TB infections are often present in HAT suffers. (44–47). Tests based on metabolic biomarkers for use in diagnosis techniques are not completely novel (6).

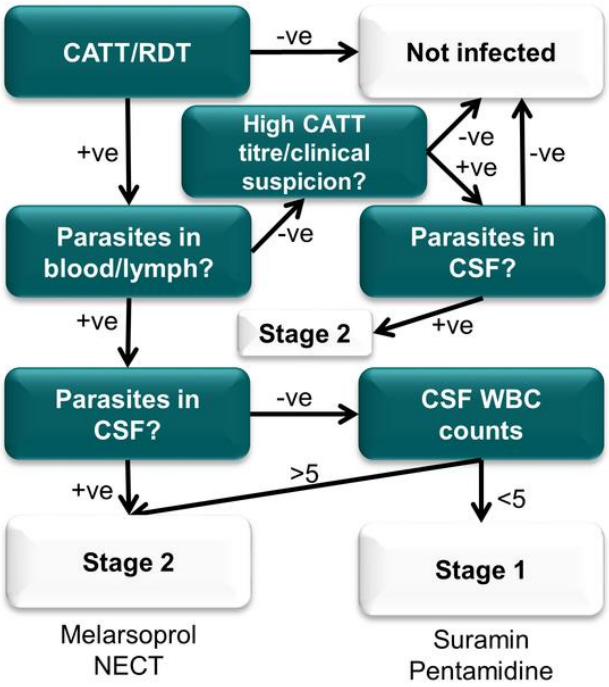

Figure 1.4 Current Diagnosis of Human African Trypanosomiasis

CATT: card agglutination test for trypanosomiasis. CSF: cerebrospinal fluid. RDT: Rapid Diagnostic Test.

Image taken from Vincent *et al*, 2016 (6)

1.1.5 Treatment

Treatment of HAT is dependent on the species of trypanosome and the stage of disease progression (48). Infections in the early stage are treated with pentamidine for *T. b. gambiense* and suramin for *T. b. rhodesiense* (49). The highly toxic drug melarsoprol is currently the only treatment that is effective, against both forms of the disease, once the parasite has invaded the CNS and can only be administered in a hospital setting due to its severe side effects (6). Unfortunately, melarsoprol treatment results in the development of severe post-treatment reactive encephalopathy (PTRE) in approximately 10% of patients, and has an approximate 50% mortality rate (50). PTRE is characterized by the development of meningoencephalitis with diffuse astrocytosis, along with the presence of lymphocytes, plasma cells and macrophages in the cerebral tissue. Perivascular cuffing is also observed (51,52). A combination treatment comprising of nifurtimox and eflornithine is also available for treatment of the later encephalitic stage (stage 2) of the disease (53,54). In 2018, Fexinidazole Winthrop, the first oral-only tablet for the treatment of both stages of HAT was approved by the European Medicines Agency (EMA) and is now incorporated into the WHO interim guidelines as one of the first-line treatments for HAT (55,56).

A number of preclinical studies have been conducted, aimed at testing the potential of novel compounds in the treatment of HAT. For example, Kristensson and colleagues investigated the effect of minocycline – a tetracycline antibiotic – on the brain parenchyma invasion by *T. b. brucei* in a murine model of the infection (57). They found that treatment with minocycline reduced parasite and CD45 leukocyte penetration into the brain parenchyma, prevented weight loss, reduced microglia and astrocyte activation, and prolonged the survival of infected animals (57). More recently

Steverding et al, 2017 (58) described the anti-trypanocidal potential of temozolomide, a well-established chemotherapeutic able to cross the BBB and currently used to treat glioblastomas. The findings revealed that temozolomide displayed trypanocidal activity, targeted trypanosomes but not human myeloid leukaemia HL-60 cells in cell culture, induced DNA damage and subsequent cell-cycle arrest in trypanosomes, and even potently enhanced the efficacy of melarsoprol and eflornithine (again in cell culture). These effects are yet to be tested *in vivo*. Although results of such chemotherapy studies are indeed preliminary yet promising, there remains a pressing need for an effective and safe drug development for both stages of the disease.

1.1.6 Co-evolutionary Arms Race: Implications for Antigenic Variation & Vaccine Development

It has not been possible to develop an effective vaccine against HAT (16). This is because the entire *Trypanosoma brucei* genome has 9,000 genes, and 10% of those are variable surface glycoprotein (VSG) genes (17). These encode the VSG covering the entire surface of the parasite, which aids immune evasion (59). The VSG coat is the key to long-term infection due to a phenomenon called antigenic variation, whereby the parasite is able to switch expression of the VSG genes in such a rapid manner that the trypanosome is constantly able to evade the consequences of an activated host immune response (Figure 1.5) (60). Indeed, bloodstream parasites are able to switch the surface VSG coat at a rate of 10^2 to 10^7 switches/doubling time of 5–10 hours (61–63). Thus, antigenic variation and switching of the VSG coat allows the parasites to stay one step ahead of the host's immune response – an elegant example of The Red Queen's evolutionary arms race (64).

On the other hand, the complex evolutionary arms race has also birthed some counter-measures by the mammalian hosts (65). Indeed, the first line of defence towards the majority of trypanosome infections in humans and other primates is the trypanolytic apolipoprotein-L1 (APOL1), present within protein complexes known as Trypanosome Lytic Factor 1 and 2 (TFL-1 and TFL-2) (66). After exposure to human serum, trypanosomes are rapidly lysed, a phenomenon facilitated by TFL-1 and TFL-2 (67). The two serum factors exploit nutrient scavenging pathways to deliver lytic APOL1 to the parasite's lysosome (68). Here APOL1 is released, exposing its lytic domains, allowing the formation of anionic pores in the membrane of the cell, leading to osmotic dysregulation and eventual cell lysis (69). It has been postulated that primates have evolved this innate immunity because of the parasite's ability to evade the adaptive immune response due to the aforementioned antigenic variation (70,71). Nonetheless, as previously mentioned, despite this mechanism humans are still susceptible to *T. b. rhodesiense and T. b. gambiense*. In the case of *T. b. rhodesiense*, expression of a truncated VSG called *SRA* confers resistance to lysis, by binding APOL-1 and preventing it from forming pores (72). For *T. b. gambiense* a more complex counter-mechanism has evolved. In brief, the expression of a gambiense specific truncated VSG known as *TgsGP* increases the resistance of the lysosomal membrane to APOL-1 interference and also enhances the activity of cysteine proteases (CP), which aid the degradation of APOL-1 (65). This information is summarised in Figure 1.6.

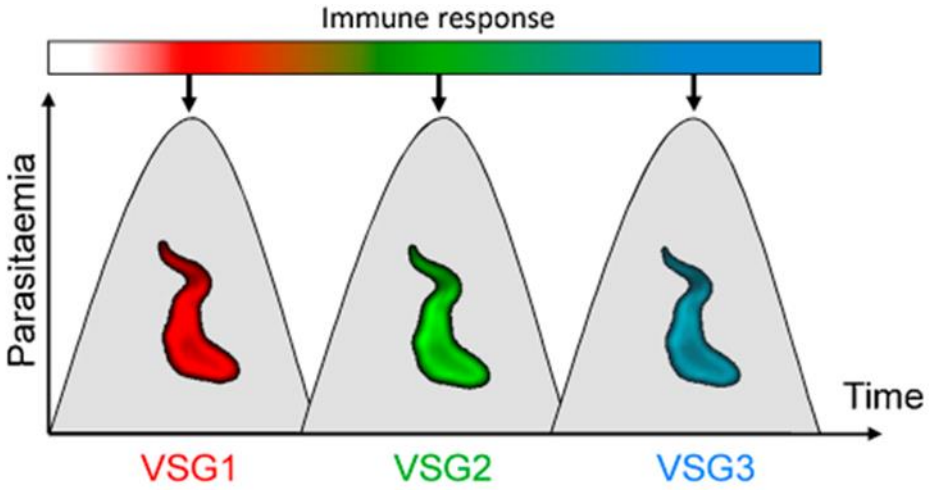

Figure 1.5 Variant Surface Glycoprotein Expression and Switching

VSG switching brings about antigenic variation. Combined with successive immune responses, this can generate a relapsing parasitemia. Please note natural infections are more complex than this highly simplified schematic.

Image adapted from Horn, 2014 (61)

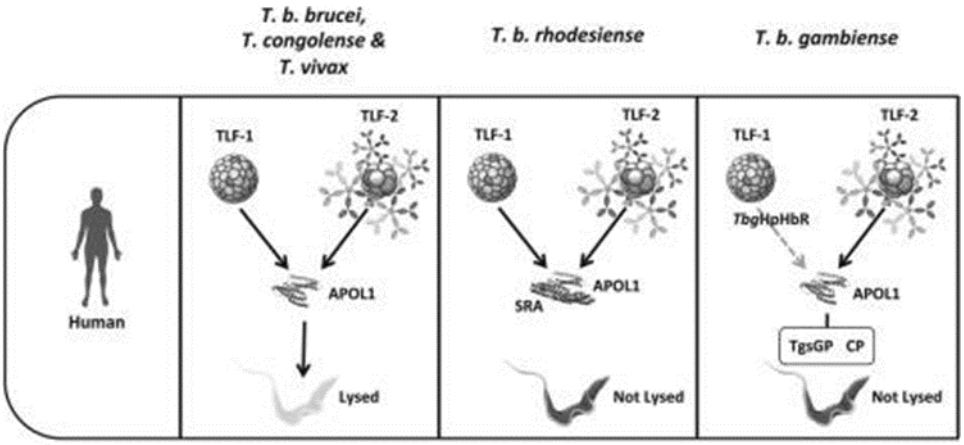

Figure 1.6 Summary of the co-evolutionary arms race between African Trypanosomes and the primate host

Image adapted from Capewell *et al*, 2015 (65)

1.2 Parasitic invasion of the Central Nervous System (CNS)

Trypanosome parasitic infections of the CNS are often "silent", with symptoms such as headaches, seizures and eventual coma appearing long after initial microbe infection of the brain has occurred (73). It has been postulated that this may work in the parasite's favour; remaining hidden from the threat of the immune system, as well as remaining unsymptomatic for long enough to allow an infection to establish (74). Nonetheless invasion of the CNS is notoriously difficult, requiring methods of evading the immune response and the potential need for cellular structures that allow for the mechanical penetration into the brain parenchyma (75).Further, parasites localised to the CNS are no longer accessible for further transmission by insect vectors, which is disadvantageous for reproductive success. So what is the evolutionary advantage of such a niche? The brain is a highly nutritious environment in which microorganisms can thrive, providing the distinct advantage of high rates of glucose flux (76) whilst providing some degree of immune-privilege (77).

Trypanosomes are able to invade the CNS, resulting in neurological disturbances including psychiatric symptoms, as well as changes in personality and alterations in irritability, confusion and aggression (31). Patients successfully cured of sleeping sickness continue to experience long-term neurological symptoms, such as sleep disturbance, ataxia and psychiatric disorders, although a lack of relevant health care and follow-up means that these potential symptoms are very poorly characterised (85). Currently, we have a very poor understanding of the mechanisms through which trypanosomes impact on the brain to induce neuropsychopathology (86). Further research is required to examine the relationship between the trypanosome parasite and the CNS (87). Specifically, it is necessary to understand how neurological invasion

occurs, and the brain regions and neurotransmitter systems affected, to elucidate the mechanisms of stage 2 HAT infections, and the neurological symptoms involved.

1.2.1 Mechanisms of CNS Invasion

Although often-debated, the mechanism by which African Trypanosome parasites enter the brain has, for many years been thought to occur through the crossing of the BBB, and subsequent colonisation of the brain parenchyma (88). Nonetheless, the mechanisms employed by the cells to enter and survive within the CNS remain little understood (89), with recent emerging evidence supports potential alternative mechanism of entry; including crossing of the blood-cerebrospinal border (BCB) and localizing within the meninges (90). Both theories remain hotly debated, although it is generally accepted that the trypanosome CNS invasion occurs first by the initial parasite arrival in the circumventricular organs (CVOs) and choroid plexus (Figure 1.7) (91). Later, in a highly debated step, trypanosomes are thought to follow the path of T-cells across the BBB into the brain (92).

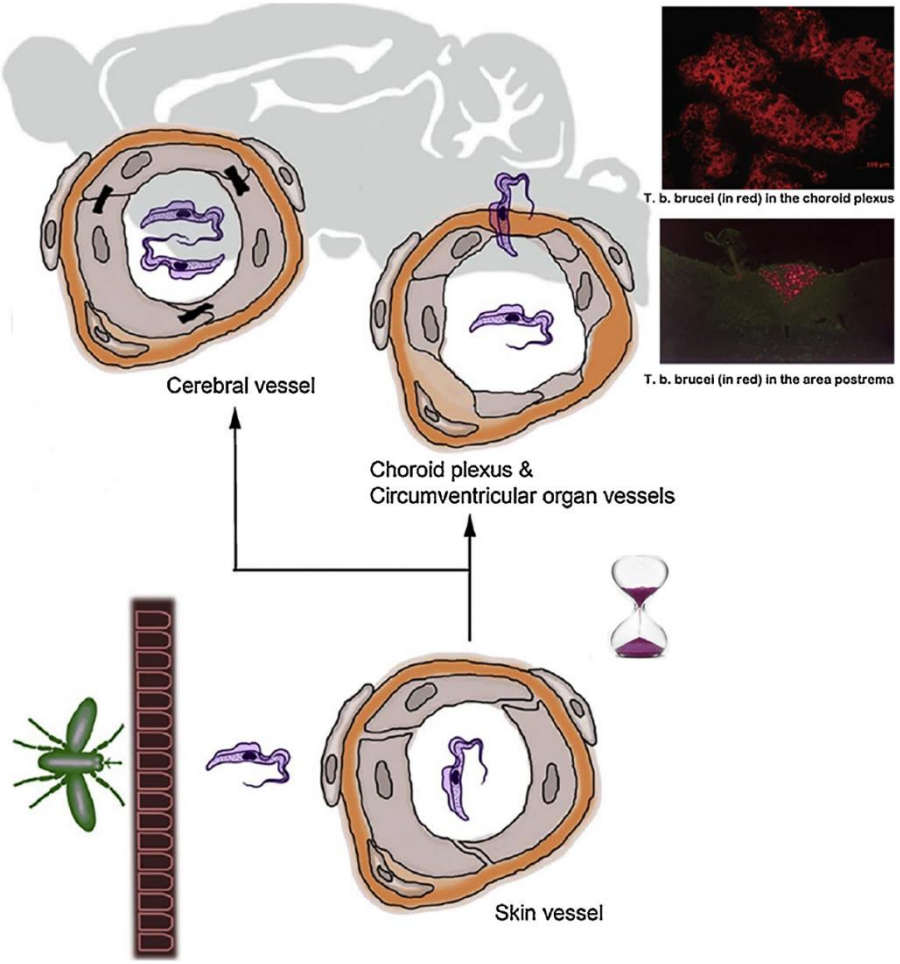

Figure 1.7 Initial Trypanosome invasion of the CNS

Following infection, trypanosomes spread through haemolymphatic vessels and, when reaching the brain, they first localize to the choroid plexus and CVOs, which have fenestrated vessels, while the BBB with tight junctions (black) prevents the passage into the brain parenchyma. For latter passage through BBB, they follow the highly regulated multi-step process of T cell invasion into the CNS (not depicted). Insert upper right immune labelled parasites (red) in the choroid plexus and in the CVO area postrema at 21 day post infection in rats.

Image taken from Masocha *et al*, 2019 (91)

1.2.2 Passage of Parasites Across the Blood-Brain Barrier (BBB)

The BBB is a structural and functional barrier, protecting the CNS from most blood-borne pathogen invasions, and modulating the flux of compounds from the blood to the brain (Figure 1.8) (93). In turn, the BBB regulates ionic homeostasis and nutrient transport necessary for the healthy functioning of the CNS, whilst protecting the nervous system from xenobiotics (94). Endothelial cells, astrocytes and pericytes are the three cellular components of the brain microvasculature comprising the BBB (95). Pericytes are morphologically similar to brain endothelial cells and share a common basement membrane, whilst astrocytes are known to induce the formation of inter-endothelial tight junctions (94). Tight junctions play an important structural role, preventing diffusion of molecules between the endothelial cells into the brain parenchyma (96).

Although the exact mechanisms by which trypanosomes cross the BBB, and how they cause neurological disturbances, are not well characterised, it is known that both parasite-derived and host-derived molecules play important roles during brain invasion (97). In addition, differences in the vessel permeability within the brain parenchyma, leptomeninges and the choroid plexus play a role in the targeting of different parasites to the brain (88,97–99). Studies have indicated both paracellular (between cells) and transcellular (through cells) routes as potential pathways for the passage taken by the trypanosome parasite across the BBB, although the potential contribution of each route remains highly debated (97,100–102).

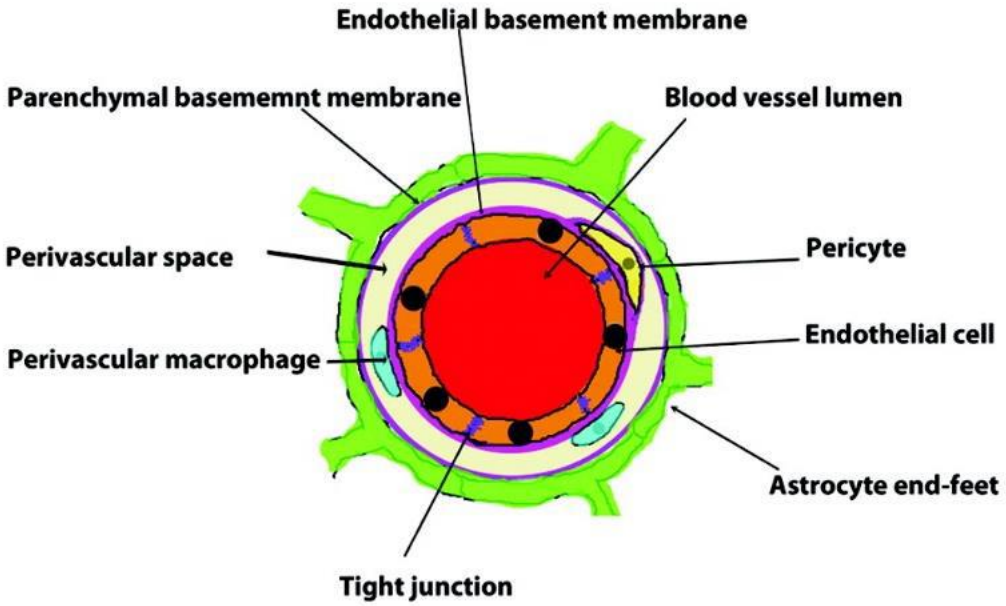

Figure 1.8 Main features of the Blood-Brain Barrier

Illustration of a cerebral post-capillary vessel showing the BBB, consisting of a complex of cerebral endothelial cells and their tight junctions, basement membranes and pericytes as well as astrocytic end-feet. Note the perivascular space that is noticeable during inflammation.

Image adapted from Masocha & Kristensson, 2012 (103)

1.2.2.1 Parasite-derived Factors Promoting Passage Across the BBB

The active penetration of Trypanosomes through the BBB occurs at or near intracellular tight junctions (104). Several molecules expressed and released from *Trypanosoma brucei* spp. aid this passage (105,106). For example, phosphatase expression and cysteine and metallo-protease secretions promote parasite penetration across endothelial cells in *in vitro* models of the BBB (105). This includes a potential role for the cysteine protease cathepsin L molecule, brucipain. Research from Abdulla and co-workers (107) revealed RNA interference against brucipain, reduced passage of *T b brucei* across the BBB *in vitro*. Moreover, Grab et al (108,109) have also suggested that *T b brucei* migration across the BBB involves parasite-derived cysteine proteases which may actually interact with host endothelial cell G protein-coupled receptors (protease-activated receptor-2) resulting in an increase in BBB permeability that allows the protozoa to transverse the BBB.

1.2.2.2 Host-derived Factors Promoting Passage Across The BBB

Host-derived molecules such as chemokines, cytokines, metalloproteases and adhesion molecules play an important role in the passage of WBCs across the BBB, and in turn the neuroinvasion of trypanosome parasites (97). Unlike other protozoal parasites, such as *Toxoplasma gondii* which utilises a "Trojan horse mechanism" to be carried within immune cells across the BBB, trypanosomes have been speculated to follow the path paved by T-cells into focal opening of the BBB (Figure 1.9) (97,110,111). Thus it has been reported that *T. b. brucei* crosses the BBB into the brain parenchyma in a similar manner to that observed for WBCs during inflammation (57,92). Indeed, infection of gene knockout C57BL/6 mice has been used extensively to study trypanosome passage

into the brain (97,112). The findings have revealed that mice deficient of Tumour Necrosis Factor (TNFα) had reduced numbers of parasite and WBCs in the CNS, as well as reduced expression of the adhesion molecule ICAM-1 on endothelial cells when compared with wild type mice (113,114). Moreover Interferon Gamma (IFNγ) deficient mice, had higher blood parasitemia when compared with wildtype (111).

Traditionally, infections with extracellular pathogens such as *Trypanosoma brucei* elicit a Th2 immune cell response, whereas infections with intracellular pathogens activate a predominate Th1 cell response (115,116). It is interesting to note, therefore, that infections of mice with *T. b. brucei* elicit mainly the Th1 arm of the host's immune response (117). This in turn results in elevated levels of pro-inflammatory cytokines such as IFNγ and TNFα, both of which are known to facilitate the WBC infiltration across the BBB (118,119). This mechanism, while potentially limiting the magnitude of infection, may paradoxically promote parasite neuroinvasion, with the immune system eliciting a double-edged sword response (120,121).

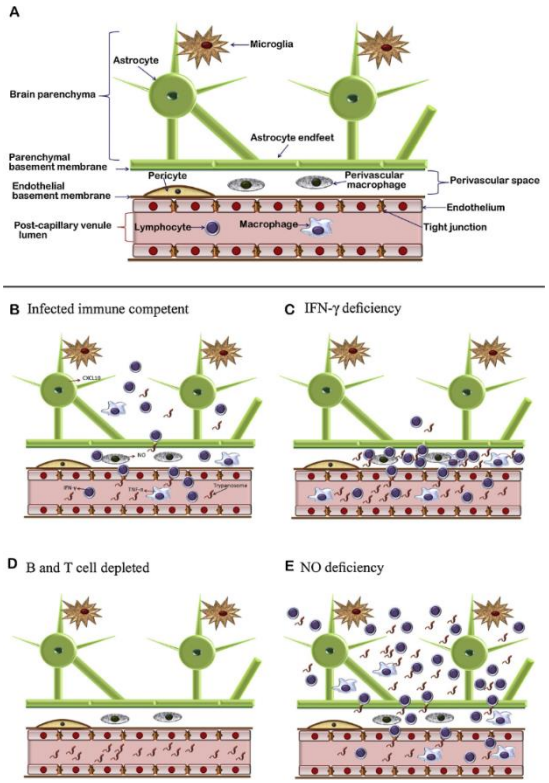

Figure 1.9 T. b. brucei and T-cell infiltration of the brain parenchyma across the BBB

(A) A postcapillary venule with the perivascular space between the endothelia- and astrocyte-derived basement membranes. (B) In infected wild-type (WT) mice activated immune cells and astrocytes release molecules that cause T cells, followed by trypanosomes to cross the barriers of endothelial cells linked by tight junctions and the astrocyte basement membrane into the brain parenchyma. (C) In the absence of IFN-γ and its receptor, parasites and T cells accumulate in the perivascular space and show a much reduced passage across the astrocyte basement membrane into the brain parenchyma. (D) In RAG $^{-/-}$ mice there are no B or T cells, and the trypanosomes remain in high numbers inside the blood vessel and do not pass into the brain. (E) In iNOS$^{-/-}$ mice both trypanosomes and T cells continue to move into the brain parenchyma

Image taken from Masocha & Kristensson, 2019 (91)

1.2.3 Passage of Parasites Across the Blood-Cerebrospinal fluid Barrier (BCB)

The theory that African Trypanosomes are able to cross the epithelial blood-cerebrospinal fluid barrier to penetrate into the cerebral ventricles and colonise the meninges, is founded on experimental evidence by Pentreath et al (122) suggesting parasites are unable to survive within the brain parenchyma or cerebrospinal fluid. From here, others have theorised that similar to the BBB theory, parasites are able to migrate from the choroid plexus stroma into the subarachnoid space, and instead of breaching the Virchow-Robin space as in the case of the BBB theory, Trypanosomes sequester between cells in the pia mater of the meninges (Figure 1.10) (101,123–125). However, Laperchia et al (99) report that parasite DNA is detected within the brain early in infection, accompanied by high levels of $CD4^+$ and $CD8^+$ T-cells, potentially consistent with the BBB theory's mechanism that parasites follow the path created by lymphocytes into the brain. Overall, more evidence is needed for the support of the BCB theory as it seems likely that the long-held dogma that Trypanosomes penetrate the BBB is indeed the most appropriate. However, one should not outright dismiss the notion that perhaps the parasites utilise both mechanisms of invasion.

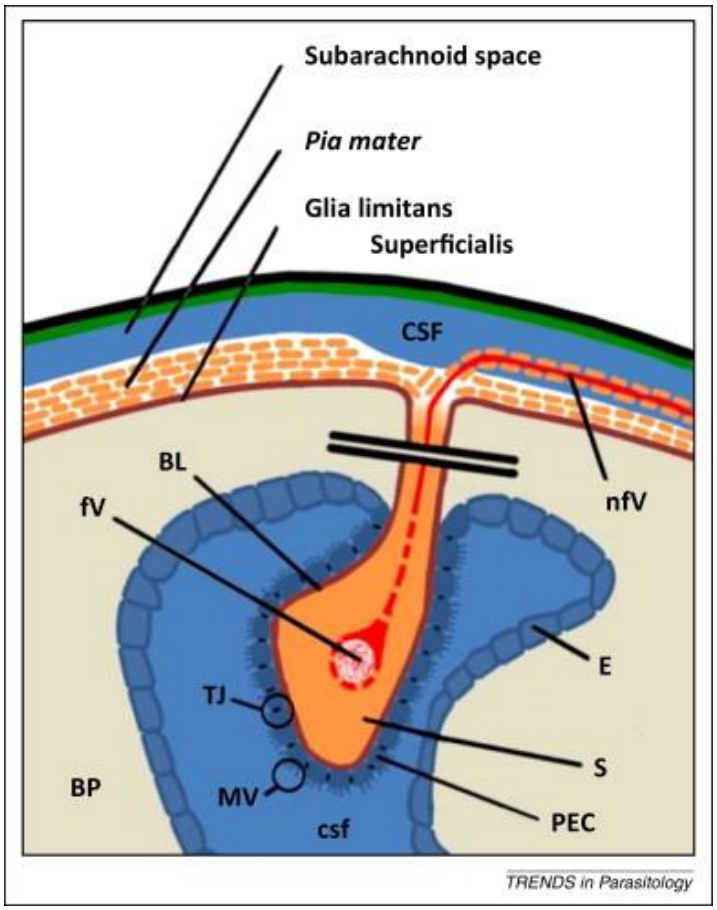

Figure 1.10 Morphological organisation of the choroid plexus and ventricles

Anatomically the choroid plexus has continuity with the pia mater. Therefore, the glia limitans develops to the basal lamina underlying the epithelial cells of the choroid plexus. Grey denotes brain parenchyma; blue denotes cerebrospinal fluid (CSF); green denotes arachnoid mater; black denotes dura mater; BL, basal lamina; BP, brain parenchyma; E, ependyma; fV, fenestrated vessel; MV, microvilli; nfV, non-fenestrated vessel; PEC, plexus epithelial cell; S, stroma; TJ, tight junction

.**Image taken from Mogk *et al*, 2014** (101)

1.2.4 Brain Regions Affected by African Trypanosomiasis

Sleeping sickness is hallmarked by sleep and neuropsychiatric disturbances (126). While there is a great deal of paucity of information on the regions of the brain affected by Trypanosomiasis infection, and the influence of the parasite itself on host behaviour and neurobiological function, it is well known that the parasites localise to the CVO's (127), choroid plexus (86) and dorsal root ganglia during early stages of CNS invasion (128). Interestingly CVOs are located around the third and fourth ventricles of the brain, and similarly to the choroid plexus, have vessels devoid of BBB making them regions susceptible to microbe attack (129). Trypanosomes are then thought to seed into the ventricles from the choroid plexus, infiltrating further into periventricular areas (130). It has also been postulated that some parasites directly enter the brain parenchyma from another CVO, the median eminence located at the base of the third ventricle, by passage across the border into the hypothalamic arcuate nuclei (91). Indeed, inflammation elicited by targeted hypothalamic structures contributes to cerebral dysfunction and malaise; however the mechanisms underlying sleep-disruption and altered host behaviour as a result of Trypanosome infection remain elusive (99)

The suprachiasmatic nucleus (SCN), located in the hypothalamus, has long been documented as a key site for Trypanosome influence (131). The SCN is known as the "master regulator", using input from photosensitive cells in the retina to coordinate sleep, as well as immune, hormonal and behavioural functioning (132–135). A study by Tesoriero et al (136), using a rodent infection model of *T. b. gambiense* reported a 30% neuronal loss within the SCN, exacerbated by significant activation of astrocytes contributing to typical neuroinflammatory pathology in this brain region. Further, Lundkvist and colleagues (137) have previously reported that trypanosome infected

mice experience reduced excitatory synaptic activity within the SCN. Moreover, the SCN harbours melatonin receptors, binding the hormone produced by the pineal gland in a circadian rhythm manner (138). Melatonin is known to act as an endogenous circadian rhythm synchronizer, stabilizing or reinforcing the body's natural rhythm (139). Interestingly, clinical studies on patients with HAT found that while the circadian nature of melatonin plasma levels is maintained its phase of release is shifted, with a significant phase-advance in its peak to within the daytime (the peak is usually nocturnal) (140). This finding was further corroborated in studies using *T. b. brucei* infected rats, whereby binding of melatonin to its receptor in the SCN was phase-advanced, and a melatonin agonist was found to restore sleep fragmentation during infection (141).

Motor function impairment is the next most prevalent pathology associated with stage 2 HAT (142), suggesting possible perturbations in the function of the cerebellum, basal ganglia system and/or peripheral motor nerves. Despite this, a paucity of data means only one study by Stiles et al (143) in the early 2000's has described significant apoptosis in the cerebellum of *T. b. brucei* infected mice. However, in the absence of a greater body of literature corroborating their results, the authors were hesitant to link their findings to motor symptoms.

Apart from sleep perturbations, very little to no research has focused on the other, equally as likely to develop, symptoms of HAT. Behavioural and psychiatric changes, often variable in presentation, are well recognised pathologies associated with the disease (144). Emotional responses, governed in part by the amygdala such as fear, aggression, sexual drive and anxiety have been often noted in HAT patients (145,146).

However a direct link between infected brain region colonisation and altered behaviour is yet to be established. Further, parasite infiltration of the thalamus, hippocampus and corpus callosum has also been documented, regions directly or indirectly associated with cognition and emotion regulation (99,147–149). Further research is warranted to link brain region colonisation and dysfunction to the symptomology of HAT.

1.2.5 ^{14}C-2-deoxyglucose (^{14}C-2-DG) Functional Brain Imaging

A technique allowing for *in vivo* quantification of glucose use within distinct brain regions, ^{14}C-2-DG functional brain imaging, was first developed and put forward by Sokoloff et al (150). The energy requirements of the brain are largely met by the oxidative catabolism of glucose, and as such it is possible to see which regions of the brain are active over a given period time of interest by measuring glucose utilisation. This can be achieved through the use of radiolabelled 2-Deoxy-D-glucose, an analogue with a hydrogen atom bound to the second carbon atom instead of the hydroxyl group present in glucose, as illustrated in Figure 1.11. This chemical modification means that 2-DG is unable to undergo further phosphorylation beyond 2-DG-6-phosphate, and so is metabolically trapped intracellularly. From this, a labelled version of 2-DG with the radioactive carbon isotope ^{14}C can be used as a indicator of glucose utilisation by the tissue, and as such a marker for brain regions with high or conversely low energy demands.

Since the publication of the Sokoloff method, a modified protocol by Dawson et al (151) has been developed, refining some aspects of the methodologies such as putting experimental animals under restraint and the requirement for surgical cannulation which would interfere with behavioural studies. The revised protocol has been

repeatedly used in studies (152),with maintained accuracy of results comparable with the original protocol developed in the 1970's.

A number of studies do exist looking at the impact of parasite infection on tissues. For example, ^{14}C-2-DG imaging was used to look at glucose utilisation in *Trypanosoma cruzi* infected mouse hearts, with authors observing a significant increase in glucose use (153). However, no published studies to date have attempted to use ^{14}C-2-DG imaging to assess the impact of Trypanosoma infection on brain activity.

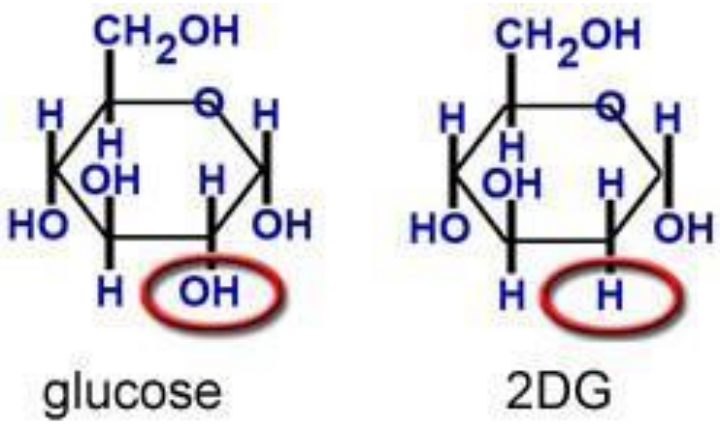

Figure 1.11 Chemical structures of glucose and 2-Deoxy-D-glucose

2-Deoxy-D-glucose shares the same molecular structure as glucose, but with the substitution of a hydrogen atom on the second carbon instead of a hydroxyl group as highlighted by the red circle.

Image taken from Balagura & Kanner, 1971 (154)

1.2.6 Parasite Modulation of Host Behaviour

1.2.6.1 Parasite Infection and Sleep Rhythms

Trypanosomes can modulate mammalian host behaviour by altering neuronal functions (86). The most well characterized modulation of behaviour are disturbances to the sleep-cycle, which has been demonstrated in HAT and in experimental rodent infections (36). The complex phenomena of wakefulness and sleep rhythms are a direct result from total brain function, requiring sophisticated coordination from various neuronal networks which control endocrine outputs, behaviour and humoral factors (86,155). To give a concise synopsis on the pathogenesis of the sleep disruptions presented in *Trypanosoma brucei* infections, it is important to note that knowledge on the function of the sleep-cycle and wake regulatory circuits during HAT infection of the CNS remain largely unclarified (137).

In a paper published by Kristensson and colleagues (86) the authors highlighted various recent studies which elucidated to the role of parasite localisation in the brain as a key player in sleep rhythm disturbances during Trypanosome infection. The authors highlighted the importance of parasite localisation to the basal meninges and CVOs, resulting in the potential release of molecules, such as prostaglandins, that could hamper the activity of neurons involved in sleep regulation. The authors also suggested that just as prostaglandins can be produce by both the parasite and the host, cytokines such as TNF-α and IFN-γ are released by the host in response to infection and may also play a part in the pathogenesis of sleep-wakefulness during HAT.

1.2.6.2 Modulation of Tsetse Fly Behaviour

An increasing number of publications to date, have revealed the ability of vector-borne parasites such as *Trypanosoma brucei*, to modulate the phenotypic traits of their vectors in such a way to increase the probability of successful parasite transmission (156,157). For example, parasite-induced alterations in vector feeding behaviour and physiology have been shown for the *Plasmodium*-mosquito, *Leishmania*-sandfly, *Wuchereria*-worm, and indeed even for *Toxoplasma gondii* and its rodent vector the mouse (158–161). However there are a paucity of studies and contradictory evidence regarding the modulation of Tsetse fly feeding behaviour by *T. brucei* that has made it difficult to decipher the complex parasite-vector relationship that might exist between these organisms (162). For example, whilst some research groups suggest that trypanosomes found in the salivary glands of the tsetse fly do not alter the fly's feeding behaviour (163,164), others observed a more frequent probing behaviour in infected flies, suggesting that this was a result of parasite interference with labral mechanoreceptor function (165).

Research from Van Den Abbeele and colleagues (162) also suggests that *Trypanosoma brucei* parasites modify salivary composition in the tsetse fly, and in turn alter their fly feeding behaviour in such a manner that parasite transmission is favoured. Indeed, findings published revealed that *T. brucei*- infected flies displayed significantly prolonged feeding time when compared with wild type flies, with the authors proposing that this thereby promotes the increased likelihood of infecting multiple hosts during a single blood meal cycle. Further experimental evidence regarding the potential alterations of salivary composition by *T. brucei* is suggested by the observation that parasite-induced changes drastically reduced salivary gland gene transcription, and thus

resulted in a decrease in salivary protein content. As a consequence, biological activities such as the anti-thrombin activity and inhibition of thrombin-induced coagulation were hampered as a result of trypanosome infection. Modulation of anti-haemostatic activities in flies, such as anti-platelet aggregation was also observed, with a clear suppression of these activities.

1.3 Neuropsychiatric Manifestations of Human African Trypanosomiasis

During stage II of HAT infection almost all regions of the nervous system are involved, producing a wide range of neurological symptoms and signs (31). In brief, the symptoms can be divided into neuropsychiatric, motor and sensory abnormalities (166). Particularly psychiatric symptoms include hallucinations, schizophrenic-like psychosis, delirium, anxiety, depression and irritability (167). Florid mental symptoms such as mania, violence and suicidal tendencies have also been reported (142). Unfortunately, psychiatric conditions resulting from CNS infections in the tropics are not well researched, with paucity of data investigating the link between the two (168). To further complicate the issue, factors such as stigma and discrimination, exclusion from local communities, accusations of witchcraft and limited access to health service is likely to exacerbate HAT patients' poor mental health and to result in the under-reporting of these symptoms in infected patients (169).

1.3.1 Schizophrenic-Like Symptomology in HAT

It has been well documented that infections during early life may play an important role in the etiology of schizophrenia (170). Schizophrenia is defined as a heterogeneous psychiatric disorder, displaying positive, negative and cognitive symptoms (171). Similar to the neuropsychiatric symptomology of stage II HAT patients (127), the main positive psychotic symptoms in schizophrenia include hallucinations and delusions

(172). The cognitive symptoms are described as perturbed cognitive flexibility and reduced working memory (173), whilst the negative symptoms include lack of motivation and enthusiasm (174). The exact cause of schizophrenia is unknown, with a complex interplay between genetic and environmental factors postulated to be at play (175–177). In brief however, the current core tenet is that schizophrenia is associated with hypofunction of the N-methyl D-aspartate receptor (NMDAr), which leads to hypostimulation of Gamma aminobutyric acid (GABA) inhibitory interneurons and a simultaneous disinhibition of glutamate release (178–180). Furthering the glutamatergic hypothesis of schizophrenia, ketamine a non-competitive NMDAr antagonist can induce neuropsychological effects in healthy volunteers, similar to those of schizophrenia (181).

Moreover past infectious disease research on schizophrenia has focused almost exclusively on viruses and bacterial pathogens, with research now describing *Toxoplasma gondii*, a microscopic protozoa, as a potential candidate for some cases of schizophrenic-like symptoms of infected patients (182). Indeed other protozoa such as *Plasmodium* and *Trypanosoma* also invade the CNS and cause behavioural changes (105). Interestingly antipsychotic drugs such as phenothiazines, traditionally used to treat schizophrenia, have also been shown to have antiprotozoal effects (183). Here, the authors describe in vitro studies which have shown that the phenothiazine chlorpromazine inhibits the growth of *Trypanosoma brucei* and *Trypanosoma cruzi*, *Plasmodium vivax* and *Leishmania donovani*.

Unlike the *T. gondii* research field which is very substantial, very little is known about the potential link between African Trypanosomiasis and the development of

schizophrenic-like symptoms. Nonetheless, there is a very small body of research which has attempted to address the link between infection, the tryptophan catabolite pathway and NMDA receptor hypofunction in the neuroprogression towards schizophrenia. For example back in the late 1980's, Amole et al (184) reported on neurochemical measurements in the brains of *T. b. brucei* infected mice and described profound alterations in the monoaminergic, but not cholinergic, neurotransmitter system which they postulated could form contribute to neuropsychiatric abnormalities observed in cases of stage II HAT. Further, Anderson and Maes (185) reviewed the role of an activated immune-inflammatory pathway in accounting for neurodevelopmental pathology linked with cytokine induction of the tryptophan pathway and consequent modulation of the NMDAr glutamate production. Here the authors describe how immune-inflammatory pathways activated due to infection, may stimulate the Tryptophan pathway, resulting in increased levels of neurotoxic metabolites from the kynurenine pathway which could contribute to neuropsychiatric symptoms similar to those seen in schizophrenia.

1.4 Metabolism

1.4.1 Tryptophan Metabolism by *Trypanosoma brucei brucei*

African Trypanosomes are obligate parasites and as such obtain their nutrients such as glucose and amino acids, from their mammalian host (186,187). Interestingly, Trypanosomes cultured *in vitro* significantly deplete tryptophan (Figure 1.12) from the media, using it in both protein synthesis and transamination reactions (188). Indeed, serum levels of aromatic amino acids such as tryptophan in infected animals are significantly decreased (189). Moreover, trypanosomes secrete the unused biochemical intermediates of these reactions as aromatic keto-acids such as sleep-inducing tryptophol, indole-3-pyruvate, and phenylpyruvate at levels correlating with

parasitemia (190–192). The significance of these aromatic ketoacids in the circulation of infected animals remains to be clarified, however it has been postulated that they may contribute to the neuropsychiatric pathogenesis of trypanosomiasis through biogenic amine pool perturbations (189,190).

Analysis of the *T. b. brucei* genome in 2005 has identified trypanosome proteins putatively involved in tryptophan uptake and metabolism, including metabolic genes such as aromatic transamidases (Cytosolic Aspartate Aminotransferase; Tb927.10.3660 and Alanine Aminotransferase; Tb927.1.3950), an aromatic dehydrogenase (Aromatic L-2-hydroxyacid dehydrogenase; Tb927.11.11250), a kynurinase (Tb927.9.2010) and putative aromatic amino acid transporters (AAT6; Tb927.8.5450) (186,193–196). However, the potential effect of protein ablation upon tryptophan uptake, incorporation and excretion remains to be elucidated (197).

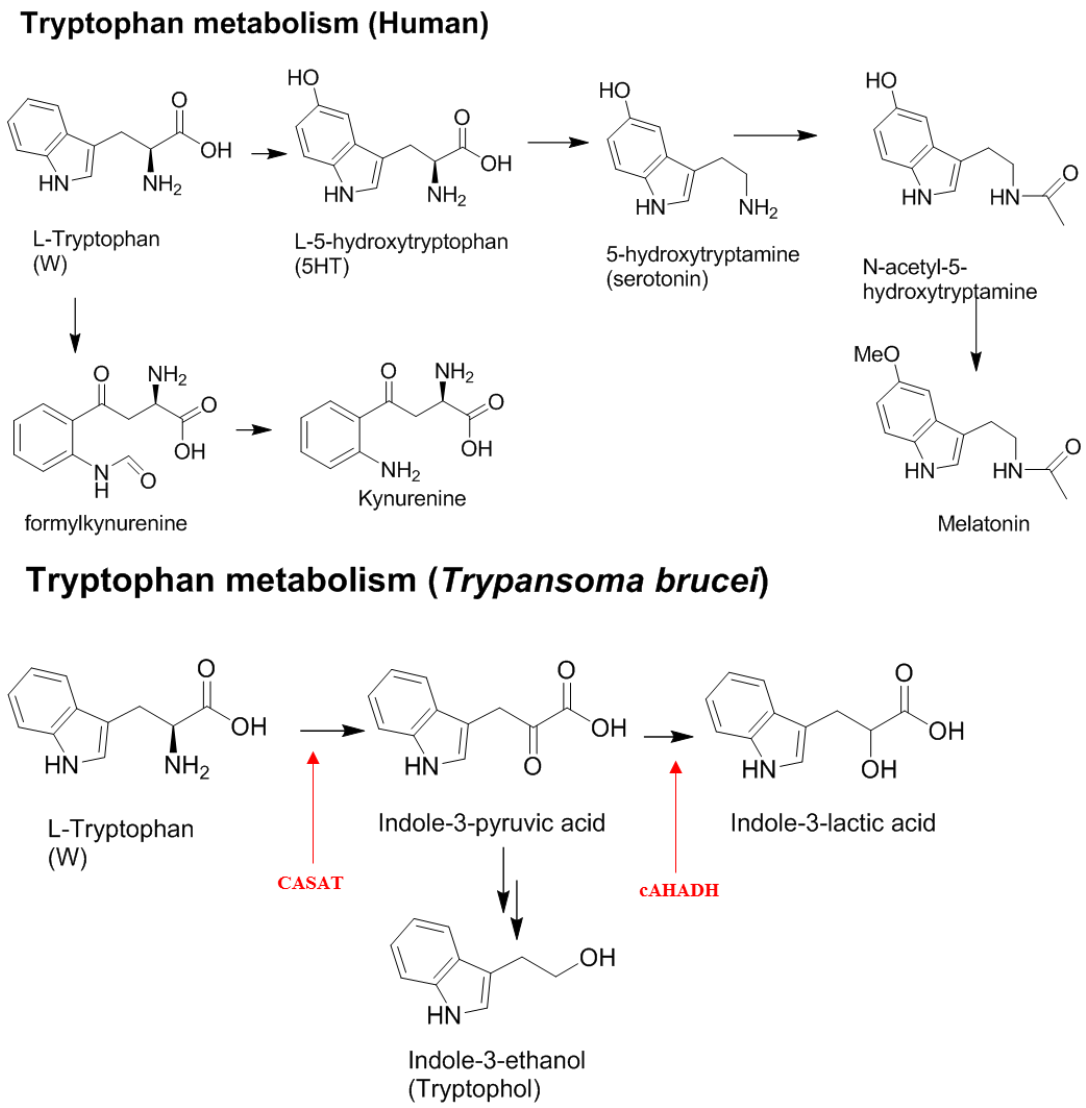

Figure 1.12 Tryptophan Metabolism in Humans and in Trypanosoma brucei

The enzymes (red) present along the pathway are shown.

1.4.2 Tryptophan and Its Main Metabolites in the Brain

In the mammalian brain, tryptophan is the essential amino-acid precursor of the neurotransmitter serotonin (5-Hydroxytryptamine) and the hormone melatonin (Figure 1.12), both of which are implicated in sleep regulation (175–177). Serotonin is synthesized from tryptophan in a multistep pathway involving the tryptophan hydroxylase enzyme, and is found mainly in the brain, gastrointestinal tract and blood platelets (198–200). Serotonin has been associated with depressive disorders, sleep, appetite, sex and temperature control (201,202). The complex relationship between sleep regulation and serotonin has been the subject of intense debate and remains incompletely understood (203). As a neurotransmitter serotonin acts on many different areas of the brain associated with the control of sleep and wake cycles, and a multitude of serotonin receptors are selectively involved in the regulation of the different sleep states (204). For example, Sangare et al (205) investigated the effect of serotonin application to the ventrolateral preoptic nucleus (VLPO), a structure that triggers non-rapid eye movement (NREM) sleep. Here, it was found that serotonin either inhibited (Type-1) or excited (Type-2) putative sleep-promoting neurons *ex vivo*. Further, serotonergic neurons of the Dorsal Raphe Nucleus (DRN) region of the brain, the primary origin of serotonergic innervation in the brain, fire at a steady rate during wakeful periods, decrease firing activity during slow wave sleep (SWS) and cease activity during rapid-eye-movement sleep (REM) (206). Nonetheless, it is not entirely clear how serotonin is involved in the modulation of the circadian rhythm, although we do know that the SCN known as the “master regulator” of the circadian rhythm in mammals, hosts one of the densest serotonergic terminal innervations in the brain (207).

Melatonin (N-acetly-5-methoxytryptamine) is produced by the pineal gland and released into the bloodstream exclusively at night (208), synchronizing the circadian rhythm whilst improving the onset, duration and quality of sleep (209–212). Endogenous melatonin levels begin to increase around 2 hours before the onset of natural sleep, with levels peaking 5 hours later (210) whereby it binds melatonin 1 (MT1) and melatonin 2 (MT2) receptors present within the SCN (213). From this, circulating melatonin levels provide feedback to the SCN circadian clock, affecting the phase-shifting effects on the firing rate of the SCN neurons (214). Specifically, it is reported that melatonin affects sleep as a consequence of its involvement in increasing sleep propensity by manipulating the circadian clock oscillations via MT1 receptors, while MT2 receptors are involved in synchronization of the circadian clock (215,216). Administration of melatonin has been reported to improve a number of neurological disorders such as Parkinsonism (217), Alzheimer's disease (218), depression (219), cerebral ischemia (220), and brain edema (221) as well as sleep disorders (222). However, no research thus far has focused on the impact of melatonin supplementation on modulating the disrupted sleep cycle of Trypanosomiasis patients.

In addition to its importance in serotonin and melatonin metabolism, tryptophan is an essential component of the kynurenine pathway (KP, Figure 13), which has both neurotoxic and neuroprotective branches, regulated by the two mammalian enzymes kynurenine 3-monooxygenase and kynurenine aminotransferase respectively (223). Kynurenine metabolism occurs in all cells within the brain, though the highest levels are found in the liver and kidney (224). Indole-2,3-dioxygenase (IDO), and to a lesser extent in the brain tryptophan-2,3-dioxygenase (TDO), are rate-limiting enzymes involved in the primary conversion of tryptophan to N-formylkynurenine (225,226).

IDO is expressed in various immune cells throughout the body (227) and is induced by proinflammatory cytokines during an immune response (228). Further, in recent years the KP of tryptophan metabolism has been implicated in the modulation of CNS inflammatory pathways, brain function, anti-microbial mechanisms and the immune system (229). Through its involvement in the KP pathway, tryptophan can regulate the function of the glutamatergic excitatory neurotransmitter system in the brain. For example quinolinic acid produced in the KP pathway can activate a subpopulation of neuronal glutamate receptors sensitive to N-methyl-D-aspartate (NMDA), producing depolarization and excitotoxicity (230,231). On the other hand, kynurenic acid is a well-known antagonist of several glutamate receptor subtypes (232). In addition, 3-hydroxykynurenine and 3-hydroxyanthranilic are both part of the pathway, and able to produce neuronal damage via the generation of reactive oxygen species (233). A schematic representation illustrating the main components in the kynurenine pathway of tryptophan metabolism is demonstrated by Figure 1.13.

Overall, there is unfortunately a very poor understanding of how African Trypanosomes impact on the brain to cause neuropsychopathology. Thus research investigating metabolism of tryptophan by Trypanosomes in the brain is warranted, indeed to understand disruptions to brain function due to potential neurotransmitter system function disruption, and also to explore the use of tryptophan and its metabolites as key biomarkers of HAT disease.

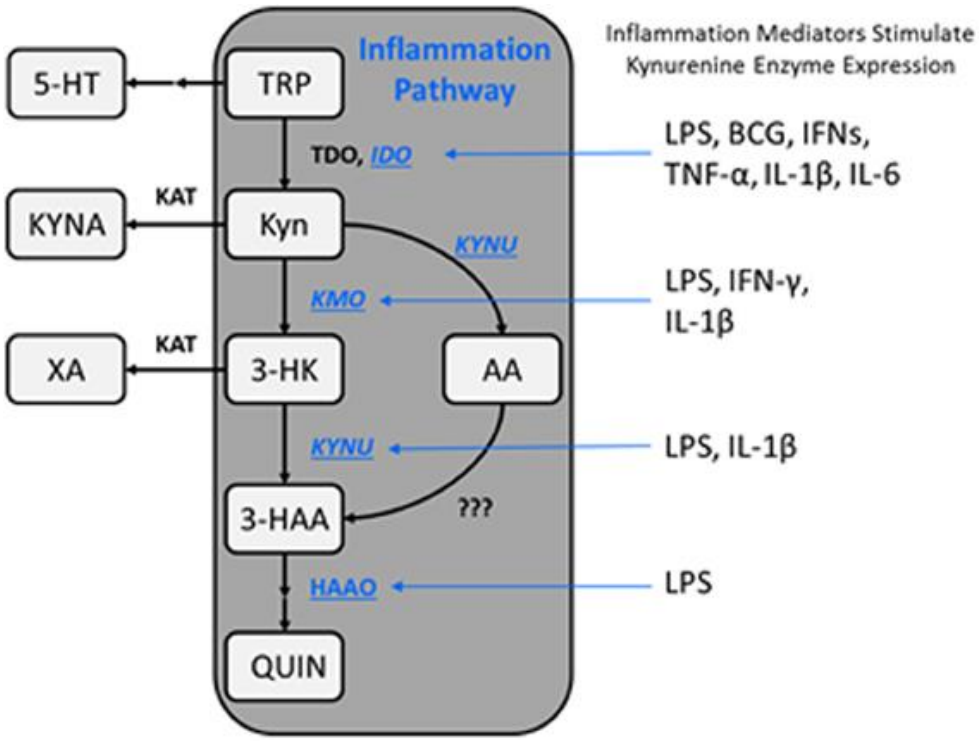

Figure 1.13 Schematic representation of the kynurenine metabolic pathway

The kynurenine pathway is theoretically segregated into two distinct branches that are regulated by KATs and KMO, as well as the availability of l-kynurenine within the brain. Additionally, kynurenine metabolism is regulated by a variety of proinflammatory mediators which impact enzyme expression levels, thereby altering substrate availability and metabolite formation favoring the KMO branch of the pathway under immune-related pathological conditions. TRP, tryptophan; 5-HT, serotonin; Kyn, kynurenine; KYNA, kynurenine acid; 3-HK, 3-hydroxykynurenine; AA, anthranilic acid; XA, xanthurenic acid; 3-HAA, 3-hydroxyanthranilic acid; QUIN, quinolinic acid; IDO, indoleamine-2,3-dioxygenase; KAT, kynurenine aminotransferase; KMO, kynurenine 3-monooxygenase; KYNU, kynureninase; HAAO, 3-hydroxyanthranilic acid oxidase; LPS, lipopolysaccharide; BCG, bacillus Calmette-Guerin; IFNs, interferons; TNF, tumor necrosis factor; IL, interleukin.

Image taken from Campbell *et al*, 2014 (223)

1.4.3 Kynurenine Pathway Activation in Parasitic Infections

In 2009 Rodgers et al (233) used a highly reproducible rodent model of early CNS and late CNS HAT infection with a kynurenine-3-monooxygenase (KMO) inhibitor, Ro-61-8048, to investigate the effects of kynurenine pathway (Figure 1.14) catabolite manipulation on the neurological consequences of HAT disease. Their findings revealed that Ro-61-8048 treatment had no significant effect on the severity of the neuroinflammation recorded in rodents during the early CNS stage of disease characterized by low level of inflammatory pathology. However, Ro-61-8048 treatment administered to animals exhibiting the late CNS stage of the infection resulted in a significant reduction in the severity of the neuroinflammatory responses measured. Results from further *in vitro* assays suggested that the anti-inflammatory action of Ro-61-8048 was due to a direct effect on host cells and not as a secondary response to the parasite. This protection by Ro-61-8048 was similarly observed in mice infected with the malaria parasite *Plasmodium falciparum*, whereby the inhibitor protected against ataxia and death (234).

Following on from Rodgers' seminal publication, Sternberg et al (235) investigated the tryptophan and kynurenine metabolite concentrations in CSF from patients infected with *T. b. rhodesiense.* Here the authors reported an increased kynurenine concentration in CSF in both early and late stage disease, with an associated increase in neuroinflammatory markers. However, no clear association with neurological sequelae was found. Given the widespread distribution of African Trypanosomiasis in the mammalian host, and the interplay between Tryptophan metabolism and neuroinflammation, the link between infection and neuroactive metabolites is a priority area for further study

Looking at *Trypanosoma cruzi*, a close relative of *T. brucei* , Knubel et al (236) reported on the critical role of IDO in host defence against the pathogen. Their findings described how blocking IDO activity *in vivo* impaired resistance to the infection and exacerbated pathology. In the case of *Toxoplasma gondii*, Tryptophan and in turn activation of the KP appears to have a toxoplasmostatic effect (237). Here it is thought that IFNγ plays a role in the host anti-parasite response to *T. gondii* via induction of IDO expression and activity, leading to Tryptophan starvation of the parasite (238). Indeed, this theory was found to be true in the case of culture human fibroblasts (239). A depletion in Tryptophan levels, and consequently reduced synthesis of serotonin, has been postulated to increase the likelihood of behavioural changes in animals and neuropsychiatric symptoms in humans being infected with *T. gondii* (81,240–242). Interestingly, in 2006 Hunt et al (243) put forward the concept that in the case of cerebral malaria, activation of the KP in the brain of the host is actually a protective response, as a means of producing antioxidant compounds and generating NAD. The damage to astrocytes that occurs (244) however, would deplete kynurenic acid (neuroprotectant) and may allow quinolinic acid (excitotoxic) formation to predominate (243). Several other associations between parasitic diseases and the kynurenine pathway have been reported; including alterations in response to Leishmania (245,246), Eimeria (247), Trichuris (248) and Encephalitozoon infection (249).

.

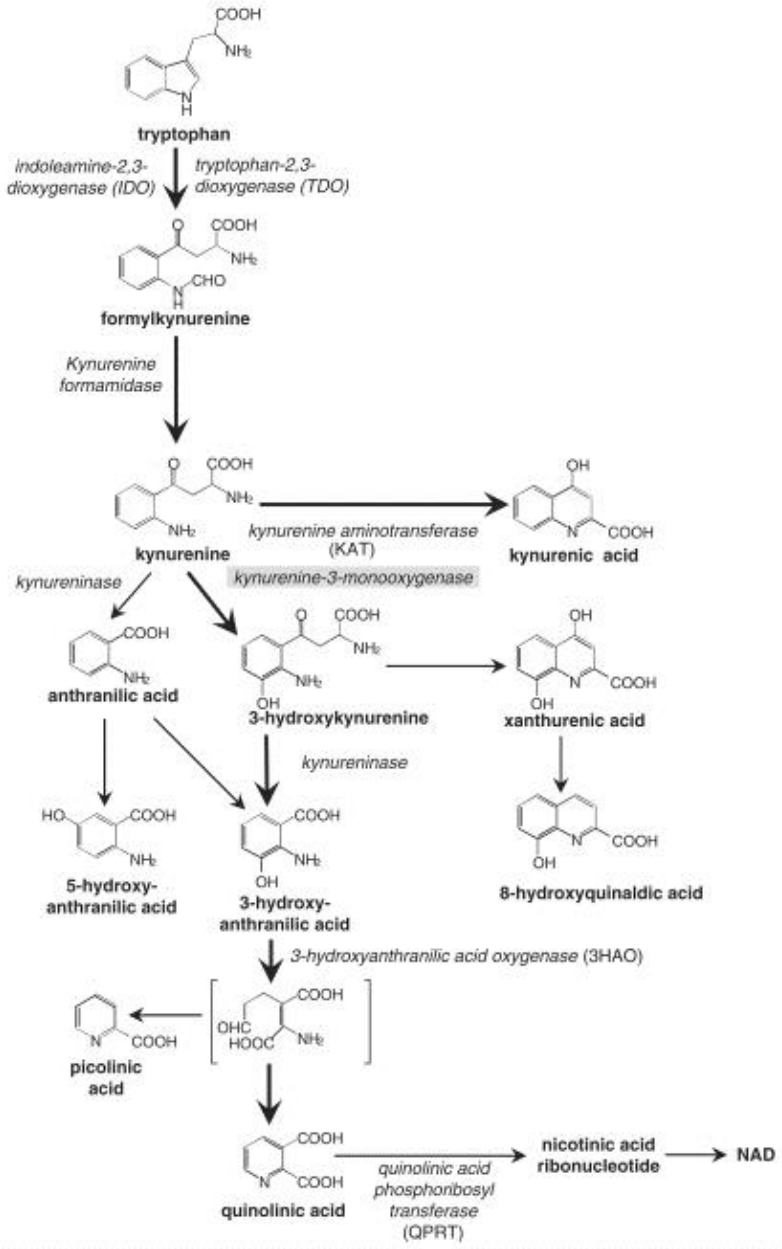

Figure 1.14 Schematic representation illustrating the main components in the kynurenine pathway of tryptophan metabolism

The enzymes (italics) and catabolites present along the pathway are shown. Ro-61-8048 inhibits the enzyme KMO (grey highlight).

Image taken from Rodgers *et al*, 2009 (233)

1.4.3.1 The Kynurenine Pathway in Neuropsychiatric Disease

In recent years, the dysregulation of kynurenine metabolism has been described in the pathophysiology of psychiatric disorders such as schizophrenia, anxiety and mood disorders (250,251). The notion that Kynurenic Acid (KYNA) is thought to function as an endogenous antagonist of the NMDA receptor co-agonist site has inspired interest in the involvement of KYNA in schizophrenia (252). This is based on a leading hypothesis proposing that NMDA receptor hypofunction is significant mechanism underlying the disease (253,254). Indeed open channel blockers, such as ketamine and phencyclidine, targeting the ion-channel of the NMDA receptor found at most excitatory synapses, have been found to exacerbate symptoms in patients whilst recapitulating a spectrum of common symptomology in healthy subjects (255). Further, increased KYNA levels have been reported in post-mortem prefrontal cortex (256) of schizophrenic patients and in CSF (257) compared with healthy control patients.

Increased availability of L-kynurenine for metabolism into KYNA by KAT II (kynurenine aminotransferase II), an enzyme found in human and rat brain (258), may account for the elevated levels of brain KYNA in schizophrenic patients. Guidetti et al (259) proposed astrocyte-specific enhancement of L-kynurenine (L-KYN) production as the mechanism by which this might occur, since it is known that brain KAT II is primarily expressed in astrocytes compared with other neuronal cells (260). Supporting this possibility, increased tissue levels of L-KYN were found in the anterior cingulate cortex (post-mortem) of patients with schizophrenia and bipolar disorder when compared with healthy subjects (261). Moreover, it has been reported that expression of TDO_2 (Tryptophan 2,3-dioxygenase) is upregulated in white matter astrocytes of the frontal cortex of schizophrenic patients (262). Put together, a leading hypothesis posits

that elevated levels of KYNA in brain regions implicated in the cognitive impairment commonly seen in schizophrenic patients may, in part, be due to upregulated astrocyte-specific TDO_2- mediated L-KYN synthesis (263).

Based on this, research efforts in the last few years have focused on the use of KAT II inhibitors to reduced KYNA brain levels, with preclinical data supporting a pro-cognitive phenotype in schizophrenic-related behavioural assays. For example, systematic administration of the brain penetrant KAT II inhibitor PF-04859989 (264) significantly reduced brain KYNA levels by 70% and improved performance in a sustained attention task. In addition, the drug reversed ketamine-induced working memory deficits in rodents and monkeys, supporting the ability of the drug to limit the pact of disease-relevant changes in glutamate system, function. More recently in early 2019, Fujigaki et al (265) reviewed the relationship between phencyclidine (PCP) intoxication and the tryptophan-kynurenine pathway. Here the authors discuss the similarities between PCP, a dissociative anaesthetic that induces psychotic-like symptoms, and KYNA since both act as NMDA receptor antagonists.

Research investigating the potential association between KP metabolites and immune-related imbalances predisposing individuals to depression-associated symptomology is still in its infancy. However, evidence from multiple research groups suggests that activated inflammatory responses, particularly the release of cytokines, may contribute to the pathogenesis of MDD (266–268). Indeed, one theory is that activation of the enzyme indoleamine 2, 3-dioxygenase (IDO) may be a route by which inflammatory stimuli may contribute to the symptoms associated with mood disorders (269). More specifically, once activated by various cytokines including IFN-γ, IFN-α and/or tumor

necrosis factor (TNF)-α (270–272), IDO mediates the catabolism of L-tryptophan into kynurenine (273). This metabolism in turn reduces the availability of tryptophan, which has an important role in T-cell regulation (274), as well as a precursor for serotonin which has a prominent function in the neurobiology of mood disorders (275).

Raison et al (276) reported that peripheral administration of IFN- α activated IDO in conjunction with central cytokine responses, lead to increased brain kynurenine levels and quinolinic acid, which correlated with depressive symptoms. Further, Savitz and colleagues (277) conducted a study with severely depressed un-medicated subjects whereby blood samples were taken for kynurenine metabolomic analysis and structural MRI scans taken. The authors reported on the KYNA/quinolinic acid (QA) index, a neuroprotective index, being lower in the MDD group compared with healthy subjects, and correlating positively with total hippocampal and amygdala volume in MDD subjects.

1.5 Concluding remarks

HAT is a complex disease, with numerous interactions between the host immune system, the parasite and the CNS which remain to be fully elucidated. Although progress has been made in recent years to reduce the number of HAT cases recorded, further studies are required to examine and clarify the effect of the parasite on the host CNS. Research investigating the role of tryptophan metabolism by African Trypanosomes in the brain would help elucidate whether this metabolism directly interferes with host neurotransmission by either depleting tryptophan in the brain, or through the production and secretion of neuroactive metabolites such as sleep inducing tryptophol or metabolites of the KP pathway. Further experimental work characterising

the metabolites produced during tryptophan metabolism could also provide essential data, adding to the growing body of literature.

1.6 General Project Aims

The aim of this project was to bring together two areas of research, namely *Trypanosoma brucei* parasite metabolomics and preclinical rodent phenotyping to further understand host-parasite relationship with regard to the neurological symptoms of HAT. The four main research aims were:

Aim 1. Map mammalian body system localisation of Trypanosomes throughout infection.

Aim 2. Define impact of Trypanosome infection on tryptophan levels in the brain.

Aim 3. Determine impact of Trypanosome infection on rodent behaviour and cerebral glucose metabolism.

Aim 4. Develop novel, genetically modified Trypanosome cell lines with altered tryptophan metabolism for use in future *in vivo* studies.

Chapter 2.0 Utilisation of VSL2 red-shifted GVR35 *T. b. brucei* to map parasite tissue localisation across infection in a mouse model of Human African Trypanosomiasis (HAT)

2.1 Introduction

Animal models of disease are useful tools in studying infectious diseases (278). Currently, a murine model of stage II trypanosomiasis makes use of the pleomorphic strain *T. b. brucei* GVR35 (279). Commonly, a tagged bioluminescent cell line is used for whole body imaging of infected rodents to monitor disease progression and localisation, allowing the correlation of bioluminescent signal with pathogen load. However, the localisation of parasites to specific tissue, particularly the brain, still requires *ex vivo* imaging. Here we report the use of a reporter cell line (280) that constitutively expresses a red-shifted firefly luciferase for the bioluminescent detection of *T. b .brucei* during infection in a murine model of stage II HAT. Tissue localisation data from infected mice will provide important information as to which tissues are potentially most likely to show altered tryptophan metabolism due to the presence of Trypanosomes, and at which point during infection. Mapping of tissue localisation will also tell us at which infection timepoint Trypanosome colonisation of the brain is evident, and if there are any brain regions that are more readily colonised by the parasite. Attempting to identify localised Trypanosome colonisation in the brain may also indicate the types of behavioural deficits that the animals are likely to show.

2.2 Research Objective

i. To establish the murine model of Human African Trypanosomiasis at Lancaster University
ii. To map tissue localisation in CD-1 *T. brucei* infected mice, at different stages of infection, using *ex vivo* imaging
iii. Generate samples for HPLC and infections for animal behaviour experiments

2.3 Method Summary

Methods in this chapter include *in vivo* mice infections, *in vitro* luciferase reporter assay, luciferase reporter assay of infected blood and *ex vivo* bioluminescent imaging of rodent tissue.

2.4 Summary of findings

1. A small subset of animals experience early CNS parasitic invasion
2. Parasitic tissue tropism is wide spread during *Trypanosomiasis* infection
3. *Ex vivo* imaging data reveals punctate parasite localisation in the gut from early stages of infection
4. Route of infection does not influence the detected tissue distribution of *T. b. brucei*

2.5 Results

2.5.1 Characterising the murine model of Human African Trypanosomiasis in CD-1 female mice

The well-established *Trypanosoma brucei brucei* (*T. b. brucei*) mouse model of human African trypanosomiasis was used throughout the study (280). Initially, a stage I infection is established with cyclical fluctuations in parasite load in the blood and lymphatic system. Which after 14 days begins to progress into the CNS reaching stage II by day 21, with a reported mean survival time of 35 days. In our study, adult albino female CD-1 mice (from 8 weeks old) were infected and subsequently sub-divided into three cohorts assigned to study disease progression and parasite localisation at 7 (n = 9), 14 (n = 10) and 22 (n = 12) days post-infection (Figure 2.1). Age and sex-matched uninfected animals were included for all three experimental groups to act as controls.

First, two mice were used as part of a starter infection, infected with approximately 10^4 VSL2 red-shifted GVR35 *T. b. brucei*, and animals euthanised at day 5 post-infection and blood samples collected. Tail-vein blood smears were used during starter infections to monitor parasitemia levels, with day 5 being deemed as the optimal time to collect slender parasite forms. Blood taken from starter mice with high levels of parasitemia (approximately 10^7 cells/ml) was then diluted with phosphate buffered saline (PBS) to achieve stabilates with a parasitemia load of 2 x 10^4 parasites per mouse in 200ul PBS, and used to set up subsequent mouse infections with *T. b. brucei*.

Infections were run for 7, 14 and 22 days to obtain samples representative of stage I, intermediate stage I-II, and stage II of the disease. On the final day of infection, luciferin was administered *intraperitoneal* (*i.p*) 10 minutes prior to sacrifice by cervical

dislocation and decapitation. Tissues collected included half of the brain, liver, heart, spleen, muscle, fat, small intestine, colon, eye and mesenteric lymph nodes, into clear 12-well plates for imaging. Luciferin was used to enable the bioluminescent visualisation of VSL2 red-shifted GVR35 *T. b. brucei* in infected rodent tissues.

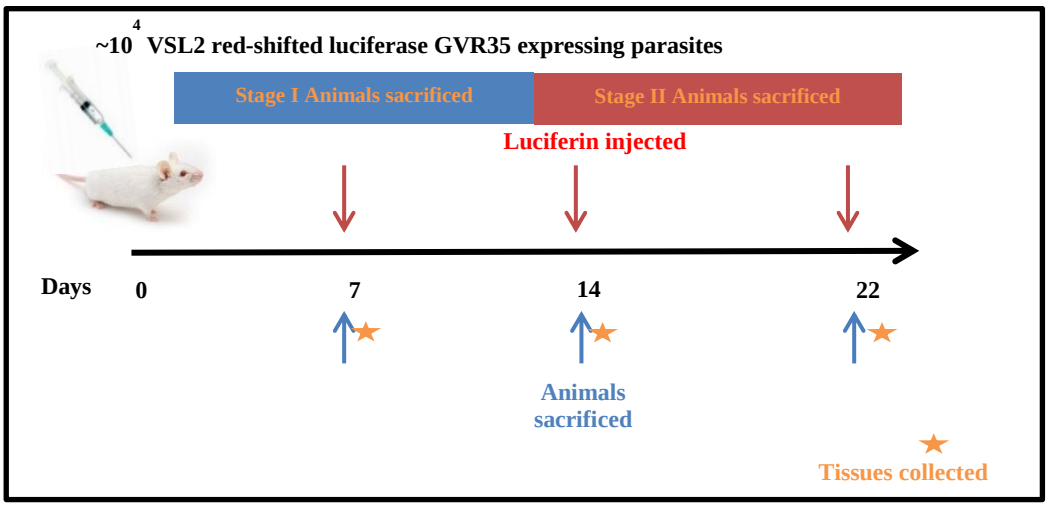

Figure 2.1 Schematic detailing the methodology and workflow of the described in vivo animal experiments

Adult CD-1 female mice (from 8 weeks old) were infected and subsequently sub-divided into three cohorts assigned to study disease progression and parasite localisation at 7 (n=9), 14 (n=10) and 22 (n=12) days post-infection. Age and sex-matched uninfected animals were included for all three experimental groups to act as controls. Luciferin was administered *intraperitoneal* (*i.p*) 10 minutes prior to sacrifice by cervical dislocation and decapitation. Tissues collected included half the brain, liver, heart, spleen, muscle, fat, small intestine, colon, eye and mesenteric lymph nodes.

.

2.5.2 Characterising the limit of detection for the *T. b. brucei* luciferase assay

To investigate the limit of detection of the *T. b. brucei* luciferase assay, and to asses if the relationship between parasite number and the bioluminescence signal, a luciferase assay on serial dilutions of VSL2 parasites was conducted. Data analysis revealed a significant ($p < 0.001$) positive correlation between parasite levels and the level of bioluminescence detected (Figure 2.2). Limit of detection was also ascertained by serially diluting VSL2 cells in a 96-well microtitre plate and measuring luciferase signal upon the addition of luciferin (see methods section). 30 parasites (in 1ml) could be readily detected above background levels of luminescence (media signal only).

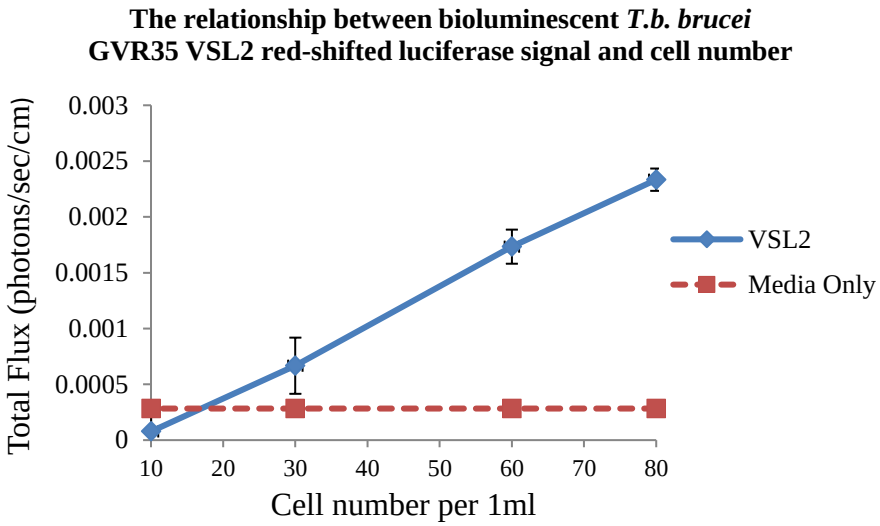

Figure 2.2 In vitro limit of detection for the T. b. brucei luminescence assay

In vitro plots generated from 96-well microtitre plates containing serial dilutions of the *T. b brucei* GVR35 clone VSL2 and wells with media only for background readings. Each point corresponds to bioluminescence represented by the total flux recorded from a single well. The data show readings from triplicate wells.

2.5.3 *Ex vivo* bioluminescent imaging of *Trypanosoma brucei* infected CD-1 mice from a blood stabilate reveals a wide range of host tissue tropism

The course of Trypanosome infection in female albino CD-1 mice was assessed following the infection (*i.p*) with approximately 2 x 10^4 VSL2 red-shifted *T. b. brucei* GVR35 parasites from a blood stabilate. To ensure the moderate severity of the protocol was not breached, we used a scoring system of 0 - 2; 0 indicating no symptoms; 1 indicating shivering, lassitude or parasite burden 1-5 x 10^8 cells/ml; 2 indicating tremor, inactivity or parasite burden > 5 x 10^8 cells/ml. Animals were monitored daily and scored every other day; if any animals reached a score of 1, the infected cohort was scored twice daily, and if the score >0 after 48 h or immediately upon reaching a score of 2 the animal was humanely sacrificed. The mice were humanely sacrificed at day 7 (stage I infection), 14 (intermediate infection) and 22 (late stage II infection) of infection and tissues imaged *post mortem* as previously described (Figure 2.1).

At day 7 (n = 4 infected) bioluminescent imaging revealed clear evidence of widespread parasitemia (Figure 2.3). Visually, in animals at day 7 the highest trypanosome load was evident in the small intestine, colon and mesenteric lymph node shown as distinct highly luminescent foci of parasitic infection, with lower levels of trypanosome burden evident in the spleen and fat. Trypanosome localisation to the liver, heart and eye was also evident. Interestingly, brain infection could be tentatively identified within 7 days of infection in one of the mouse brains imaged. The lack of bioluminescent signal was confirmed in control non-infected animals (n = 5) at the same time point.

Visually, in animals at day 14 (n = 5 infected) of infection, *ex vivo* examination of tissues showed that the highest trypanosome load was evident in the fat, heart, muscle

and mesenteric lymph node as characterised by 100% of the cohort (as seen in 5/5 animals) (Figure 2.3). Visually, during dissection it appeared that animals suffered severe splenomegaly and hepatomegaly. Punctate parasitic localisation was found in the gut. Animals had strongly identifiable brain infection as seen in 80% (4/5) of mice, with 60% (3/5) suffering from trypanosome infection of the eye.

Finally, at day 22 (n = 6 infected) efforts to map whole body system localisation of parasites at the chronic stage II trypanosomiasis revealed once more the highest trypanosome load evident in the spleen, fat, liver, heart, muscle, small intestine, colon and mesenteric lymph node (Figure 2.3). Similar to animals from the day 14 cohort, 83% (5/6) of animals characterised at day 22 suffered with brain infections. Overall, the majority of animals from all three cohorts had clear trypanosome localisation to the same main tissue types, with the proportion of animals with parasites in the eye and brain increasing across the duration of the infection (Figure 2.4).

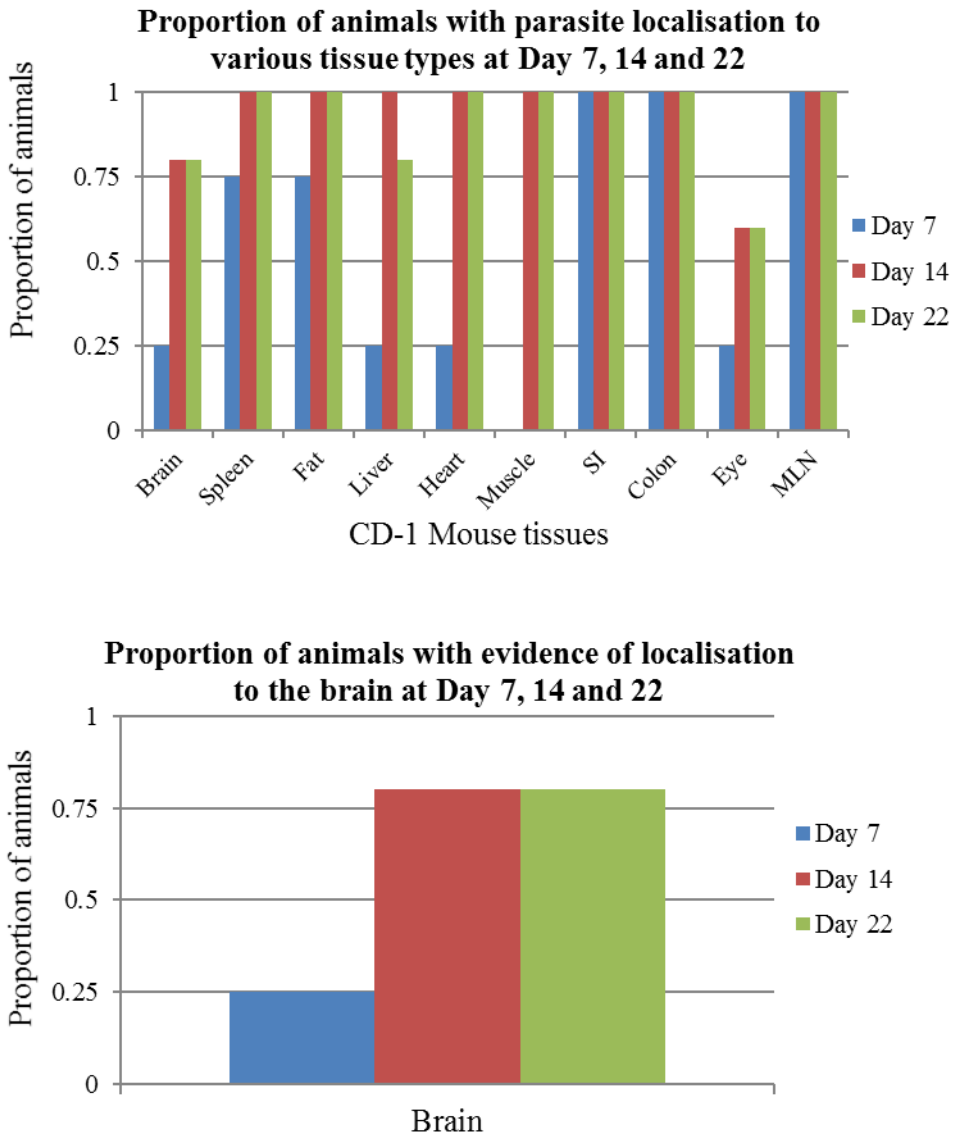

Figure 2.3 Parasite tissue localisation at day 7,14 and 22 post infection with VSL2 red-shifted T. b. brucei GVR35 parasites

Data shown are the proportion of animals with confirmed parasite localisation to the brain, spleen, fat, liver, heart, muscle, small intestine (SI), colon, eye and mesenteric lymph node (MLN) at day 7 (n=4) ,14 (n=5) and 22 (n=6) post infection (A). At day 7 post-infection (p.i) 25% of animals (1/4) have a bioluminescent signal from the brain, compared with 80% and 83% of animals at day 14 (4/5) and 22 (5/6) respectively (B).

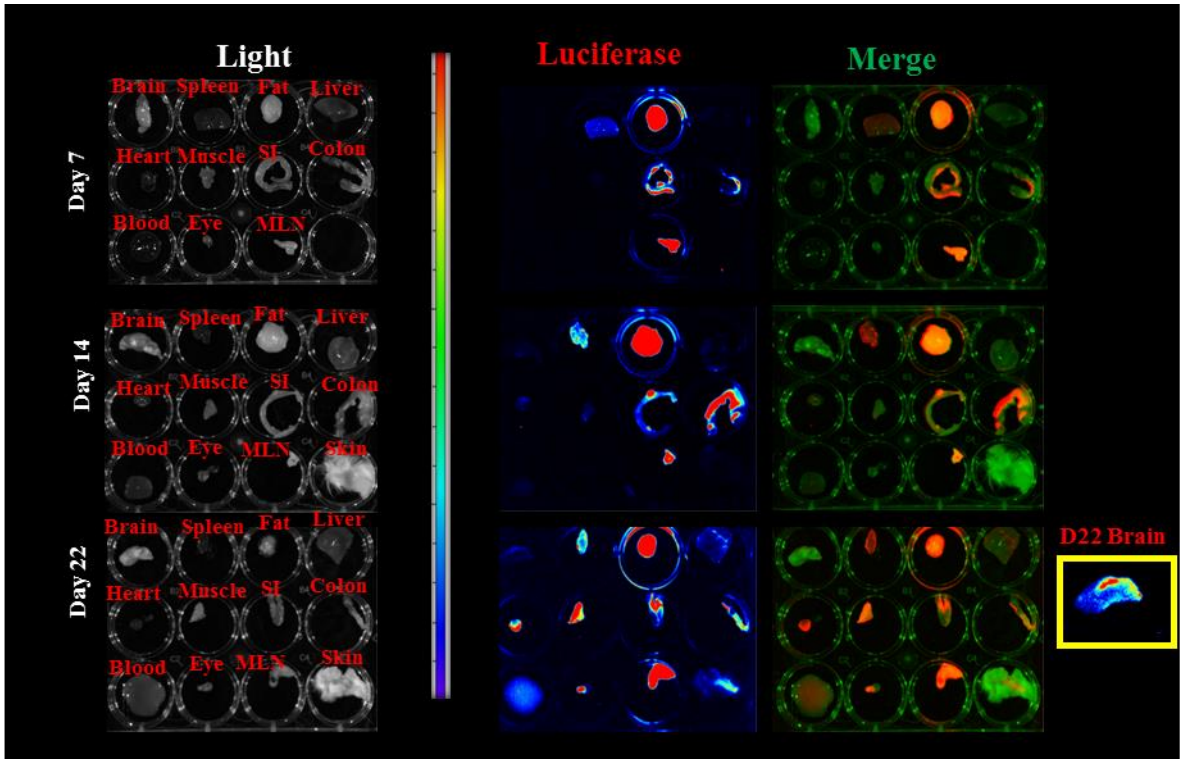

Figure 2.4 Representative ex vivo bioluminescent images of infected rodent tissues at day 7, 14 and 22 post infection

Post mortem bioluminescent imaging of representative infected mice following *intraperitoneal (i.p)* infection with 1 x 10^4 parasites, in the early stage I phase (Day 7), intermediate phase (Day 14), and late stage II infection (Day 22). The images in the left panel indicate arrangement of the dissected tissues in a 12-well plate format, images in the middle panel detailing the bioluminescent signal and images in the right panel showing the bioluminescent signal overlaying the tissue sample. All images are calibrated to the same scale. Full data is given in Appendices 1-3. SI, Small Intestine; MLN, Mesenteric Lymph Nodes.

2.5.4 Route of injection with *Trypanosoma brucei* does not affect parasite tissue localisation

The course of Trypanosome infection in female albino CD-1 mice infected subcutaneously (*s.c*.) was assessed following the infection with approximately 2 x 10^4 VSL2 red-shifted *T. b. brucei* GVR35 parasites from a blood stabilate, generated as previously described. This was undertaken to determine whether parasite localisation, particularly to the gut and organs within the abdominal cavity, was a consequence of parasite infection through intraperitoneal injection.

Parasites were injected *s.c*. in the neck scruff to provide an alternative site of initial infection. The mice were humanely sacrificed at 7 days of infection and tissues imaged *post mortem*, using the same approach taken for tissues from *i.p*. infected animals (Figure 2.4). At day 7 (n=2) bioluminescent imaging revealed clear evidence of widespread parasitemia, with localisation to the fat, mesenteric lymph node, spleen and eye (Figure 2.5). In addition, distinct highly luminescent foci of parasitic infection, similar to that seen in animals infected *i.p.*, was also seen in the small intestine and colon (Figure 2.6). While no brain infection was determined in this cohort, at 7 days of infection, as the sample size was very small and brain penetration seems to occur only in a proportion of animals by 7 days of infection, no firm conclusions of brain localisation following *s.c.* injection can be made. However, as the animals had very similar parasite tissue localisation profiles to the cohort of day 7 animals infected *i.p.*, including localisation to the small intestine and colon, the localisation of parasites to the gut does not appear to be the result of *i.p.* infection.

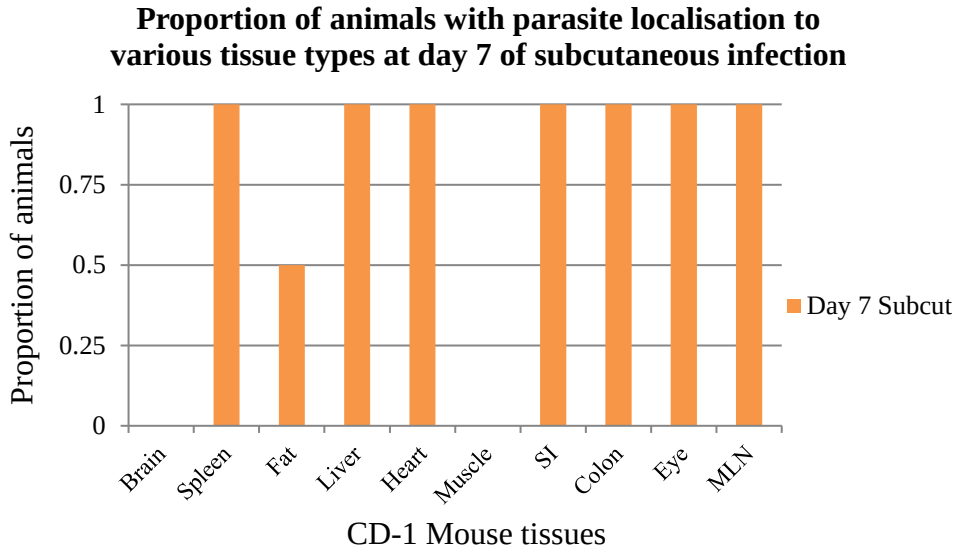

Figure 2.5 Parasite tissue localisation at day 7 post subcutaneous infection with VSL2 red-shifted T. b. brucei GVR35 parasites

Data shown are the proportion of animals with confirmed parasite sequestration to the spleen, fat, liver, heart, small intestine (SI), colon, eye and mesenteric lymph node (MLN) at day 7 (n=2) post subcutaneous *(s.c.)* infection.

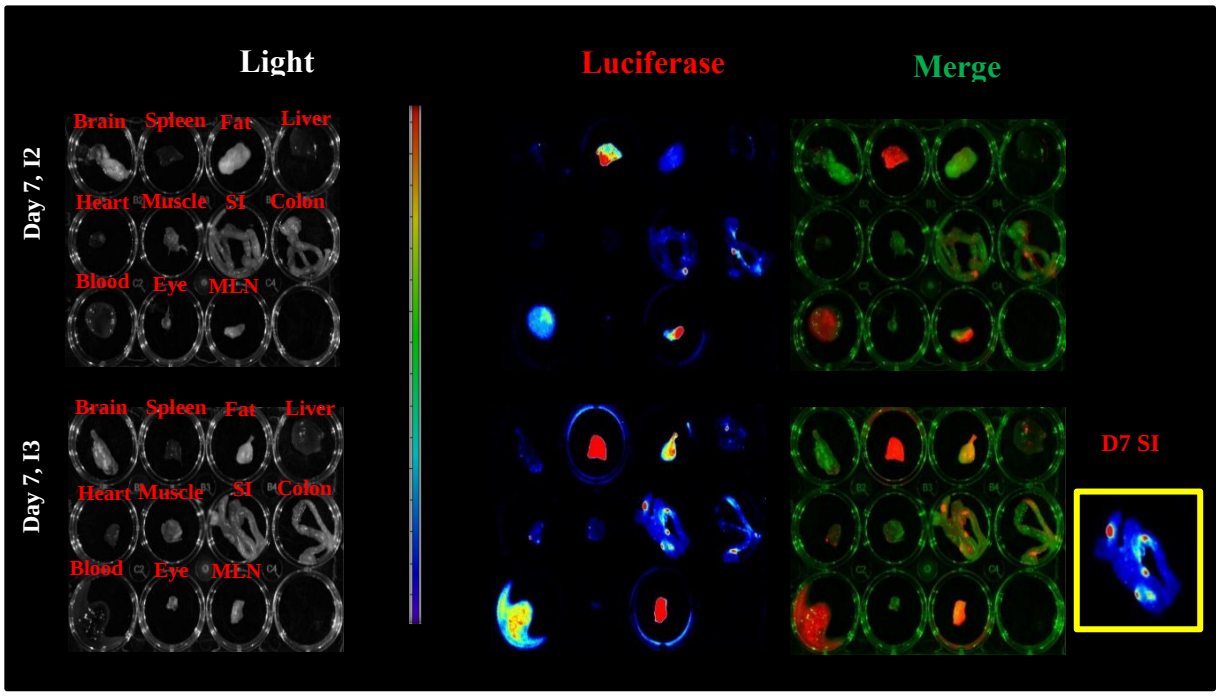

Figure 2.6 Ex vivo bioluminescent images of infected rodent tissues at day 7 post subcutaneous infection

Post mortem bioluminescent imaging of infected mice following *subcutaneous (s.c.)* infection with 1 x 10^4 parasites, in the early stage I phase of infection (Day 7). The images in the left panel indicate arrangement of the dissected tissues in a 12-well plate format, images in the middle panel detailing the bioluminescent signal and images in the right panel showing the bioluminescent signal overlaying the tissue sample. All images are calibrated to the same scale and undertake under the same conditions as animals analysed for *i.p.* infection. SI, Small Intestine; MLN, Mesenteric Lymph Nodes.

2.6 Discussion

In an attempt to bridge the gaps in our knowledge of the systemic time course of Trypanosome infection and its infiltration of the brain, in this work we used *ex vivo* bioluminescent imaging of *Trypanosoma brucei brucei* infected rodent tissues at day 7, 14 and 22 post infection. *In vitro* luciferase assays were employed to determine limit of detection for the tagged cell line and corroborate findings with the existing literature (280). The overall primary aim was to understand the developing nature of Trypanosome infection in the murine model, with respect to tissue localisation and to detect exactly when during this process parasites infiltrate the brain.

Based on the use of the GVR35 red-shifted luciferase VSL *Trypanosoma brucei brucei* cell line developed by Mclatchie et al in 2013 (280), we were able to bioluminescently image infected tissues and visually compare levels of parasitemia in different tissues types across infection in the murine model. Unlike Mclatchie and colleagues, we made us of *ex vivo* imaging of the tissues with the intention to overcome issues associated with scattering of the light by the skull when imaged *in vivo* and the relatively poor anatomical resolution of *in vivo* imaging. Similarly, Myburgh et al in 2013 (294) monitored parasite distribution in infected mice following treatment with trypanocidal compounds using bioluminescence imaging. Using a combination of *in vivo* and *ex vivo* tissue imaging, their data showed that trypanosomes enter the brain meninges as early as day 5 post-infection, with parasites found in the spleen, liver, heart, lungs and mesenteric lymph nodes at 35 days post-infection.

One main limitation of our study is that we made use of a cross-sectional sampling design rather than a longitudinal design. The main advantage of a longitudinal design

is that inter-individual variability is reduced, and it could allow for potentially more accurate tracking of the infection time course. Individual variability, particularly at earlier stages of infection, were detected in our experiment. It must also be mentioned that although this technology represents exciting opportunities for further development with regards to cerebral parasite localisation, it does not provide direct information on brain tissue dysfunction. Combining *ex vivo* imaging with functional brain imaging methods, such as by the use of ^{14}C-2-DG (Chapter 5) would be a worthwhile route of investigation.

It is important to note that although murine models are accepted as appropriate methods of furthering the field's stage II trypanosomiasis knowledge, the results reported in this work may be limited to their translatable relevance to the clinical setting in humans. For example, it is well known that *T b brucei* is not capable of propagating infection in human hosts (281) ; however *T b gambiense* and *T b rhodesiense* are not routinely used in *in vitro* murine models of infection due to compromised survival time of the mammalian host (282).

2.6.1 Infection with *Trypanosoma brucei* reveals a wide range of host tissue tropism

Our work studied tissue tropism of *T. b. brucei* at distinct time points of infection to try and elucidate the time course of tissue invasion and, with specific regard to the aims of this thesis, correlate brain invasion and colonisation with behavioural phenotypes and tryptophan metabolism in the brain. In doing so, we took a broad systems approach by investigating trypanosome colonisation of diverse tissue types throughout the course of infection. In doing so, we aimed to elucidate the interaction between the pathogen parasite with the organ and tissue niches at set time-points, which is critical in the wider

context of understanding immune evasion, virulence, treatment failure, transmission and the negative consequences for the host.

It comes as no surprise that our study found widespread parasitemia of various tissue types throughout the course of infection, since *Trypanosoma brucei* has for a long time been known as a tissue parasite (22). Previous reports suggest that the parasite can be found in several organs, with splenomegaly and hepatomegaly being a common feature (283,284). To date the CNS, skin, heart, testes and adipose tissue have been the most well characterised reservoirs of the pathogen (25,27,146,285,286). It has also been noted that *T b brucei* is one of the best characterized of the African Trypanosomes (22), with the support of a vast body of animal studies.

Recent advances in technology and imaging systems have allowed researcher to undertake a more in depth, systemic analysis of tissue tropism during infection. Indeed, using novel *ex vivo* bioluminescent imaging technology of infected tissues we were able to clearly identify foci hot spots in the gut of infected animals at all three time-points analysed. In particular we were able to visually distinguish punctate parasite sequestration to the small intestine, in small distinct pockets. These could potentially be putatively peyer's patches, forming part of the gut associated lymphoid tissue (287), although this suggestion requires further systemic characterisation. Further work is necessary to characterise the exact location of the Trypanosome cells; for example are the parasites sequestered inside blood vessels of specific tissues or are they localised to the extravascular compartment of those tissues? The use of a dual luminescent-fluorescently tagged cell line, such as that developed by Costal *et al* (288) for *Trypanosoma cruzi*, would allow investigations into the micro-niche of the parasites at

a microscopic level. Nonetheless the novel finding that Trypanosomes localise to the gut during early stages of infection should catalyse future investigations regarding this potentially over-looked reservoir of African Trypanosomes, with potentially broad implications for nutrient absorption, tryptophan-serotonin depletion, the gut microbiome and the neuro-immuno-gut-brain axis. Importantly, if the integrity of the gut is impaired this could have severe implications for nutrient uptake, potentially contributing to the wasting phenotype observed in sick animals (289), particularly in the economic context of nagana in cattle.

Furthermore recent research by the Sternberg group (290), investigating the relationship between endotoxaemia and inflammatory responses, demonstrated a clear association between low-grade systemic toxaemia and *T. b. rhodesiense* infection. This finding was proposed to be independent of late-stage neuroinflammation. It was further postulated that the potential source of endotoxin reported was most probably a result of increased permeability of the gastrointestinal tract. However, contrary to our findings, the authors suggested that this phenomenon was "certainly parasite-independent," and potentially induced by localised inflammatory responses in the gut which does not align with our gut colonisation findings. Although our work also seems to indicate a potential role for the immune system in contributing to pathology in the gut of infected experimental animals due to parasite localisation to the immune sites such as the Peyer's patches and MLN, it is too simplistic to declare the phenomenon parasite-independent when the authors provided no tissue tropism data to suggest the presence or indeed absence of parasites in the gut. It is important to note that our work used whole rodent tissues, whereas the Sternberg group made use of CFS and plasma samples from human

volunteers, which may account for the discrepancies. Clearly more work is warranted to understand the role of the gut as a novel niche for *Trypanosomes*.

Trypanosome entry in to the brain marks the beginning of clinical stage 2 infection, followed by subsequent neurological perturbations, sleep disturbance, and progressive dementia (91,99). Although there is heated debate regarding the timing of cerebral penetration and staging of disease (291,292), our findings from *ex vivo* imaging of the brain seem to generally corroborate the existing dogma regarding the late stage time-points at which parasites are detectable in the brain tissue. However, we also identified a small subset of animals with early parasitic CNS invasion at day 7, with similar findings reported elsewhere (293). The current literature suggests that once parasites are in the brain, several lesions in the brain parenchyma begin to form with the brain stem, cerebellum and cortical regions most affected (294). From our data, images of day 22 brains reveal strong bioluminescent signals from the cerebellum and visual cortex which substantiates previous reports (280). Locomotor disturbances such as ataxia, tremors and choreiform movement have been described as common symptomologies of HAT (142), with the cerebellum having an established role in producing coordinated movement (295). Thus damage to the cerebellum is associated with perturbed equilibrium and fine movement (296), both of which have been reported to be altered in experimental animal studies as well as in humans with late stage trypanosomiasis (297,298). Disturbed cerebellar function may account for some of hypolocomotory phenotype we observed in Trypanosome infected animals (Chapter 4).

Albeit less reported than for other strains of Trypanosomes, old clinical reports have described the presence of vascular lesions in the eyes of *T. brucei* infected patients,

noting an ocular form of Trypanosomiasis (11,299). Indeed, a myriad of visual pathologies have been reported such as optic neuritis, diplopia, iritis, keratitis and conjunctivitis (146). *Trypanosoma vivax* parasites have also been identified in the aqueous humor of the eye in goats, with authors suggesting that as a potential source of relapse infection following chemotherapy due to the parasites localised in the eye being relatively protected from trypanocide treatment (300). Similarly, the cornea has also been reported as a tissue reservoir of *Trypanosoma cruzi* (301), with the authors highlighting the risk of the ocular environment as a potential source of transmission through parasitized corneal transplants. Intriguingly, our study identified bioluminescent parasites in the eyes of some late stage II animals at day 22. In the context of our stage II characterisation work, trypanosome eye infection is extremely important due to the eye's high blood irrigation and close proximity to the brain with the optic nerve projecting into the brain (302). This could provide an entry route for the parasites into the brain, yet this awaits further investigation.

2.6.2 Route of infection does not influence parasite tissue tropism

To better understand the effect of route of *T. b brucei* infection on parasite tissue tropism, we used a whole system approach to characterise parasite localisation, with rodents infected *s.c*. We assessed impact of the route of infection on parasite tissue localisation, given our previous observation that the parasites localised to multiple organs in the abdominal cavity, including the gut, we wanted to ascertain whether these observations were an artefact of *i.p.* injections, or whether they were independent of infection route. Arguable, the *s.c.* infection route more closely resembles the route of the 'natural' infection, conveyed by bite of the teste fly vector to the mammalian host dermis, than *i.p.* injection (10). Visualising infected tissue *post mortem* at one time-point (day 7), our data suggested a similar tissue localisation profile in *s.c.* infected

animals to that of day 7 animals infected *i.p.* Notably, despite the *s.c.* infection route, clear parasitic foci were evident in the small intestine, colon and MLN. Further, despite the early time-point clear widespread parasitemia was observed, similar to that seen in animals infected by the *i.p*. route. No animals had bioluminescent parasites in the brain during this stage I phase. Infection route, therefore appeared to play no significant role in determining pathogenicity in terms of tissue tropism spread in the murine mouse model of African trypanosomiasis. In turn, parasite localisation to the gut tissues appears to be a biologically relevant observation, as it is not simply a result of *i.p.* infection.

Interestingly, Ndgungu and colleagues (303) have indeed reported infection route to be a critical determinant of pathogenicity of *Trypanosoma congolense* and of *Trypanosoma brucei brucei* in the murine model of HAT using Swiss white mice. Here, the authors compared five different routes of parasite infection- intraperitoneal (*i.p.*), subcutaneous (*s.c.*), intramuscular (*i.m.*), intradermal (*i.d.*) and intravenous (*i.v.*). Looking at parasitemia progression, the authors found no significant difference between *s.c.* and *i.p.* infection with *T. b brucei*, corroborating the findings from our work. However, route of infection with *T. congolense* did appear to affect progression to peak parasitemia. This suggests that differing parasitic strains, not infection routes, play a bigger part in determining pathogenicity in the mouse model. Additionally a study (304) monitoring parasite dissemination in mice following two routes of infections with *Trypanosoma vivax*, namely *s.c.* and *i.p.* , found parasitemia and survival rates were very similar for mice from both cohorts, except with a longer prepatent period following subcutaneous infections. This longer prepatent period resulted in delayed onset parasitemia as compared with mice infected via the intraperitoneal route.

Expanding on the elegant work of the MacLeod group (25) defining the skin as a significant reservoir of Trypanosome parasite, Caljon et al (19) described the use of 'natural' infections as a better alternative for parasite infections of model organisms. In 2016, the authors reported the use of *Glossina morsitans* flies infected with fluorescently tagged *T. brucei* parasites to initiate infection in mice. Here, metacyclic cells were found to be highly infectious, with parasites capable of emigrating from the original dermal infection site to the peripheral blood within 42 hours. The authors championed the use of naturally initiated infections to refine future *in vivo* models of HAT, perhaps providing a better representation of clinical settings.

2.7 Methods

2.7.1 Ethics statement

CD-1 mouse studies were carried out under UK Home Office regulations under project license number P15EA559A. The work was performed with the approval of Lancaster University Animal Welfare and Ethics Review Boards (AWERB). All experiments were carried out in compliance with the UK Animals (Scientific Procedures) Act 1986.

2.7.2 Red-shifted Luciferase GVR35 cell line

The VSL2 red-shifted luciferase *T. b. brucei* GVR35 strain was kindly gifted to the Urbaniak lab from Dr Martin C. Taylor (London School of Hygiene and Tropical Medicine). In brief, McLatchie et al (280) created a reporter system which allows the detection of approximately 100 bioluminescent parasites in the *in vivo* rodent model of HAT. This was done following the targeted integration of the red-shifted *Photinus pyralis* luciferase gene (PpyRE9H) into a ribosomal DNA locus of *T. brucei*, flanked by a 5′-variant surface glycoprotein untranslated region and a 3′-tubulin untranslated region. PpyRE9H has a peak emission of 617 nm.

2.7.3 Luciferase reporter assay

Luciferase activity was measured using the OneGlo luciferase assay system (Promega, UK) following the manufacturer's instructions. In brief, reporter fLUC gene expression was quantified by incubating 100µl of cells/ml *T.b .brucei* GVR35 VSL red-shifted culture in white 96-well plates with an equal volume of the reagent OneGlo luciferase. After 5 min, the luciferase activity was measured in a Fluoroskan ascent FL plate reader (Thermo Scientific) with a 10 sec acquisition time per well.

2.7.4 Mouse infection, welfare monitoring and *ex vivo* imaging

Female CD1 mice (8-12 weeks) were purchased from Charles River (Margate, UK) and housed together in ventilated cages (I.V.Cs, Techniplast, UK), experiencing a 12 hour light/dark cycle (lights on 07:00) with access to food and water *ad libitum.* Two mice were infected intraperitoneally (*i.p.*) with 2×10^4 parasites in 200 µl 1 x PBS and monitored for peripheral parasitemia levels using tail vein bleeds. At the peak of parasitemia (Day 5- post infection), the mice were sacrificed and the infected blood collected. The pleomorphic cells (approximately at 1×10^7) were diluted to approximately 2×10^4 in 200 µl PBS and injected *i.p.* into each CD-1 mouse. To ensure the moderate severity of the protocol was not breached, we used a scoring system of 0 - 2; 0 indicating no symptoms; 1 indicating shivering, lassitude or parasite burden 1-5 x 10^8 cells/ml; 2 indicating tremor, inactivity or parasite burden > 5 x 10^8 cells/ml. Animals were monitored daily and scored every other day; if any animals reached a score of 1, the infected cohort was scored twice daily, and if the score >0 after 48 h or immediately upon reaching a score of 2 the animal was humanely sacrificed.

At specific time-points after the infection (day 7 n = 9; day 14 n = 10; day 22 n = 12), the mice were injected *i.p.* with 200 µl D-luciferin (Perkin Elmer) for imaging, and 10 minutes later sacrificed using cervical dislocation and decapitation. A blood sample was collected and tissues dissected out including the brain, liver, heart, spleen, muscle, fat, small intestine, colon, eye and mesenteric lymph nodes. Half of the tissues were used for bioluminescent imaging, and the other half snap frozen in cold isopentane (-40^0C), and then stored at -80^0 C for future analysis. Light emission was recorded using the GelDoc EZ Imager machine (Bio-rad) using Image Lab Software (Bio-rad) with exposure time varying from 1 to 5 minutes depending on signal intensity.

Chapter 3.0 Brain specific biphasic tryptophan alterations during Trypanosomiasis Infection

3.1 Introduction

Tryptophan metabolite perturbations are associated with several neurological and inflammatory disease (305–308). Analytical quantification of tryptophan and its metabolites in tissue is therefore highly desirable, with numerous valuable potentials such as possible biomarkers of disease (309). Changes in the relative ratios and peak size of the metabolites provide can insight in the progression of neuroinflammatory disorders such as Alzheimer disease, schizophrenia and multiple sclerosis (309).

Trypanosomes are obligate parasites and as such obtain their nutrients such as glucose and amino acids, from their mammalian hosts (310). Bloodstream form *Trypanosoma brucei* cultured *in vitro* significantly deplete the amino acid tryptophan from the media, using it in both protein synthesis and transamination reactions (188). *In vivo* models of Trypanosomiasis infection have also revealed depressed serum levels of aromatic amino acids such as tryptophan (189), but this is yet to be characterised in the different tissues where we have detected parasite localisation (Chapter 2). In addition, research by the Barrett group has also shown decreased tryptophan levels and increased 5-Hydroxytryptophan in stage II clinical samples (6).

Tryptophan catabolism occurs via three main pathways in the mammalian host; forming an essential component of the kynurenine pathway with both neurotoxic and neuroprotective branches, via the serotonin pathway acting as a precursor for melatonin, with both serotonin and melatonin heavily implicated in sleep regulation, and via intestinal bacterial degradation (311–314). In this study we measured tissue tryptophan

concentrations in the *Trypanosoma brucei brucei* rodent model of infection using high performance liquid chromatography (HPLC) and liquid chromatography-tandem mass spectrometry (LC-MS/MS).

3.2 Research objectives

i. To set up the HPLC protocol by Lesniak *et al* (315) and utilise the intrinsic spectroscopic properties of tryptophan metabolites for detection in murine tissues infected with *Trypanosoma brucei brucei.*
ii. To determine the impact of Trypanosomiasis infection and disease stage on tryptophan levels in the murine brain.
iii. To investigate whether Trypanosomiasis infection impacts on the tryptophan profile of selected other murine tissues.

3.3 Methods Summary

Sample preparation of rodent tissue for HPLC and LC-MS/MS analysis was conducted following the established protocol by Lesniak *et al* (315). In brief, tissue samples were homogenised with zirconium beads, processed and lyophilized to be dissolved in 1 ml of the mobile phase required for HPLC analysis (0.1% TFA in H20: ACN 90:10 v/v).

For HPLC analysis, infected and non-infected samples were run through a TSKgel ODS-80TS column with an isocratic flow of 10% acetonitrile, 0.1% TFA with selected tryptophan metabolites detected by UV and fluorescence. Tissue sample measurements were taken in triplicate.

For LC-MS/MS analysis, samples were separated on an Atlantis T3 reverse-phase column with an increasing acetonitrile gradient of X to Y% prior to electrospray

ionisation into a triple quadrapole mass spectrometer operating in multiple reaction monitoring (MRM) mode.

3.4 Summary of Findings

1. There was a significant increase in brain tryptophan levels of animals at day 7 post infection as compared with non-infected control animals.
2. Animals at stage II *Trypanosomiasis* infection (Day 22) have significantly decreased levels of tryptophan in the brain.
3. In contrast to the brain, tryptophan levels were elevated in animals with stage II Trypanosomiasis infection in multiple body tissues including the colon, spleen, liver and skeletal muscle.

3.5 Results

3.5.1 Set up of HPLC Method

Following a protocol by Lesniak *et al* (315), the quantification of tryptophan and its main metabolites was carried out based on dual UV absorbance and fluorescence detection. Standard compounds were used to validate the HPLC separation, and to enable quantification of tryptophan metabolites produced in body tissues of mice during *Trypanosomiasis* infection. Initially, commercial standards of each analyte were run through the HPLC system to determine retention times (RT) and validate chromatographic separation.

Standard mixtures of tryptophan (W), serotonin (5-HT), 5-hydroxyindolacetic acid (5-HIAA), kynurenine (KYN) and kynurenic acid (KYNA) at concentrations of 100ug/ml were analysed by HPLC separation. Chromatographic analysis for each standard and their retention times (RT) are summarised in Table 3.1

Table 3.1 Spectroscopic and chromatographic properties of tryptophan and its major metabolites

Analyte	λ_{Ex} (nm)	λ_{Em} (nm)	Abs (nm)	RT (min)
Tryptophan	297	348	220	30.7
			280	
			300	
5-Methoxy-DL-tryptophan	297	348	220	29
			280	
			300	
5-Hydroxyindoleacetic acid (5-HIAA)	297	348	220	20.2
			280	
			300	
5-Hydroxytryptophan (5-HT)	297	348	220	9.4
			280	
			300	
5-Hydroxytryptamine (Serotonin)	297	348	220	8.8
			280	
			300	
Kynurenine (KYN)	364	480	226	12.3
			254	
			364	
Kynurenic acid (KYNA)	330	390	216	20.9
			242	
			330	

Commercial standards were separated by HPLC to determine retention times (RT) and validate chromatographic separation. Spectroscopic properties for each analyte were reproduced from an established protocol (315). λ_{Em}, wavelength of excitation; λ_{Em}, wavelength of emission; Abs, wavelength of absorbance; RT, Retention time.

3.5.2 Tissue Sample Preparation, Data collection and Analysis

In vivo Trypanosome infection experiments using the murine model for stage II HAT were conducted (see Chapter 2 for detail) and after 7 (Stage I), 14 (Stage I-II) and 22 days (Stage II) post infection the animals were humanely sacrificed. The brain and various other body tissues, including the spleen, muscle, liver and gastrointestinal organs, were dissected out and snap frozen in liquid nitrogen then stored at -80^0 C (see Methods section).

For analysis of tryptophan levels, tissues were defrosted, weighed and mechanically disrupted using a zirconium bead shaker system (Figure 3.1). An acetonitrile/chloroform extraction technique was employed, after which samples were aliquoted into three collection tubes and lyophilised. Samples were then stored (-80^0 C), prior to analysis. Data was collected by dissolving the lyophilised material in running buffer A and injecting the sample into the analytical instrument, with each samples injected in triplicate.

Initially HPLC analysis of half of control murine brain tissues were conducted, to check that the system worked, and that separation of metabolites could be achieved, with clear assignment of the Tryptophan peak (Figure 3.2). Most peaks shifted retention time substantially between different control animals, which limited the confidence with which we could assign the peaks to metabolites based on our HPLC RT data. Tryptophan peaks for different control brain tissues remained the most consistent, with peaks appearing between 29-32 minutes. Based on this, we decided to focus the rest of the HPLC-MS study on tryptophan levels in rodent tissues

After data collection, the sample fluorescence values (arbitrary units) were normalised to 100mg of tissue, followed by subsequent normalisation of the data to the control mean. The variability between the triplicate measurements and between animals from the same experimental cohort was also examined. Statistical analysis of Mass Spectrometry (MS) data included normalisation to the internal tryptophan standard 5-Methoxy-DL-tryptophan, per 1 kilogram of brain tissue. Tryptophan concentrations in different tissues were compared between infected and control animals using Student's t-test.

At day 7 post infection, tissues from 9 animals (n = 4 infected, n = 5 non-infected control) were recovered as one infected animal had to be humanely euthanised due to exhibiting hind leg paralysis (see Chapter 2). At day 14, tissues from 10 animals (n = 5 infected, n = 5 non-infected control) were recovered and from 12 animals (n = 6 infected, n = 6 non-infected control) at day 22 post infection. Differences between absolute tryptophan levels recorded for the control group animals across the different cohorts was observed. However, as infected and control tissues for each cohort were processed by HPLC-MS at the same time, results were still deemed to be comparable.

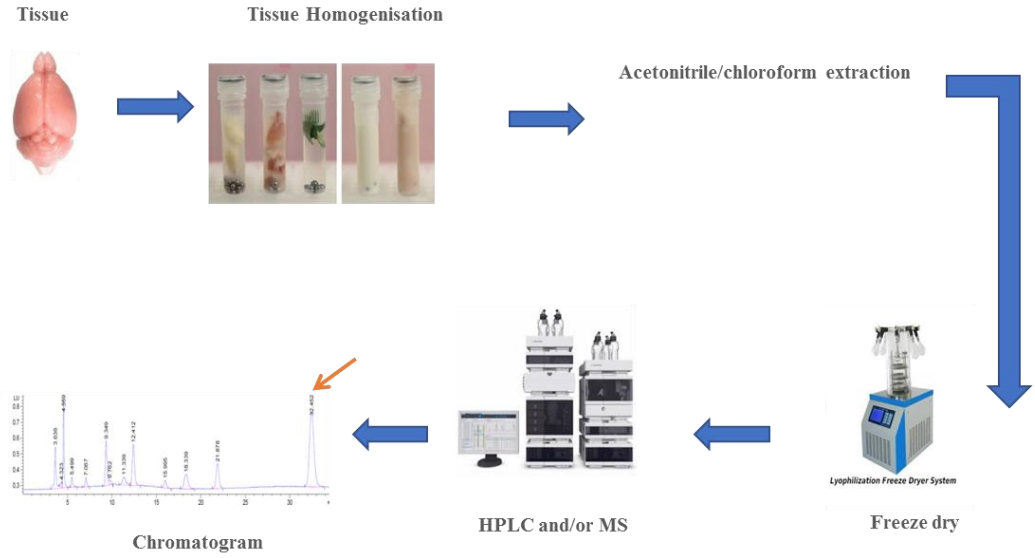

Figure 3.1 Schematic detailing the methodology and experimental workflow for the tryptophan HPLC/MS experiments

Murine tissues, homogenised mechanically using zirconium beads and a high-speed tissue disrupter, extracted with acetonitrile/chloroform, lyophilised and stored at -80 ^{0}C. Samples were analysed by HPLC using an Agilent Technologies 1260 Infinity II system (Böblingen, Germany) equipped with UV and fluorescence detection. Chromatograms were analysed, and tryptophan metabolite concentrations compared between control and infected animals. Red arrow on chromatogram defined the metabolite peak for tryptophan.

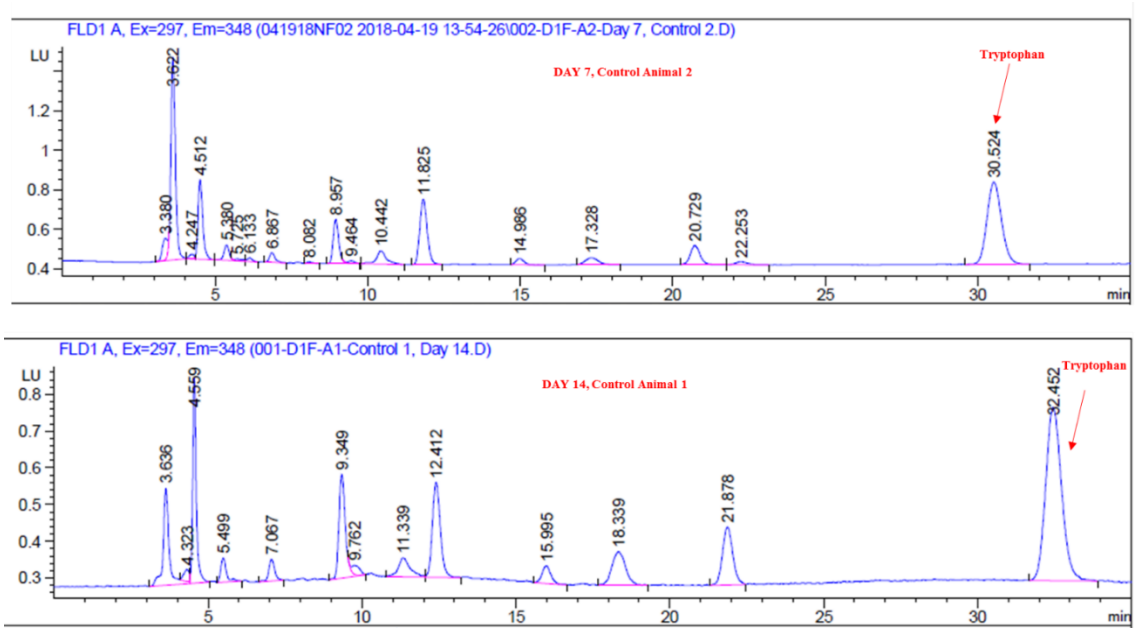

Figure 3.2 Representative HPLC chromatograms of control murine brain tissues at Day 7 and 14

Control rodent brain tissues were weighed, homogenised mechanically, extracted with acetonitrile/chloroform, lyophilised and stored at -80 ^{0}C. Samples were analysed by HPLC using an Agilent Technologies 1260 Infinity II system (Böblingen, Germany) equipped with UV and fluorescence detection. Chromatograms were analysed, and tryptophan metabolite concentrations quantified. Red arrow on chromatogram defined the metabolite peak for tryptophan.

3.5.3 Brain specific biphasic tryptophan alterations during Trypanosome infection

Trypanosome-infected brain tissue from CD-1 female mice was profiled via HPLC analysis with the abundance of tryptophan quantified by fluorescent detection. Intra-cohort variability is apparent in Figure 3.3 (panels 2B and 3B for day 14 and day 22 cohorts), with a broad range of brain tryptophan levels observed between animals in the same cohort. Despite this, a clear general trend of changes in tryptophan levels in infected animals compared to uninfected animals is evident. As the variation between the triplicate technical replicates is smaller than the variation in the biological replicates (each animal), the intra-cohort variability is likely to be mainly due to biological variation. Differences between absolute tryptophan levels recorded for the control group animals across the different cohorts was also observed (Figure 3.3, panel B), potentially due to differences in sample processing. As infected and control tissues for each cohort were processed at the same time, fluorescence values per 100 mg of tissue were normalised to the control mean to allow comparison between cohorts

The normalise HPLC data revealed a significant 2.4-fold increase in brain tryptophan levels for the infected cohort (Figure 3.3 panel 1A) as compared with the control group at day 7 post infection ($n = 9$, $p \leq 0.001$). By contrast, a significant 1.7-fold decrease in tryptophan levels in the infected cohort at both day 14 ($n = 10$, $p \leq 0.01$) and a significant 1.8-fold decrease at day 22 ($n = 12$, $p \leq 0.001$) post infection was found compared to the relevant control group (Figure 3.3 panels 2A and 3A respectively).

To verify the identity of the peak assigned as tryptophan during HPLC analysis, LC-MS/MS analysis was conducted on the same sample to independently determine

tryptophan levels from the brain samples of day 14 and day 22 infected animals. MS data was normalised to both tissue weight and the internal tryptophan standard 5-Methoxy-DL-tryptophan. Diversity between animals in the same cohort was again observed (Figure 3.4 panel 1B, Figure 3.5 panel 1B), although the variation between technical triplicates is in some cases as large as the variation between biological replicates. Differences between absolute tryptophan levels recorded for the control group animals across the different cohorts was also observed (Figure 3.4 and 3.5 panel B), as previously, so the data was again normalised to the control mean to allow comparison between cohorts.

There was no significant difference between tryptophan levels observed between infected and control animals at day 14 when using MS analysis and when normalising the tryptophan concentration to the internal tryptophan standard (units per kilogram of brain tissue) ($p = 0.472$, Figure 3.4 panel 1A). Conversely, the MS data from the day 22 cohort corroborated the LC data, with a significant 1.7-fold decrease of tryptophan observed for the infected brains in comparison to the non-infected controls. This was found when data was normalised to the internal tryptophan standard ($p \leq 0.001$) (Figure 3.5 panel 1A). The different outcomes in tryptophan levels at day 14 when comparing HPLC and LC-MS/MS may be down to using two different analytical systems with inherent variations in analysis, having a lower number of samples for the LC-MS/MS run due to loss of samples during sample preparation or perhaps down to LC-MS/MS providing slightly higher sensitivity and specificity.

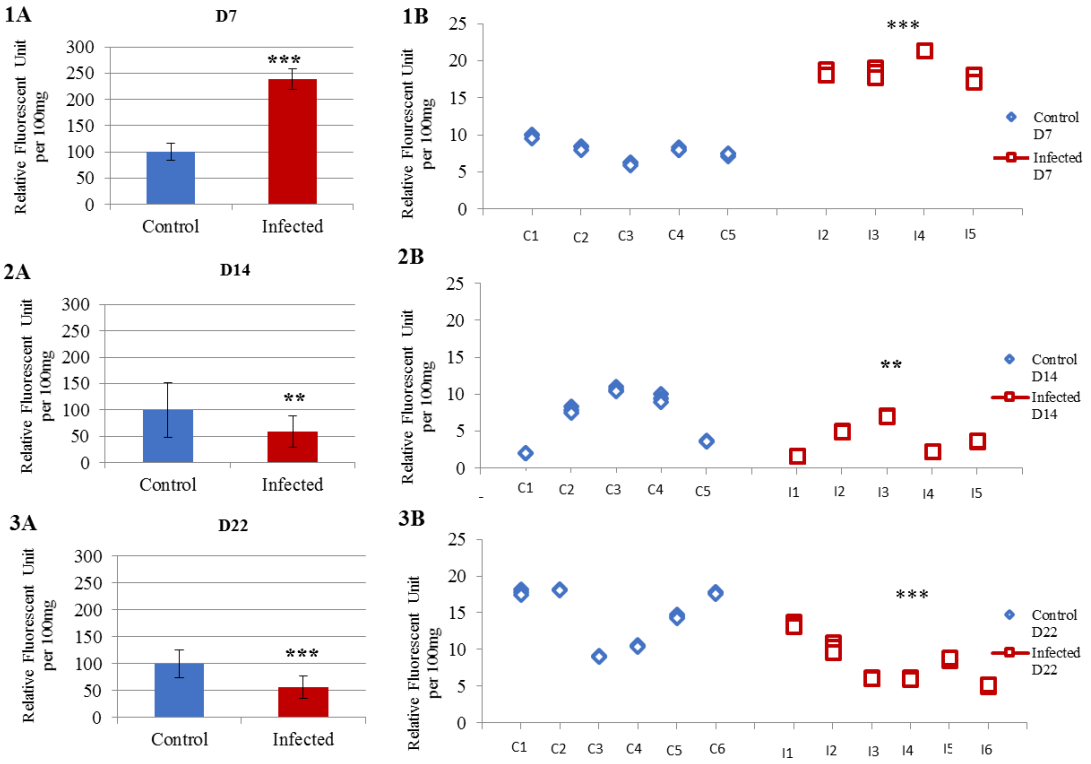

Figure 3.3 Tryptophan levels in the brain show a biphasic response during Trypanosome infection: HPLC quantification

HPLC data showing tryptophan levels for trypanosome-infected brain tissue from CD-1 mice. Data was analysed per 100mg of tissue and normalised to the control group mean. HPLC data is shown for day 7 post infection (n = 4 infected, n= 5 non-infected control) (1A), for day 14 post infection (n= 5 infected, n= 5 non-infected control) (2A) and for day 22 post infection (n= 6 infected, n= 6 non-infected control) (3A)). Scatter graphs depict the intra- animal and technical replicate variability in tryptophan levels within the cohorts of animals when data is normalised per 100mg of tissue (1B-3B). Samples were injected in triplicate and statistically analysed using an unpaired two-tailed Student's *t* test. ** denotes $p \leq 0.01$ and *** $p \leq 0.001$ significant differences from non-infected control**.**

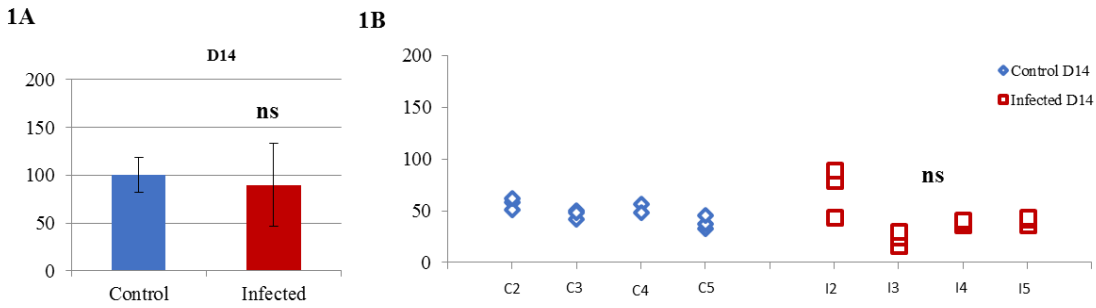

Figure 3.4 Mass Spectrometry data for brain tissue at day 14 post infection

Mass Spectrometry (MS) data showing tryptophan levels for Trypanosome-infected brain tissue from CD-1 mice (n = 4 infected, n= 4 non-infected control). Data was normalised to the internal standard per kilogram of brain tissue, and the mean of the control group (1A). Scatter graphs show the intra- animal and technical replicate variability in tryptophan levels within the cohorts of animals when data is normalised per kilogram of tissue to the internal standard (1B). Samples were injected in triplicate and statistically analysed using an unpaired two-tailed Student's *t* test. ** denotes $p \leq 0.01$ and *** denotes $p \leq 0.001$ significant differences from non-infected control. **NS** denotes no statistical significance.

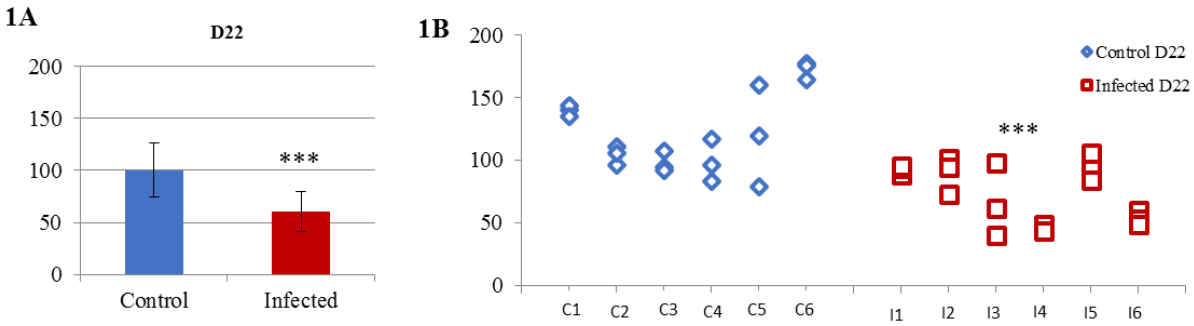

Figure 3.5 Mass Spectrometry data for brain tissue at day 22 post infection

Mass Spectrometry (MS) data showing tryptophan levels for Trypanosome-infected brain tissue from CD-1 mice (n = 6 infected, n= 6 non-infected control). Data was normalised to the internal standard per kilogram of brain tissue, and the mean of the control group (1A). Scatter graphs showing the intra- animal and technical replicate variability in tryptophan levels within the cohorts of animals when data is normalised per kilogram of tissue to the internal standard (1B). Samples were injected in triplicate and statistically analysed using an unpaired two-tailed Student's *t* test. ** denotes $p \leq 0.01$ and *** denotes $p \leq 0.001$ significant differences from non-infected control.

3.5.4 Impact of infection on tryptophan levels in the spleen, muscle and liver

HPLC was used to analyse the tryptophan profile of Trypanosome infected CD-1 rodent tissue identified as having high levels of parasitemia such as the spleen, muscle and liver across all three time-points (Chapter 2). This work aimed to ascertain whether the tryptophan alterations observed in our study were brain specific or reflecting a more general system wide perturbation. At early stage infection (Day 7 post- infection), HPLC analysis revealed no significant difference in the levels of tryptophan in the spleen ($p = 0.245$) and muscle ($p = 0.178$) recovered from infected as compared to control rodents (Figure 3.6, panels 1A and 1B). However, tryptophan levels in the liver from infected animals at day 7 were significantly higher ($p = 0.003$) than that seen in control animals (Figure 3.6, panel 1C), with a 1.9-fold increase.

At day 14 of infection, no significant difference in tryptophan levels was found for any of the three tissues types (spleen $p = 0.237$; muscle $p = 0.719$; liver $p = 0.401$ (Figure 3.6, panel 2A-2C).

At late stage II infection (Day 22 post-infection), HPLC analysis revealed the spleen ($p = 0.0198$), muscle ($p = 0.001$) and liver ($p = 0.0007$) of infected rodents to have significantly elevated levels of tryptophan as compared with that seen in control, non-infected animals (Figure 3.6, panel 3A-3C), with respective fold changes of 1.3, 2.3 and 1.9.

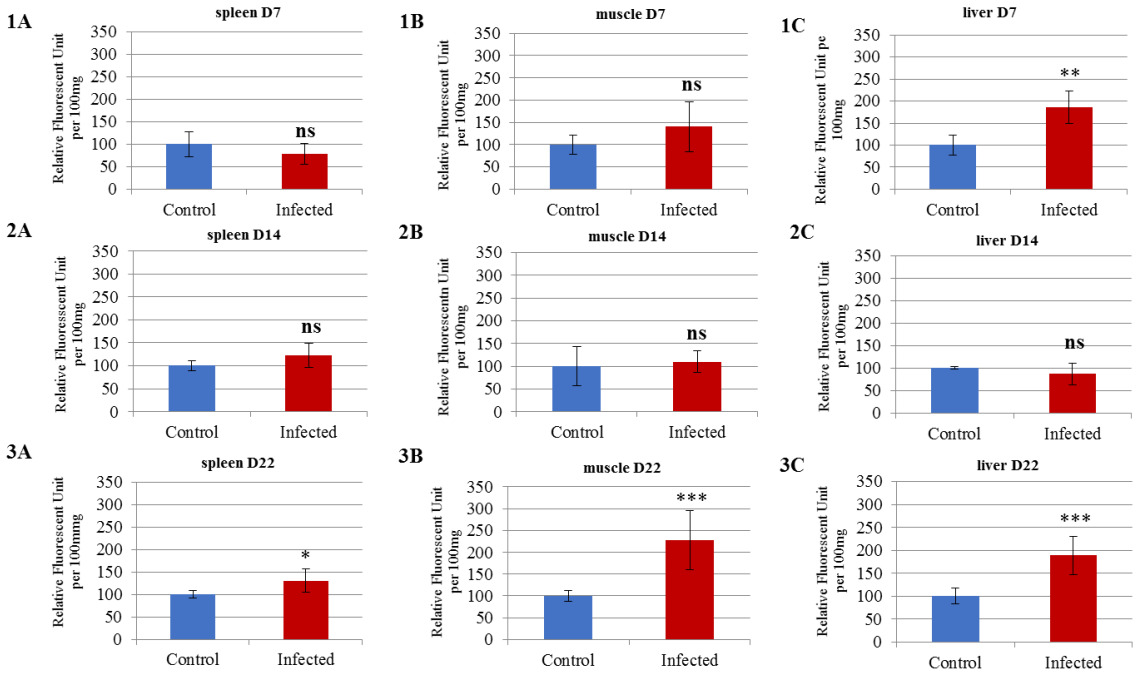

Figure 3.6 Tryptophan levels in the spleen, muscle and liver tissue at day 7, 14 and 22 post infection

HPLC analysis of tryptophan levels in Trypanosome-infected spleen, muscle and liver tissue from CD-1 mice. Data is at day 7 (n = 4 infected, n= 5 on-infected control) (1A-1C), day 14 (n= 5 infected, n= 5 non-infected control) (2A-2C) and day 22 (n= 6 infected, n= 6 non-infected control) (3A-3C) post infection. Samples were injected in triplicate, normalised per 100 mg of tissue, and then normalised to the control group mean and statistically analysed using an unpaired two-tailed Student's *t* test. * denotes $p \leq 0.05$, ** denotes $p \leq 0.01$ and *** denotes $p \leq 0.001$. **NS** denotes no statistical significance.

3.5.5 Late stage II infection reveals elevated levels of tryptophan in the distal colon

Parasite localisation and imaging data (Chapter 2) guided our study towards investigating the level of tryptophan of the small intestine (SI) and distal colon (COL) at late stage II infection (22 days post-infection). Here the small intestine and colon were dissected *ex vivo* mechanically using cell scrapers to isolate the mucus layer and tissue, discarding the faecal matter.

In our study, HPLC analysis revealed there to be no significant difference in the levels of tryptophan found in the mucus layer of the small intestine between infected and control animals at day 22 of infection (Figure 3.7 panel 1A). This was also found to be the case when the small intestine tissue was isolated and analysed independently (Figure 3.7 panel 1B). Interestingly, at late stage infection the colon mucus layer as well as the colon tissue itself was found to have significantly higher levels of tryptophan as compared with that in control, non-infected animals (Figure 3.7 panels 2A, 2B). A significant 1.4-fold increase was found for the colon mucus and a 2.8-fold increase for the colon tissue.

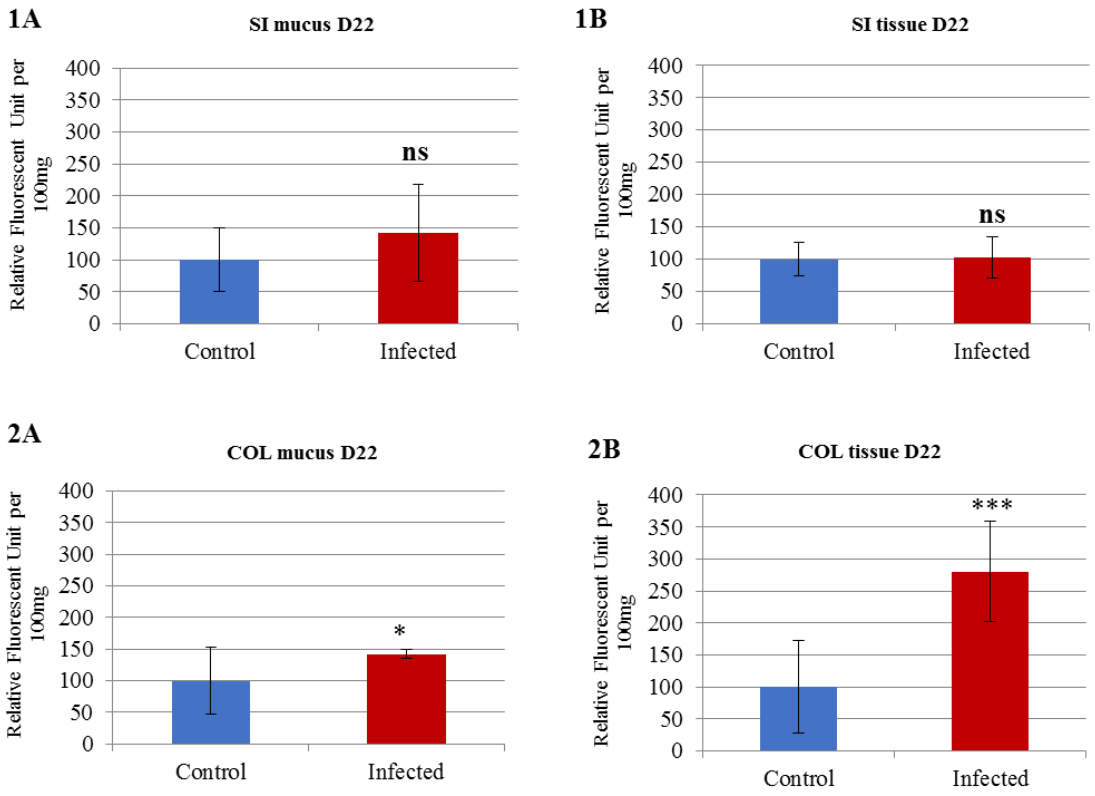

Figure 3.7 HPLC data normalised per 100mg of the small intestine and colon at day 22 post infection

HPLC data showing tryptophan levels for Trypanosome-infected and control mice in the small intestine (SI) and distal colon (COL). HPLC data is shown for small intestine mucus (1A), small intestine tissue (1B), colon mucus (2A) and colon tissue (2B) at day 22 post infection (n = 3 infected, n= 3 non-infected control). Samples were injected in triplicate, normalised per 100 mg of tissue, then normalised to the control group mean and statistically analysed using an unpaired two-tailed Student's t-test. * denotes $p \leq 0.05$ and *** denotes $p \leq 0.001$. **NS** denotes no statistical significance.

3.6 Summary

Table 3.2 Summary Table

Tissue	HPLC Tryptophan Levels for Infected Tissue		
	D7	D14	D22
Brain	↑2.4^{x}	↓ 1.7^{x}	↓1.8^{x}
Spleen	**ns**	**ns**	↑1.3^{x}
Muscle	**ns**	**ns**	↑2.3^{x}
Liver	↑1.9^{x}	**ns**	↑1.9^{x}
Small Intestine			**ns**
Small Intestine Mucus			**ns**
Colon			↑1.4^{x}
Colon Mucus			↑2.8^{x}

A summary table of the HPLC tryptophan data for various tissues types from *Trypanosoma brucei* CD-1 infected mice. At day 7 post infection, tryptophan levels in the brains of infected mice were significantly higher when compared with controls. At late stage infection (day 14 and day 22), tryptophan levels are significantly reduced in the brains of infected animals. HPLC analysis of other tissues such as the spleen, muscle and liver with known parasite infection revealed significantly elevated levels of tryptophan at late stage infection. This was also found at day 7 post infection for the liver. Interestingly at day 22 post infection, the distal colon and the mucus layer from the colon had significantly higher concentrations of tryptophan as compared with the control. Small intestine and colon data is not shown for D7 & D14, as we decided to focus on late stage II disease and the potential effects on the gut tryptophan levels.

3.7 Discussion

HPLC/MS analysis aims to identify and quantify low molecular weight chemicals within a defined biological sample (316). There has been a tradition of metabolic research on the pathogens of the Kinetoplastida order (317–321). However the development of metabolomics technology to facilitate our understanding of the neuropsychopathology underlining stage II Trypanosomiasis is lacking (144). In this way, the work presented in this chapter aimed to investigate the impact of stage II *Trypanosoma brucei brucei* infection on tryptophan and its metabolites in rodent brain tissue using a High-Pressure Liquid Chromatography-Mass Spectrometry (LC-MS/MS) system. Based on bioluminescent localisation data (see Chapter 2), the impact of infection on tryptophan levels in other body tissue types such as the spleen, liver, muscle and gastrointestinal organs with high parasitemia was also of interest. There were four main findings from our work: (A) Increased brain tryptophan levels at early stage Trypanosomiasis infection was observed, (B) By contrast, animals at late stage II infection had decreased levels of cerebral tryptophan, (C) Elevated tryptophan levels in the spleen, muscle and liver are evident at late stage II infection, and (D) Increased tryptophan levels are also present in the distal colon at late stage II infection.

3.7.1 Increased brain tryptophan levels at early stage Trypanosomiasis infection

The impact of Trypanosomiasis infection on brain tryptophan levels was first investigated by examining samples from early stage, 7 days post-infection rodent brain tissues. Based on the existing literature, central nervous system (CNS) invasion by the pathogen does not occur until approximately 14-21 days post infection (322) and so these animals represented the systemic haemolymphatic stage of infection. In the CNS both fates of tryptophan, which acts as a precursor to both kynurenine and serotonin

synthesis, are of interest given the role of the metabolites in the pathomechanism of neuroinflammatory and neurodegenerative disorders (306,323–325). Our HPLC data revealed significantly increased levels of brain tryptophan for the infected cohort at day 7 post-infection, suggesting that perturbed metabolism of this essential amino acid occurs in the brain before parasite entry into the brain parenchyma. Over-activation of the tryptophan-kynurenine pathway (TRYP-KYN) has previously been reported to lead to immune system activation and leads to the accumulation of potentially neurotoxic compounds (326). Previous studies have shown that acute stress and infection influence tryptophan influx into the brain, resulting in an increase in brain tryptophan availability (327). The authors in the same review mention that although the exact mechanisms behind this stress-induced increase in brain tryptophan is no entirely understood, stress, infections and changes in the gut microbiome have all been shown to direct available tryptophan towards the kynurenine pathway thus reducing 5-hydroxytryptamine (serotonin) synthesis (328,329). Acute stress and its influence on increased brain tryptophan concentrations may in part be due to sympathetic nervous system activation and increased levels of circulating catecholamines (330). Here activation results in increased permeability of the blood-brain barrier (BBB), which may represent another mechanism by which increased brain tryptophan levels occurs (331). In terms of the behavioural effects of elevated brain tryptophan, studies have demonstrated a relationship between dietary tryptophan levels and aggression, whereby tryptophan supplementation induced a dose dependant effect on aggressive responses in humans, rats and birds (332–336). We did not characterise levels of aggression in this study but testing this in future experiments would be of potential interest.

In humans and rats, manipulating dietary tryptophan has been shown to influence tryptophan availability to the brain (337,338). The amount of tryptophan entering the brain depends on levels of plasma tryptophan in relation to other large neutral amino acids or LNAA' such as valine, tyrosine and methionine which enter the brain through a common transporter protein (327,339). Here dietary carbohydrates, in contrast to dietary protein, are able to significantly increase brain tryptophan levels due to the action of elevated circulating insulin levels that increase the tryptophan/LNAA ratio and in turn increase tryptophan influx into the brain (340). The potential clinical relevance of dietary tryptophan availability on tryptophan levels in the brain at early stage human Trypanosomiasis infection is not currently understood. Most individuals subject to the disease are from remote rural areas, and are often malnourished and impoverished (341). Afflicted with food insecurity and other socio-economic burdens mean that those individual are dependent on subsistence agriculture with little scope on diverse food choice (342). In the case of our study however, perhaps the nutritious content of the food provided to the experimental rodents has a minor influence on the data recorded. Further testing may be able to define the relationship between dietary tryptophan availability and the brain changes in tryptophan that results from infection.

3.7.2 Animals at late stage II infection have decreased levels of cerebral tryptophan

It has been well established in previously published data that *Trypanosoma brucei gambiense* significantly deplete tryptophan in both *in vivo* and *in vitro* settings (188,189), with this also shown to be true in cases of stage II clinical samples (6). Based on this rationale, we wanted to investigate brain specific tryptophan levels at stage II Trypanosomiasis. HPLC-MS analysis was used to investigate tryptophan concentrations of samples from day 14 and day 22 post-infection rodent brain tissues.

Our liquid chromatography (LC) results revealed that tryptophan was significantly increased in animals on day 7 of infection but decreased in the brains of mice at both day 14 and 22 post-infection, whilst MS corroborated our findings for the day 22 cohort.

Perturbations to the tryptophan-kynurenine and tryptophan-serotonin pathway have both been implicated in the neuropathogenesis of psychiatric disorders such as schizophrenia (343) and bipolar disorder (344), and so we were interested in correlating potential imbalances in the tryptophan levels of infected animals to any behavioural phenotypes observed in our animal behaviour studies (see Chapter 4). It has long been reported that tryptophan depletion can trigger a depressive episode in humans (345) amongst other effects, and can produce a profound change in mood even in healthy individuals (201). Further, since approximately 95% of tryptophan is metabolised towards the kynurenine pathway (346), depletion of tryptophan results in the reduction of kynurenine metabolites. In the case of schizophrenia, it has been reported that patients had elevated kynurenine levels particularly in the prefrontal cortex, which has been associated with the "hypofrontality" phenomenon (reduced metabolic activity in this region) which can contribute to key symptoms and cognitive disturbances of this disorder (347,348). Rodents treated with neuroleptics showed a significant reduction in frontal kynurenine levels (349). Based on that, significantly depressed levels of brain tryptophan at late stage infection in our study therefore correlates with the finding of "hypofrontality" in infected brain samples observed in our functional brain imaging study (see Chapter 5). Other detrimental effects of kynurenine catabolites include activation of oxidative pathways, cause mitochondrial dysfunction and direct neurotoxic effect (350)- all of which could potentially contribute to the neuropathogenesis observed during African Trypanosomiasis. Taken together, the

ability to influence the metabolism of the kynurenine pathway towards the neuroprotective branch (i.e. towards kynurenic acid rather than kynurenine synthesis) may be a potential option for ameliorating the symptoms of some psychiatric disorders and may have relevance to the psychiatric symptoms seen in HAT. Our aim is to springboard further discussion on the interplay between metabolomics and neuropsychiatric symptomology observed in cases of infectious disease based on the findings presented herein. Expansion of our work should include further research looking exclusively at the kynurenine levels in the brains of Trypanosome-infected rodents to decipher whether changes in the concentration levels of kynurenine can shift the balance towards non-pathological conditions.

Reduced availability of brain tryptophan also means that there is less substrate for the synthesis of serotonin, which is crucial for healthy cognitive function (351). Reduced serotonin concentrations have been implicated in the pathogenesis of depression (352), perturbed emotional processing in memory and attention (353), and cognitive inflexibility (354). Although our behavioural studies revealed no significant differences in terms of anxiety-like states or memory consolidation in our infected cohort (see Chapter 5), perhaps future work focusing exclusively on serotonin depletion in Trypanosomiasis and cognitive behavioural testing is warranted. This would help us better understand how serotonin depletion may or may not contribute to the neuropsychiatric symptoms of HAT.

In terms of other infectious diseases, in Chagas disease caused by *Trypanosoma cruzi* for example, increased kynurenine is seen in patients and this was also found to correlate with disease severity (355). Indoleamine-2, 3-dioxygenase (IDO), the enzyme involved in the first step of tryptophan catabolism, has also been shown to dampen

protective host immunity, indirectly leading to increased pathogen burden as in the case of *Toxoplasma gondii* replication in the lung (356). Here, cell activated-immune responses via the effect of Interferon gamma (IFN- γ) induces the expression of IDO enzyme, and begins the process of enhanced tryptophan catabolism (357). There is a growing body of research investigating the link between metabolism and immune responses and their relationship to disease outcome, with the aim of unravelling novel biochemical pathways susceptible to clinical management (358). In terms of tryptophan depletion, effector T- cells are sensitive to depressed tryptophan concentrations in the microenvironment, resulting in T-cell anergy and apoptosis (359). The general control non-derepressible-2 kinase (GCN2) detects the depletion of tryptophan, and its activation elicits a stress-response programme resulting in cell-cycle arrest and apoptosis (359). Further the direct interaction between kynurenine and the aryl hydrocarbon receptor (AHR) has been shown to generate regulatory T-cells from T-helper cells (360). AHR is a transcription factor that has been known to cause immunosuppression following binding to dioxin, which does not occur until kynurenine activates AHR (361). Thus the depletion of tryptophan and subsequent accumulation of immunosuppressive tryptophan catabolites acts to suppress antigen-specific T-cell responses, and induces the formation of regulatory T-cell which provides a more regulatory immune environment. This may provide a potential explanation for the interplay between perturbed brain tryptophan levels and neuropathogenesis observed at late stage African Trypanosomiasis, given the decreased tryptophan levels seen in the brain at later stages of infection.

3.7.3 Elevated tryptophan levels in the spleen, muscle and liver at late stage II infection

The impact of Trypanosomiasis infection on brain tryptophan levels was first investigated by examining samples from early stage and late stage infected rodent brain tissues. Following on from our brain tryptophan findings, we wanted to investigate whether our results were brain specific or more reflective of a whole system metabolomic profile. We decided to use HPLC to analyse the tryptophan levels for the spleen, muscle, liver and gut due to them being identified as tissue with high parasitemia (see Chapter 2). Our aim was to decipher whether the tryptophan perturbations recorded were tissue specific (i.e. to the brain) or more related to general tissue parasitemia. Our LC data revealed that at late stage infection (22 days post-infection) the spleen, muscle and liver tissue had significantly elevated tryptophan concentrations as compared with the control tissues. Interestingly no significant difference was found for the samples at day 14 or 7 post-infection; significance was limited to the liver in animals 7 days after infection.

Tryptophan-2, 3-dioxygenase (TDO), along with IDO, is involved in the first step of tryptophan catabolism and is expressed at high levels in the liver (362). TDO, unlike IDO, is not induced by signalling from the immune system but is regulated by glucocorticoids and has been shown to have a key role in regulating systemic tryptophan levels (363). TDO acts as a house-keeping enzyme, keeping systemic levels of tryptophan constant by shunting tryptophan to the Krebs cycle or to nicotinamide synthesis in the case of tryptophan overload, or the need of direct energy (364). Interestingly increased TDO expression has been found in the anterior cingulate cortex from individuals with schizophrenia (262), with the authors suggesting an involvement of the kynurenine pathway in the pathogenesis of the disease (261). Rats treated with the glucocorticoid dexamethasone had increased liver TDO activity, and consequently

reduced tryptophan levels in the liver, serum and brain (365). On the other hand, studies using TDO -/- knockout mice revealed that the knockout mice had a 10-fold increase in the plasma concentration of tryptophan (366). Authors from the same study also found TDO ablation resulted in the increase of tryptophan and serotonin in the brain, and as such proposed TDO as a modulator of anxiety-like behaviour, as supported by their observation of increased anxiety-like behaviour in TDO -/- mice. Therefore, further studies are therefore warranted to explore the potential involvement of TDO dysfunction as a consequence of Trypanosome infection. For example, quantitative endpoint RT-qPCR can be used to measure mRNA transcripts, to compare the TDO expression in the liver and brains of infected and control animals to see if expression correlates with the metabolomics data. It also important to note however that all our experimental rodents were female, with some data suggesting that liver TDO activity is greater in females compared to males (367) conjuring the hypothesis that there may be a gender related difference in tryptophan turnover by TDO.

Numerous well established studies have explored the relationship between tryptophan catabolism in the lymphoid tissues following inflammatory assault (273,368,369). Traditionally during inflammation, activity of TDO decreases and IDO is induced in extra hepatic sites for tryptophan degradation, with the substantial formation of the kynurenine downstream metabolite quinolinic acid occurring in the select lymphoid regions such as the spleen (370). Indeed outside of the placenta, functional IDO expression was reported to be highest in the spleen, lymph nodes and thymus (371). To our surprise therefore, tryptophan levels were found to be significantly elevated in the spleen exclusively at late stage II Trypanosomiasis, rather than decreased as initially postulated based on the literature. He et al (372) analysed the transcriptome of global

changes in cytokine expression in mouse spleens following *T. gondii* infection, and revealed that although IFN- γ- induced IDO was upregulated, most differentially expressed genes involved in tryptophan metabolism pathway were downregulated. Further Drewes et al (373) reported that following simian immunodeficiency virus (SIV) infection of pigtailed macaques, tryptophan levels were stable in tissues sites such as the spleen despite robust depletion in the circulating plasma and CSF. The authors suggested that their findings reveal insights into tissue-specific mechanisms by which cells seek to prevent tryptophan starvation during inflammation. For example it is known that IFN-γ, a major inducer of IDO, also upregulates tryptophanyl-tRNA synthetase (TTS) – an enzyme which catalyzes the ligation of intracellular tryptophan to its cognate tRNA during translation (374,375). Thus cells expose to IFN-γ may maintain or even accumulate intracellular levels of tryptophan-tRNA, protecting them from GCN2 Kinase mediated anergy (359,376,377). Based on these findings, we posit that perhaps tryptophan levels are elevated in our study due to either the downregulation of genes required for tryptophan degradation or through the upregulation of TTS. Future work could test this hypothesis, and correlate gene expression with our metabolic data. IDO activity in the spleen of Trypanosome-infected rodents can also be characterised in future work by characterising the kynurenine to tryptophan ratio, which correlates with concentrations of the immune activation marker neopterin (378).

Tryptophan is an essential amino acid required for protein synthesis and transamination reactions, and the availability of amino acids is crucial for the regular turn-over of proteins of the muscle tissues (379). During inflammatory processes and infectious disease, metabolic changes occur which can modify this availability (380). For example, immunological stress can induce redistribution of amino acids from protein

synthesis towards tissues involved in the immune response (381). Newport et al (382) discovered that the aromatic amino acids tyrosine and tryptophan underwent the most profound drop in field voles infected with *T. b. gambiense*. Free amino acid concentrations in the skeletal muscle of voles following infection with the same pathogen was then explored further by Newport and Page (383), with authors revealing a 45% reduction of tyrosine in the muscle of infected voles. Based on these studies, we assumed tryptophan levels would be reduced in the muscle of infected animals. However, in our study late stage Trypanosomiasis infection resulted in significantly increased tryptophan concentrations of the muscle tissue. It has been proposed that acute stress (such as handling of the rodents during our behavioural studies, see Chapter 5), can increase free amino acid concentrations in muscle and liver (384). A human study demonstrated that cortisol can induce amino acid transport from the liver to the muscle when amino acids are needed during stress (385). Further Agudelo et al (386) identified a mechanism by which skeletal muscle PGC-1α1 expression induced by exercise can change tryptophan-kynurenine metabolism towards the production of the neuroprotective kynurenic acid. Here, the activation of the PGC-1α1-PPARα/δ pathway increased muscle expression of kynurenine aminotransferases, thus reducing plasma kynurenine and increasing kynurenic acid concentrations. This strategy provides a translation opportunity by which a more neuroprotective environment can be accomplished simply by exercise training. Finally, since tryptophan levels in the muscle tissue was only elevated at late stage infection, quantifying level of parasitemia and correlating that to our HPLC data would help to elucidate whether the trend is associated with parasite burden.

3.7.4 Increased tryptophan concentration in the distal colon at late stage II infection

Bioluminescent imaging data (see Chapter 2) revealed punctate parasite localisation to the gut, which appeared more pronounced at stage II infection. Following on from our tryptophan findings for the brain and other tissues types, we therefore investigated the tryptophan profile of the gut at late stage II Trypanosomiasis infection. We decided to use HPLC to analyse the tryptophan levels for the small intestine, small intestine mucus layer, distal colon and distal colon mucus layer with the aim of deciphering whether the tryptophan perturbations were correlated with parasite localisation and if this had any implicated for the brain-gut axis. Moreover, the microbiota plays a key role in the generation of tryptophan (387), so the modification of the gut microbiome of gut function by Trypanosomiasis infection could contribute to alterations in tissue tryptophan levels during the modification of the amino acid availability from the gut. The mucus layer was isolated for autonomous analysis due to it representing the bacterial colonies of the gut. Our LC data revealed at late stage infection, tryptophan concentrations were significantly elevated in the infected distal colon as well as in the distal colon mucus layer.

A growing body of research and data is emerging, whereby the impact of tryptophan metabolism and the serotonergic system is being implicated in the regulation of the brain and host behaviour by the gut microbiome (329). Research in this area is based on the principles of the bidirectional communication network between the brain and the gut, the so called brain-gut axis (388). Here, serotonin synthesis via tryptophan metabolism is established as the key signalling molecule in both the enteric nervous system and the central nervous system (389). Taken together, it has been theorised that the gut microbiota can directly or indirectly recruit tryptophan metabolism, and in turn influence serotonergic signalling to modulate host behaviour via the gut-brain axis

(390). For example germ-free animals raised in a sterile environment have demonstrated increased plasma tryptophan concentrations which can be successfully normalised following microbiota colonisation of the mice (391). Other groups have also reported elevations in both plasma levels of tryptophan and serotonin in germ-free mice compared to their control counter parts (392). Following chronic gastrointestinal inflammation induced by *Trichuris muris* infection of mice, an increase in circulating kynurenine as well as in the kynurenine: tryptophan ratio was observed (393). Importantly however, the gut microbiota has also been shown to directly utilise tryptophan and in turn influence its availability for the host (394). Unlike eukaryotes, certain bacterial strains possess a tryptophase enzyme that produces indole from tryptophan (395,396). This enzymatic activity found in *Bacteroides fragilis* has been linked to gastrointestinal abnormalities in autism spectrum disorder (397). It is important to note that further work remains necessary to explore the impact of different mouse strains, potential species-specific serotonergic profiles as well as any sex-dependent alterations.

The immune system also plays an important role in the signalling pathway of the gut-brain axis (398). Indeed, gut associated lymphoid tissue is dependent on the microbiota for development (399). More specifically in relation to tryptophan metabolism and inflammation, enterochromaffin cells (which produce gut serotonin) have been shown to be in close contact with $CD3^+$ and $CD20^+$ rat lymphocytes, suggesting a direct interaction between these gut and immune system cells (400). In cases of inflammatory gastrointestinal disorders, the role of serotonin in the immune system is becoming increasingly significant in the pathogenesis of the disease (401). Infection induced inflammation in the colon of animal models also shows increased enterochromaffin cell

numbers and subsequent increase in serotonin levels (402). Taken together, these studies underline the critical role played by serotonin in gastrointestinal inflammation, and the modulation of serotonergic signalling in the gut-brain axis during infection.

It would have been beneficial therefore, if our data revealed what, if any serotonin perturbations were happening in the gut in tandem with progressing disease pathogenesis. Further since approximately 80% of serotonin is produced in the gut by enterochromaffin cells (200,403), future work expanding on our findings could make use of gut tissue staining to investigate whether any changes in cell number or morphology is correlated with HPLC data and Trypanosomiasis disease progression. Nonetheless, based on the literature we theorise that perhaps due to inflammation of the gut induced by Trypanosomiasis infection, the microbiome of the gut is adversely affected as seen for other diseases (404). In turn the normal healthy microbiota may no longer utilise the available tryptophan, and thus we see an increase in the levels of tryptophan. This could be investigated experimentally through the study of the gut microbiome in infected animals, with significant implications for the animal form of the disease Nagana. Alternatively due to the compromised gut architecture, the gut may have become more "leaky" and so cannot successfully absorb the available tryptophan for serotonin synthesis- although we did not see any significant changes in the small intestine. Characterisation of gut morphology and structure may be able to provide more insight into the potential contribution of this mechanism.

3.8 Methods

3.8.1 Materials and reagents

Tryptophan, 5-hydroxytryptamine (serotonin), 5-hydroxytryptophan (5-HT), 5-hydroxyindoleacetic acid (5-HIAA), kynurenine (KYN), kynurenic acid (KYNA), acetonitrile, trifluoroacetic acid (TFA) and chloroform were purchased from Sigma-Aldrich (UK).

3.8.2 Murine tissue preparation for HPLC and LC-MS/MS analysis

To acquire infected and control murine tissues for HPLC/MS analysis, *in vivo* Trypanosomiasis infections were established (see Chapter 2). At day 7 (n = 4 infected, n = 5 non-infected control), day 14 (n = 5 infected, n = 5 non-infected control) and day 22 (n = 6 infected, n = 6 non-infected control) post infection, animals were sacrificed and the brain, spleen, muscle, liver and gastrointestinal tissues harvested, snap frozen in ice cold isopentane (-40 ^{0}C) and stored at -80 ^{0}C until further use.

To prepare for HPLC/MS experiments tissues were defrosted, weighed and homogenised using zirconium beads (BeadBug™ prefilled tubes, Sigma Aldrich). Body tissues were placed in tubes containing the beads along with 1 ml of molecular grade water and broken up using a high-speed mechanical tissue homogenizer (FisherScientific, UK). Zirconium bead tubes were then centrifuged at 15,000 x g at 4 ^{0}C for 10 min to isolate the homogenized material after which an established acetonitrile/chloroform extraction procedure by Lesniak *et al* (315) was employed. To ensure consistency, the same tissue types from animals from the same cohort (i.e. all day 7 animal brain tissues) were processed at the same time. Processed samples were lyophilised and stored at -80 ^{0}C until further use.

3.8.3 High-Pressure Liquid Chromatography (HPLC)

For HPLC analysis an established protocol was followed (315), and samples were analysed using an Agilent Technologies 1260 Infinity II (Böblingen, Germany) HPLC equipped with UV and fluorescence detectors. Samples were run on a TSKgel ODS-80TS column (0.5 µm, 4.6 x 250 mm, Tosoh Bioscience LLC) with 0.1% TFA in H_20: ACN 90:10 *v/v* at a flow rate of 0.8 ml/min. The column was kept at 25 ^{0}C.

All processed and lyophilized samples were dissolved in 1 ml of the mobile phase (0.1% TFA in H_20:ACN 90:10 *v/v*). Triplicate technical injections of 100 µl for each biological sample were analysed. To compare between control and infected animals, tissues from the same post-infection time-point were run on the same day as one batch to reduce batch to batch variability.

The fluorescence detectors were set at the following channels: for analysis of tryptophan (λ_{Ex}) excitation at 297 nm and (λ_{Em}) emission at 348 nm, with UV wavelengths set at 220nm, 280nm, 330nm and 364nm. The retention time (RT) for tryptophan in this study was 30.7 minutes.

The RT for each analyte was obtained by injecting commercial standards into the HPLC for use as reference for the quantification of metabolite in the various tissue types (see Table 3.1).

3.8.4 Liquid Chromatography- Tandem Mass Spectrometry (LC-MS/MS)

A Waters Atlantis T3 (2.1 x 150-mm i.d., 3µm) reversed-phase column with mobile phases A (0.1% *v/v* formic acid in water) and B (0.1% *v/v* formic acid in acetonitrile) was used on the Shimadzu LCMS-8040 instrument. The column was kept at 35 ^{0}C. A linear gradient was used for the chromatographic separation of the analytes as previously described (405). In brief, the gradient was as follows: 0-10 min linear increase from 0% to 40% B, 10-12 min from 40% to 95% B, 12-17 min hold at 95% B, 17-20 min from 95% to 0% B. The flow rate was 0.4 ml/min. All analytes were detected in positive ion multiple reaction monitoring (MRM) mode. For MRM parameters see table 3.3 with data taken from Zhu *et al* (405).

For the analysis of samples, lyophilized material was dissolved in 100 µl of mobile phase B (0.1% formic acid in acetonitrile, *v/v*). 10 µl of the internal standard 5-Methoxy-DL-tryptophan (1 mg/ml) was added to the recuperated biological samples for each run (total volume of 110 µl for each sample in microvolume tubes). Triplicate technical injections of 15 µl for each biological sample were performed. To compare between control and infected animals, tissues from the same infection time-point were run on the same day as one batch to reduce batch to batch variability.

3.8.5 Statistical Analysis

All statistical analysis was undertaken using an unpaired two-tailed Student's t-test. Significance was set at * $p \leq 0.05$ throughout.

3.8.6 Data Analysis

Data was first analysed per 100mg of tissue and then normalised to the control group mean for each respective time-point. In this way the area under the peak was recorded for each tissue and normalised to a 100mg of tissue depending on the original recorded weight. Then, all the analysed data points were normalised to the control group mean so as to make the control group mean 100%. For the MS data, after normalisation per kilogram of brain tissue, data was also normalised to the internal 5-Methoxy-DL-tryptophan standard.

3.8.7 Software

BioInert Software on the 1260 Infinity II LC System was used for data collection. LabSolutions LCMS Version 5 integrated workstation software was used for data collection on the Shimadzu system.

Table 3.3 List of chromatographic RT and selected MRM parameters for each analyte

Analyte	RT (min)	Q1 Mass	Q3 Mass
Tryptophan	7.122	205.1	118.1
Serotonin	5.303	177.2	160.0
5-Hydroxytryptophan	5.599	-	-
5-Hydroxy-indole-3-acetic acid	8.212	192.2	146.0
Kynurenine	5.563	209.1	192.0
Kynurenic Acid	7.858	190.2	144.0
Tryptophol	11.565	-	-
5-Methoxy-DL-tryptophan	7.5	-	-
Indole-3-lactic acid	10.5	206.2	130.0

A table detailing the chromatographic properties of analytes investigated in this study for the quantitative profiling of tryptophan and its metabolites by LC-MS. Q1 and Q3 mass data was taken from Zhu et al (405).

Chapter 4.0 Trypanosomiasis infection impacts on locomotion but not novel object recognition behaviour

4.1 Introduction

The Open Field Test (OFT) involves measuring parameters such as walking distance, velocity, duration and frequency as a test for locomotor activity (406). In addition, analysis of centre zone duration and frequency of visits to the central zone are used to test for anxiety-like behaviours. In general, rodents prefer to spend more time at the perimeter of arenas as compared to the centre, a phenomenon known as Thigmotaxis whereby a preference towards physical contact with the arena wall is observed (407). Therefore, changes in this natural behaviour (spending more or less time in the centre of the arena) can provide a proxy measure of the animal's anxiety like-behaviour. Here, the OFT is used to assess infected rodent ambulation levels which may be useful in indicating the neurological decline associated with Trypanosomiasis, with the first noticeable symptoms being abnormal gait and loss of motor function in humans (144). Analysis of behaviour in the OFT may provide a more robust approach to determining the impact of Trypanosomiasis on locomotor function than direct observation and thus determine effects at earlier time points during infection.

The Novel Object Task (NORT) is used to investigate learning and memory (408), based on the observation that mice naturally exhibit a preference towards exploring novel objects rather than familiar objects (409). The task therefore takes advantage of this by initially presenting the mouse with two identical objects (acquisition phase), followed by the testing period in which the mouse is presented with one "familiar" object (from the acquisition phase) and one novel object. If a mouse investigates the novel object for a longer duration or more frequently than the familiar object, it can be

inferred that the mouse has learned and formed a memory of the original, "familiar" object. During the NORT different inter-trial intervals (ITIs) can be applied, between the acquisition and test phase, to probe short and long-term memory.

4.2 Research objectives

i. To determine impact of Trypanosome infection on locomotion and anxiety-like behaviour at different stages of infection using the OFT.
ii. To investigate the effect of late stage *Trypanosomiasis* infection on short-term and long-term memory using the NORT.

4.3 Methods Summary

The OFT was used to measure the response of female CD-1 Trypanosome infected mice to a novel environment. The NORT was used to test short-term recognition; learning and memory (1 hour ITI) and long-term recognition memory (24 hour ITI) in female CD-1 Trypanosome infected mice.

4.4 Summary of findings

1. At late, but not early, stage of infection Trypanosome infection induces hypolocomotion in a novel OFT environment.
2. Trypanosome infected CD-1 mice show a reduction in exploratory behaviour in the OFT
3. Anxiety-like behaviour is not altered in Trypanosome infected CD-1 mice in the OFT
4. Late stage Trypanosome infection does not impact on short or long-term memory in female CD-1 mice, assessed using the NORT.

4.5 Results

4.5.1 Trypanosome infected CD-1 mice show hypolocomotion in a OFT novel environment at later stages of infection

CD-1 Trypanosome infected mice showed reduced locomotor activity in comparison to (non-infected) control mice at late stages of the infection. Infection status significantly impacted on velocity of movement at infection day 12[$F_{(1,8)} = 5.489$, $p = 0.047$] and 20 [$F_{(1,1)} = 26.217$, $p \leq 0.001$] but not at day 5 [$F_{(1,7)} = 0.776$, $p = 0.407$] as illustrated in figure 4.1, with Trypanosome infected mice being significantly slower than non-infected controls at day 12 and 20 of infection. Similar effects were observed when analysing distance moved. While there was no significant difference between infected and non-infected mice in terms of distance moved on day 5 of infection [$F_{(1,7)} = 0.379$, $p = 0.558$] there was a strong statistical trend towards reduced distance moved in infected animals on day 12 of infection [$F_{(1,8)} = 5.09$, $p = 0.054$] and infected mice at day 20 showed a significant reduction in distance moved during the experiment [$F_{(1,1)} = 24.99$, $p \leq 0.001$]. Taken together, these data show that at later stages of infection, mice moved slower and covered an overall shorter distance during the test than non-infected controls.

For all data sets, when velocity and distance data were statistically analysed over the 15 minute time frame (using repeated measures ANOVA with data in 30 second time bins), a characteristic pattern of behaviour was evident in both infected and non-infected mice. In this way, as time progressed distance moved per 30 seconds significantly decreased, as did velocity. For distance moved this effect was significant in mice measure at day 5 [$F_{(29,203)} = 14.269$, $p \leq 0.001$], day 12 [$F_{(29,232)} = 16.548$, $p \leq 0.001$], and day 20 [$F_{(29,1014)} = 56.437$, $p \leq 0.001$] of infection. A similar significant

effect for velocity was also found in the different cohorts of animals measured at velocity day 5 [$F_{(29,203)} = 14.571$, $p \leq 0.001$], day 12 [$F_{(29,232)} = 18.897$, $p \leq 0.001$], and day 20 [$F_{(1,34)} = 26.217$, $p \leq 0.001$] of infection. This finding was representative for both infected and non-infected animals, with both animal cohorts at all three time points moving slower and less over the time course of the experiment and supports the habituation of animals to the OFT environment. There was no evidence that this pattern of habituation was significantly different between control and Trypanosome infected mice, at any stage of infection (no significant x time bins interaction).

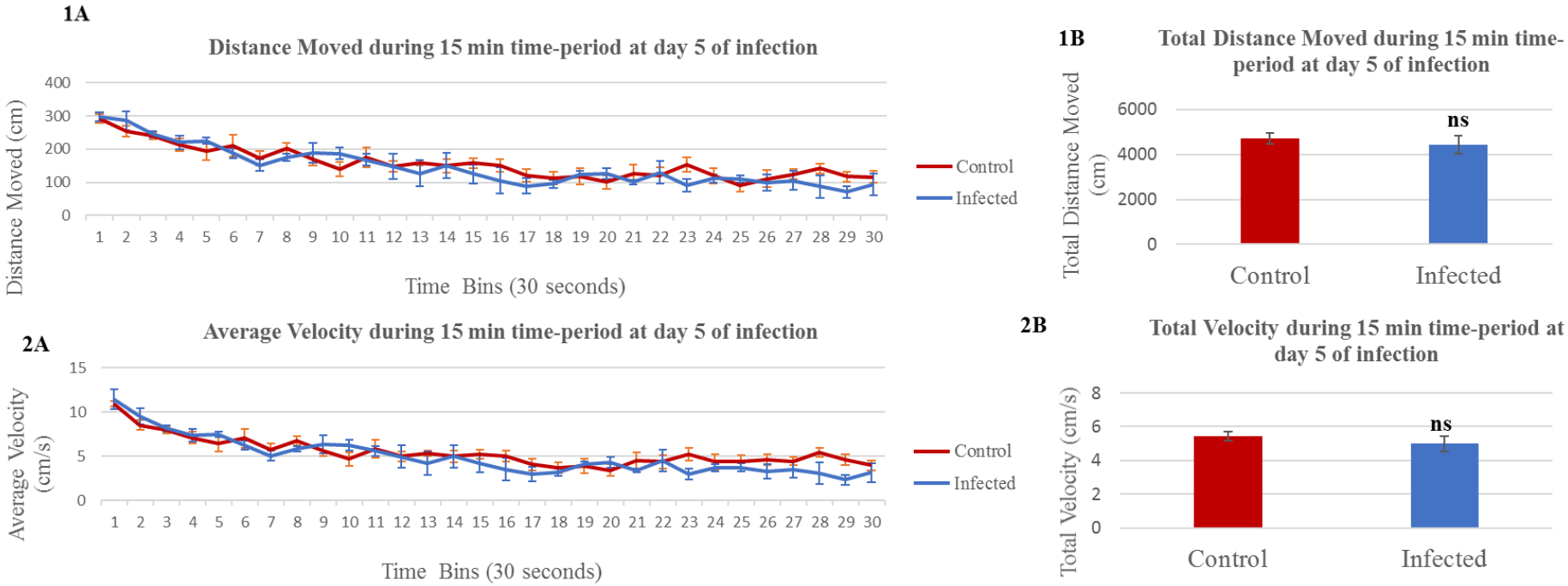

Figure 4.1 Infection at day 5 does not significantly impact on locomotor activity in CD-1 female mice

Data shown are mean ± SEM. Measures of locomotion include distance moved (1A, 2A) and velocity (1B, 2B). 1A and 2A show distance moved across the 15-minute testing period (30 seconds time bins) while 1B and 2B show total distance moved and the average velocity over the 15-minute test period. Time bin significantly influenced the distance moved (cm) and velocity (cm/s), with mice from both cohorts moving less and more slowly over the 15-minute time-period. There was no evidence that infection status impacted on this behavioural response (no significant infection x time bin interaction) or that infection itself impacted on either distance moved or velocity at day 5 of infection. *** denotes $p \leq 0.001$ significant effect of time bin (repeated measures ANOVA).

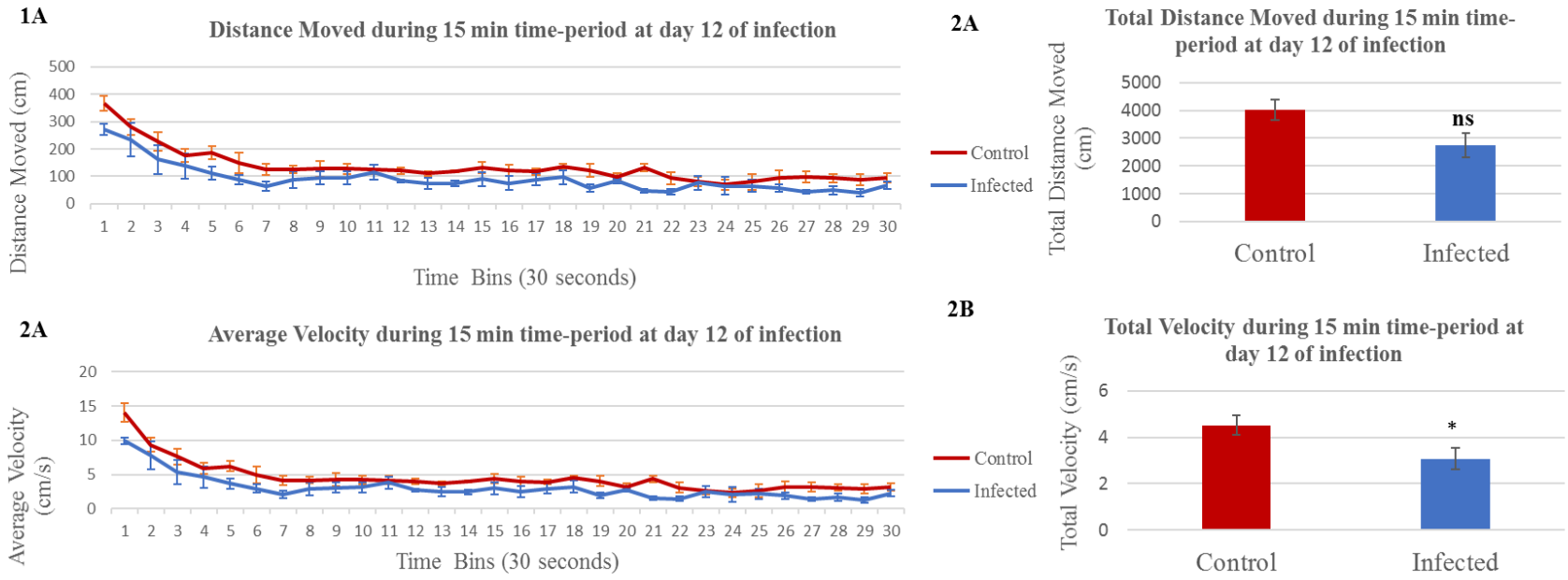

Figure 4.2 Infection at day 12 significantly impacts on locomotor activity in CD-1 female mice

Data shown are mean ± SEM. Measures of locomotion include distance moved (1A, 2A) and velocity (1B, 2B). 1A and 2A show distance moved across the 15-minute testing period (30 seconds time bin) while 1B and 2B show total distance moved and the average velocity over the 15-minute test period. Time bin significantly influenced the distance moved (cm) and velocity (cm/s), with mice from both cohorts moving less and more slowly over the 15 minute time period. There was no evidence that infection status impacted on this behavioural response (no significant infection x time bin interaction), however there was evidence that infection itself impacted on velocity at day 12 of infection. * denotes $p \leq 0.05$ significant effect of infection on velocity. *** denotes $p \leq 0.001$ significant effect of time bin (repeated measures ANOVA).

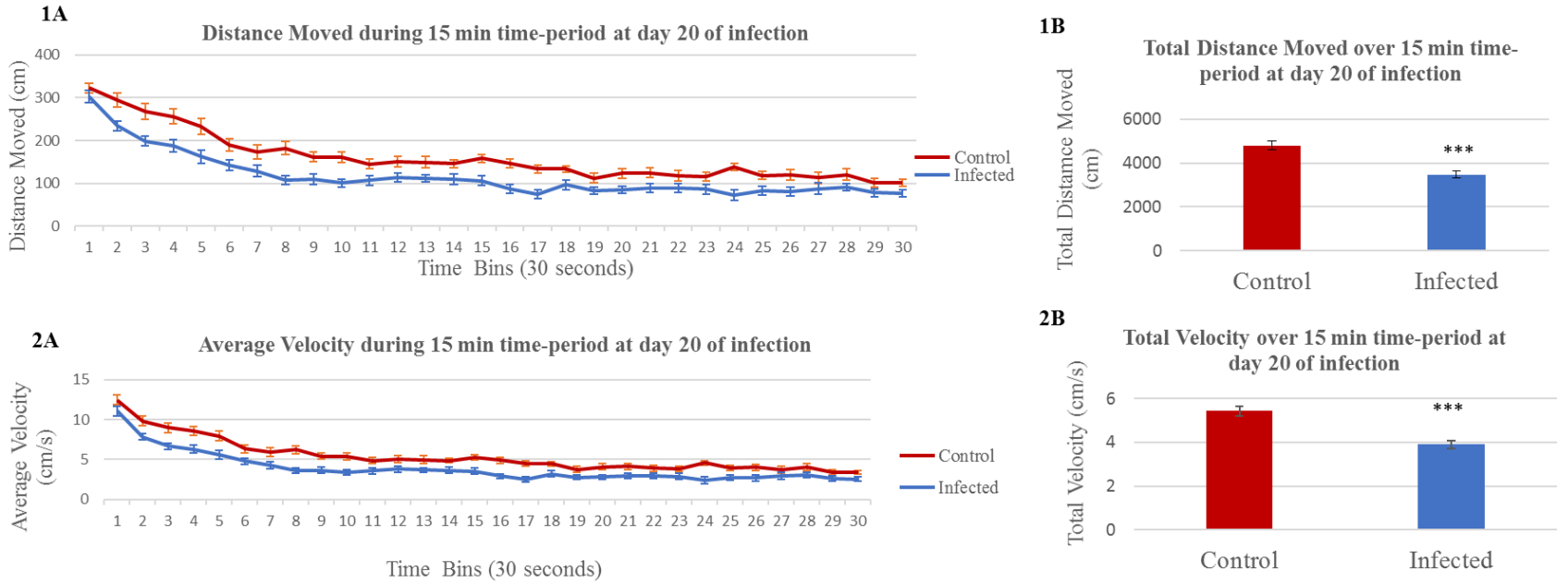

Figure 4.3 CD-1 infected female mice at day 22 exhibit hypolocomotion in a novel environment

Data shown are mean ± SEM. Measures of locomotion include distance moved (1A, 2A) and velocity (1B, 2B). 1A and 2A show distance moved across the 15-minute testing period (30 seconds time bin) while 1B and 2B show total distance moved and the average velocity over the 15-minute test period. Time bin significantly influenced the distance moved (cm) and velocity (cm/s), with mice from both cohorts moving less and more slowly over the 15 minute time period. There was no evidence that infection status impacted on this behavioural response (no significant infection x time bin interaction). However there was evidence that infection status impacted on distance moved and velocity at day 20 of infection. *** denotes $p \leq 0.001$ significant effect of time bin and infection on distance moved and velocity (repeated measures ANOVA).

4.5.2 Deficits in movement duration and frequency also contribute to the decreased locomotory activity seen during late stage Trypanosome infection

Trypanosome infected mice showed a deficit in both movement duration and frequency during late but not early stages of infection. *ANOVA* testing revealed a significant impact of infection on movement duration at day 12 [$F_{(1,8)} = 8.75$, $p = 0.018$] and 20 [$F_{(1,34)} = 19.409$, $p \leq 0.001$] of infection, which was not present at day 5 [$F_{(1,7)} = 2.199$, $p = 0.182$] (figures 4.4, 4.5 and 4.6). With infected mice showing decreased movement duration on day 12 and 20, but not on day 5, similar effects were seen for movement frequency, with infected animals showing significantly reduced frequency of movement at day 12 [$F_{(1,8)} = 25.27$, $p \leq 0.01$] and 20 [$F_{(1,34)} = 8.075$, $p \leq 0.01$], but not at day 5 [$F_{(1,7)} = 1.336$, $p = 0.286$], in comparison to non-infected controls. Thus, mice at later stages of infection moved less frequently and for shorter durations than non-infected controls.

Data from all 15 minutes of open field recording were used in the analysis to determine if there was any impact of time on these measures of locomotor activity, and if these effects were impacted by infection status. Testing revealed that as time progresses through the test, animals moved significantly less frequently, an effect evident for all cohorts (day 5 [$F_{(29,203)} = 2.434$, $p \leq 0.001$], 12 [$F_{(29,232)} = 1.613$, $p = 0.029$], 20 [$F_{(29,1014)} = 5.360$, $p \leq 0.001$]), and that movement duration also significantly decreased as time progressed, again this was evident in all cohorts tested ((day 5 [$F_{(29,203)} = 4.691$, $p \leq 0.001$], 12 [$F_{(29,232)} = 8.335$, $p \leq 0.001$], and 20 [$F_{(29,1014)} = 28.320$, $p \leq 0.001$]).

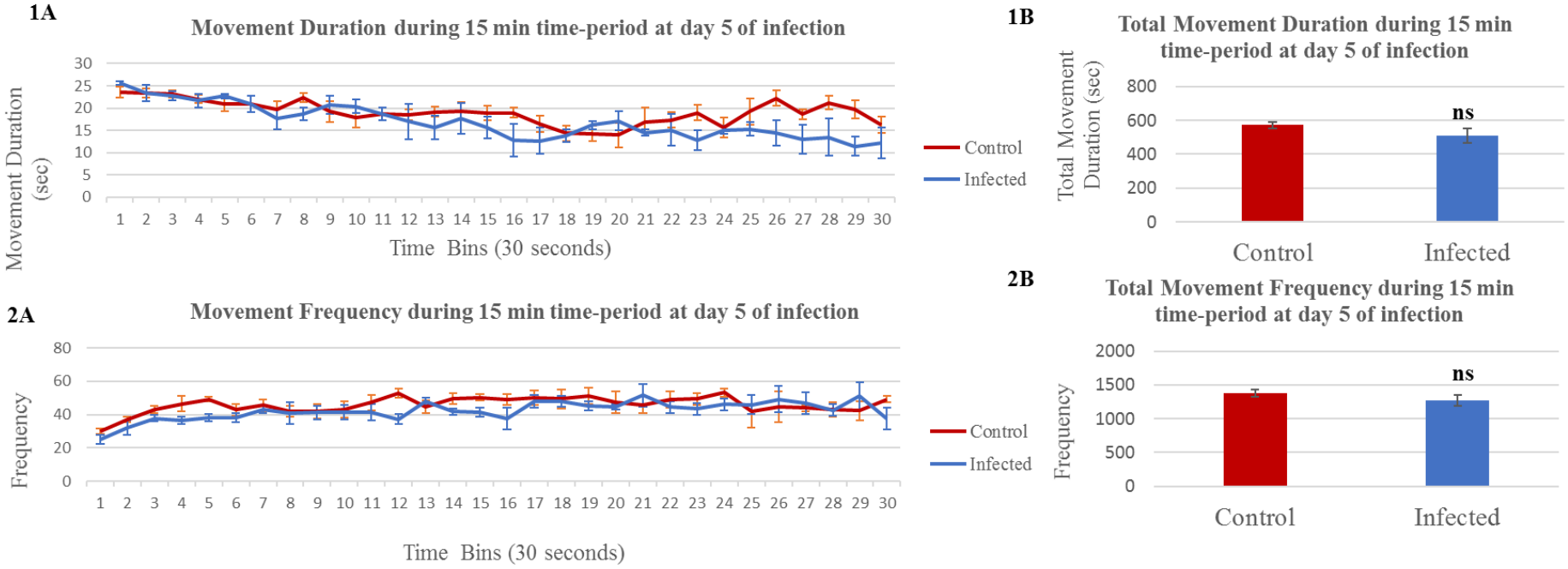

Figure 4.4 CD-1 infected female mice at day 5 display no significant exploratory type behaviour deficits in a novel environment

Data shown are mean ± SEM. Measures of exploratory behaviour include movement duration (1A, 2A) and movement frequency (1B, 2B). Significant interaction was found between movement duration x time bin and movement frequency x time bin over the 15 minute time-period for both animal cohorts with recorded animal behaviour changing over time. No significance was found for infection x movement duration (1B) or for infection x movement frequency (2B) meaning infection was no impact at that time point. A trend towards infection and time bin interaction was found for movement duration ($p = 0.0539$). *** denotes significance at $p \leq 0.001$ (repeated measures ANOVA).

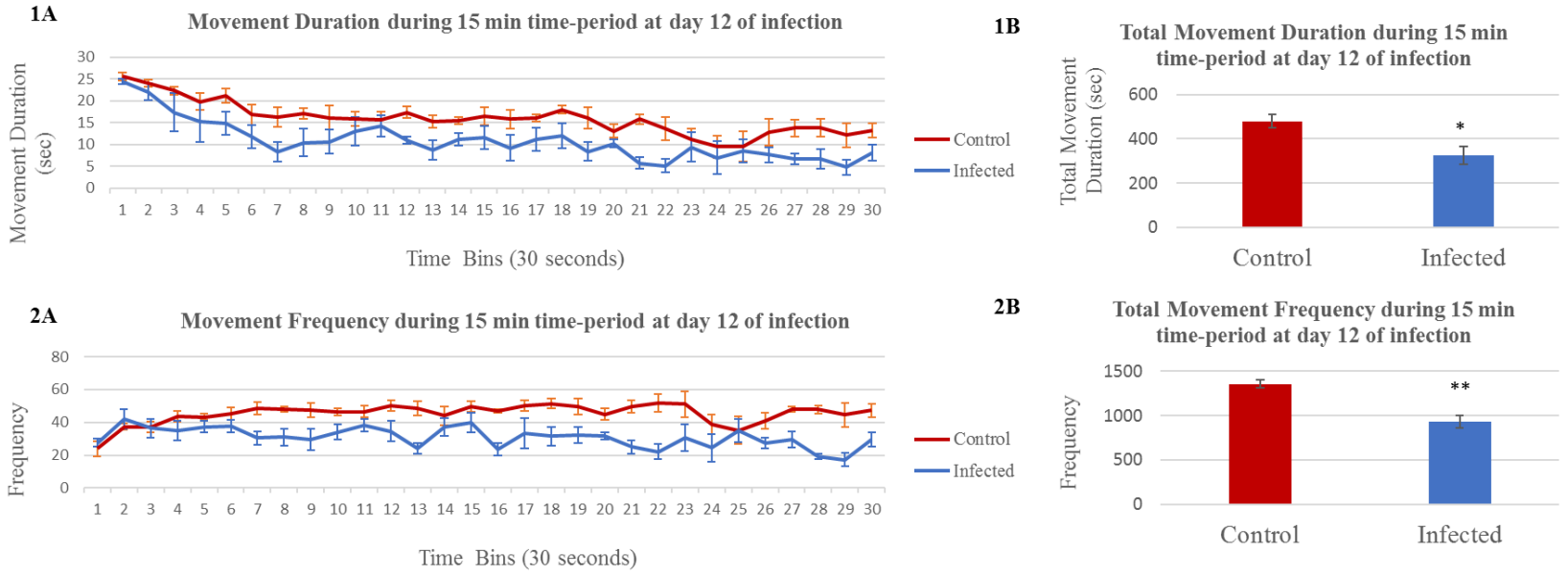

Figure 4.5 CD-1 infected female mice at day 12 display significant exploratory behaviour deficits in a novel environment

Data shown are mean ± SEM. Measures of exploratory behaviour include movement duration (1A, 2A) and movement frequency (1B, 2B). Significant interaction was found between movement duration x time bin and movement frequency x time bin over the 15 minute time-period for both animal cohorts with recorded animal behaviour changing over time. Significance was found for infection x movement duration (1B) and for infection x movement frequency (2B) meaning infection contributed to reduced exploration in a novel environment. An infection and time bin interaction was also found for movement frequency. *Post-hoc* analysis using a Pairwise t-test revealed that infected mice had significantly lower frequency of movement (day 12 $p = 0.048$) over the time course of recording * denotes significance at $p \leq 5$, ** denotes significance at $p \leq 0.01$ and *** denotes significance at $p \leq 0.001$ (ANOVA).

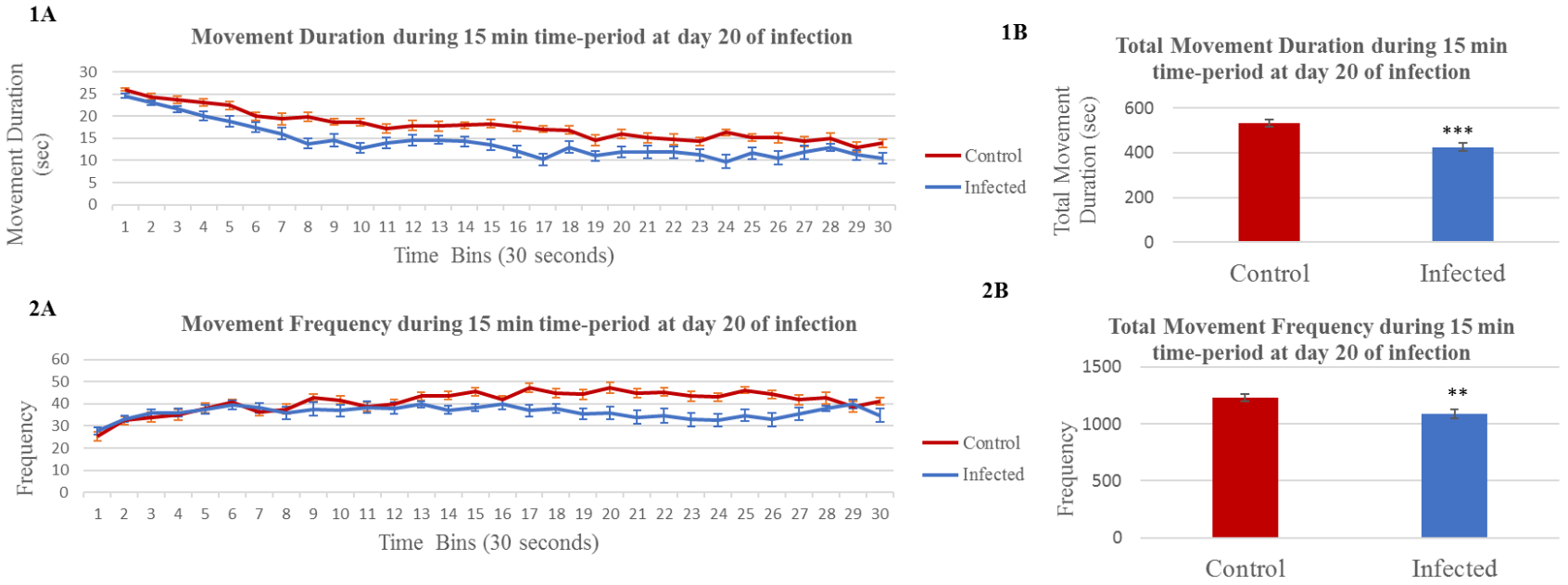

Figure 4.6 CD-1 infected female mice at day 22 display significant reductions in exploratory behaviour in a novel environment

Data shown are mean ± SEM. Measures of exploratory behaviour include movement duration (1A, 2A) and movement frequency (1B, 2B). Significant interaction was found between movement duration x time bin and movement frequency x time bin over the 15 minute time-period for both animal cohorts with recorded animal behaviour changing over time. Significance was found for infection x movement duration (1B) and for infection x movement frequency (2B) meaning infection contributed to reduced exploration in a novel environment. An infection and time bin interaction was also found for movement frequency. *Post-hoc* analysis using a Pairwise t-test revealed that infected mice had significantly lower frequency of movement (day 20 $p = 0.04$) over the time course of recording. ** denotes significance at $p \leq 0.01$ and *** denotes significance at $p \leq 0.001$ (ANOVA in R statistical software).

4.5.3 Trypanosome infected mice show no alteration in anxiety-like behaviour when exposed to a novel environment

Anxiety –like behaviour in a novel environment was measured by analysing the duration of time mice spent inside the central zone (1/3 the size of the completed arena size) of the testing arena. Infected mice at all time-points of infection (day 5, 12 and 20) showed no significant difference in the duration spent in the central zone of the arena as compared to control animals, as shown in figures 5.7, 5.8 and 5.9 respectively. Analysis also showed that centre zone duration was not significantly affected by time in the arena, i.e. the amount of time spent in the central zone per 30-second time bin did not change during the course of the 15 minutes of recording. This effect was independently observed in each cohort of mice (day 5, 12 and 20).

Anxiety-like behaviour was also measured by calculating the frequency of visits to the central zone of the testing arena. Interestingly, infected mice at day 12 [$F(_{1,8}) = 9.042$, $p = 0.016$] and 20 [$F\ (_{1,34}) = 14.894$, $p \leq 0.001$] frequented the centre significantly less than control animals. This analysis was based on the frequency of visits to the centre zone across the 15 minute testing period. Significant reduction in centre zone frequency was also found to be true when including data from all 15 minutes of recording and analysing the behaviour over time for infected animals at day 5 [$F\ (_{29,203}) = 1.992$, $p \leq 0.01$], 12 [$F(_{29,232}) = 3.976$, $p \leq 0.001$] and 20 [$F(_{29,1014}) = 5.780$, $p \leq 0.001$].

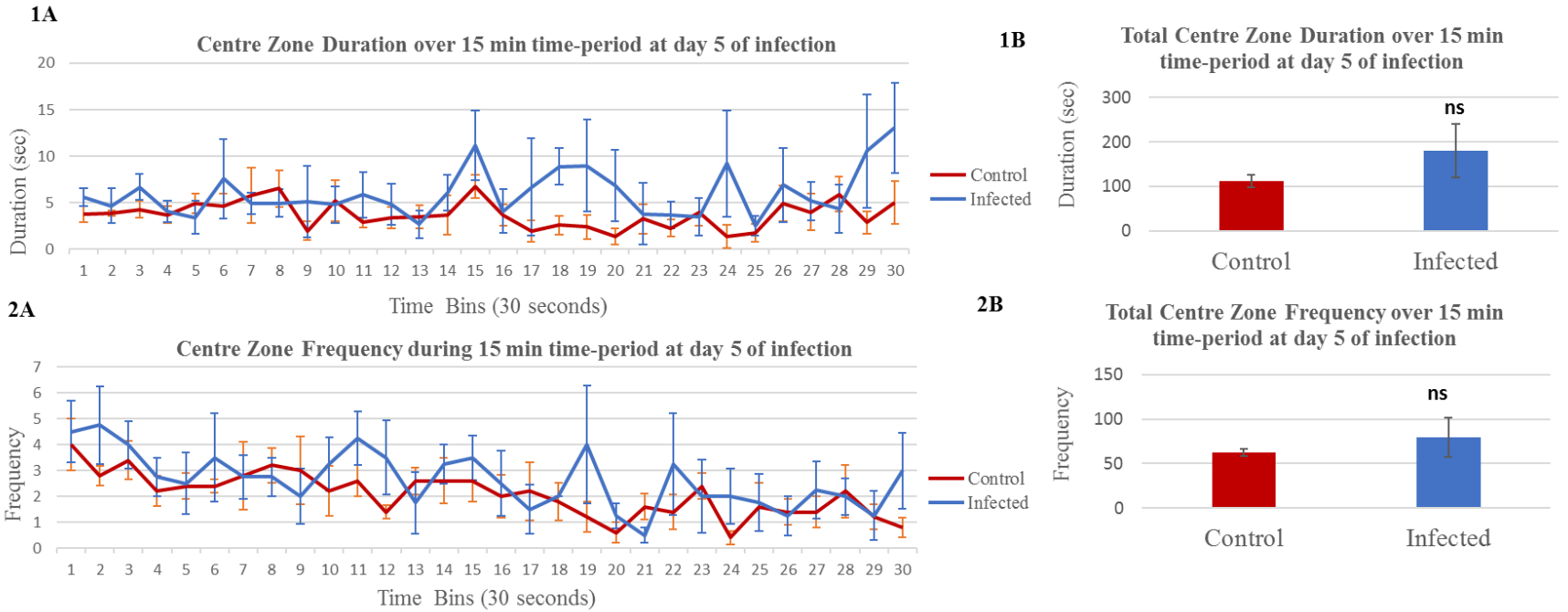

Figure 4.7 CD-1 infected female mice at day 5 display no significant anxiety-like behaviour in a novel arena

Data shown are mean ± SEM. Measures of anxiety-like behaviour include centre zone duration (1A, 1B) and centre zone frequency (2A, 2B). Significant interaction was found between centre zone frequency x time bin over the 15 minute time-period for both animal cohorts with recorded animal behaviour changing over time. Centre zone duration was not significantly affected by time bins. No significance was found for infection x centre zone duration (1B) or for infection x centre zone frequency (2B) meaning infection did not contributed to anxiety-like behaviour at day 5 of infection. ** denotes significance at $p \leq 0.01$ (ANOVA in R statistical software). Sample sizes were infected n=4, control n=5.

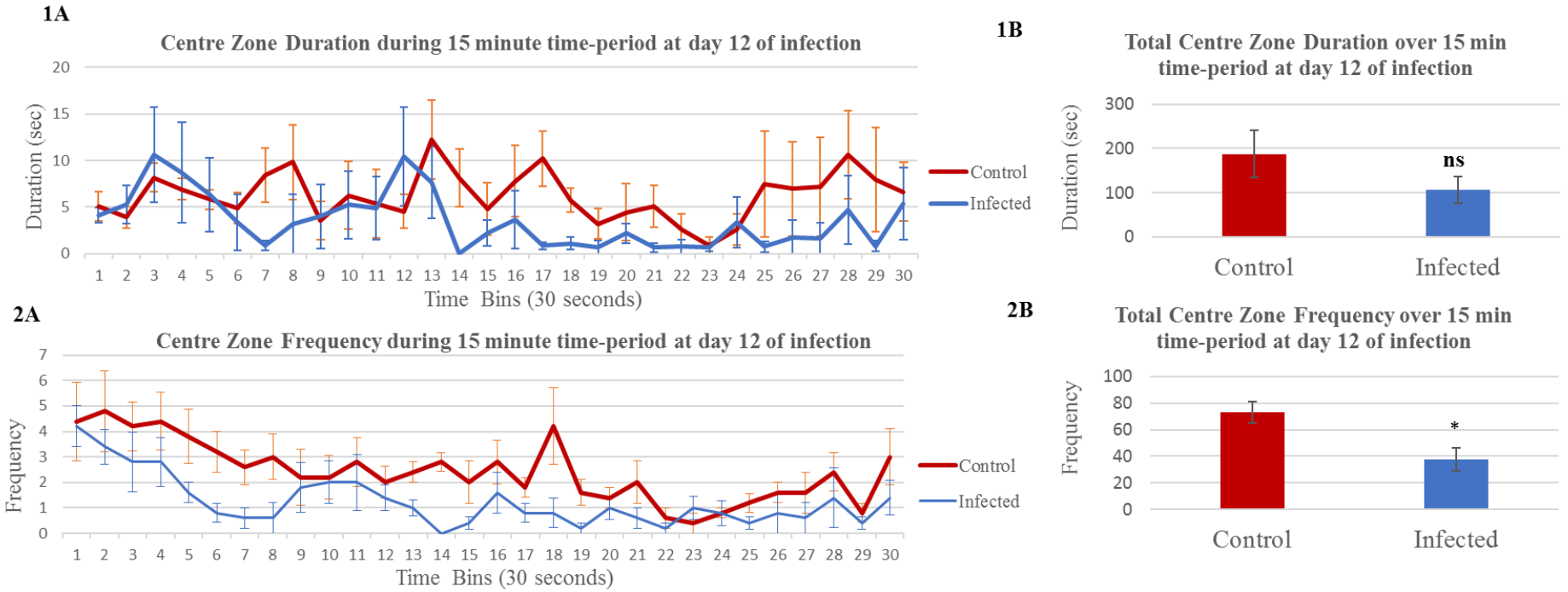

Figure 4.8 CD-1 infected female mice at day 12 display no significant anxiety-like behaviour in a novel arena

Data shown are mean ± SEM. Measures of anxiety-like behaviour include centre zone duration (1A, 1B) and centre zone frequency (2A, 2B). Centre zone duration (1A) was not significantly affected by time bins, or by infection (1B). Significant interaction was found between centre zone frequency x time bin over the 15 minute time-period for both animal cohorts with recorded animal behaviour changing over time. Significance was also found between centre zone frequency x infection (2B) * denotes significance at $p \leq 0.05$, *** denotes significance at $p \leq 0.001$ (ANOVA in R statistical software). Sample sizes were infected n=5, control n=5.

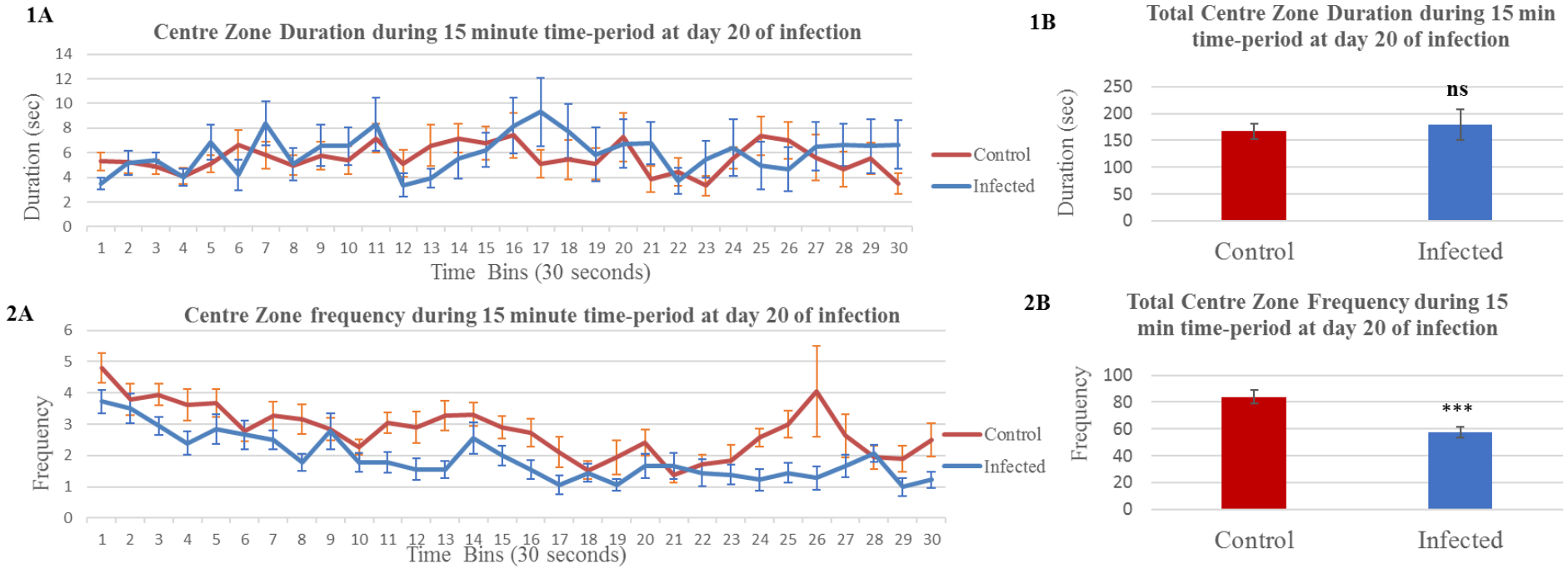

Figure 4.9 CD-1 infected female mice at day 22 display no significant anxiety-like behaviour in a novel arena

Data shown are mean ± SEM. Measures of anxiety-like behaviour include centre zone duration (1A, 1B) and centre zone frequency (2A, 2B). Centre zone duration (1A) was not significantly affected by time bins, or by infection (1B). Significant interaction was found between centre zone frequency x time bin over the 15 minute time-period for both animal cohorts with recorded animal behaviour changing over time. Significance was also found between centre zone frequency x infection (2B) *** denotes significance at $p \leq 0.001$ (ANOVA in R statistical software). Sample sizes were infected n=18, control n=17.

4.5.4 Trypanosome infected mice show no significant difference in object exploration during the acquisition phase of NORT

Trypanosome infected mice and their non-infected control counterparts spent a similar amount of time exploring the two objects (familiar) presented to them in the 10 minute acquisition phase of the NORT. No significant difference was found for the duration of visit (sec), with both groups interacting with the objects for an average duration of 130 seconds ($p= 0.65$, figure 4.10). By contrast, a student's t-test revealed a significant difference in the frequency of visit to the objects, with control animals visiting the objects more often than infected animals ($p= 0.046$). This decrease in frequency was be related to the decreased locomotor activity seen in infected animals (figure 4.1). Nonetheless, the total object interaction time composed of both parameters revealed no significant difference. This data is presented in figure 4.10

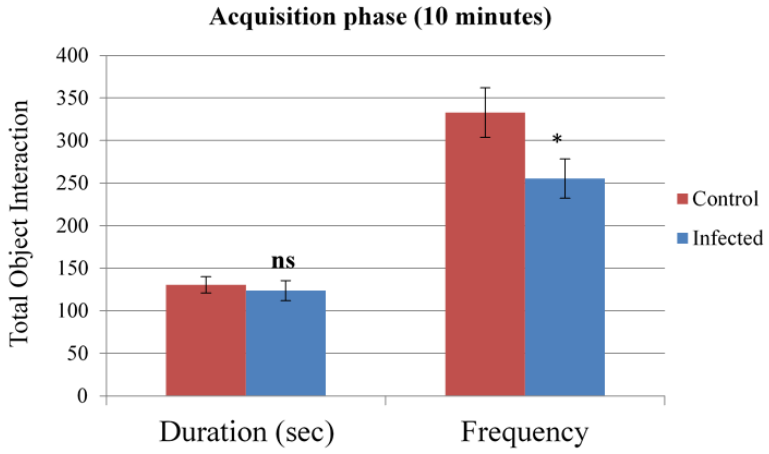

Figure 4.10 Trypanosome infected mice show no difference to non-infected controls in object exploration during the acquisition phase of the NORT

Data shown are mean ± SEM. Total object interaction comprised of total duration of time (seconds) interacting with objects and frequency of visit to object during 10 minutes of the acquisition phase. No significant effect of infection on object duration interaction was found, with a significance found for object frequency (p= 0.046, Student's t-test). Sample sizes were infected n=18, control n=17.

4.5.5 Trypanosome infected mice display no significant deficit in object recognition after a 24 hour delay period

In the test phase of the NORT, Trypanosome infected mice showed no significant deficit in novel object recognition after a 24-hour delay when compared to non-infected controls (figure 4.11). In this way, both infected and non-infected animals were able to successfully differentiate between the familiar and the novel objects, with both experimental groups showing a significant preference for exploring the novel, as compared to the familiar object (infected, $p < 0.001$; non-infected $p= 0.001$). This was further supported by the finding of no interaction between infection status and object on the Recognition Index (RI) [$F_{(1,68)} = 0.0$, $p=0.98952$], indicating that there was no difference in object exploration preference between the two experimental groups.

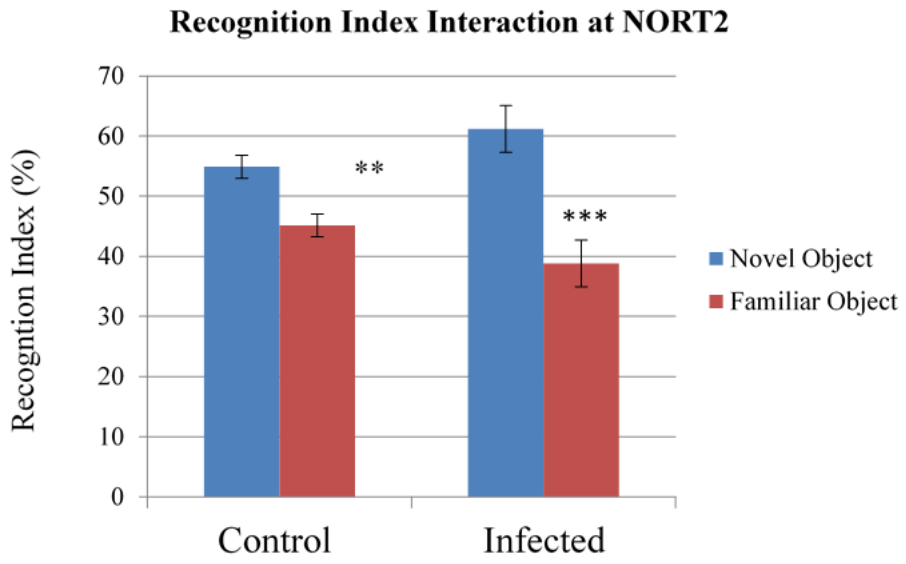

Figure 4.11 Infection at day 22 does not impact on performance of the NORT in CD-1 female mice

Data shown are mean ± SEM. Recognition Index (RI) for CD-1 female mice infected with *Trypanosoma brucei brucei* for 22 days. The recognition index (RI) parameter reported here includes both measures of object exploration duration (seconds) and object visit frequency, determined over a 10 minutes NORT test phase, 24 hours after acquisition phase. A significant novelty preference (Student's t-test) was found independently for both infected and control animals, and no significance was found for the object x infection status interaction (ANOVA, [$F_{(1,68)} = 0.0$, $p=0.98952$]). ** denotes $p \leq 0.01$, *** denotes $p \leq 0.001$. Sample sizes were infected n=18, control n=17.

4.6 Summary

Table 4.1 Summary table of findings from the Open Field test at day 5, 12 and 20 of infection

Open Field Parameters	Impact of Infection		
	Day 5	**Day 12**	**Day 20**
Velocity (cm/sec)	-	↓	↓
Distance moved (cm)	-	↓	↓
Movement Duration (sec)	-	↓	↓
Movement Frequency	-	↓	↓
Duration in centre zone (sec)	-	-	-
Frequency of centre zone visit	-	↓	↓

Table showing a summary of infection impact on locomotor activity and anxiety-like behaviour in CD-1 female mice at three time-points (D7, D12 and D20). No significant effects of infection were found at day 5 post inoculation. Late stage infection resulted in a significant reduction in locomotion and exploratory behaviour.

4.7 Discussion

The aforementioned experimental studies present an experimental model of African trypanosomiasis with CD-1 female mice infected with *Trypanosoma brucei brucei*. Open-field tests showed that infected mice display decreased locomotor activity in a novel environment, with infected animals moving slower and for shorter durations. This was only evident at later stages of infection (day 12 and 20) and not at earlier time-points of 5 days. The NORT revealed that infected mice could successfully differentiate between the familiar and novel objects, with a preference for novelty observed. This suggests that novel object recognition memory is not impaired at later stages of infection, when Trypanosomes are present in the brain (Chapter 2).

4.7.1 Trypanosome infected CD-1 mice show hypolocomotion in a novel environment at the late stage of infection

Mice observed during the entire 15 minute period of the OFT, moved more slowly and for over shorter distances as the test period progressed (Figures 5.1 and 5.2). This pattern of behaviour was found to be true for both infected and control animal at all three infection time points. This finding corroborates previous evidence, with research suggesting mice placed in a novel environment such as the OF arena will naturally move less over time as their interest in their new environment declines (410).

Further, upon closer investigation of the relationship between movement and infection, infected mice at a later stage of the disease progression (Day 20) were found to move for significantly shorter durations than their healthy control counterparts. This was also found to be true when looking at speed of movement (velocity), with infected mice at both day 14 and 20 moving slower than non-infected controls. Reduced velocity and distance moved are both parameters which may reflect the neurological perturbations

of motor activity reported in humans during stage II trypanosomiasis (144). Infected mice were also found to have reduced speed of movement, which parallels the altered gait behaviour of affected human individuals (144). Interestingly, these observations parallel those of *Trypanosoma cruzi* infected rodents subjected to the OFT, where animals at 30 days of infection (acute phase) also exhibited significantly reduced locomotor and exploratory behaviour as compared to control animals during 5, 10 and 30 minute testing sessions (411).

Few studies have investigated the interaction between tryptophan metabolism and its role in motor function. Research describing the effects of acute tryptophan depletion (ATD) on affective behaviour and cognition in rats, found no significant effect of depletion on locomotion as assessed by the OFT (412). This finding was corroborated by an independent group, who found no significant effect of ATD on affective behaviour in adult rats (413). Even more paucity surrounds information on the potential link between tryptophan depletion and perturbed motor activity during late stage II HAT. However, studies have been published describing the effect of ATD on motor function in Parkinson's disease- another disorder of the central nervous system. Research focused on psychomotor ability- a parameter used to describe the relationship between cognitive function and physical movement- found that there was a reduced latency of response during ATD in the Parkinson's disease group compared to controls (414).

The kynurenine pathway, a major component of tryptophan metabolism, has been demonstrated to be involved in many CNS disorders and diseases with motor function perturbations including amyotrophic lateral sclerosis, Huntington's disease,

Alzheimer's disease and AIDS dementia complex (415). Involvement of the pathway appears to be attributed to imbalances in tryptophan levels. Indeed researchers have found that under various neuropathological conditions, degradation of tryptophan is usually followed by an increase in kynurenine metabolites observed in the CSF, brain and serum (306). The metabolism of tryptophan via the kynurenine pathway is preferentially routed towards the production of quinolinic acid, an endogenous neurotoxin which acts as a N-methyl-D-aspartic acid (NMDA) receptor agonist (326,416). Further, a study by Parrott et al (417) found a correlative link between increased kynurenine metabolism in the dorsal hippocampus and increased depressive behaviours during inflammation. Based on tryptophan observations (chapter 3), one could expect that kynurenine will be increased as a result of tryptophan depletion in brain of Trypanosome infected mice.

Taken together, researchers theorise that the significant imbalances of tryptophan and its main metabolites could play a significant pathological role in the development of neurodegenerative disorders, with direct pathological consequences as well as indirect psychiatrics attributes (416). However more mechanistic insight is needed, beyond correlative interpretations, to ascertain the potential role of tryptophan depletion on psychiatric measures, mostly in relation to mood and anxiety, in human studies.

CD-1 infected mice showed a deficit in exploratory behaviour in a novel environment, as reflected by the parameters movement duration and frequency. Mice at late stage infection moved less frequently and for shorter durations than age and sex matched controls. No significance for either parameter was established for rodents at day 5 early stage infection.

It is important to note that reduced exploratory behaviour could come about as a result of impaired locomotory activity as seen for late stage infection mice. Indeed previous research by Darsaud et al (418) reported the same behavioural disturbances in infected rats, with authors postulating the cause to be the onset of meningoencephalitis. On the other hand, it could perhaps be argued that this behavioural phenotype of reduced exploratory behaviour and movement is indicative of parasite manipulation aimed to increase the chance of transmission. Decreased host activity increases the chances of being bitten by the tsetse fly vector, increasing the likelihood of transmission from the vertebrate host to the vector.

Furthermore, a study in 2006 (419) looking at behaviour of serotonin transporter knockout mice with more serotonin in the synapses as reuptake is reduced, found a striking reduction in exploration and activity during the open field test. Authors concluded that pronounced thigmotaxis and anxiety could drive the behavioural phenotype and thus lead to less exploration in a novel environment. It is also well known that serotonin transporters are key for healthy processes in the central nervous system, with dysregulation implicated in neuropsychiatric disorders such as anxiety and depression (420,421). From this, one could postulate that perhaps increased serotonin levels as a consequence of less tryptophan in the brain could in some way contribute to the reduced exploration of infected CD-1 mice at late stage disease. Hillegaart *et al* (422) reported that when given acutely, administration of serotonin drugs was accompanied by slight decrease in total activity and an increased activity in the periphery of the open-field arena.

4.7.2 Trypanosome infected mice show no significant anxiety-like behaviour in a novel environment

During the OF test, no animals at any of the three time-points seemed to exhibit altered anxiety-like behaviour. This was found to be true by analysing the time spent by animals in the central zone, with no significant difference observed between infected and control animals. Interestingly, animal at day 12 and 20 of infection had a lower frequency of visit to the central zone when compared to controls which would initially suggest the exhibition of anxiety-like behaviour. However, given that the animals at late stage infection appear to move less, slower and for shorter durations, it suggests that hypolocomotion may confound the significance of the centre zone frequency results. Animals are simply moving around less and therefore as a result would frequent the centre zone less. However, our data indicate that infected animals spend a similar amount of time in the central zone to non-infected controls, supporting the idea that anxiety-like behaviour is not altered in infected animals.

Darsaud et al (423) have previously reported that in a rat experimental model of African Trypanosomiasis using the *T. b. brucei* AnTat l.lE strain, behavioural disturbances evaluated through the OFT revealed no significant effect on anxiety-like behaviours, reporting only increased lassitude in infected animals. On the other hand previous research using rats as model organisms for *Trypanosoma evansi* infection looked at the state of anxiety-like behaviour in animals as measure for neural function during disease. The researchers described a correlative link between infection and increased anxiety-like behaviour, with the progression of disease (424). Clearly there are discrepancies in the findings reported from different research groups depending on the strain and rodent model organism used, with few to no studies examining the anxiety-like states of mice infected with *T. b. brucei*.

It is also known that in humans suffering from HAT, anxiety is one of the common neuropsychiatric symptoms associated with infection. Unfortunately, most accounts of patients with mental health issues associated with Trypanosomiasis are anecdotal, with very little known about the underlying aetiology. A review by Litt et al in 2012 (169) suggested that perhaps suffering from neglected tropical diseases in the first place may actually predispose individuals to poor mental health. Stigma, discrimination and exclusion from local society are just some of the contributing factors. This is further compounded by the fact that mental health and psychiatric illness in the African diaspora have historically been associated with witchcraft and the black arts (425). This could contribute to the unwillingness of patients experiencing with such symptoms from coming forward to clinicians, highlighting the need for further collaborative work between parasitologists, psychiatrists and psychologists on NTDs.

4.7.3 Trypanosome infected mice at day 22 display no deficit in object recognition learning and memory

Infection with *T. brucei brucei* for 22 days did not result in any significant perturbation in novel object preference behaviour after a 24 hour acquisition-test inter-trial interval. Indeed, both control and infected mice showed significantly increased exploration of the novel object in comparison to the familiar object, as determine by the RI. Further, both cohorts of mice explored the two objects presented to them during the acquisition phase for equal amounts of time. Taken together, these findings suggest that in the test phase the mice did recognise the familiar object initially presented to them during the acquisition phase, had formed a memory of the familiar objects and that after a 24-hour delay period that memory remain intact, and thus the mice opted to explore the novel object more during the test phase. This indicates that *T. brucei brucei* infected mice do

not suffer from an object recognition memory deficit and that learning and memory consolidation is unaffected in these animals.

Our findings support the notion that in the animal model of HAT, there are no significant deficits in objects recognition memory and learning capabilities. However, considering the noteworthy reduction in tryptophan levels of late stage infected mice (Chapter 3); one would assume serotonin levels to be depressed, as supported in tryptophan depletion models (201) and so a decrease in novelty interactions mechanisms as well as impaired memory formation to be observed (426). Indeed, an early study by Riedal and colleagues (427) describes how tryptophan depletion in humans specifically impairs long-term memory formation, with the authors proposing reduced serotonin turnover in the brain as the potential cause. This finding has been mirrored by the work of other groups, again demonstrating the impact of tryptophan depletion on human cognitive function, revealing impairments in learning and memory (428–430). Numerous independent studies have also implicated a potential role for tryptophan and therefore serotonin depletion on impaired memory and learning in rats (431–433). For instance data from Lieben et al (413) using acute nutritional manipulations of tryptophan in rats suggests that lowered tryptophan levels may not be associated with changes in affective behaviour (i.e. anxiety) but do play a role in impairing object memory.

The results from this study may not corroborate these previous findings for two main reasons. The first being we used mice and not rats as our model organism and existing research suggests that acute tryptophan depletion in mice does not result in the depletion of serotonin (434) as it does in rats. Therefore, even though our previous work (Chapter

3) displays the significant reduction of tryptophan levels, serotonin may not be depleted or depleted enough to result in cognitive deficits in the mouse model of disease. Moreover, our results are based on the mouse model of HAT and therefore cannot be extrapolated to be compared to results from healthy human volunteers not suffering with infection. The studies on acute tryptophan depletion in humans also rely on artificial or nutritional means to induce acute tryptophan depletion whereas our research suggests the effects of tryptophan depletion occurring naturally in the brain during the course of infection are more biphasic, which adds additional complexity. Our work also specifically focused on learning and long-term memory formation after a 24-hour delay, whereas the human studies described focused on short-term memory. Future studies could employ shorter ITI (1 hour) to investigate short term memory in Trypanosome infected mice, but if there is no deficit observed at 24hr this strongly suggests that there won't be a deficit at 1 hour.

In summary: Trypanosoma infected CD-1 mice show hypolocomotion in a novel environment at late stage infection, show no anxiety-like behaviour in a novel environment and display no deficit in object recognition learning and memory.

4.8 Methods

4.8.1 Open Field Test (OFT)

In preparation for the OFT, CD-1 female mice were placed individually into empty holding cages in order to habituate to the room in which the experiment was held. After 10 minutes, animals were placed individually into one of the four circular testing arenas, comprising of a black Perspex background (diameter of 38cm, central zone diameter of 12cm), and video recorded for 15 minutes. Four animals were recorded per run. 70% ethanol was used to clean and remove any prior scent markings before the beginning of the test, and between succeeding runs. A camera was secured to the ceiling and connected to the desktop PC, saving videos for further analysis. The number of animals for each experimental group (infected and control) were day 5 n= 9, 14 n=10 and 22 n=35.

4.8.2 Novel Object Recognition Task (NORT)

The day following after the OFT, mice were subjected to the Novel Object Recognition Task (NORT). Again, the mice were allowed to habituate to the room in individual holding cages prior to the task. After 10 minutes, four mice per run were placed individually into the empty arenas and activity recorded for 5 minutes. Following this, mice were removed and two identical objects (blue pyramids 5.5 x 2.5 x 3cm, wooden squares 3 x 3 x 3cm or red oblongs 9 x 3 x 1cm) were placed into each arena as part of the acquisition phase, placed 15cm from the arena wall. Mice were allowed 10 minutes to explore the objects, with their activity being recorded by video, before returning to the home cages. A 24-hour delay was imposed, after which mice were returned to the arenas, now containing one familiar object and a novel object. In this phase, behaviour was video recorded for 10 minutes.

For both phases of the test, both arenas and objects were cleaned with 70% ethanol between runs. All object allocations to each animal were randomised, as was the side (left or right) of novel object presentation. The number of animals for each group were day 14 n=10 and 22 n=35.

4.8.3 Data and Statistical Analysis

Ethovision XT v8.5, Noldus software was used to track and analyse the OFT and NORT videos. For the OFT this allowed parameters such as walking distance, velocity, duration and frequency to be analysed as measures of locomotor activity. Duration and frequency in the centre zone of the arena were analysed as measures of anxiety-like behaviour. The effect of infection and time bin (30 seconds), on output parameters were analysed using repeated measures Analysis of Variance (ANOVAs) in R software. Significance was determined at $p<0.05$.

Chapter 5.0 The impact of Stage II Trypanosomiasis infection on cerebral glucose metabolism

5.1 Introduction

^{14}C-2-Deoxyglucose (^{14}C-2DG) functional brain imaging is a technique used to measure regional brain cerebral glucose metabolism (151,152). As an analogue of glucose, the more metabolically active a region of the brain is, the more glucose it metabolises, and so more of the ^{14}C-2DG accumulates in that region. Here, this method was used to elucidate the effect of Trypanosomiasis brain infection on the cerebral metabolism of particular areas of the brain. Data obtained from any changes in cerebral metabolism are useful in understanding the potential interaction between Trypanosomes and cognitive function, with relevance to the behavioural changes observed in infected rodents.

5.2 Research objectives

i. To investigate impact of Trypanosomiasis stage II infection on brain function, determined by cerebral glucose metabolism.

5.3 Methods Summary

Methods in this chapter include *in vivo* mouse infections, *in vivo* application ^{14}C-2-deoxyglucose as a glucose analogue tracer, cryostat brain sectioning, the generation of autoradiographic brain imaging and computer-based brain image analysis.

5.4 Summary of findings

1. A significant global reduction in cerebral glucose utilisation was observed in infected animals.
2. Trypanosome-infected mice show reduced metabolism in the prefrontal cortex, also known as “hypofrontality.”
3. Brain regions associated with circadian rhythm, motor function, cognition and serotonergic activity in the brain were affected.
4. No significant difference was found in the amount of tracer in the blood circulation of infected versus control animals.

5.5 Results

5.5.1 Infected animals show a significant global reduction in cerebral glucose utilisation

Following on from physiological analysis of the mice in the study, the whole brain average concentration of ^{14}C 2-DG (WBAv^{14}C) was characterised for each animal. Here, the WBAv^{14}C represents the average ^{14}C-2-DG concentrations determine across 6 brain levels as part of functional brain imaging. As illustrated by Figure 5.1, infected animals show a significant global reduction in cerebral glucose utilisation ($p< 0.001$**)**. While the plasma glucose levels were significantly lower in the infected group, there is no evidence that the ability of the ^{14}C-2DG to enter the brain is hampered as supported by no significant different in the blood plasma ^{14}C concentration (Table 5.1). Therefore, the global cerebral glucose utilisation reduction found for infected animals appears to be genuine, validating the findings from the study.

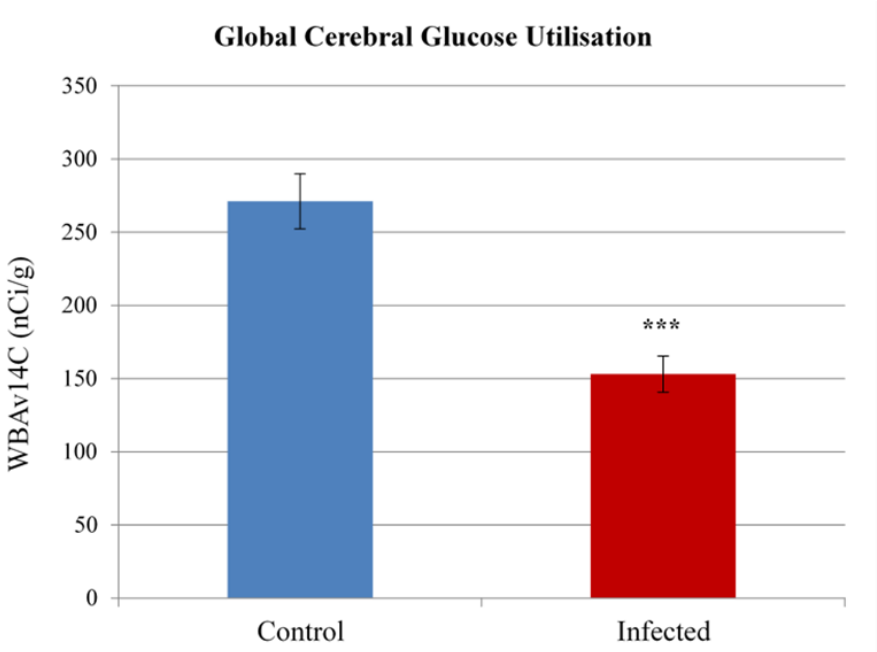

Figure 5.1 Global cerebral ^{14}C-2-DG auto-radiographic tracer utilisation

Data shown are Mean ± SEM. WBAv^{14}C= Whole brain average ^{14}C-2-Deoxyglucose (^{14}C-2-DG) tracer. A significant global cerebral glucose utilisation was found for the infected cohort at day 21 post infection (p=0.000033**)** as compared with the control animals. Statistical analysis was conducted using a Student's t-test. Significant was set at $p \leq 0.05$. *** denotes $p \leq 0.001$.

5.5.2 Infected animals show decreased cerebral glucose metabolism in brain regions involved in locomotor function

Regions of the basal ganglia and cerebellum were found to have significantly decreased ^{14}C-2-DG cerebral metabolism as compared with control animals (Figure 5.2). In terms of the basal ganglia, this was evident in the dorsolateral striatum (DLST, $p<0.001$), ventromedial striatum (VMST, $p= 0.002$), globus pallidus (GP, $p= 0.001$), substantia nigra pars reticulata (SNR, $p<0.001$) and substantia nigra pars compacta (SNC, $p<0.001$). In addition, cerebral metabolism was significantly reduced in the cerebellum (CB, $p= 0.001$) of the infected mice relative to the non-infected controls.

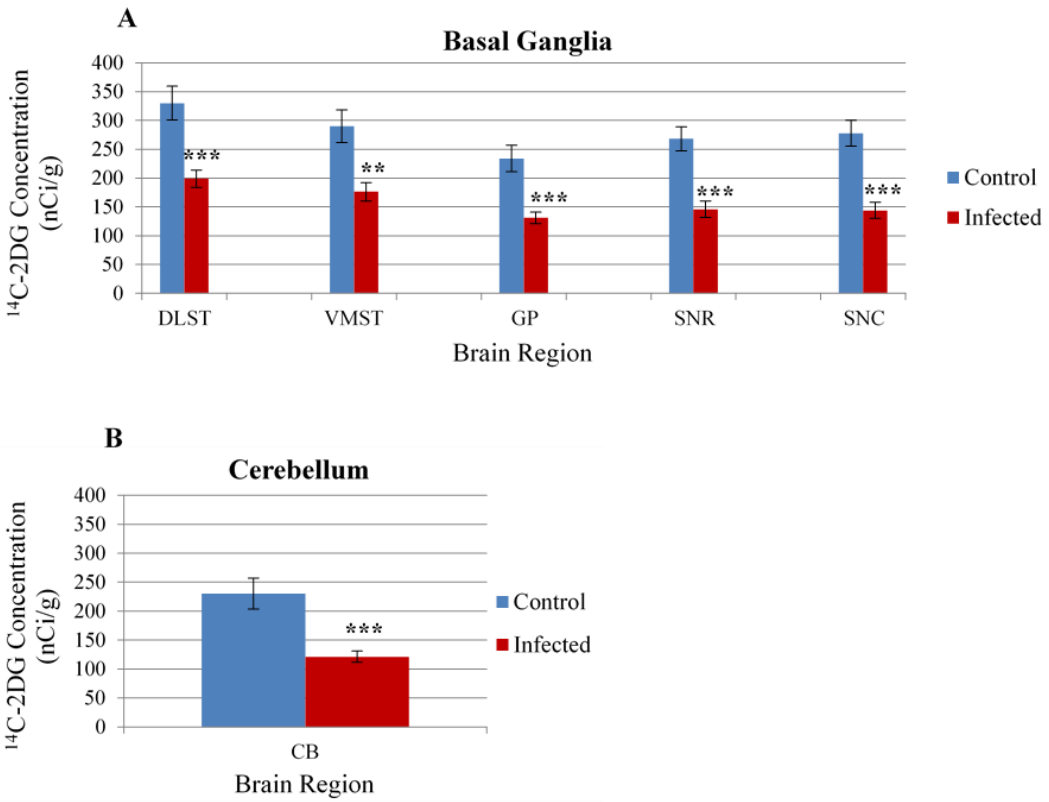

Figure 5.2 Trypanosome-infected mice show decreased cerebral metabolism in motor brain regions

Data shown are mean ± SEM. ^{14}C-2-Deoxyglucose tracer (^{14}C-2-DG) concentration (nCi/g) for the Basal Ganglia (**A**) and Cerebellum (**B**). A significant effect of infection on reduced cerebral metabolism was found for every brain region analysed, namely; for the dorsolateral striatum (DLST), ventromedial striatum (VMST), globus pallidus (GP), substantia nigra pars reticulata (SNR), substantia nigra pars compacta (SNC) (**A**). Cerebellum (CB) (**B**). Samples sizes were n= 13 infected, and n=12 control mice. Statistical analysis was conducted using a Student's t-test. ** denotes significance at $p \leq 0.01$. *** denotes significance at $p \leq 0.001$.

5.5.3 Infected animals show reduced metabolism in the prefrontal cortex (PFC)

Given that the whole brain average ^{14}C-2-DG concentration is significantly reduced in infected mice, supporting a potential global reduction in glucose utilisation in these animals, we wanted to assess whether this reduction in metabolism was also evident across the different brain regions analysed. It is plausible that some specific brain regions are affected but others are not, even when a significant change in the WBAv^{14}C concentration is observed. Therefore, we statistically compared the ^{14}C-2-DG concentration in each brain region of interest (RoI) using Student's T-test. Overall, we found evidence for significantly reduced cerebral metabolism in all brain regions analysed in Trypanosome infected mice, as evidence by a significant reduction in ^{14}C-2-DG, with the exception of the nucleus reuniens (Re) where the decreased in ^{14}C-2-DG concentration seen failed to reach significance.

Trypanosome brucei brucei-infected mice showed significantly decreased cerebral glucose metabolism, as reflected by the decreased local glucose utilisation (LCGU), in all regions of the prefrontal cortex analysed, supporting a phenotype in these animals (Figure 5.3). As such, cerebral metabolism was significantly reduced in the anterior Prelimbic (aPRL, $p< 0.001$), motor (M2, $p<0.001$), dorsolateral orbital (DLO, $p<0.001$), lateral orbital (LO, $p<0.001$), medial orbital (MO, $p<0.001$), medial prelimbic (mPRL, $p=0.008$), infralimbic (IL, $p=0.01$), and cingulate (Cg1, $p<0.001$) cortices.

5.5.4 Infected animals show decreased cerebral glucose metabolism in the amygdala and hippocampus

Infected mice also showed significantly decreased cerebral metabolism in the amygdala when compared to the non-infected control group, as evident in all the amygdala nuclei measured including basolateral (BLA, $p=0.004$), medial (MeA, $p=0.002$) and central (CeA, $p=0.002$) amygdala. A significant decrease in local cerebral metabolism was also found in multiple subfield of the dorsal [(cornu ammonis 1, DHCA1, $p=0.007$), (cornu ammonis 2, DHCA2, $p=0.007$), (molecular layer, DHML, $p=0.01$), (dentate gyrus, DHDG, $p=0.008$)] and ventral [(cornu ammonis 1, VHCA1, $p<0.001$), (cornu ammonis 2, VHCA2, $p<0.001$), (molecular layer, VHML, $p<0.001$), (cornu ammonis 3 VHCA3, $p<0.001$)] and ventral subiculum (VHSub, $p<0.001$) hippocampus. This data is presented in Figure 5.3.

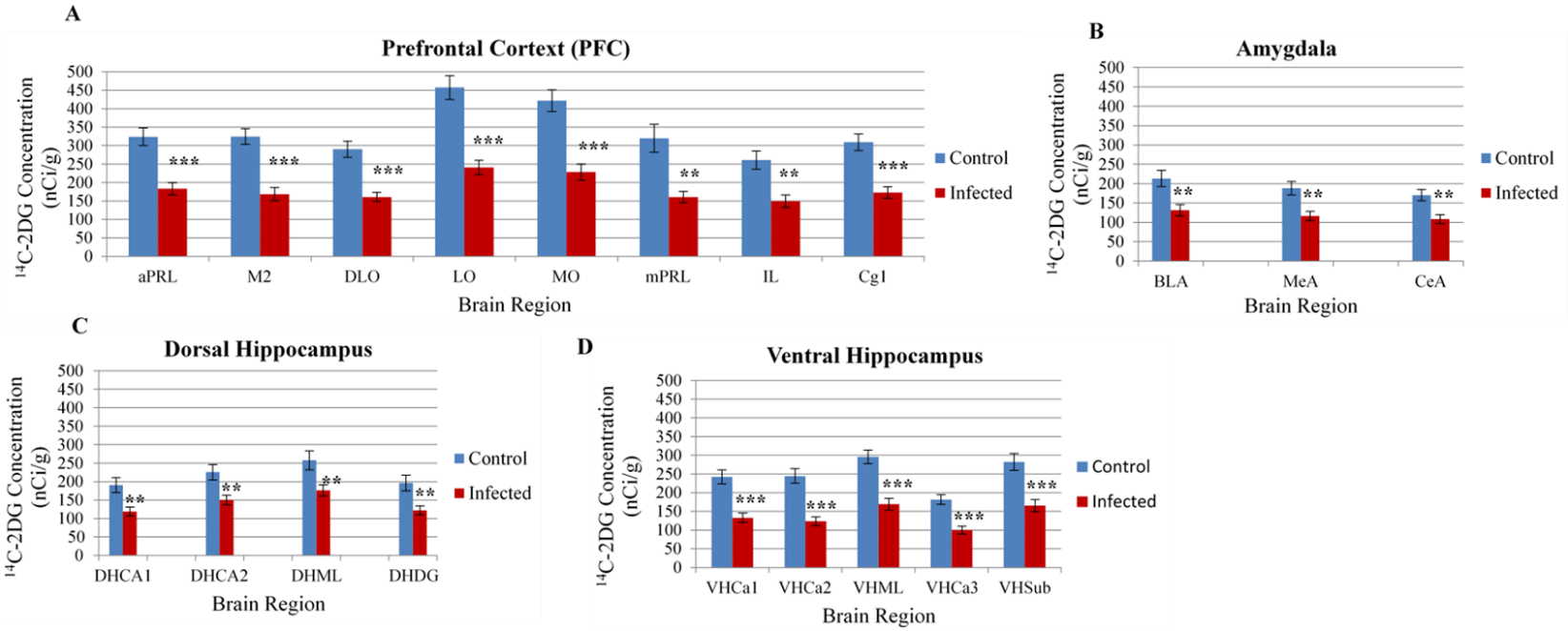

Figure 5.3 Trypanosoma-infected mice show hypofrontality and decreased cerebral metabolism in the amygdala and hippocampal brain regions

Data shown are mean ± SEM. ^{14}C-2-Deoxyglucose tracer (^{14}C-2-DG) concentration (nCi/g) for the Prefrontal Cortex (**A**), Amygdala (**B**), Dorsal Hippocampus (**C**) and Ventral Hippocampus (**D**). A significant effect of infection on reduced cerebral metabolism was found for every brain region analysed, namely; for the anterior Prelimbic (aPRL), motor (M2), dorsolateral orbital (DLO), lateral orbital (LO), medial orbital (MO), medial Prelimbic (mPRL), infralimbic (IL) and cingulate area 1 (Cg1) cortices (**A**). Basolateral (BLA), medial (MeA) and central (CeA) (**B**). Dorsal hippocampus (DHCA1) (DHCA2) (DHML), (DHDG (**C**). Ventral hippocampus (VHCa1), (VHCa2), (VHML), (VHCA3) and ventral hippocampus subiculum (VHsub) (**D**). Samples sizes were n= 13 infected, and n=12 control mice. Statistical analysis was conducted using a Student's t-test. ** denotes significance at $p \leq 0.01$. *** denotes significance at $p \leq 0.001$

5.5.5 Animals at late stage infection show decreased regional glucose metabolism in the striatum, thalamus and hypothalamus

Animals sacrificed at day 21 post inoculation also showed substantially depressed cerebral metabolism in the striatum as evidence by significant p-values for the dorsomedial (DMST, $p=0.001$) and ventrolateral (VLST, $p<0.001$) regions. Further, thalamic regions encompassing the mediodorsal thalamus (MD, $p=0.001$), ventromedial (VPM, $p=0.001$), dorsolmedial thalamus (DM, $p=0.01$) and the medial geniculate [(MG, $p=0.00$, medial dorsal (MD, $p=0.001$), ventromedial (VPM, $p=0.001$) and dorsomedial (DM, $p=0.01$)]. In relation to the hypothalamus, decreased levels of cerebral metabolism were found in infected animals as compared with the non-infected controls in the medial preoptic (MPOM, $p=0.006$), lateral preoptic (LPO, $p=0.008$), anterior (AHC, $p=0.001$), paraventricular (PVN, $p=0.01$), lateral hypothalamic (LH, $p=0.006$) nuclei. This data is shown in Figure 5.4.

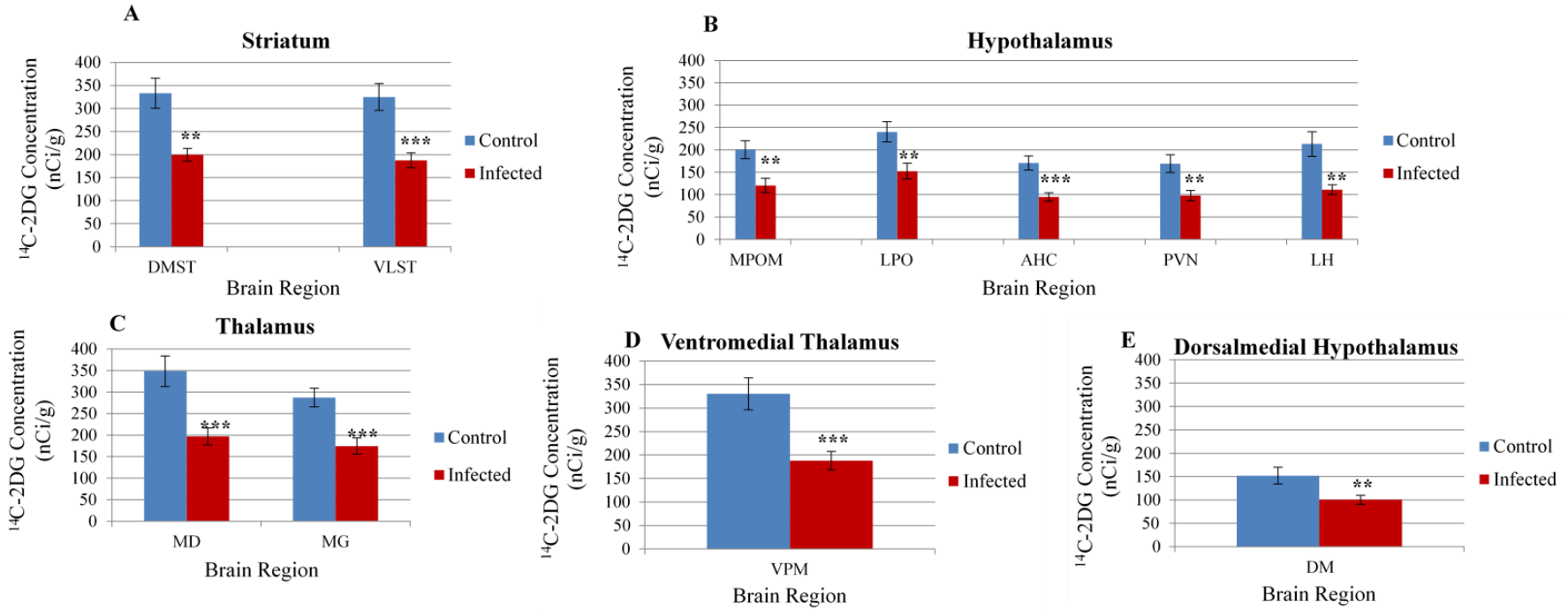

Figure 5.4 Trypanosome-infected mice show decreased cerebral metabolism in the striatum and thalamic brain regions

Data shown are mean ± SEM. ^{14}C-2-Deoxyglucose tracer (^{14}C-2-DG) concentration (nCi/g) for the Striatum (**A**), Hypothalamus (**B**), Thalamus (**C**), Ventromedial Thalamus (**D**), and Dorsalmedial Hypothalamus (**E**). A significant effect of infection on reduced cerebral metabolism was found for every brain region analysed bar one, namely; for the dorsomedial (DMST) and ventrolateral (VLST) striatum (**A**). Medial preoptic (MPOM), lateral preoptic (LPO), anterior (AHC), paraventricular (PVN), lateral (LH) hypothalamus (**B**). Medial dorsal (MD), Medial Geniculate (MG) (**C**). Ventromedial (VPM) (**D**). Dorsomedial (DM) (**E**). Samples sizes were n= 13 infected, and n=12 control mice. Statistical analysis was conducted using a Student's t-test. ** denotes significance at $p \leq 0.01$. *** denotes significance at $p \leq 0.001$.

5.5.6 Infected animals show a decreased cerebral glucose metabolism in a number of cortical brain regions

There was a significant decrease in cerebral metabolism in multiple cortical regions (Figure 5.5), including the lateral entorhinal cortex (Lent, $p< 0.001$), somatosensory cortex barrel field (S1BF, $p< 0.001$), the retrosplenial cortex (RSG, $p= 0.006$), visual cortex (V1, $p <0.001$), perirhinal cortex (Prh, $p< 0.001$), piriform (Pir, $p=0.002$) and insular(Ins, $p=0.004$).

5.5.7 Rodent Stage II Trypanosomiasis results in decreased cerebral glucose metabolism in dopaminergic, serotonergic and cholinergic brain regions

Significantly reduced cerebral glucose metabolism was also found in areas of the mesolimbic system and raphé brain regions, dopaminergic and serotonergic areas respectively, in infected as compared to non-infected control animals (Figure 5.6). In terms of the serotonergic raphé, this included hypometabolism in the dorsal raphé (DR, $p<0.001$) and median raphé (MR, $p<0.001$). For the mesolimbic system this included a significant decrease in metabolism in the nucleus accumbens core (NaC, $p<0.001$), nucleus accumbens shell (NaS, $p<0.001$) and the ventral tegmental area (VTA, $p<0.001$).

Further, in the septal/diagonal band of broca, regions such as the medial septal nucleus (MS, $p=0.001$), lateral septal nucleus (LS, $p=0.001$), the vertical limb of the diagonal band of broca (VDB, $p<0.001$) and the horizontal limb of the diagonal band of broca (HDB, $p<0.001$) significantly reduced metabolism in infected animals was found. These brain regions send cholinergic projections to the hippocampus, and are a primary

source of cholinergic innervations in the brain (435). This data is highlighted in Figure 5.6.

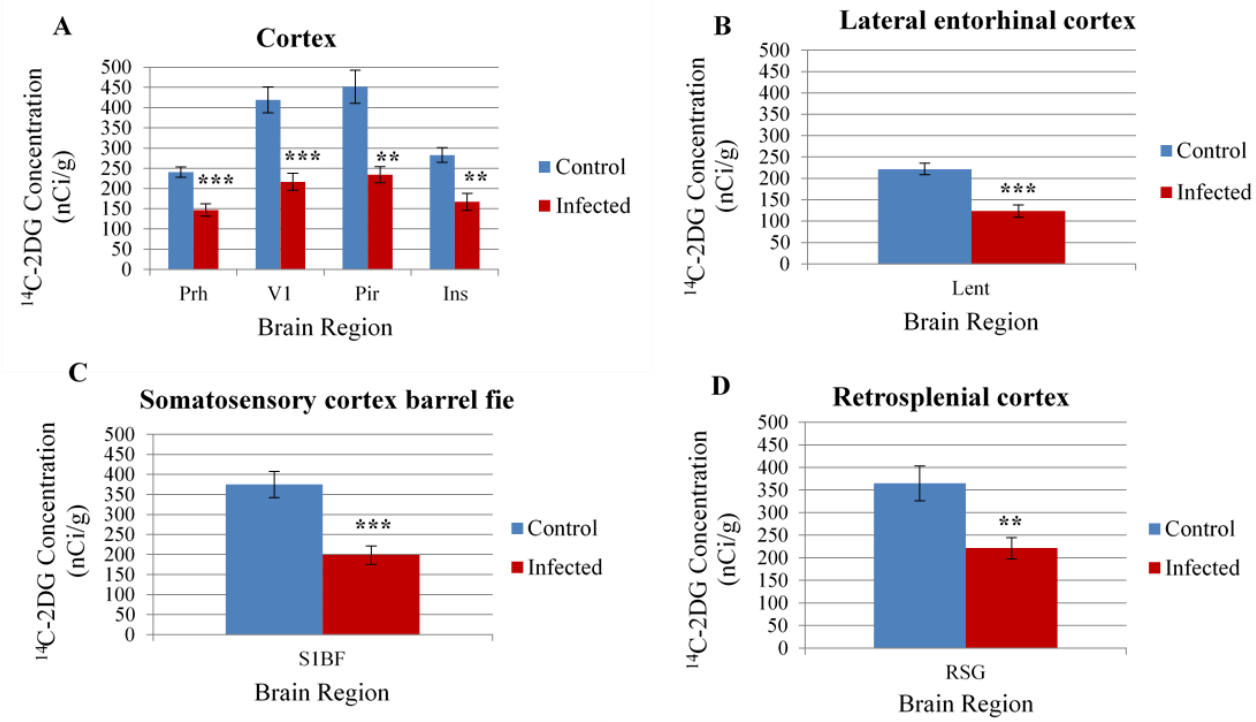

Figure 5.5 Trypanosome-infected mice show decreased cerebral metabolism in a number of cortical brain regions

Data shown are mean ± SEM. ^{14}C-2-Deoxyglucose tracer (^{14}C-2-DG) concentration (nCi/g) in cortical regions including visual cortex (**A**), Lateral entorhinal cortex (**B**), Somatosensory cortex barrel fie (**C**), and Retrosplenial cortex (**D**). A significant effect of infection on reduced cerebral metabolism was found for every brain region analysed, namely; for perirhinal cortex (Prh), visual cortex (V1), piriform (Pir) and insular (Ins) (**A**). Lateral entorhinal cortex (Lent) (**B**). Somatosensory cortex barrel fie (S1BF) (**C**). Retrosplenial cortex (RSG) (**D**). Samples sizes were n= 13 infected, and n=12 control mice. Statistical analysis was conducted using a Student's t-test. ** denotes significance at $p \leq 0.01$. *** denotes significance at $p \leq 0.001$.

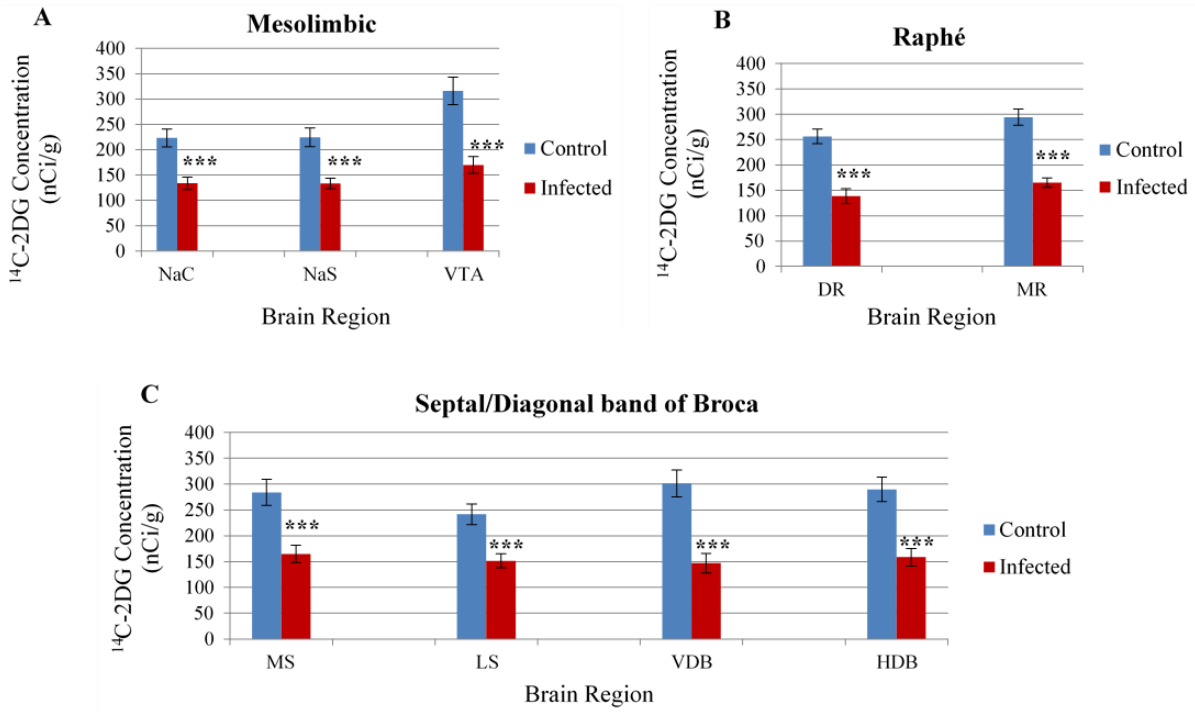

Figure 5.6 Trypanosome-infected mice show decreased cerebral metabolism in a number of dopaminergic, serotonergic and cholinergic brain regions

Data shown are mean ± SEM. ^{14}C-2-Deoxyglucose tracer (^{14}C-2-DG) concentration (nCi/g) for the Mesolimbic (**A**), Raphé (**B**), and Septal/Diagonal band of Broca (**C**). A significant effect of infection on reduced cerebral metabolism was found for every brain region analysed, namely; for the nucleus accumbens (NaC), nucleus accumbens septi (NaS), ventral tegmental area (VTA) (**A**). Dorsal raphé (DR), median raphé (MR). (**B**). Medial septal nucleus (MS), lateral septal nucleus (LS), vertical limb of the diagonal band of broca (VDB) and the nucleus of the horizontal limb of the diagonal band of broca (HDB) (**C**). Samples sizes were n= 13 infected, and n=12 control mice. Statistical analysis was conducted using a Student's t-test. *** denotes significance at $p \leq 0.001$.

5.5.8 Trypanosome-infected mice show decreased cerebral glucose metabolism in multimodal brain regions

Brain regions with known multimodality such as the periaqueductal grey (PAG, $p < 0.001$) and habenula (Hab, $p=0.012$) were found to have decreased metabolism as compared with non-infected, control animals (Figure 5.7).

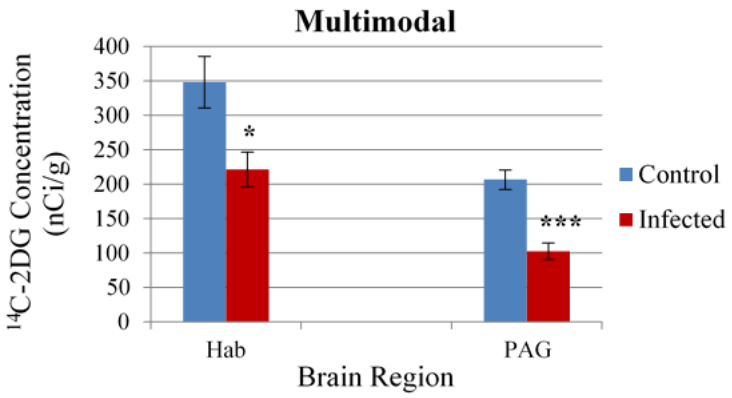

Figure 5.7 Trypanosome-infected mice show decreased cerebral metabolism in multimodal brain regions

Data shown are mean ± SEM. ^{14}C-2-Deoxyglucose tracer (^{14}C-2-DG) concentration (nCi/g) for Multimodal brain regions. A significant effect of infection on reduced cerebral metabolism was found for Periaqueductal grey (PAG) and Habenula (Hab). Samples sizes were n= 13 infected, and n=12 control mice. Statistical analysis was conducted using a Student's t-test. * denotes significance at $p \leq 0.05$. * denotes significance at $p \leq 0.05$. *** denotes significance at $p \leq 0.001$.

.

5.5.9 Physiological Tests

As displayed in Table 5.1, no significant difference was found between the blood plasma concentration of the ^{14}C-2-deoxyglucose tracer between the control and infected group. Further, no significant difference was found between animal weights when both cohorts were compared, with the average weights for both groups falling within the expected range for female adult CD-1 mice at 10 weeks old (approximately 33 grams +/- 2.3g, Charles River Factsheet). From this, any significant differences found in the ^{14}C-2-DG brain image analysis can be concluded to be independent of any physiological compounding factors such as animal weight or blood concentration of the tracer.

Interestingly, a significant difference was found in plasma glucose levels ($p= 0.028$, Student's t-test), with an average value of 7.25 mmol/L for the control group and 5.89 mmol/L for the infected group. Theoretically, low comparative levels of circulating plasma glucose could allow for greater entry of ^{14}C-2-deoxyglucose into the brain, resulting in potentially higher levels of the tracer in the brain, due to a lack of competition from glucose for the glucose transporter across the blood brain barrier. However, thus occurs only in severe hypoglycaemia. Plasma glucose values in both experimental groups are within the normal, expected physiological range (436,437), and so although the difference is significant, it is not outside the normal physiological bounds and is unlikely to impact on the amount of ^{14}C-2-deoxyglucose taken into the brain of infected versus control animals. In mice, the normal concentration of plasma glucose ranges from 7.15-12.69 mmol/L (437).

Table 5.1 Blood plasma ^{14}C concentration, glucose levels and mouse weights

	^{14}C (nCi/mL)		Plasma Glucose (mmol/L)		Weight (g)	
	Control	**Infected**	**Control**	**Infected**	**Control**	**Infected**
Mean	38.73	44.31	7.25	5.89*	34.52	35.69
SD	15.37	24.39	1.01	1.66	4.87	4.88
SE	4.86	7.36	0.32	0.50	1.54	1.47
%SD	39.67	55.06	13.92	28.15	14.10	13.66
T-test	**0.541**		**0.028**		**0.553**	

Table showing a summary of mean carbon-14 concentrations (nCi/mL), plasma glucose levels (mmol/L) and mouse weights (g) for animals used in the functional brain imaging study. Control mice were found to have a significantly higher average plasma glucose levels as compared with the infected group (p= 0.028). By contrast, infected mice showed no significant difference in weight or plasma concentrations of ^{14}C as compared with control mice. Statistical analysis was conducted using a Student's t-test. Significant was set at $p \leq 0.05$.

5.6 Discussion

5.6.1 Trypanosomiasis infected mice show reduced cerebral glucose metabolism

This work aimed to use ^{14}C-2-Deoxyglucose functional brain imaging as a measure of cerebral glucose metabolism within specific mouse brain regions, to investigate the effect of Stage II Trypanosomiasis infection on neuronal activity. There were two main findings of altered cerebral metabolism in infected mice. Infected mice show reduced activity in the motor brain regions, which align with the hypolocomotion seen in these animals. However, we believe these effects must be interpreted cautiously with regard to their potential relationship to neuronal activity and the specificity of these effects as late stage Trypanosomiasis infection caused a significant, widespread decrease on cerebral glucose metabolism throughout the rodent brain, evident at both the global and regional level.

5.6.2 Stage II Trypanosomiasis results in reduced regional cerebral metabolism

Locomotor disturbances have been reported as the second most common symptom associated with stage II HAT (142), and as such the hypofunction seen in the basal ganglia and cerebellum in this study are of particular interest. Our findings from previous behavioural experiments (Chapter 4), revealed reduced locomotor activity in infected mice subjected to the Open Field Test (OFT) and as such we proposed that neuronal activity would be reduced in regions of the brain associated with motor function. HAT associated cerebellar ataxia has been well established, with Stiles et al (143) describing how infection with *Trypanosoma brucei* induced direct apoptosis in the cerebellum of experimental rodents. Cerebral ataxia is not uncommon to brain infection, with cases described as part of the neurological complications that follow

Plasmodium falciparum (438), *Naegleria fowleri* (439) and chikungunya meningoencephalitis (440).

Hippocampal brain regions were investigated due to their role in memory consolidation from short-term to long-term, encompassing regions such as the dentate gyrus and Cornu Ammonis (441). Our previous behavioural findings suggest no significant difference learning and memory, as characterised using the NORT, between infected and control mice (Chapter 4), and as such we were expecting to see no differences in cerebral metabolism for this particular brain region. Further, memory dysfunction is rarely, if ever mentioned in the literature as a symptom of neurological dysfunction in humans or animal models of HAT. Significantly reduced cerebral metabolism in the hippocampal brain regions of infected mice may therefore come about as a compensatory mechanism, to make up for the lack of activity in another region, as the brain is extremely complex and interlinked with no one region acting autonomously (442), although there is no evidence for the potential role of hypometabolism in contributing to pathogenesis. D'Aiuto et al (443) reported on the association between persistent infection by Herpes simplex virus type 1 (HSV-1) and functional brain changes affecting working memory. Here the authors described their functional magnetic resonance imaging (fMRI) data among schizophrenia cases exposed to the virus, suggesting significantly increased neurobiological efforts in the hippocampus to increase functional working memory.

Trypanosome-infected mice showed significantly decreased cerebral metabolism in both dorsal and median raphé nuclei, as compared with the control animals. The dorsal raphé contains a large group of serotonergic neurons, with interconnected

neuromodulatory functions in the CNS homeostasis (444,445). Dysregulation of circadian rhythm is a hallmark feature of African sleeping sickness (446), and so trypanosome-related damage to the raphé nuclei may impact on the feedback system between the raphé nuclei and suprachiasmatic nucleus (SCN)- the SCN signals to the raphé nuclei to modulate serotonin release, whilst the raphé nuclei project to SCN to regulate levels of awareness (447). This correlates with previously published data, revealing reduced levels of serotonin in *T. b. gambiense*-infected mice brains (448). Serotonin depletion has long been associated with insomnia (449), which may be exacerbated in cases of Trypanosomiasis as our findings (Chapter 3) reveal decreased levels of the serotonin precursor tryptophan in the brains of infected mice. Taken together, Trypanosome-mediated reduced serotonergic neuronal activity in the raphé nuclei and depletion of available tryptophan may both contribute to an overall reduction in levels of serotonin in the brain, further impairing the sleep/wake cycle of the host.

Due to its proposed role in base emotional responses, such as fear, aggression and sexual drive (450), all of which have been noted as often increased in patients of stage II HAT (52), the metabolism of the amygdala was investigated with hypometabolism also found. It is important to note however, that complex emotional responses are not solely governed by one area of the brain, which makes it difficult to propose that the reduced neuronal activity in the amygdala is the sole reason for the emotional responses associated with the disease. For example in the case of *Toxoplasma gondii* infection, dendritic retraction in the basolateral amygdala is also accompanied by reduced corticosterone secretion, both of which may contribute to reduced predator aversion in rats (451–453).

5.6.3 Trypanosoma-infected mice show hypofrontality

Significantly reduced cerebral metabolism was recorded in the prefrontal cortex (PFC), a phenomenon known as hypofrontality (Figure 6.3). The PFC was chosen due to the many implications of its role in modulating behaviour, personality and impulse control (454). This is relative to cases of HAT, as Stage II patients are noted in the literature as exhibiting "odd behaviours" with poor control of sexual impulses, suggesting perturbed PFC activity (142).

Hypofrontality is well established in the pathology of psychiatric disorders, and particularly in schizophrenia during both resting-state (455) and task-based behaviour (456). In our study, the tracer signal represents neuronal activity over a prolonged period of 45 minutes, and therefore more closely mimics resting-state behaviour rather than task-based. It has been shown that under conditions of rest, patients with psychiatric disorders showed decreased cerebral metabolism in areas of the PFC, and in particular the Dorsolateral Prefrontal Cortex (DLPFC) (457). The DLPFC (Brodman's areas 9 and 46) in humans is a functional and anatomical homologue of the Prl cortex in rodents (458), and so the reduced cerebral metabolism recorded for the Prelimbic cortices (mPrl and aPrl) in our study is translationally relevant to hypofrontality associated dysfunction of the DLPFC in schizophrenic patients. In studies on major depressive disorders (MDD), glucose metabolic abnormalities have also been reported for prefrontal cortex structures by Positron emission tomography (PET) neuroimaging techniques (459). These studies support the reported notion of schizophrenic-like symptomologies associated with Stage II HAT, as our functional brain images also reveal hypofrontality in infected mice.

Hypofrontality of infected mice also encompasses the medial prefrontal cortex, which has been associated with generation of slow-wave sleep (460). Under normal conditions, sleep is characterised by progressive reduction of neuronal activity, known as NREM sleep, the deepest phase of which is called slow-wave sleep (461). After the slow-wave sleep, REM sleep takes place which comprises of activated neurons and dreaming (462). The cycle then begins again with NREM until wakefulness is achieved (463). The most characteristic symptom of HAT is sleep perturbations, with reversed sleep-wake cycles and disturbed sleep architecture so that REM sleep is directly followed by wakefulness (464). Our study noted reduced utilisation of the ^{14}C-2-DG tracer in the medial prefrontal cortex, alluding to metabolic disturbances caused by infection, which may exacerbate the sleeping sickness.

5.6.4 Infected mice show globally reduced cerebral metabolism

Our study revealed a significant, global cerebral reduction in glucose utilisation of infected rodents as compared with their non-infected, control counterparts (Figure 6.1). Unfortunately, there have been no previous studies investigating cerebral glucose metabolism using functional brain imaging in Trypanosome-infected mice or rats for comparison. Nonetheless, the functional brain imaging protocol used in this study is widely utilised and has been highly effective in elucidating alterations in cerebral metabolism in multiple other independent mouse studies (152,465). The experimental approach used represents a refinement in relation to animal experimentation as it eliminates the need for prolonged restraint as utilised in the original protocol (150) and consequently reduces the suffering experienced by the animals. Interestingly, stress hormones such as the glucocorticoid cortisol in humans (466), and corticosterone in rodents (467), are associated with reduced levels of glucose metabolism within the brain and in particular of the hippocampus (468,469), so the potentially confounding

effects of stress are somewhat reduced by this protocol. However, parasitic neuroinvasion of the brain has also been associated with increased release of glucocorticoids (470), and so the relationship between stress, brain infection metabolism and glucocorticoid release may be an avenue for future research. However, we did not determine the impact of Trypanosome infection on circulating glucocorticoid levels in our animals, and so the potential contribution of this mechanism is unknown.

Ezeh and colleagues (471) reported reduced blood glucose levels in fasted *Trypanosoma brucei* infected rats following relapse of infection observed after diminazene aceturate treatment. This finding of hypoglycaemia following trypanosomal infection was corroborated by others in rabbits and cattle and parallels our own observations in here (Table 6.1) (472–474). Ezeh et al (471) postulated the reduced blood glucose levels could be attributed to increased metabolic rate due to fever, leading to increased glucose metabolism by the host or extensive utilisation of host glucose by the parasite (475).

5.7 Methods

5.7.1 Ethics Statement

All experiments were carried out under UK Home Office regulations; under project license number P15EA559A. The work was performed with the approval of Lancaster University Animal Welfare and Ethics Review Boards (AWERB). All CD-1 mouse studies were carried out in compliance with the UK Animals (Scientific Procedures) Act 1986.

5.7.2 Parasite Strain and Mouse Model

8-12 week old female CD-1 mice were purchased from Charles River (Margate, UK). 12 mice were randomly assigned to the control groups and 13 mice to the infected group. Animals were housed in groups, in individually ventilated cages (i.v.c's) with access to food and water *ad libitum*. Animals were subjected to standard housing conditions (21 ± ^{0}C, 45-65% humidity) with a 12 hour dark/light cycle (lights on 07:00).

Mice were infected intraperitoneally (*i.p.*) with an initial dose of 1 x 10^4 *Trypanosoma brucei brucei* GVR35 red-shifted luciferase VSL 2 in 200 µl of 1 x PBS, and infection allowed to progress for 21 days.

5.7.3 ^{14}C-2-Deoxyglucose Functional Brain Imaging

In accordance with previously published protocols by Dawson *et al* (151), cerebral glucose metabolism was determined using *14*C-2-DG functional brain imaging. In brief, mice were injected i.p. with the 4.635 MBq/kg of the isotope 2-deoxy-D-[^{14}C] glucose (dose volume of 2.5ml/kg) over a 10 second period, diluted in physiological saline. After injection, mice were returned to home cages for 45 minutes. Subsequently,

animals were sacrificed by cervical dislocation followed by decapitation. Brains were dissected out and immediately snap frozen in cold isopentane (-40^{0}C) and stored at -80^{0}C until further use. A blood sample was taken to measure blood glucose (mM/L) levels directly using an AccuChek Aviva glucose monitor.

A terminal blood sample was also collected from each mouse, taken from the neck via torso inversion. Samples were centrifuged at 13,000 rpm to separate the plasma, and stored at -80^{0}C until required. Liquid scintillation analysis (Packard) was conducted in triplicate to determine plasma ^{14}C levels, by placing 10ul plasma in 1ml scintillation fluid (Ecoscint XR, National Diagnostics).

Frozen brains were mounted with Shandon^{TM} M-1 Embedding Matrix (ThermoFisher Scientific), and were sectioned coronally at 20 μm within a cryostat (-20^{0}C). A series of three consecutive brain slices were collected, thaw mounted onto cover slips (50 x 20mm) and rapidly dried on a hot plate at 70^{0}C. The following series of three slices were discarded, and this process was repeated for the whole brain with the exception of the region surrounding the suprachiasmatic nucleus, whereby every section was collected.

The coverslips containing brain slices and ^{14}C standards (40-1069 nCi g^{-1} tissue equivalents; American Radiolabelled Chemicals, Inc) were opposed to autoradiographic film (Kodak, Biomax MR) within a darkroom for seven days. Then according to manufacturer's instructions, films were developed using an automated film developer (Konica Minolta, SRX-101A).

5.7.4 Brain Imaging Analysis

Analysis of the autoradiographic images was conducted using computer-based image analysis (MCID/M5+), following established protocol in Dawson et al (152). Local isotope concentration for each brain region of interest (RoI) was derived from the optical density of the autoradiographic image relative to the co-exposed ^{14}C standard. A total of 50 anatomically distinct RoI were chosen (Figure 6.7), and measured with reference to a stereotaxic mouse brain atlas (476). Each region was measured between 10-12 times per animal (in both hemispheres of 10 brain slices if quality of sectioning allowed). Average whole slice isotope concentration was also measured at each level of the brain analysed, to determine the whole brain average ^{14}C level for each animal.

5.7.5 Statistical Analysis

The effect of Trypanosome infection on the tissue ^{14}C-2-deoxyglucose concentration was analysed using a Student's t-test, with significance set at $p < 0.05$.

5.8 Representative brain sections

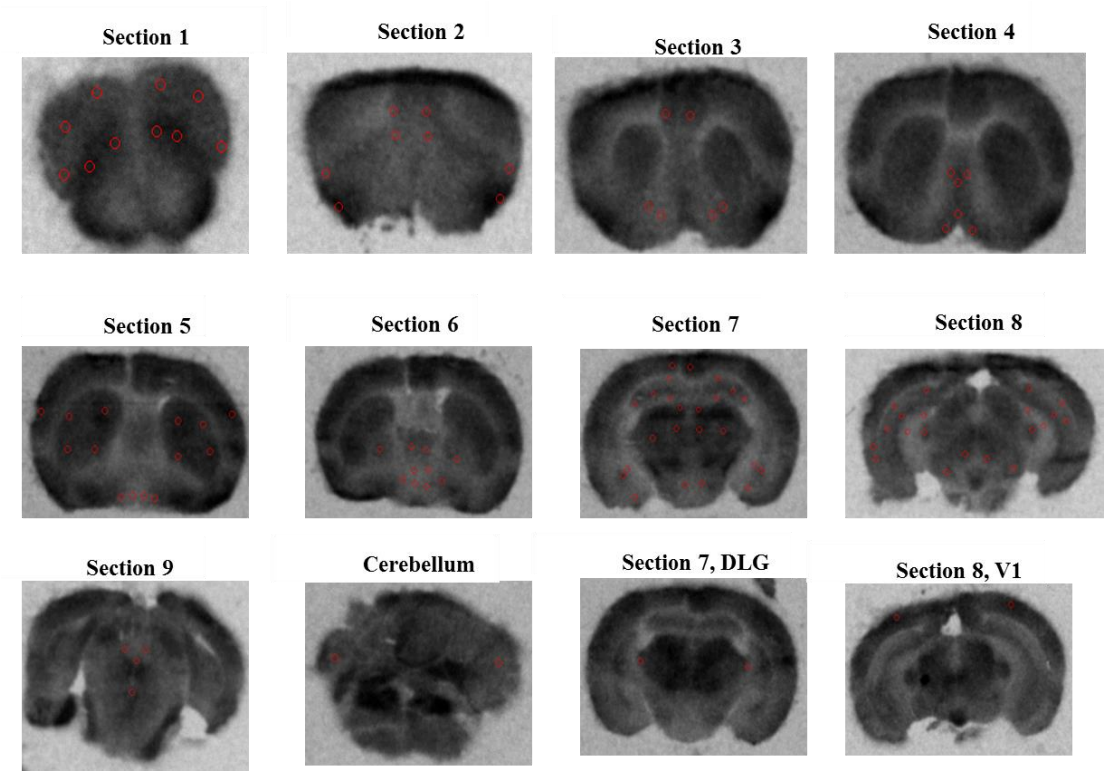

Chapter 6.0 Genetic manipulation of *Trypanosoma brucei brucei*

6.1 Introduction

Tryptophan is an essential amino acid and as such must be supplied in the diet, usually as a constituent of protein (477). Analysis of the *Trypanosoma brucei* genome (196) identified trypanosome proteins putatively involved in tryptophan uptake and metabolism, including metabolic genes such as aromatic transamidases (Cytosolic Aspartate Aminotransferase, CASAT; Tb927.10.3660), a cytosolic malate dehydrogenase (Aromatic L-2-hydroxyacid dehydrogenase, CAHADH; Tb927.11.11250), a kynurinase (Tb927.9.2010) and amino acid transporters (AAT6; Tb927.8.5450) (186,193–195). However, the potential effect of these specific proteins upon tryptophan uptake, incorporation and excretion remains to be elucidated (197).

Through the use of tetracycline inducible RNA interference (RNAi), our work aimed to investigate whether the aforementioned genes were essential to *T. b. brucei* blood-stream form cell proliferation, morphology or cell cycle. In addition, we aimed to develop these genetic manipulation tools to interfere with the tryptophan pathway for future characterisation.

6.2 Research objectives

i. To use RNAi techniques to knock-down genes putatively involved in tryptophan uptake and/or metabolism in *Trypanosoma brucei brucei.*

ii. To utilise RT-qPCR to verify the effectiveness of the knockdown system.

iii. To characterise the impact of gene knock-down on cell proliferation, morphology and the cell cycle.

iv. To employ *In Silico* analysis to create a three-dimensional (3D) model structure of *Trypanosoma brucei brucei TbCASAT* using comparative protein structure homology modelling.

v. To investigate the potential effect of structural changes to the metabolic enzyme *TbCASAT* that would result from site-directed mutagenesis.

6.3 Methods Summary

Methods in this chapter include molecular biology techniques, transfections, tetracycline inducible RNA interference (RNAi), real-time quantitative PCR (qPCR), and comparative protein structure homology modelling.

6.4 Summary of findings

1. *TbCASAT,* but not *TbCAHADH* or *TbKynurinase,* is essential for blood-stream form *T. b. brucei* cell proliferation.
2. A 3D model structure of *Trypanosoma brucei brucei TbCASAT* was built using the SWISS-MODEL programme.
3. The Serine-131 residue identified on the model CASAT crystal structure of *Trypanosoma brucei brucei* was recognised as a potential target for site-directed mutagenesis.

6.5 Results

6.5.1 Generation of RNAi constructs

6.5.1.1 Cloning into inducible stem-loop pRPa vector plasmid

RNAi cell lines *TbAAT6*, *TbCAHADH* and *TbKYNURINASE* (Figure 6.1, panels 1A and 3A respectively) were made by transfecting 2TI blood-stream form *Trypanosoma brucei brucei* with RNAi plasmids. Plasmids were made by amplifying a portion of the target genes using PCR primers that incorporate two pairs of restriction enzyme site that allow the amplified PCR fragment to be ligated into the stem-loop pRPa ($pRPa^{iSL}$) vector (478) in the sense and antisense direction, and digestion with *Xba*I & *Apa*I (Figure 6.1, panels 1B and 3B), produced an antisense fragment, whereas digestion with *Kpn*I & *Afl*II produced a sense fragment (Figure 6.1, panels 1C and 3C), each with the correct over-hang sequences for sequential integration into the $pRPa^{iSL}$ vector (Figure 6.2, panel A). The PCR inserts for target genes *TbAAT6* and *TbCAHADH* were created and provided by Yasmine Kumordzi (Summer Intern at Lancaster University). A tagged, stem-loop RNAi vector was chosen to eliminate positional effects of integration (479) and to provide more efficient knock-down as a consequence of RNAi transcript intramolecular base pairings. DNA sequencing was used to confirm that the cloning strategies had been successful in ligating the RNAi constructs with the vector. Figure 6.2 provides a schematic of the RNAi strategy used (479).

6.5.1.2 Cloning into p2T7-117 vector plasmid

The RNAi cell line for *TbCASAT* was initially made by attempting to transfect 2TI blood-stream form *Trypanosoma brucei brucei* with RNAi plasmids as detailed in section 6.5.1.1. Unfortunately, despite several attempts, no clones were recovered for *TbCASAT* after transfection of 2TI cells, and thus RNAi induction using this technique could not be conducted for that gene.

Following on from this, the RNAi cell line for *TbCASAT* was made by transfecting Single Marker (SM) blood-stream form *Trypanosoma brucei brucei* with the RNAi construct. The target gene was amplified by PCR (Figure 6.1, panel 2A), and digested with restriction enzymes *BamH*I and *Xho*I (Figure 6.1, panel 2B) for integration into the p2T7-117 RNAi vector. This genetic manipulation method was used based on work by McGettrick et al (190), whom published their publication at the same time as this work, and I attempted to reproduce their work using the exact same primers and RNAi vector.

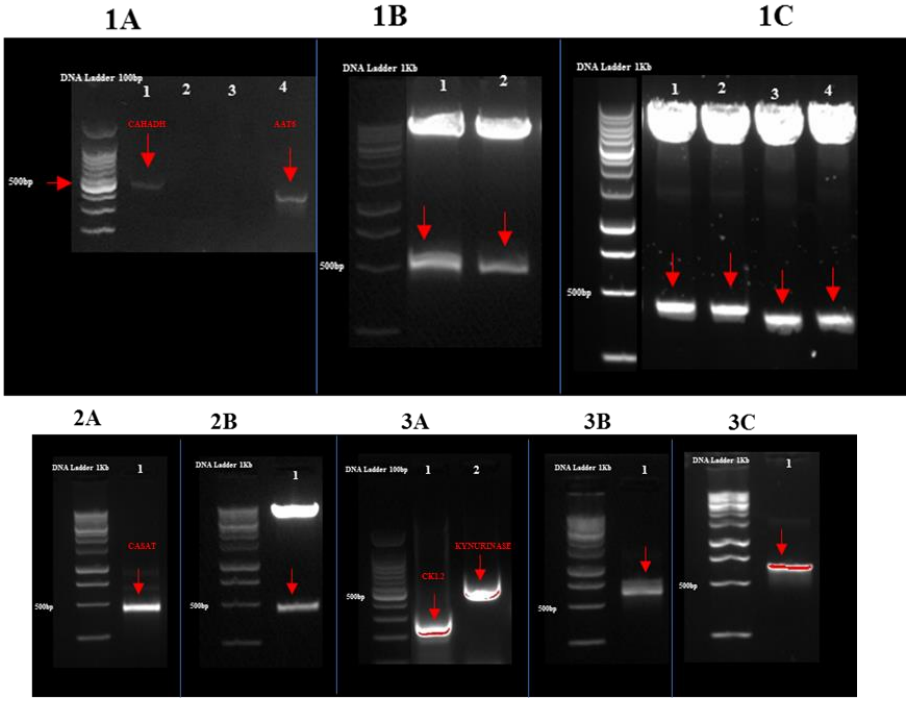

Figure 6.1 Generation of RNAi constructs by amplification of target fragments by PCR and restriction enzyme digests of PCR inserts

Agarose electrophoresis gels of the PCR gene inserts and respective restriction enzyme digest products, used for molecular cloning of RNAi constructs (**1A**) Lane 1: *TbCAHADH* fragment amplified by PCR. Lanes 2 & 3: Negative *TbCAHADH* and *TbAAT6* controls respectively, with no template genomic DNA. Lane 4: *TbAAT6* fragment amplified by PCR. (**1B**) Lane 1: *TbCAHADH* PCR product digested with antisense restriction enzymes *Xba*I and *Apa*I. Lane 2: *TbAAT6* PCR product digested with antisense restriction enzymes *Xba*I and *Apa*I. (**1C**) Lanes 1 & 2: *TbCAHADH* digested with sense restriction enzymes *Kpn*I & *Afl*II. Lanes 3 & 4: *TbAAT6* digested with sense restriction enzymes *Kpn*I & *Afl*II. (**2A**) Lane 1: *TbCASAT* fragment amplified by PCR. (**2B**) Lane 1: *BamH*I and *Xho*I analytical restriction enzyme digest of the p2T7-117 vector ligated with the *TbCASAT* gene, to confirm integration of construct. (**3A**) Lane 1: PCR amplified *TbCK1.2* fragment (positive control.) Lane 2: *TbKynurinase* gene amplified by PCR. (**3B**) Lane 1: *TbKynurinase* PCR product digested with antisense restriction enzymes *Xba*I and *Apa*I. (**3C**) *TbKynurinase* digested with sense restriction enzymes *Kpn*I & *Afl*II. 1kb and 100bp DNA molecular weight ladders are indicated as appropriate.

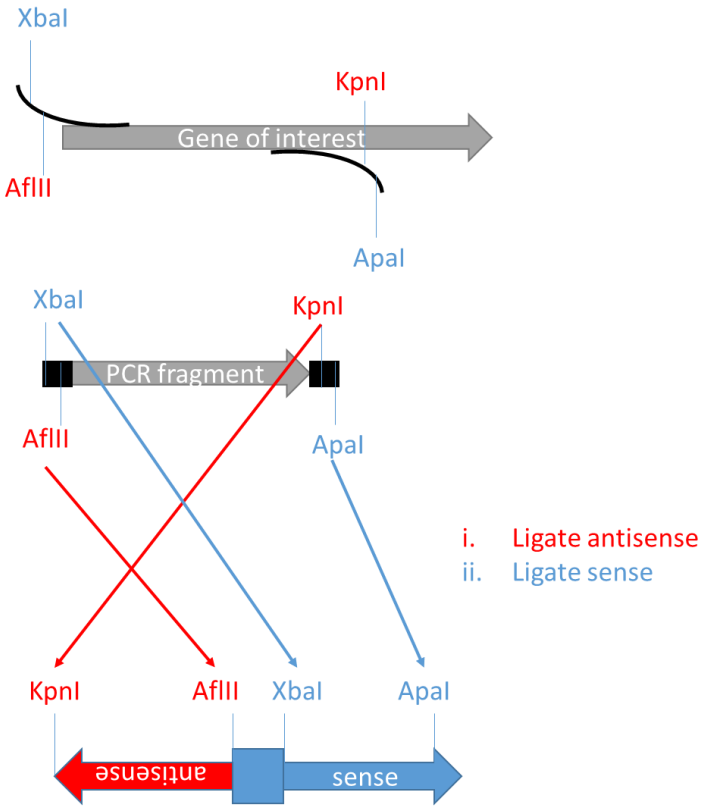

Figure 6.2 RNAi Plasmids pRPa^{iSL} and p2T7-117

Cloning strategy for inducible expression of stem loop RNA in *T. b. brucei* from a tetracycline-responsive RRNA promoter. RNAi plasmid was a gift from Dr Sam Alsford from the London School of Hygiene and Tropical Medicine (479).

6.5.2 *TbCAHADH, TbKynurinase and TbAAT6* are not essential genes for cell proliferation

The results presented in Figure 6.3 (panel 1A-3A) indicate that none of the three genes putatively involved in tryptophan metabolism, namely an aromatic dehydrogenase cAHADH (Aromatic L-2-hydroxyacid dehydrogenase; Tb927.11.11250), a kynurinase (Tb927.9.2010) and a putative aromatic amino acid transporter (AAT6; Tb927.8.5450) are essential in bloodstream forms of *T. b. brucei* for cell proliferation**.** We tested the efficiency of RNAi ablation by qRT-PCR analysis of mRNA expression in the knock-down cell lines (Figure 6.3 panels 1B-3B). Actin was used as a reference house-keeping gene, with log fold changes in mRNA expression portrayed as relative to un-induced cell cultures for each respective gene. Upon tetracycline induction for 48hours, *TbCAHADH* knockdown of around 88% mRNA expression and *TbKynurinase* of 89% mRNA was achieved (Figure 6.3 panels 1B, 2B). This certifies the system and confirms that gene knockdown has occurred. Surprisingly however, RNAi of *TbAAT6* resulted in a more modest reduction of mRNA expression, with only a 14% knockdown observed (Figure 6.3 panel 3B). Therefore, since the knockdown of *TbAAT6* is considerably modest, if the gene was to be essential it is unlikely that any significant effects would be observed for cell proliferation. Cells from all three cell lines grown in the absence and presence of tetracycline grow at rates comparable with the parental 2T1 strain, with no effect of induction up to 72 hours on cell proliferation or survival (Figure 6.3 panels1A-3A).

6.5.3 Knockdown of *TbCAHADH, TbKynurinase and TbAAT6* does not impact on cell cycle or cell morphology

Next, we sought to characterise whether inducible RNAi knockdown of *TbCAHADH*, *TbKynurinase* or *TbAAT6* impacted on cell cycle or cell morphology. Microscopy of DAPI stained cells (Figure 6.3 panels 1C-3C) was conducted to ascertain if RNAi knockdown resulted in any morphological changes or influenced the cell cycle. No changes in cell morphology were observed, and induction of RNAi did not alter the proportion of cells in each cell cycle phase.

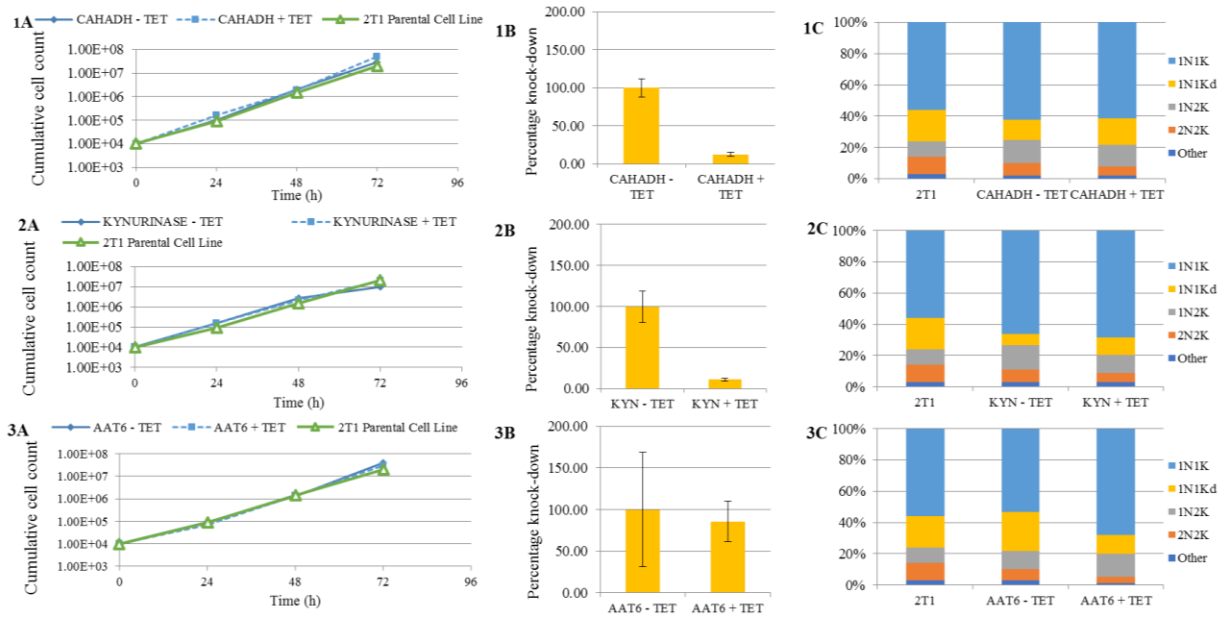

Figure 6.3 Representative growth curves for TbCAHADH, TbKynurinase and TbAAT6 RNAi transfected cells

Growth of RNAi cells for *TbCAHADH* (**1A**), *TbKynurinase* (**2A**) and *TbAAT6* (**3A**) in the absence (- Tet) and presence (+Tet) of tetracycline. Growth curves are representative examples of multiple experiments (n=3). Percentage knockdown of mRNA levels was determined using RT-qPCR for *TbCAHADH* (**1B**), *TbKynurinase* (**2B**) and *TbAAT6* (**3B**). DAPI staining for the three RNAi knockdown cell lines was conducted (**1C**, **2C**, and **3C** respectively).

6.5.4 RNAi knockdown of *TbCASAT* proves its essentiality for cell proliferation

For *TbCASAT* RNAi cells, 24 hours of induction with tetracycline resulted in the arrest of cell proliferation (Figure 6.4 panel 1). *TbCASAT* cells grown in the absence of tetracycline continue to grow at levels comparable with the parental SM BSF cell line. To confirm successful knockdown of the target gene, mRNA was extracted from lysed cells and used to quantify percentage knockdown of TbCASAT mRNA at 8, 24 and 48 hours post induction. RT- PCR data presented in Figure 6.4 panel 2 demonstrates a clear level of mRNA knockdown of around 20% as early on as 8 hours post induction, dropping to 78% at 24 hours and finally to 97% knockdown at 48hours.

6.5.5 RNAi knockdown of *TbCASAT* does not impact on cell morphology or cell cycle

Microscopy of DAPI stained cells (Figure 6.4 panel 3) was conducted to investigate whether knockdown of *TbCASAT* resulted in changed cell morphology and to determine if any of the induced cells had any clear cell cycle defects. Neither distinct morphological abnormalities nor any noticeable cell cycle defects were observed for the *TbCASAT* cell line (Figure 6.4). Although knockdown of *TbCASAT* resulted in the arrest of cell proliferation, it is important to note that the cells appeared relatively unchanged with regards to K/N status. This suggests that the down-regulation of this enzyme does not affect kinetoplast division and cytokinesis, which could potentially be explored further using flow cytometry analysis to look at DNA replication for example. Data presented in this chapter show that *TbCASAT* is essential for bloodstream form *Trypanosoma brucei brucei* proliferation in culture.

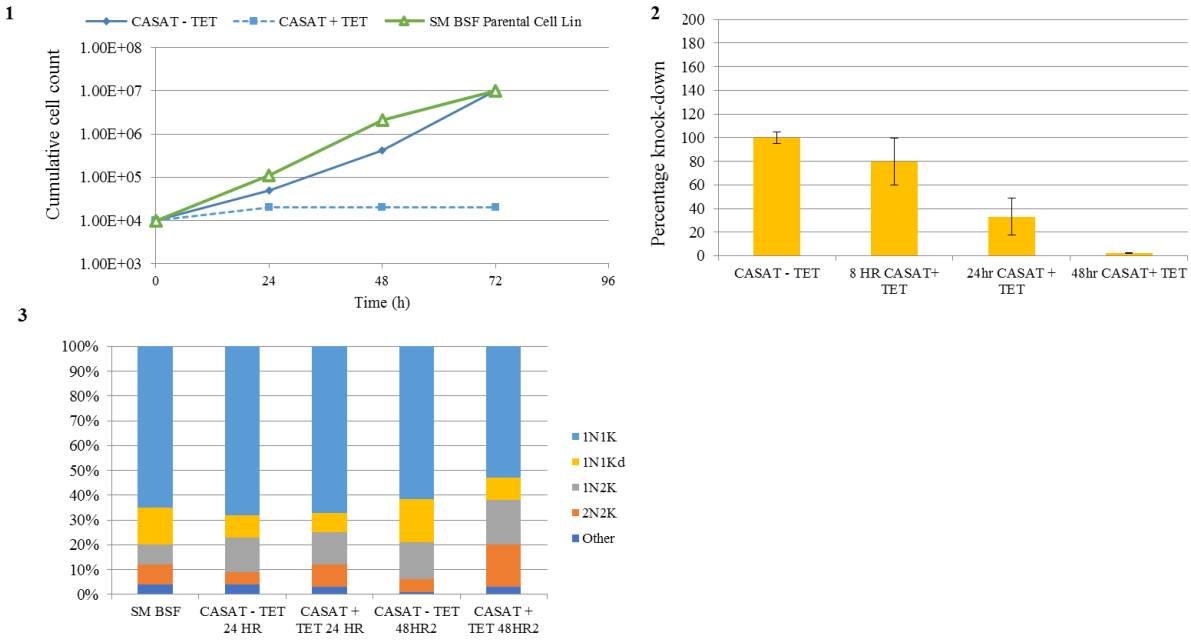

Figure 6.4 Representative growth curve for TbCASAT knockdown cells

Growth of knockdown cells *TbCASAT* (**1**) in the absence (- Tet) and presence (+Tet) of tetracycline. The growth curve is a representative example of multiple experiments (n=3). Percentage knockdown of mRNA levels was determined using RT-qPCR (**2**). DAPI staining for the RNAi knockdown cell line was conducted (**3**).

6.5.6 Protein Homology Modelling

Findings from the study by McGettrick *et al* (190), corroborated by the work presented in this chapter, revealed *TbCASAT* to be essential for cell survival and proliferation in *T. b. brucei*. Since genetic ablation of *TbCASAT* is lethal, we decided to investigate whether we could use genetic modification of the enzyme active site to reduce its turnover of tryptophan without effecting it transamidase activity towards other substrates. The strategy would be to alter the tryptophan binding properties of *TbCASAT*, rather than knocking the gene down, to further develop targeting the function of this enzyme to further understand the role of trypanosome tryptophan metabolism on the changes seen in the host. To investigate the potential influence of structural changes to the enzyme on its ability to bind large substrates such as tryptophan, we decided to employ protein homology modelling to determine suitable targets for site-directed mutagenesis. The tertial structure of *TbCASAT* is yet to be determined, and therefore the 3D model of the *T. brucei* ASAT protein (TbCASAT) (Figure 6.5) was built by comparative protein structure homology modelling with the program SWISS-MODEL. TbCASAT (Tb_cASAT Accession Number AAK73815) was aligned with orthologues from closely related flagellated protozoa and mammals consisting of *L. mexicana* BSAT (Lmex_BSAT, AAQ03600); *T. cruzi* CASAT (Tc_ASAT, XP807788) and Chicken CASAT using the T-coffee web-interface software (Figure 6.6). Identical residues among the multiple aligned ASAT isozyme sequences were identified, to determine sequence homology that might be indicative of residues essential to the function of the protein, and to determine the closest inter-species similarity for the protein. The closest template structure found, with the SEARCH FOR TEMPLATES command of SWISS-MODEL, was *Leishmania mexicana* broad specificity aminotransferase (BSAT; PDB 4WB0), which shared more

than 55% sequence identity to the target *T. brucei brucei* CASAT. Thus, the structure of *L. mexicana* BSAT was used as the structural template to generate the putative 3D ribbon structural model of the *T. b. brucei* CASAT.

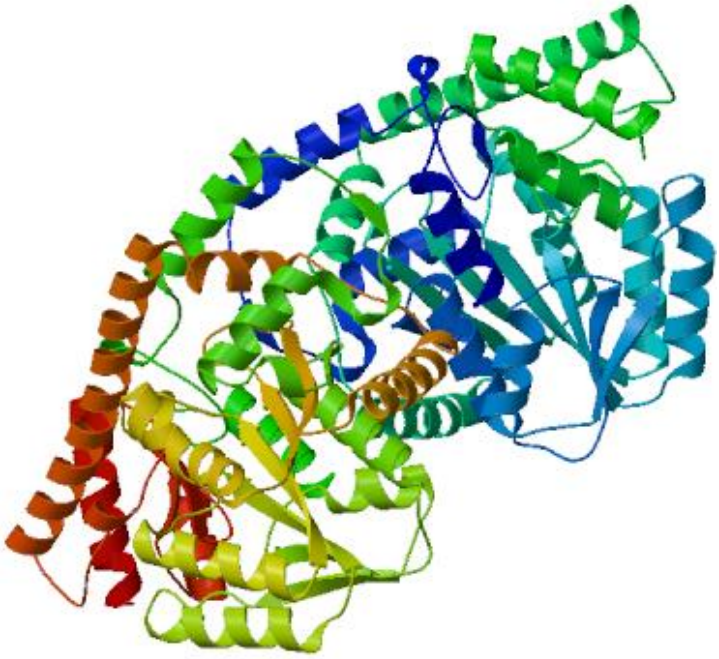

Figure 6.5 Tertiary Model of the T. b. brucei CASAT homodimer

The 3D model was built using the SWISS-MODEL programme, using *Leishmania mexicana* broad specificity aminotransferase (BSAT) as the structural template.

Figure 6.6 Comparison of the amino acid sequences of TbCASAT with L. mexicana BSAT, T. cruzi CASAT and chicken CASAT

T. brucei cASAT was aligned with orthologues from closely related flagellated protozoa and mammals using the T-coffee web-interface software. *T. brucei* cASAT (Tb_cASAT, AAK73815); *L. Mexicana* BSAT (Lmex_BSAT, AAQ03600); *T. cruzi* cASAT (Tc_ASAT, XP807788); Chicken cASAT. Identical residues among the multiple aligned ASAT isozymes are highlighted with an asterisk.

6.5.7 Putative Targets for Site-Directed Mutagenesis of *TbCASAT* to disrupt tryptophan metabolism

In a paper published in 2015 (480) the superposition of representative and structurally similar PDB 4WB0 (*L. mexicana* BSAT) and PDB 2CST (Chicken Cytosolic Aspartate Aminotransferase) revealed the conservation of important conformation residues, Arginine-291, Arginine-384 and, Arginine-328 between these proteins (Figure 6.7) in the active site. In the chicken cASAT the non-conserved Glutamic Acid-141 residue interacted with the flexible Arg-291 residue, resulting in a more closed form of the protein structure and a shallower substrate binding space unsuitable for larger substrates. In the *Leishmania* structure the Arg-292 residue does not interact with the equivalent residue (Asp-33), resulting in a large substrate binding pocket that may explain the broader specificity of the *LmBSAT* compared to the Chicken cASAT.

In the place of the residue Glu-141 on PDB 2CST (Figure 6.6), Serine-131 was found on the model CASAT crystal structure of *T. brucei*, as shown in Figure 6.8. Theoretically, this serine residue is unlikely to bind to the Arginine-292 residue. As precited for the Glu-141 in 2CST, this would allow CASAT to bind and use larger aromatic substrates, such as tryptophan. Therefore, if site-directed mutagenesis was to be carried out on template CASAT to change Serine-131 to Glutamic Acid, Proline, Threonine, Asparagine, Tyrosine and Aspartic Acid, all of which are amino acids with the potential to bind the highly conserved Arg-291 residues found on the model *T. brucei* cASAT structure, this would theoretically hinder the binding of larger substrates, such as tryptophan, to the enzyme and in turn decrease the metabolism of tryptophan to Indole-3-pyruvic acid, which has neurotoxic downstream metabolites.

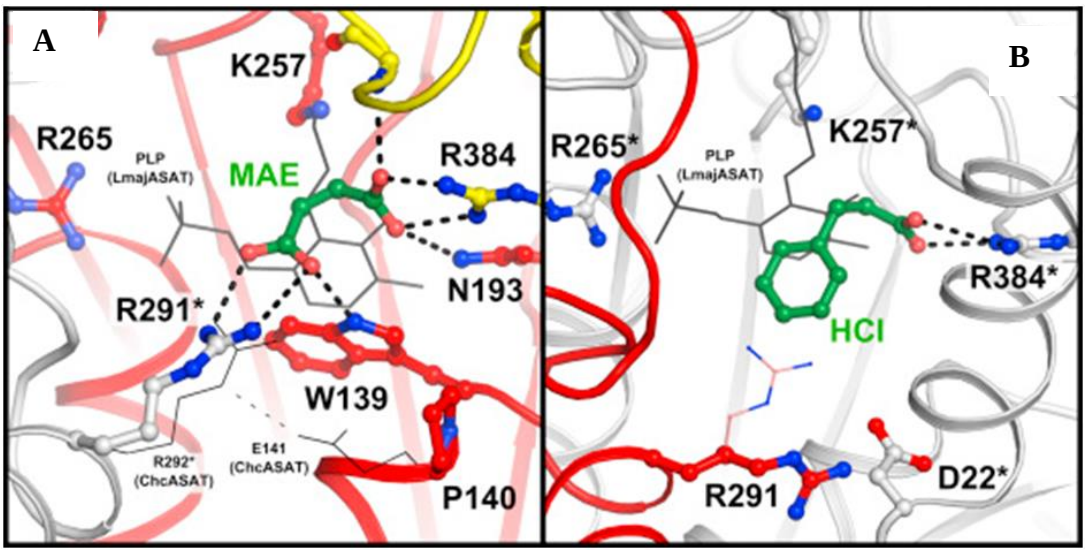

Figure 6.7 Details of the active sites of L. mexicana BSAT (PDB 4WB0) shown from similar orientations

(A) The superimposition of LmexBSAT with ChcASAT in complex with maleate (PDB entry 2CST; MAE: maleate; thin black lines show the position of PLP in LmajASAT and of E141 and R292* in ChcASAT as indicated). (B) Flexibility of R291 indicates how aromatic substrates may be bound. The ligand 3-phenylpropionate has been placed by superimposition of the more open monomer of LmexBSAT with the respective complex of PdARAT (PDB entry 1AY8; HCI:3-phenylpropionate). The smaller ball-and-stick model represents the inward conformation of R291, which would lead to unfavorable interactions with aromatic substrates.

Figure adapted from Wen, Nowicki & Blankenfeldt 2015 (480)

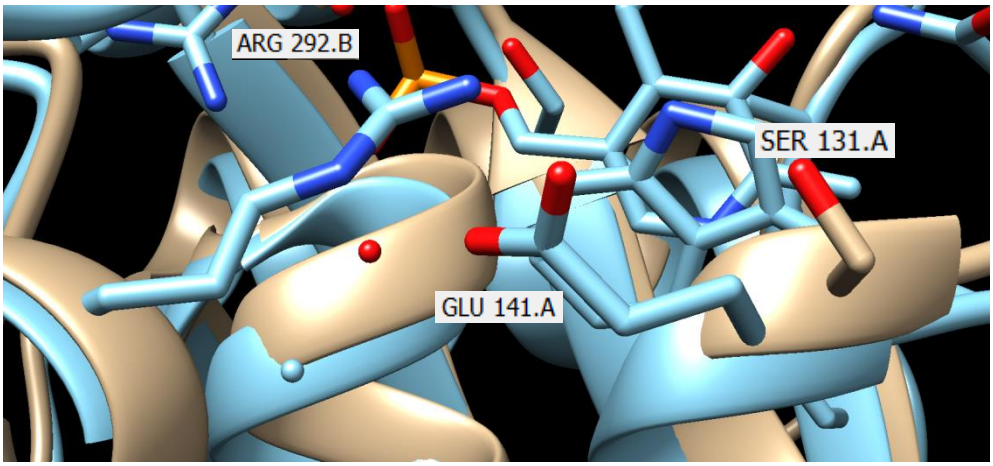

Figure 6.8 Details of residues predicted to make contact preventing the binding of larger substrates by cASAT in PDB 2CST

Model *T. brucei* cASAT enzyme is portrayed in the beige colour and the crystal structure of chicken cASAT (PDB 2CST) is portrayed in blue. Glutamic acid 141 (GLU 141.A) residue makes contact with the arginine residue 292 (ARG 292.B) in chicken cASAT to form a closed structure and disrupting the binding space available for larger substrates such as tryptophan. In place of the GLU 141.A, serine 131 (SER 131.A) is found in the model *T. brucei* CASAT, and this does not bind ARG 292.B. The lack of binding between these residues is predicted to allow an open structure that allows the binding of tryptophan. Thus, Serine 131 is identified as a candidate residue that could be subject to site-directed mutagenesis to modify the processing of tryptophan by *T. b. brucei* CASAT.

6.6 Summary

Table 6.1 Summary Table

Gene	Essential for Cell Proliferation	Percentage Knockdown after 48hrs
TbCAHADH	×	88%
TbAAT6	?	14%
TbKynurinase	×	89%
TbCASAT	✓	97%

A summary table of the *T. b. brucei* genes putatively involved in tryptophan metabolism, and genetically manipulated by tetracycline inducible RNAi methods to investigate essentiality. Out of the four genes investigated namely *TbCAHADH*, *TbAAT6*, *TbKynurinase* and *TbCASAT*, only *TbCASAT* was found to be essential for cell proliferation in culture, with arrested cell proliferation observed 24 hours after induction. Knockdown of all genes proved successful using the RNAi approach with strong mRNA suppression, apart from *TbAAT6* whereby only partial knockdown was achieved (14%).

6.7 Discussion

The work presented herein aimed to use tetracycline-inducible RNA interference to ablate *T. b. brucei* genes putatively involved in tryptophan metabolism and uptake, and to investigate their essentiality for cell survival and proliferation. In addition, potential effects on cell morphology and cell cycle were characterised. Alternative strategies to use genetic manipulation to interfere with the tryptophan metabolism in *T. b. brucei* were also developed using computational modelling. There were three main findings from this study: (A) *TbCASAT* is essential for cell proliferation in culture, (B) *TbCAHADH* and *TbKynurinase* are not essential for cell survival, and (C) RNAi knockdown of *TbAAT6* was limited.

6.7.1 *TbCASAT* is essential for bloodstream form (BSF) *T. b. brucei*

African Trypanosomiasis is characterized by alterations in plasma and urinary metabolic profiles, with glucose depletion, altered amino acid levels and hyperketonaemia mimicking states of diabetes-like phenotype (382,481–483). It has been noted that in infected animals, a significant depletion of serum levels of amino acids such as tryptophan is observed (188), accompanied by the excretion of large amounts of metabolites of aromatic acids, which have long been postulated to play a role in the neuropsychiatric symptomology associated with the disease (189,484–487). A small number of *T. brucei* genes have been assigned putative functions in the tryptophan/kynurenine pathway (196), which is of particular interest to our study due to the suggested interplay between tryptophan metabolites and pathogenesis of stage II disease, and our observations of tryptophan depletion in the brain at late stages of infection (6,316). Here we show, through RNAi analysis, that a cytoplasmic aminotransferase (*TbCASAT,* Tb927.10.3660*),* which catalyses the transamination of

aromatic amino acids, is essential in bloodstream forms of *T. brucei.* Termed an aminotransferase, this *T. brucei* enzyme has diverged evolutionary to accompany larger substrates, such as tryptophan (193). Although the precise reason for the obligatory requirement for *TbCASAT* in bloodstream forms remains to be elucidated, a number of metabolomic and kinetic studies provide some potential insight. McGettrick et al (190) indicated that aromatic amino acids such as tryptophan act as amino acid donors for transamination of oxaloacetate, generating intracellular aspartate which is essential. The same study also showed that when tryptophan was the amino acid donor, oxaloacetate was the preferred ketoacid acceptor. This substrate pair preference was corroborated by metabolic data showing that intracellular aspartate was mainly synthesized from oxaloacetate derived from glucose, and not by the uptake of aspartate (488). Further, kinetic studies have shown that *TbCASAT* has a preference (lower K_m) and higher V_{max}/K_m ratio for tryptophan as the amino donor when compared with tyrosine, phenylalanine or aspartate (193). This was in contrast with the enzymes activity in *Trypanosoma cruzi,* which was reported to be less selective and non-discriminatory towards aromatic amino acids and aspartate (195). Decreased intracellular levels of aspartate in the knockdown *TbCASAT* cell line could account for the deleterious effects observed on cell proliferation in our study for two main reasons. First, aspartate is essential for the production of the nucleotide uridine monophosphate (489) and secondly, since the parasites are auxotropic for purines, aspartate is also required for the synthesis of adenine nucleotides from hypoxanthine (a purine source provided in the culture medium) (490). Taken together this suggests that aspartate produced by *TbCASAT,* through the metabolism of tryptophan, could have an essential role in the synthesis of essential nucleotides in *T. b. brucei.* This certainly warrants further systemic characterisation.

6.7.2 *TbKynurinase* is non- essential in cultured BSF *T. b. brucei*

The kynurenine pathway forms a major part of the tryptophan metabolism cascade (329). Both neurotoxic and neuroprotective catabolites are produced along this pathway, with their role in activating the immune system to generate CNS inflammation becoming increasingly documented in a myriad of diseases (306,347,491–493). Inhibition of the host kynurenine pathway has previously been shown to reduce CNS inflammation in a mouse model of human African Trypanosomiasis, supporting a key role for this pathway in the disease (233). In the same study the authors described how their findings demonstrate that catabolites produced along the kynurenine pathway are involved in the generation of inflammatory reactions associated with late stage II African Trypanosomiasis, and so further research is warranted in order to establish potential targets for ameliorating post-treatment reactive encephalopathy (PTRE) through this pathway. The authors proposed the manipulation of the pathway would provide a more neuroprotective environment, reducing overall inflammation. Based on this rationale, we decided to use RNAi analysis to knockdown a parasite gene putatively involved in the kynurenine pathway. We have shown, using a tetracycline inducible knockdown system, that the kynurinase enzyme (*TbKynurinase*, Tb927.9.2010) putatively assigned the role of catalysing the conversion of kynurenine to anthranilic acid (AA), is non-essential in cultured BSF *T. b. brucei.*

6.7.3 *TbCAHADH* is non- essential in cultured BSF *T. b. brucei*

The kynurenine pathway is responsible for around 95% of the degradation of the essential amino acid tryptophan (266). In humans, the remaining 5% of tryptophan is metabolised to 5-hydroxytryptophan and further downstream to 5-hydroxytryptamine (serotonin) and melatonin (494). In the case of procyclic form (PCF) *T. brucei,* a

cytosolic malate dehydrogenase isozyme (*TbCAHADH,* Tb927.11.11250*)* is present (495,496). Three different malate dehydrogenase isoenzymes are present in PCF *T. brucei,* namely mitochondrial, glycosomal and cytosolic, but only the latter is expressed in the BSF at seemingly more abundant levels than those found in PCF (495) In *Trypanosoma cruzi*, a similar enzyme namely aromatic α-hydroxy acid dehydrogenase is implicated in the metabolism of Indole-3-pyruvic acid into Indole-3-lactic acid (497), with the same study postulating that although the enzyme lacks malate dehydrogenase activity, it is derived from a cytosolic dehydrogenase no longer present in the parasite. Indole-3-lactic acid is a metabolite excreted by *T. b. brucei* into cell culture medium without any known neuroactive properties (498). Here we show, using RNAi genetic manipulation, that *TbCAHADH* is non-essential in cultured BSF *T. b. brucei.* CAHADH's function in tryptophan metabolism is yet to be established. In eukaryotes, the biological role of cytosolic malate dehydrogenase has been clearly established (496), namely its involvement together with aspartate aminotransferase in the transfer of reducing equivalents from the cytosol to the mitochondrion (499). Epimastigotes of *Trypanosoma cruzi* have a similar cytosolic malic enzyme (500), implicated in the pathway which leads to the generation of reduced NADP (NADPH) in the cytosol, and this is required for fatty acid synthesis (501).

6.7.4 Genetic Manipulation of *TbAAT6* was unsuccessful

Mathieu et al (502) revealed AAT6 to be a low-affinity, low-selective transporter for aromatic amino acids such as tryptophan, phenylalanine and tyrosine in *in vitro* culture settings, and a high affinity transporter has yet to be identified.

An inducible RNA interference library established by Burkard et al (503) characterised a novel drug transporter in BSF *T. brucei*. In the same study RNAi induction and selection of resistant parasites in the presence of eflornithine helped identify the amino

acid transporter AAT6 (Tb927.8.5450), whereby knockdown of AAT6 increased resistance to eflornithine by approximately 5 fold. The authors reported on the modestly reduced mRNA levels to 30-35%, and later clarified the clinical relevance of their findings as levels of eflornithine are administered at high doses with little lee-way in dosage options. Concurrent with the findings of Burkard and colleagues, two other independent research groups acknowledged AAT6 (a member of the AAAP family; amino acid/auxin permease) as the entry gate for the drug eflornithine (504,505). Eflornithine [DFMO (difluoromethylornithine)] is used as a first line defence to treat stage 2 human African Trypanosomiasis (506).

RNAi manipulation of AAT6 in our study was conducted with the aim of investigating the effect of knockdown upon the rate of tryptophan uptake and metabolism in future studies. We attempted to show using RNAi genetic manipulation and growth curves that *TbAAT6* is non-essential in cultured BSF *T. b. brucei* and did not influence cell morphology or the cell cycle. However, validation of the RNAi cell line revealed an insufficient reduction of 14% in AAT6 mRNA levels revealing a robust knockdown was not achieved, and so the findings were deemed unfounded. The transfection work outlined in our study was carried out in 2T1 BSF cells using the inducible stem-loop pRPa vector, which has been characterised as a robust and efficient technique providing a single marked locust for reliable and reproducible transgene expression (479). Nevertheless, tetracycline-responsive gene knockdown in trypanosomes also has known limitations. For example undesirably high and “leaky” expression of the target gene in the absence of induction is regarded as the main cause of reported bleed-through characteristic of RNAi-induction in non-induced cells (507). Use of the alternative p2T7-117 minichromosomal vector in the transfection of single-marker BSF cells for

AAT6, as in the case of CASAT in our study, would have ensured integration to the minichromosomal repeats (507). Although it is a transcriptionally silent region, using the minichromosomal vector would have provided a tighter state for knockdown of sensitive transcripts (507). Taken together, this vector seems a suitable option to be explored for future work. Further, while RNAi knockdown has been the most widely utilised technique to study loss of function phenotypes, there are other strategies in place to create regulated conditional null mutant *T. brucei* using Cre recombinase and loxP sites (508). This would be another mechanism by which to investigate primary effects of gene knockout on expression and functionality of genes such as *TbAAT6.* The labour-intensive generation of several constructs, transfections and clones to confirm tight regulation of the conditional allele would be worthwhile for future experiments investigating AAT6 in the context of tryptophan metabolism.

6.7.5 Site-Directed Mutagenesis to alter substrate specificity of key enzymes, to influence *Trypanosoma brucei* tryptophan metabolism

Here we show, through RNAi analysis that a cytoplasmic aminotransferase (*TbCASAT,* Tb927.10.3660*),* which catalyses the transamination of host aromatic amino acids, is essential in bloodstream forms of *T. brucei.* Termed an aminotransferase, this *T. brucei* enzyme has diverged evolutionary to accompany larger substrates such as tryptophan (193). Although the precise reason for the obligatory requirement for *TbCASAT* in bloodstream forms remains to be elucidated, a number of metabolomic and kinetic studies provide some potential insight. McGettrick et al (190) indicated that aromatic amino acids such as tryptophan act as amino acid donors for transamination of oxaloacetate, generating intracellular aspartate which is essential.

In a paper published in 2015 (480) the superposition of representative and structurally similar PDB 4WB0 and PDB 2CST (Chicken Cytosolic Aspartate Aminotransferase) revealed the conservation of conformation of residues Arginine-291, Arginine-384, Arginine-328. Residue Glutamic Acid-141 found only on the 2CST model revealed a functional role, binding the flexible Arg-291 residue resulting in a much more closed form of the structure and disrupting the substrate binding space suitable for larger substrates.

From this, we decided to utilise protein homology modelling to build the 3D model of the *T. brucei* cytosolic ASAT, since the crystal structure of cytosolic aspartate aminotransferase (cASAT) was yet to be determined. In the place of the residue Glu-141 on PDB 2CST, Serine-131 was found on the model cASAT crystal structure of *T. brucei*. This means that the serine residues does not bind the arginine 292 residue and thus allows cASAT to bind and use bigger aromatic substrates, such as tryptophan. Therefore, we planned to make use of site-directed mutagenesis conducted on template cASAT to change Serine-131 to Glutamic Acid, Proline, Threonine, Asparagine, Tyrosine and Aspartic Acid, all of which are amino acids with the potential to bind the highly conserved Arg-291 residues found on the model *T. brucei* CASAT structure. This would hinder the binding of larger substrates to the enzyme and in turn decrease the metabolism of tryptophan to Indole-3-pyrvuic acid, which has neurotoxic downstream metabolites. This output from this reduced turnover due to altered substrate specificity could then be measured by LC-MS/MS. Future research is required to develop this experimental hypothesis further.

6.8 Methods

6.8.1 *Trypanosoma brucei brucei* growth, maintenance and transfection techniques

6.8.1.1 Trypanosome Cell line and Culture

Blood-stream form *Trypanosoma brucei brucei* strain 427 2T1, created by Alsford & Horn (478) was kindly gifted to the Urbaniak research group by Prof David Horn, Dundee University. 427 2T1 cells were sustained in standard HMI 11- T Glx (10% FBS, 5% 100 x Glutamax, 1% Antibiotic/Antimycotic) with Puromycin (0.2ug/ml) and Phleomycin (0.5ug/ml). Blood-stream form Single marker (SM) 427 *Trypanosoma brucei brucei* cells were maintained in HMI 11- T Glx (10% FBS, 5% 100 x Glutamax, 1% Antibiotic/Antimycotic) with G418 (2.5 ug/ml). All cell cultures were maintained at 37°C in a humid 5% CO_2 atmosphere.

6.8.1.2 Transfections & RNAi Induction

pRPa^{iSL} plasmids containing stem-loops targeting *TbCAHADH*, *TbAAT6* and *TbKynurinase* to be used in transfection protocols were linearized using *Asc*I, and transformed into the 2TI RNAi parental cell lines using the AMAXA parasite nucleofection instrument and Roditi transfection buffer (503). 2TI RNAi cell lines were maintained by selection in hygromycin (2.5ug/ml) and phleomycin (0.5ug/ml) as described previously (509). 2T1 construct *TbCASAT* to be used for transfection was linearized with *Not*I, and transfected into the Single Marker (SM) parental cell line using the AMAXA parasite nucleofection instrument and Basic Parasite Nucleofector^{TM} Kit 2, following manufacturer's instructions (Bioscience, Lonza). Following transfection of SM, cells were maintained with G418 (2.5 ug/ml) and Phleomycin (2.5 ug/ml) as described previously (190). Expression of the dsRNA was

induced by addition of tetracycline (1µg/ml). HMI-11 medium was placed under UV in the cell-culturing hood overnight to destroy any possible UV-sensitive tetracycline in the media before use in the transfections.

6.8.2 Molecular Cloning

6.8.2.1 Polymerase Chain Reaction (PCR)

For PCR reactions, 0.5 ng of template *T. brucei* 427 genomic DNA was placed in the PCR machine in a final volume of 50 µl with 1 µl of each primer, 1 µl dNTP mixture (10mM), 6 µl of $MgCl_2$ stock, 10 µl of Green Flexi Buffer (5x), 0.25 µl of GoTaq DNA polymerase and 30.25 µl of water as recommended by the manufacturer (GoTaq G2 Flexi DNA Polymerase, Promega).

Cycling Parameters included: 94 °C for 2 min, then 35 cycles of 94°C for 1 min, 60 °C for 1.5 min, 72 °C for 2 min, 72 °C for 5 min, followed by 4 °C cooling period.

PCR-amplified from genomic DNA was used for target genes *AAT6, Kynurinase, cASAT,* and *cAHADH.* The primer were ordered from Sigma Aldrich (UK) and sequences for these are shown in Table 6.2.

6.8.2.2 Agarose Gel Electrophoresis

1% Agarose gels were made using Ultrapure Agarose (Sigma Aldrich) in 1 x TAE buffer (Tris-Acetate-EDTA; 2M Tris Base, 5.7% (v/v) glacial acetic acid, 50 mM EDTA, pH 8). This mixture was heated in a microwave until the liquid was lightly boiling. The agarose mixture was then cooled to ~ 50^0C and 1 x GelRed Nucleic Acid Gel stain (Sigma Aldrich) was added. Agarose gels were cast into a gel tray with combs in place (VWR) and allowed to set at room temperature. Set gels were placed in a gel tank filled with 1 x TAE buffer. DNA samples were mixed with 5 x DNA loading dye (50% glycerol in 1 x TAE, Bromophenol Blue, Xylene Cyanol, pH 8.0) and loaded

using gel loading pipette tips. A DNA ladder (NEB, UK) was also loaded to the gel to provide size markers. The gel was then subjected to electrophoresis at a constant voltage (150 V) for an appropriate amount of times (~45 minutes). Gels were then visualised on a GelDoc EZ Imager machine (Bio-rad) using Image Lab Software (Bio-rad).

Table 6.2 The forward and reverse oligonucleotide sequences of primers used in amplification of target genes

Oligonucleotide	Type	Sequence
TbAAT6	Forward	5'-*ttaatt* **ggtacc gggccc** ACCGGATGCAATCAGAAGAC- 3'
	Reverse	5'-*ttaatt* **cttaag tctaga** CGTAAACATGCTTCCCCAGT- 3'
TbCAHADH	Forward	5'-*ttaatt* **ggtacc gggccc** AAGCTTAATCCCCGATTCGT- 3'
	Reverse	5'-*ttaatt* **cttaag tctaga** GGGGAAAGAAAAGATGAGGC- 3'
TbKynurinase	Forward	5'-*ttaatt* **ggtacc gggccc** AGGTGGATTTTGCAAGTTGG- 3'
	Reverse	5'-*ttaatt* **cttaag tctaga** CAAGCAGCACATCCTTGAAA- 3'
TbCASAT	Forward	5'-*ttaatt* **ggatcc** AAGCAAAGATCAGTGGGCAACC - 3'
	Reverse	5'-*ttaatt* **ctcgag** ATCAGCCCTTCATAAACACC - 3'

The forward and the reverse oligonucleotide sequences of the primers used for the amplification of target genes *AAT6*, *Kynurinase*, *CASAT*, and *CAHADH*. Restriction enzyme sites are highlighted in bold. Spacer sites are highlighted in italics.

6.8.2.3 Recovery of DNA from Agarose Gels

The desired bands of DNA were visualised on a UV transilluminator (Promega, UK) and excised from the agarose gel using a scalpel blade. The DNA was recovered from the agarose using a commercially available extraction kit (GeneJET Gel Extraction Kit, ThermoFisher Scientific). Briefly, the agarose was melted by heating to 50 ^{0}C for 10 min, DNA the bound to a silica spin-column, washed with an ethanol based solution, air dried, and eluted with a buffer or nuclease free water.

6.8.2.4 Restriction Enzyme Digestion of DNA

Restriction enzyme digestions of *TbCAHADH*, *TbAAT6* and *TbKynurinase* PCR DNA products were conducted initially using a mixture of *Xba*I and *Apa*I antisense restriction enzymes at 37^{0}C overnight. The following day, the DNA from all three genes was digested with *Kpn*I and *Afl*II sense restriction enzymes at 37^{0}C overnight. Restriction enzyme digestion of *TbCASAT* was conducted using *Xba*I and *Xho*I enzymes. The RNAi plasmid vector pRPa^{iSL}, kindly gifted to the Urbaniak lab from Prof David Horn (Dundee University), was first digested with the antisense restriction enzymes, followed by digestion with the sense enzymes.

6.8.2.5 Ligations

A combination of purified PCR DNA product and purified digested vector (molar ration 1:2) was mixed with 1 µl T4 DNA Ligase, 2.5 µl Rapid Ligase Buffer (2 x), and made up with water to a total volume of 5 µl. Mixture was left to incubate at room temperature for 15 min.

6.8.2.6 Bacterial Transformation Techniques

For bacterial transformation, the procedure was carried out using New England Biolabs chemically competent cells according to manufacturer instructions. Once the ligation reaction was complete, 2.5 µl of ligation reaction was transformed using 25 µl of ice-cold competent bacterial cells (NEB 5-Alpha high efficiency *E. coli*). The mixture was placed on ice for 10 minutes, and then heat-shocked at 42 °C for exactly 30 sec. Mixture was then placed on ice again for 5 min, followed by the addition of 250 µl of room-temperature SOC outgrowth medium purchased from New England Biolabs (2% Vegetable Peptone, 0.5% Yeast Extract,10 mM NaCl ,2.5 mM KCl, 10 mM $MgCl_2$, 10 mM $MgSO_4$, 20 mM Glucose). The DNA/cell mixture was incubated at 37 °C with vigorous shaking (250 rpm) for 45 min, and then plated onto a Luria Broth-Ampicillin agar plate (15 g/L Agar, 10 g/L Tryptone, 10 g/L NaCl, 5 g/L Yeast Extract, 50µg/ml ampicillin) and left to incubate at 37 °C overnight.

6.8.2.7 DNA Miniprep

E. coli colonies on an LB plate were picked into 5ml of LB Broth with the appropriate antibiotic and grown for 16 h at 37 ^{0}C with shaking at 2500 rpm.. The cells were then harvested by centrifugation at 4,000 x g, and the plasmid DNA extracted using a commercially available kit (GeneJET Plasmid Miniprep Kit, ThermoFisher Scientific). In brief, cells were lysed with an alkaline solution, proteins removed by digestion with alkaline proteases, the resulting solution neutralised, and cell debris removed by centrifugation. Plasmid DNA was bound to a silica spin column, washed with an ethanol-based solution, air-dried, and eluted with elution buffer or nuclease free water.

6.8.2.8 DNA Sequencing & *In Silico* Analysis

Selected clones with the correct inserts were sent for DNA sequencing at the University of Dundee. *In Silico* analysis was carried out using CLC Sequence Viewer software.

6.8.2.9 Reverse Transcriptase Real-Time PCR (RT-qPCR)

T. brucei cells were lysed and total RNA extracted using the EZNA total RNA kit (Omega Bio-TEK), and treated with DNase I (ThermoFisher Scientific). The concentration of RNA was measured by using a Nanodrop 2000c spectrophotometer (ThermoFisher Scientific), and equal masses (100ng) of RNA were taken from each sample.

RNA was then reverse transcribed using the iScript cDNA Synthesis Kit (Bio-Rad Laboratories) according to manufacturer's instructions. Briefly, a 0.5 µl iScript reverse transcriptase and 2 µl 5 x iScript reaction mix was made up to 10 µl with RNA and nuclease-free water, and assembled in PCR tubes. iScript mixtures were then run on Eppendorf Master Cycler for 5 mins at 25 ^{o}C, 30 mins at 42 ^{o}C, 5 mins at 85 ^{o}C, then cooled to 4 ^{o}C

qRT-PCR amplification was carried out using 2 x FastStart Universal SYBR Green master mix (Roche; SYBR Green I dye, AmpliTaq Gold DNA Polymerase, dNTPs with dUTP Passive Reference, and optimised buffer components) on a LightCycler 96 realtime PCR instrument (Roche). The cycling parameters were as follows: initial denaturation at 95 ^{0}C for 600 sec; 40 cycles at 95 ^{0}C for 10 sec and at 60 ^{0}C for 30 sec, followed by a melt curve step. Quantification cycle (Cq) for the mRNA's of interest were normalised to Actin reference mRNA. Data was expressed as fold change and normalised to cells without tetracycline induction. PCR primers were synthesized by

Sigma Aldrich, for sequences see Table 6.3. Primers were designed to be specific only for the gene of interest.

Table 6.3 The forward and reverse oligonucleotide sequences of primers used in RT-qPCR

Oligonucleotide	Type	Sequence
TbAAT6	Forward	5'- GAACCTGCATGGAGATAAAC - 3'
	Reverse	5'- GCCAACAGCGAGTTCAATAC - 3'
TbCAHADH	Forward	5'- CTGCAGCTATTGGATATTAG - 3'
	Reverse	5'- GTGGTTACCCCAAATAATGC - 3'
TbKynurinase	Forward	5'- GCTAATAGCCTTCTACAAGC - 3'
	Reverse	5'- CAGGCTCAAATTTATAGGAC - 3'
TbCASAT	Forward	5'- CATTAAAAGTAGTGCGGAAG - 3'
	Reverse	5'- GGACTGTAGTAACGGTATTC - 3'

The forward and the reverse oligonucleotide sequences of the primers used for Reverse-Transcriptase PCR (RT-PCR) of target genes *TbAAT6, TbKynurinase*, *TbCASAT,* and Tb*CAHADH* to determine relative amounts of mRNA. This would act as a qualitative measure of RNAi gene knockdown.

6.8.3 Protein Comparative Structural Homology Modelling

The three-dimensional (3D) protein model of the *T. brucei* cytosolic ASAT was built by comparative protein structure homology modelling with the program SWISS-MODEL (510). The closest template structure found with the SEARCH FOR TEMPLATES command of SWISS-MODEL was *Leishmania Mexicana* broad specificity aminotransferase (BSAT; PDB 4WB0), which shared more than 55% sequence identity to the target ASAT.

Chapter 7.0 Summary and Future Work

The aim of this project was to develop the existing murine African Trypanosomiasis model to further characterise the host-parasite relationship in the generation of the neurological symptoms of HAT. The four main research objectives were to: (1) Map mammalian body system localisation of trypanosomes throughout infection. (2) Define the impact of trypanosome infection on tryptophan levels in the brain and other tissues. (3) Determine impact of trypanosome infection on rodent behaviour and brain metabolism. (4) Develop genetically modified trypanosomes with targeted disruption of genes putatively involved in tryptophan metabolism and uptake for use in future studies to further characterise the relevance of trypanosome tryptophan metabolism in African Trypanosomiasis neuropsychopathology.

7.1 African *Trypanosomiasis* infection causes wide spread tissue tropism, with a subset of infected animals experiencing early CNS invasion

In this study I attempted to bridge the gaps in our knowledge of the systemic time course of trypanosome infection and its infiltration of the brain in murine models. I addressed this aim by use of *ex vivo* bioluminescent imaging of *Trypanosoma brucei brucei* infected murine tissues at day 7 (early Stage I), 14 (intermediate Stage I-II) and 22 (late stage II) of infection. The findings showed that throughout the infection time course, parasite localisation throughout the body tissues is wide spread (discussed in detail in section 2.5). I was also able to detect a small subset of infected animals experiencing early CNS invasion, further evidencing the complexity of disease staging for HAT and highlighting the heterogeneity present in preclinical murine models of HAT CNS invasion. Interestingly, the data highlighted some important novel body tissue reservoirs, with potentially significant implications for HAT disease and as such are

worthy of further, in-depth exploration. For example, I identified punctate parasite localisation to gastrointestinal organs at all three time points of infection, highlighting the potential of neuro-gut-immune axis cross-talk in HAT. The identification of bioluminescent parasites in the eyes of some late stage II animals at day 22 was also interesting, due to the eye's high blood irrigation and the anatomical connectivity of the eye with the optic nerve projecting directly into the brain (302). I posited that this could provide an entry route for the parasites into the brain, yet very little is known about ocular *Trypanosomiasis,* with most clinical reports describing this pathology originating in the late 1970's (511–513). Parasites found in the aqueous humor of the eye may have profound implications, potentially serving as a source of relapse infection following chemotherapy (289). Future investigations are warranted to understand the degree of protection that the ocular environment provides the parasites from trypanocide treatment and the potential role of the eye in relation to CNS invasion by African Trypanosomes.

Due to technical limitations, I was unable to detect, with high anatomical resolution the exact brain regions colonised by the parasite. This somewhat limited my ability to correlate parasite regional colonisation with my observations in terms of the effects on rodent behaviour and regional cerebral metabolism. This highlights the need to further expand the *in vivo* imaging toolbox for *Trypanosoma brucei* (discussed in detail in section 2.5), which is considerably lagging as compared to currently available *Trypanosoma cruzi in vivo* imaging techniques (286, 514).

7.1.2 Future Investigations: Generation of dual-labelled Red-shifted Luciferase-mNeon Green construct for expanding *in vivo* localisation and phenotyping of *T. brucei*

Our *ex vivo* bioluminescent study of Trypanosome-infected mouse body tissues spring boarded the development of further appariaches to enhance currently available *in vivo* imaging techniques of rodent body tissues, with emphasis on improving *in vivo* imaging techniques of the brain in the context of late stage II *Trypanosomiasis*. Due to time constraints, this experimental investigation was not completed in its entirety during this PhD study.

Based on work by Costa *et al* (288) in *Trypanosoma cruzi,* I attempted to generate a dual-labelled Red-shifted Luciferase-mNeon Green construct for subcellular parasite localisation in *Trypanosoma brucei brucei*. I attempted this technical innovation, by transfecting a *T. brucei* reporter strain with the construct expressing a fusion protein comprising red-shifted luciferase and green fluorescent protein domains from Costa and colleagues. Given my previous observations on tissue localisation we wanted to generate a construct that allowed the specific foci of infection to be visualized, with individual parasites in tissue sections identified, to study host-parasite interactions at the cellular level. Unfortunately, while I was able to incorporate the construct into the reporter Red-shifted Luciferase GVR35 VSL2 *T. brucei* strain from culture, these trypanosomes proved too virulent when introduced into mice. Further work is required to carry on the experimental investigation, and to attempt the incorporation of the dual-labelled construct into less virulent pleomorphic VSL2 stock, by transfecting parasites obtained freshly from infected blood.

7.2 Brain specific biphasic tryptophan alterations occur during infection

It has been well established in previously published data that *Trypanosoma brucei gambiense* significantly deplete tryptophan in both *in vivo* and *in vitro* settings (188,189), with this also shown to be true in cases of stage II clinical samples (6). Perturbations to the tryptophan-kynurenine and tryptophan-serotonin pathway have

been implicated in the neuropathogenesis of psychiatric disorders such as schizophrenia (343) and bipolar disorder (344), and so we were interested in correlating potential imbalances in the tryptophan levels of infected animals to any behavioural phenotypes observed in behaviour studies (see Chapter 4). The data presented in this chapter aimed to investigate the impact of stage II *Trypanosoma brucei brucei* infection on tryptophan and its metabolites in rodent brain tissue using a LC-MS/MS system. We also expanded our study to investigate other body tissues such as the spleen, muscle, liver and gastrointestinal organs with varying degrees of parasite colonisation, based on the bioluminescent imaging data (see Chapter 2). There were three main findings from this work (discussed in detail in Section 3.7): (A) Brain tryptophan levels are increased at early stage I *Trypanosomiasis* infection (day 7). (B) By contrast, animals at late stage II (day 22) infection had decreased levels of tryptophan in the brain. (C) Elevated tryptophan levels in the spleen, muscle, liver and colon were evident at late stage II but not at early stage (day 7) infection.

We aimed to use HPLC-MS to investigate tryptophan and its associated metabolites. However, due to technical limitations, we were only successful in reporting on perturbations in tryptophan concentrations and not on the other downstream compounds. This was disappointing as we were particularly interested in also characterising serotonin and kynurenine metabolite level alterations during the early and late stage of infection. Unfortunately, the chromatographs obtained after analytical runs with brain samples yielded a strong signal for the peak assigned as tryptophan, with little to no signal for the other metabolites. In some cases, new peaks were detected for unknown compounds and as such we found that data obtained by HPLC was unsuitable for untargeted metabolite characterisation. Future work warrants the

inclusion of stable isotope-labelled internal standards for each metabolite of interest, as well as the incorporation of MS technology with ultra-high mass accuracy for the identification of the unknown metabolites (515). Further, a major consideration for our study was the sample preparation. We followed a well-established extraction technique (315) achieved by simultaneous cell lysis and extraction with organic solvent mixtures. However, perhaps rapid quenching of metabolism (516, 517) is recommended for future work, in order to capture the metabolites as close to their natural physiological state as possible.

7.3 Infection impacts on behaviour and causes a significant global reduction in cerebral glucose utilisation

This study presents an experimental model of African trypanosomiasis with CD-1 female mice infected with *Trypanosoma brucei brucei*, assessing the impact of infection on locomotor activity, anxiety-like behaviour and cognition. To our knowledge, this is one of the first models used to describe behavioural disturbances observed during the course of infection at three individual time-points representing the progression from the haemolymphatic phase (5 days) to the late stage meningoencephalitic phase (20 days). This work also used ^{14}C-2-Deoxyglucose functional brain imaging as a measure of cerebral glucose metabolism, to investigate the effect of Stage II *Trypanosomiasis* infection on cerebral glucose utilisation.

The OF test showed that infected mice display decreased locomotor activity in a novel environment, with infected animals moving slower and for shorter durations. This was only evident at later stages of infection (day 12 and 20) and not at the earlier time-point (5 days). These findings suggest that the OF test may act as a proxy for translationally relevant parameters of functional alterations observed in motor function during the later stages of HAT infection, particularly around the encephalitic stage of HAT (144). The

NORT revealed that infected mice could successfully differentiate between the familiar and novel objects, with a preference for novelty observed. This suggests that object recognition learning and memory is not impaired at later stages of infection, when trypanosomes are present in the brain (Chapter 2). This observation was somewhat surprising given that in the brain imaging study we identified reduced glucose utilisation in all brain regions of interest assessed. The results obtained from this study therefore strongly support a global impact on cerebral glucose utilisation.

The existing human literature indicates that general feelings of weakness and malaises are prominent early on, during the haemolymphatic stage of the disease (518). However, we found no significant difference between infected and control animals in terms of locomotor activity on day 5 of infection in rodents. Novelty of environment may act to counteract these feelings in mice, and thus future study could investigate early infected animals in a familiar environment (e.g. Home cage recording) to see if similar effects on activity are found (519). Home cage monitoring would also allow the characterisation of the sleep-wake cycle which would also be of interest in the context of *T. brucei* infection.

The NORT in the current study used both a 1 hour and a 24-hour delay to assess object recognition learning and memory in mice. A 24-hour delay allows the assessment of long-term memory consolidation thought to occur during sleep (520), and this is perturbed by sleep disturbances (521). This is particularly relevant to the clinical situation, as HAT patients are known to suffer from sleep perturbations (522). Areas of the brain known to be involved in the process of object recognition and long-term memory consolidation include the prefrontal cortex (523), hippocampus (524) and the amygdala (525). These cerebral regions were included in the brain imaging study we

undertook in *T. brucei brucei* infected mice (Chapter 5), with regions in each of these structures showing significantly decreased glucose utilisation (hypometabolism).

One of our initial leading hypotheses connoted a potential for the parasites themselves to be metabolising and utilising host glucose, in particular niches of the brain. This theory was proposed because it is known that trypanosomes depend upon glycolytic phosphorylation for energy generation (526) and can induce changes in host blood glucose levels following infection. However, if this were the case, we would have observed increased cerebral ^{14}C-2-DG utilisation in specific regions of the brain. Future work would expand on the findings presented in this study to ascertain; firstly what the parasitic burden of the infected brains was, to see if this correlates with decreasing cerebral metabolism, and secondly to investigate levels of brain glucose in infected rodents. Defining the relationship between quantified parasitic brain infection and the degree of cerebral glucose utilisation could be beneficial for treatment, allowing clinicians to modulate drug dosage based on this measure, and potentially avoiding the associated toxicity effects of inappropriately high doses (527). By looking at whole brain glucose levels during infection, we would be able to elucidate whether the brains of infected mice contained more glucose. The presence of high glucose concentrations within the brain may act to compete with the^{14}C-2-DG tracer, in terms of transport across the BBB and metabolism. Thus, this could potentially result in the observation seen here, a global reduction in brain ^{14}C-2-DG levels.

7.4 Generation of novel genetic *Trypanosoma brucei brucei* tools for the future characterisation of tryptophan metabolism in the host-pathogen relationship

This study aimed to use tetracycline inducible RNA interference to ablate *T. b. brucei* genes putatively involved in tryptophan metabolism and uptake, and to investigate the essentiality of these genes and their effects on cell cycle and morphology. To address

this research objective, trypanosome proteins putatively identified as being involved in tryptophan metabolism were chosen as targets for genetic manipulation. These included metabolic genes such as aromatic transamidases (Cytosolic Aspartate Aminotransferase, CASAT; Tb927.10.3660), a cytosolic malate dehydrogenase (Aromatic L-2-hydroxyacid dehydrogenase, CAHADH; Tb927.11.11250), a kynurinase (Tb927.9.2010) and amino acid transporters (AAT6; Tb927.8.5450) (186,193–195). There were three main findings from our study: (A) *TbCASAT* is essential for cell proliferation in culture, (B) *TbCAHADH* and *TbKynurinase* are not essential for cell survival, and (C) RNAi knockdown of *TbAAT6* was unsuccessful. Interestingly, the essentiality of the *TbCASAT* gene for cell proliferation (190) was also established by other researchers and published whilst this study was being undertaken. It is important to note that following the aforementioned publication, I made use of the same plasmid and primers detailed in their work.

7.4.2 Future Investigations: Could over-expression of key metabolic enzymes influence the tryptophan pathway towards a more neuroprotective branch?

Our data showed using RNAi genetic manipulation that *TbCAHADH* is non-essential in cultured BSF *T. b. brucei.* To date CAHADH's function in tryptophan metabolism is yet to be established. In eukaryotes, the biological role of cytosolic malate dehydrogenase has been clearly established (496), namely its involvement together with aspartate aminotransferase in the transfer of reducing equivalents from the cytosol to the mitochondrion (499). Epimastigotes of *Trypanosoma cruzi* have a similar cytosolic malic enzyme (500), implicated in the pathway which leads to the generation of reduced NADP (NADPH) in the cytosol, required for fatty acid synthesis (501). Further research could investigate the potential role of *TbCAHADH* in tryptophan metabolism

and examine if its role is analogous to that of the *T. cruzi* aromatic dehydrogenase. For example over-expressing the enzyme in BSF *T. brucei* would manipulate the pathway towards the production of lactic acid as opposed to pyruvic acid, providing a more neurostable environment which could potentially be beneficial in reducing neuroinflammation (528) in stage II HAT disease.

7.5 Conclusion

Overall the data presented in this thesis have shown that African *Trypanosomiasis* infection results in widespread tissue tropism in a mouse model of HAT, with some animals experiencing early CNS invasion. From these findings, parasite localisation to the eye represented a potential direct pathway into the brain, with punctate parasite localisation to the gut also implicating a potential role for neuro-immune-gut axis cross talk in HAT. Parallels between parasite entry to the brain and changes in tryptophan levels were observed, with findings of brain specific biphasic alterations in tryptophan throughout the course of infection identified that ultimately results in brain tryptophan depletion at the later stages of infection. Data presented showed that African *Trypanosomiasis* infection caused a hypolocomotor phenotype, and significantly influence global cerebral glucose utilisation. Finally, data presented in this thesis highlighted the development of novel genetically modify *Trypanosoma brucei brucei,* generated with the aim of influencing trypanosome tryptophan metabolism for utilisation in future *in vivo* studies. In conclusion, the data presented herein have developed novel approaches for understanding and have increased our knowledge of the neuropsychopathology associated with late stage II African *Trypanosomiasis*.

8.0 Appendix

Appendix 1. Bioluminescent images of *ex vivo* tissues from *i.p* infected day 7 mice

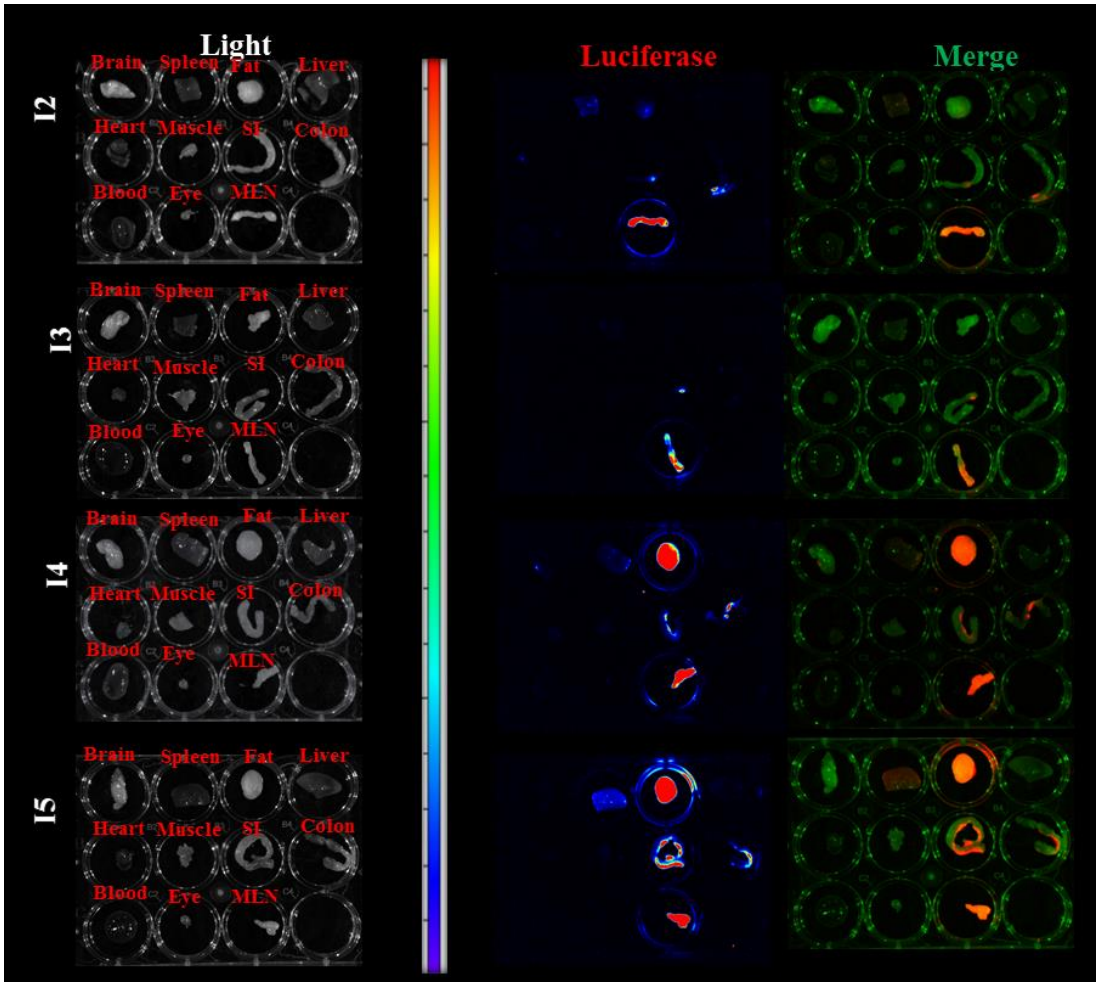

Post mortem bioluminescent imaging of representative infected mice following *intraperitoneal (i.p)* infection with 1 x 10^4 parasites, in the early stage I phase (Day 7) infection. The images in the left panel indicate arrangement of the dissected tissues in a 12-well plate format, images in the middle panel detailing the bioluminescent signal and images in the right panel showing the bioluminescent signal overlaying the tissue sample. All images are calibrated to the same scale. SI, Small Intestine; MLN, Mesenteric Lymph Nodes.

Appendix 2. Bioluminescent images of *ex vivo* tissues from *i.p* infected day 14 mice

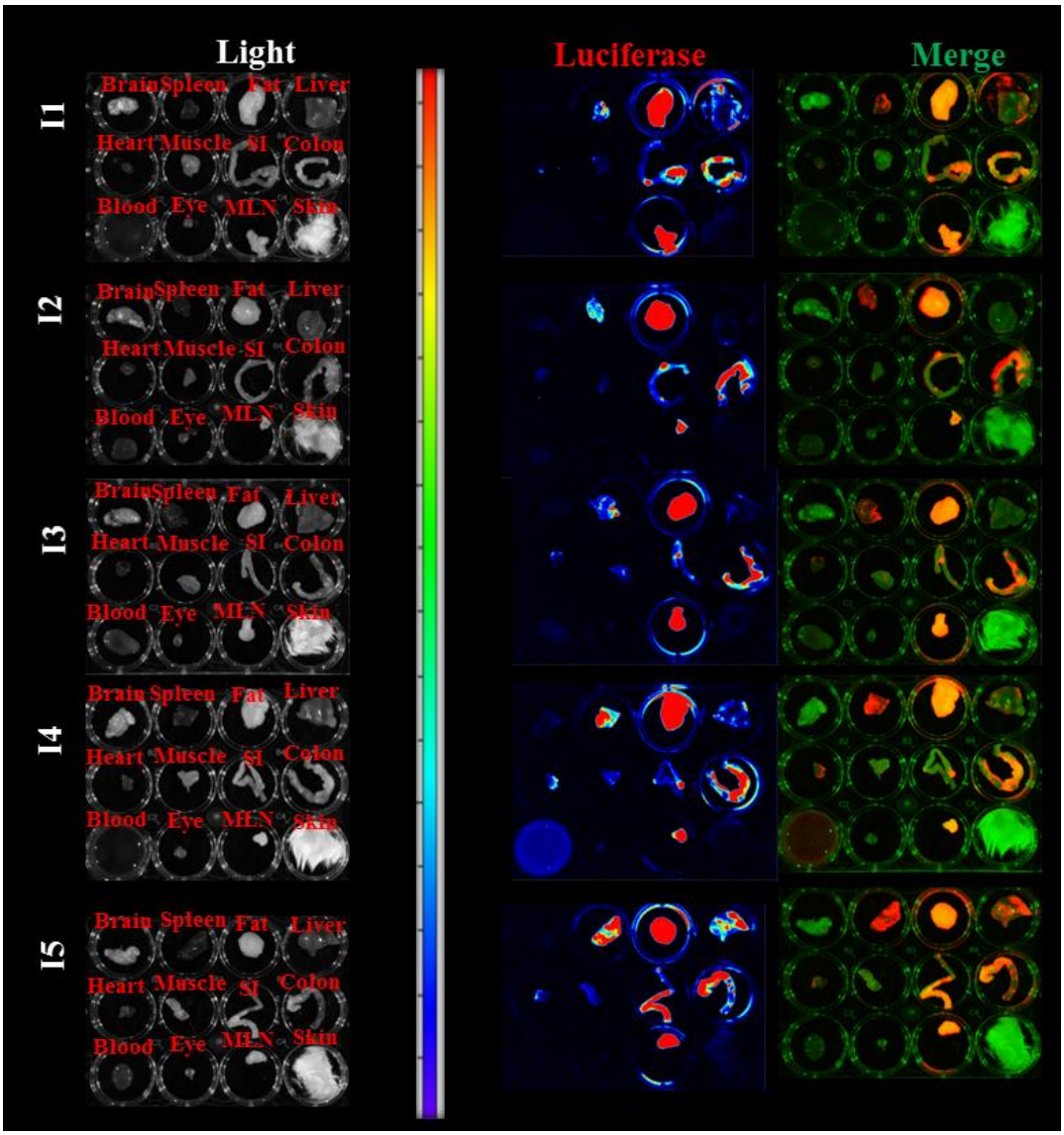

Post mortem bioluminescent imaging of representative infected mice following *intraperitoneal (i.p)* infection with 1 x 10^4 parasites, in the intermediate phase (Day 14), infection. The images in the left panel indicate arrangement of the dissected tissues in a 12-well plate format, images in the middle panel detailing the bioluminescent signal and images in the right panel showing the bioluminescent signal overlaying the tissue sample. All images are calibrated to the same scale. SI, Small Intestine; MLN, Mesenteric Lymph Nodes.

Appendix 3. Bioluminescent images of *ex vivo* tissues from *i.p* infected day 22 mice

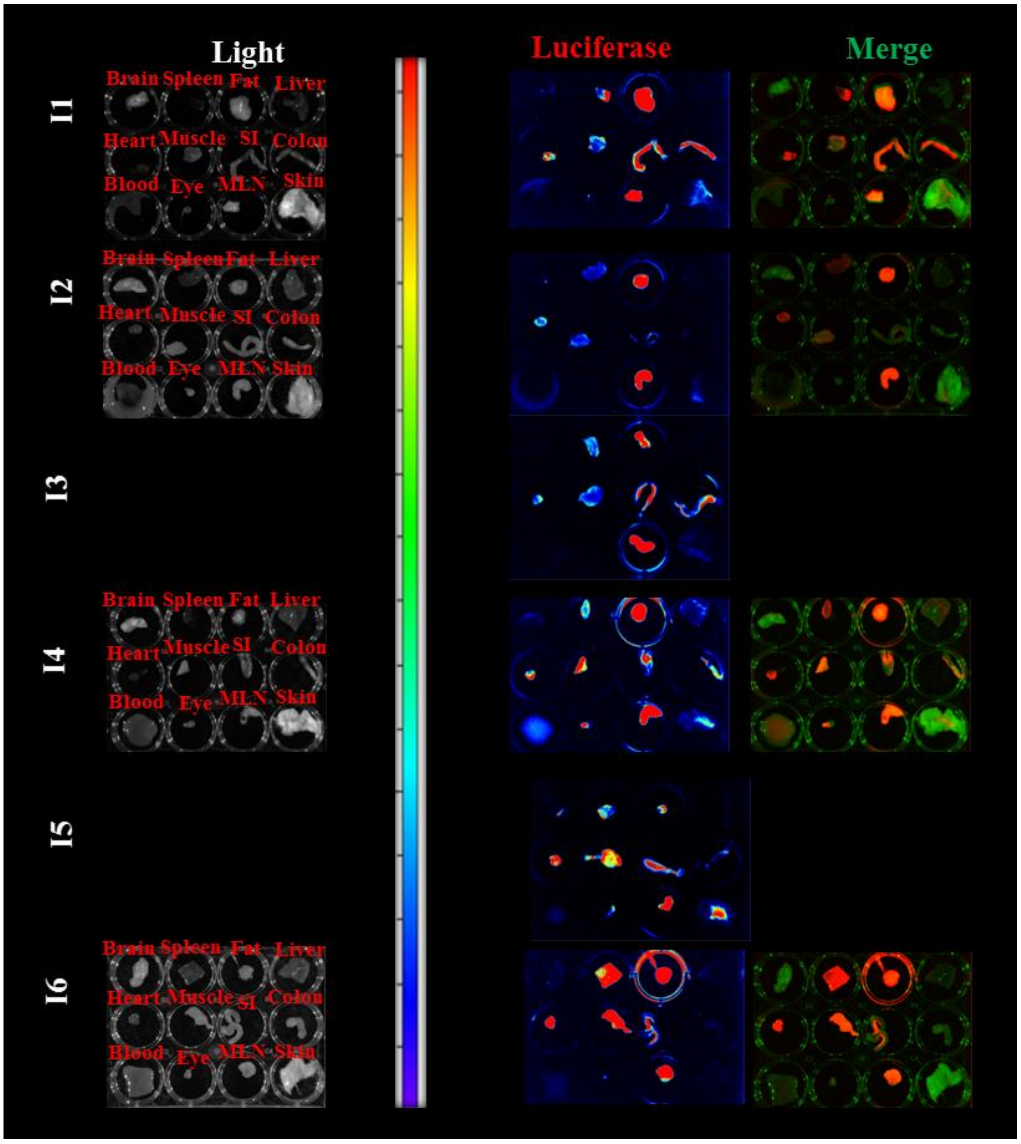

Post mortem bioluminescent imaging of representative infected mice following *intraperitoneal (i.p)* infection with 1 x 10^4 parasites, in the late stage II infection (Day 22). The images in the left panel indicate arrangement of the dissected tissues in a 12-well plate format, images in the middle panel detailing the bioluminescent signal and images in the right panel showing the bioluminescent signal overlaying the tissue sample. All images are calibrated to the same scale. SI, Small Intestine; MLN, Mesenteric Lymph Nodes.

9.0 References

1. Barrett MP *et al*., (2003) The trypanosomiases. *Lancet*. 362(9394):1469–80.
2. Fèvre EM *et al*., (2008) The Burden of Human African Trypanosomiasis. *PLoS Negl Trop Dis*. 2(12):e333.
3. Pandey A., Galvani A., (2017) Strategies for Trypanosoma brucei gambiense elimination. *Lancet Glob Heal*. 5(1):e10–1.
4. Brun R *et al*., (2010) Human African trypanosomiasis. *The Lancet*. (275):148–59.
5. Van den Bossche P *et al.*, (2010) A changing environment and the epidemiology of tsetse-transmitted livestock trypanosomiasis. *Trends Parasitol*. 26(5):236–43.
6. Vincent IM *et al.*, (2016) Metabolomics Identifies Multiple Candidate Biomarkers to Diagnose and Stage Human African Trypanosomiasis. *PLoS Negl Trop Dis*.10(12):e0005140.
7. Molyneux DH., (2014) Neglected tropical diseases: now more than just 'other diseases'— the post-2015 agenda. *Int Health*. 6(3):172–80.
8. Molyneux DH., (2012) The 'Neglected Tropical Diseases': now a brand identity; responsibilities, context and promise. *Parasit Vectors*. 5(1):23.
9. Molyneux DH., Savioli L., Engels D., (2017) Neglected tropical diseases: progress towards addressing the chronic pandemic. *Lancet*. 389(10066):312–25.
10. Franco JR *et al.*, (2014) Epidemiology of human African trypanosomiasis. *Clin Epidemiol*.6:257–75.
11. Kennedy PGE., (2004) Human African trypanosomiasis of the CNS : current issues and challenges. *J Clin Invest*.113(4):496–504.
12. Gibson W., Bailey M., (2003) The development of Trypanosoma brucei within the tsetse fly midgut observed using green fluorescent trypanosomes. *Kinetoplastid Biol Dis*.2(1):1.
13. Hamm B *et al.*, (1990) Differentiation of Trypanosoma brucei bloodstream trypomastigotes from long slender to short stumpy-like forms in axenic culture. *Mol Biochem Parasitol*. 40(1):13–22.
14. Rico E *et al.*, (2013) Bloodstream form pre-adaptation to the tsetse fly in Trypanosoma brucei. *Front Cell Infect Microbiol*. (3):78.
15. Vickerman K., (1985) Developmental Cycles and Biology of Pathogenic Trypanosomes. *Br Med Bull*.41(2):105–14.
16. Donelson JE., (2003) Antigenic variation and the African trypanosome genome. *Acta Trop*.85(3):391–404.
17. Fenn K., Matthews KR., (2007) The cell biology of Trypanosoma brucei differentiation. *Curr Opin Microbiol*.10(6):539–46.
18. Cochran R., Rosen T., (1983) African Trypanosomiasis in the United States. *Arch Dermatol*.119(8):670.
19. Caljon G *et al.*, (2016) The Dermis as a Delivery Site of Trypanosoma brucei for Tsetse Flies. *PLOS Pathog*.12(7):e1005744.
20. Lewis MD., Kelly JM., (2016) Putting Infection Dynamics at the Heart of Chagas Disease. *Trends in Parasitology*. 32(11):899-911
21. McCall LI *et al.*, (2016) Location, Location, Location: Five Facts about Tissue Tropism and Pathogenesis. *PLoS Pathogens*. 12(5):e1005519
22. Silva Pereira S *et al.*, (2019) Tissue tropism in parasitic diseases. *Open Biol*. 9(5):190036.
23. Losos GJ., Ikede BO., (1972) Review of Pathology of Diseases in Domestic and

Laboratory Animals Caused by Trypanosoma congolense, T. vivax, T. brucei, T. rhodesiense and T. gambiense. *Vet Pathol*. 9(1): 1–79.
24. Abenga JN., (2014) A comparative pathology of Trypanosoma brucei infections. *Glob Adv Res J Med Med Sci*. 3(12):390-399
25. Capewell P *et al.*, (2016) The skin is a significant but overlooked anatomical reservoir for vector-borne African trypanosomes. *Elife*. 5: e17716
26. Caljon G *et al*., (2016) The Dermis as a Delivery Site of Trypanosoma brucei for Tsetse Flies. *PLoS Pathog*. 12(7): e1005744
27. Trindade S *et al*., (2016) Trypanosoma brucei Parasites Occupy and Functionally Adapt to the Adipose Tissue in Mice. *Cell Host Microbe*.19(6):837–48.
28. Capewell P *et al.*, (2019) Resolving the apparent transmission paradox of African sleeping sickness. *PLoS Biol*. 17(1): e3000105
29. Hotez PJ., Kamath A., (2009) Neglected tropical diseases in sub-Saharan Africa: Review of their prevalence, distribution, and disease burden. *PLoS Neglected Tropical Diseases*. 3(8): e412
30. Steverding D., (2008) The history of African trypanosomiasis. *Parasit Vectors*. 1(1):3.
31. Kennedy PG., (2013) Clinical features, diagnosis, and treatment of human African trypanosomiasis (sleeping sickness). *Lancet Neurol*. 12(2):186–94.
32. Holmes P., (2013) Tsetse-transmitted trypanosomes - Their biology, disease impact and control. *Journal of Invertebrate Pathology*. 112(1):11-14
33. Roditi I., Lehane MJ., (2008) Interactions between trypanosomes and tsetse flies. *Current Opinion in Microbiology*. 11(4):345-351
34. La Greca F., Magez S., (2011) Vaccination against trypanosomiasis. *Hum Vaccin*. 7(11):1225–33.
35. Checchi F *et al*., (2008) The natural progression of gambiense sleeping sickness: What is the evidence? *PLoS Neglected Tropical Diseases*. 2(12): e303.
36. Ponte-Sucre A., (2016) An Overview of Trypanosoma brucei Infections: An Intense Host-Parasite Interaction. *Front Microbiol*. 7(12):2126.
37. Checchi F *et al*., (2008) Estimates of the duration of the early and late stage of gambiense sleeping sickness. *BMC Infect Dis*. 8(1):16.
38. Odiit M., Kansiime F., Enyaru JC., (1997) Duration of symptoms and case fatality of sleeping sickness caused by Trypanosoma brucei rhodesiense in Tororo, Uganda. *East Afr Med J*. 74(12):792–5.
39. Kennedy PGE., (2008) Diagnosing central nervous system trypanosomiasis: two stage or not to stage? *Trans R Soc Trop Med Hyg*. 102(4):306–7.
40. Matovu E *et al*., (2012) Towards Point-of-Care Diagnostic and Staging Tools for Human African Trypanosomiaisis. *J Trop Med*. 12:1–9.
41. MacLean L., Odiit M., Sternberg JM., (2006) Intrathecal cytokine responses in Trypanosoma brucei rhodesiense sleeping sickness patients. *Trans R Soc Trop Med Hyg*.100(3):270–5.
42. Tiberti N *et al*., (2013) Neopterin Is a Cerebrospinal Fluid Marker for Treatment Outcome Evaluation in Patients Affected by Trypanosoma brucei gambiense Sleeping Sickness. *PLoS Negl Trop Dis*. 7(2):1–9.
43. Tiberti N *et al*., (2013) New biomarkers for stage determination in Trypanosoma brucei rhodesiense sleeping sickness patients. *Clin Transl Med*. 2(1):1.
44. Biemba G *et al*., (2000) Markers of inflammation in children with severe malarial anaemia. *Trop Med Int Heal*. 5(4):256–62.
45. Skogmar S *et al*., (2015) Plasma Levels of Neopterin and C-Reactive Protein (CRP) in Tuberculosis (TB) with and without HIV Coinfection in Relation to

CD4 Cell Count. *PLoS One*. 10(12):e0144292.
46. Kagira JM *et al*., (2011) Prevalence and types of coinfections in sleeping sickness patients in Kenya (2000/2009). *J Trop Med*. (11):248914
47. Kato CD *et al*., (2015) Clinical Profiles, Disease Outcome and Co-Morbidities among T. b. rhodesiense Sleeping Sickness Patients in Uganda. *PLoS One*. 10(2):e0118370.
48. Barrett MP., Croft SL., (2012) Management of trypanosomiasis and leishmaniasis. *British Medical Bulletin*. 104(1):175–196.
49. Rodgers J., (2010) Trypanosomiasis and the brain. *Parasitology*. 137(14):1995–2006.
50. Rodgers J., (2009) Human African trypanosomiasis, chemotherapy and CNS disease. *J Neuroimmunol*. 211(1):16–22.
51. Adams JH *et al*., (1986) Human African Trypanosomiasis (T.b. gambiense): a study of 16 fatal cases of sleeping sickness with some observations on acute reactive arsenical encephalopathy. *Neuropathol Appl Neurobiol*.12(1):81–94.
52. Kennedy PGE., (2006) Diagnostic and neuropathogenesis issues in human African trypanosomiasis. *Int J Parasitol.* 36(5):505–12.
53. Steverding D., (2010) The development of drugs for treatment of sleeping sickness: a historical review. *Parasit Vectors*.3(1):15.
54. Priotto G *et al*., (2009) Nifurtimox-eflornithine combination therapy for second-stage African Trypanosoma brucei gambiense trypanosomiasis: a multicentre, randomised, phase III, non-inferiority trial. *Lancet*. 374(9683):56–64.
55. Dickie EA *et al*., (2020) New drugs for human African trypanosomiasis: A twenty first century success story. *Tropical Medicine and Infectious Disease*. 19(5):1.
56. Neau P *et al*., (2020) Innovative partnerships for the elimination of human African trypanosomiasis and the development of fexinidazole. *Tropical Medicine and Infectious Disease*. 5(1):17.
57. Masocha W., Rottenberg ME., (2006) Minocycline impedes African trypanosome invasion of the brain in a murine model. *Antimicrob Agents Chemother*. 50(5):1798–804.
58. Steverding D., Rushworth SA., (2017) Front-line glioblastoma chemotherapeutic temozolomide is toxic to Trypanosoma brucei and potently enhances melarsoprol and eflornithine. *Exp Parasitol*. (178):45-50
59. Manna PT., Kelly S., Field MC., (2013) Adaptin evolution in kinetoplastids and emergence of the variant surface glycoprotein coat in African trypanosomatids. *Molecular Phylogenetics and Evolution*. 67(1): 123–128.
60. Mugnier MR., Stebbins CE., Papavasiliou FN., (2016) Masters of Disguise: Antigenic Variation and the VSG Coat in Trypanosoma brucei. *PLOS Pathog*.12(9):e1005784.
61. Horn D., (2014) Antigenic variation in African trypanosomes. *Mol Biochem Parasitol*.195(2):123–9.
62. Turner CMR., (2006) The rate of antigenic variation in fly-transmitted and syringe-passaged infections of Trypanosoma brucei. *FEMS Microbiol Lett*. 153(1):227–31.
63. Turner CMR., Barry JD., (1989) High frequency of antigenic variation in Trypanosoma brucei rhodesiense infections. *Parasitology*. 99(01):67.
64. Pays E *et al.*, (2014) The molecular arms race between African trypanosomes and humans. *Nature Reviews Microbiology*. 12(8):575-84
65. Capewell P *et al.*, (2015) A co-evolutionary arms race: Trypanosomes shaping

the human genome, humans shaping the trypanosome genome. *Parasitology*. 142(1): S108–S119
66. Stijlemans B *et al*., (2016) Immune evasion strategies of Trypanosoma brucei within the mammalian host: Progression to pathogenicity. *Frontiers in Immunology*. 7(233)
67. Pays E *et al*., (2006) The trypanolytic factor of human serum. *Nat Rev Microbiol*. (4):477–486
68. Vanhollebeke B., Pays E., (2010) The trypanolytic factor of human serum: Many ways to enter the parasite, a single way to kill. *Molecular Microbiology*.76(4):806-814
69. Shimamura M., Hager KM., Hajduk SL., (2001) The lysosomal targeting and intracellular metabolism of trypanosome lytic factor by Trypanosoma brucei brucei. *Mol Biochem Parasitol*. 115(2):227-237
70. Pays E *et al*., (2001) The VSG expression sites of Trypanosoma brucei: Multipurpose tools for the adaptation of the parasite to mammalian hosts. *Molecular and Biochemical Parasitology*. 114(1):1-16
71. Davidbarry J., Mcculloch R., (2004) Antigenic variation in trypanosomes: Enhanced phenotypic variation in a eukaryotic parasite. *Advances in Parasitology*. (49):1-70
72. Oli MW *et al*., (2006) Serum resistance-associated protein blocks lysosomal targeting of trypanosome lytic factor in Trypanosoma brucei. *Eukaryot Cell*. 5(1): 132–139
73. Carpio A *et al*., (2016) Parasitic diseases of the central nervous system: Lessons for clinicians and policy makers. *Expert Review of Neurotherapeutics*. 16(4): 401–414
74. Rosenberg GA., (2012) Neurological diseases in relation to the blood-brain barrier. *Journal of Cerebral Blood Flow and Metabolism*. 32(7): 1139–1151
75. Raman Sharma R., (2010) Fungal infections of the nervous system: Current perspective and controversies in management. *International Journal of Surgery*. 8(8):591-601
76. Mergenthaler P *et al*., (2013) Sugar for the brain: The role of glucose in physiological and pathological brain function. *Trends in Neurosciences*. 36(10):587-597
77. Louveau A., Harris TH., Kipnis J., (2015) Revisiting the Mechanisms of CNS Immune Privilege. *Trends in Immunology*. 36(10):569-577
78. Webster JP., (2001) Rats, cats, people and parasites: The impact of latent toxoplasmosis on behaviour. *Microbes and Infection*. 3(12):1037-1045
79. Webster JP., McConkey GA., (2010) Toxoplasma gondii-altered host behaviour: Clues as to mechanism of action. *Folia Parasitologica*. 57(2):95-104
80. Prandovszky E *et al*., (2011) The neurotropic parasite toxoplasma gondii increases dopamine metabolism. *PLoS One*. 6(9): e23866
81. Flegr J., (2007) Effects of Toxoplasma on human behavior. *Schizophr Bull*. 33(3): 757–760
82. Stiles JK *et al*., (2004) Trypanosome apoptotic factor mediates apoptosis in human brain vascular endothelial cells. *Mol Biochem Parasitol*. 133(2):229-40
83. Brady J., Gibson G., (1983) Activity patterns in pregnant tsetse flies, Glossina morsitans. *Physiol Entomol*. 8(4):359-369
84. Dauvilliers Y *et al*., (2008) Hypocretin and human African trypanosomiasis. *Sleep*. 31(3): 348–354.
85. Elliott I *et al*., (2014) West-African trypanosomiasis in a returned traveller from

Ghana: an unusual cause of progressive neurological decline. *BMJ Case Rep*. 2014:bcr2014204451.
86. Kristensson K *et al*., (2010) African trypanosome infections of the nervous system: Parasite entry and effects on sleep and synaptic functions. *Prog Neurobiol*.91(2):152–71.
87. Sudarshi D *et al*., (2014) Human African Trypanosomiasis Presenting at Least 29 Years after Infection—What Can This Teach Us about the Pathogenesis and Control of This Neglected Tropical Disease? *PLoS Negl Trop Dis*. 8(12):e3349.
88. Bentivoglio M., Kristensson K., (2014) Tryps and trips: Cell trafficking across the 100-year-old blood-brain barrier. *Trends Neurosci*. 37(6):325–33.
89. Mogk S *et al*.,(2017) African trypanosomes and brain infection – the unsolved question. *Biol Rev*. 92(3):1675-1687
90. Wolburg H *et al*, (2012) Late stage infection in sleeping sickness. *PLoS One*. 7(3): e34304
91. Masocha W., Kristensson K., (2019) Human African trypanosomiasis: How do the parasites enter and cause dysfunctions of the nervous system in murine models? *Brain Research Bulletin*. (145):18-29
92. Masocha W., Rottenberg ME., Kristensson K., (2007) Migration of African trypanosomes across the blood–brain barrier. *Physiol Behav*. 92(1):110–4.
93. Ballabh P., Braun A., Nedergaard M., (2004) The blood–brain barrier: an overview: Structure, regulation, and clinical implications. *Neurobiol Dis*. 16(1):1–13.
94. Nakagawa S *et al*., (2009) A new blood-brain barrier model using primary rat brain endothelial cells, pericytes and astrocytes. *Neurochem Int*.54(3–4):253–63.
95. Takeshita Y., Ransohoff RM., (2012) Inflammatory cell trafficking across the blood-brain barrier: chemokine regulation and in vitro models. *Immunol Rev*. 248(1):228–39.
96. Bauer HC *et al*., (2014) You Shall Not Pass;-tight junctions of the blood brain barrier. *Front Neurosci*. 8:392.
97. Masocha W., Kristensson K., (2012) Passage of parasites across the blood-brain barrier. *Virulence*. 3(2):192–202.
98. Strazielle N., Ghersi-Egea J-F., (2000) Choroid Plexus in the Central Nervous System: Biology and Physiopathology. *J Neuropathol Exp Neurol*. 59(7):561–74.
99. Laperchia C *et al*., (2016) Trypanosoma brucei Invasion and T-Cell Infiltration of the Brain Parenchyma in Experimental Sleeping Sickness: Timing and Correlation with Functional Changes. *PLoS Negl Trop Dis*.10(12):e0005242.
100. Untucht C *et al*., (2011) An optimized in vitro blood-brain barrier model reveals bidirectional transmigration of African trypanosome strains. *Microbiology*. 157(10):2933–41.
101. Mogk S *et al*., (2014) The lane to the brain: How African trypanosomes invade the CNS. *Trends Parasitol*. 30(10):470–7.
102. Grab DJ *et al*., (2004) African Trypanosome Interactions With An In Vitro Model Of The Human Blood–Brain Barrier. *J Parasitol*. 90(5):970–9.
103. Masocha W., Kristensson K., (2012) Passage of parasites across the blood-brain barrier. *Virulence*. 3(2):202–12.
104. Lonsdale-Eccles JD., Grab DJ., (2002) Trypanosome hydrolases and the blood-brain barrier. *Trends Parasitol*.18(1):17–9.
105. Elsheikha HM., Khan NA., (2010) Protozoa traversal of the blood–brain barrier to invade the central nervous system. *FEMS Microbiol Rev*.34(4):532–53.

106. Nikolskaia OV *et al*., (2006) Blood-brain barrier traversal by African trypanosomes requires calcium signaling induced by parasite cysteine protease. *J Clin Invest*. 116(10):2739–47.
107. Abdulla MH *et al*., (2008) RNA Interference of Trypanosoma brucei Cathepsin B and L Affects Disease Progression in a Mouse Model. *PLoS Negl Trop Dis.* 2(9):e298.
108. Grab DJ *et al*., (2009) Protease Activated Receptor Signaling Is Required for African Trypanosome Traversal of Human Brain Microvascular Endothelial Cells. *PLoS Negl Trop Dis*. 3(7):e479.
109. Grab DJ et al., (2011) How can microbial interactions with the blood-brain barrier modulate astroglial and neuronal function? *Cell Microbiol*. 13(10):1470–8.
110. Lachenmaier SM *et al*., (2011) Intracellular transport of Toxoplasma gondii through the blood–brain barrier. *J Neuroimmunol*. 232(1):119–30.
111. Masocha W *et al.*, (2004) Cerebral vessel laminins and IFN-γ define Trypanosoma brucei brucei penetration of the blood-brain barrier. *J Clin Invest*. 114(5):689–94.
112. Hertz CJ., Filutowicz H., Mansfield JM., (1998) Resistance to the African Trypanosomes Is IFN-γ Dependent. *J Immunol*.161(12).
113. Amin DN *et al*., (2012) Distinct Toll-like Receptor Signals Regulate Cerebral Parasite Load and Interferon / and Tumor Necrosis Factor -Dependent T-Cell Infiltration in the Brains of Trypanosoma brucei-Infected Mice. *J Infect Dis*. 205(2):320–32.
114. Osborn L *et al*., (1989) Direct expression cloning of vascular cell adhesion molecule 1, a cytokine-induced endothelial protein that binds to lymphocytes. *Cell*.59(6):1203–11.
115. Mosmann TR., Coffman RL., (1989) TH1 and TH2 Cells: Different Patterns of Lymphokine Secretion Lead to Different Functional Properties. *Annu Rev Immunol.* 7(1):145–73.
116. Pearce EJ., MacDonald AS., (2002) The immunobiology of schistosomiasis. *Nat Rev Immunol*. 2(7):499–511.
117. Mhlanga JD., Bentivoglio M., Kristensson K., (1997) Neurobiology of Cerebral Malaria and African Sleeping Sickness. *Brain Res Bull*. 44(5):579–89.
118. Lucas R *et al.*, (1993) A role for TNF during African trypanosomiasis: involvement in parasite control, immunosuppression and pathology. *Res Immunol*.144(5):370–6.
119. Schleifer KW *et al.*, (1993) Characterization of T helper cell responses to the trypanosome variant surface glycoprotein. *J Immunol*.150(7):2910–9.
120. Rosenberg GA *et al.*, (1995) Tumor necrosis factor-α-induced gelatinase B causes delayed opening of the blood-brain barrier: an expanded therapeutic window. *Brain Res.* 703(1–2):151–5.
121. Gloor SM *et al.*, (2001) Molecular and cellular permeability control at the blood-brain barrier. *Brain Res Brain Res Rev*. 36(2–3):258–64.
122. Pentreath VW., Owolabi AO., Doua F., (1997) Survival of Trypanosoma brucei brucei in cerebrospinal fluid. *Ann Trop Med Parasitol*. 137(6): 1369–1379
123. Ueno N., Lodoen MB., (2015) From the blood to the brain: Avenues of eukaryotic pathogen dissemination to the central nervous system. *Current Opinion in Microbiology*. (26):53-59
124. Wolburg H., Paulus W., (2010) Choroid plexus: Biology and pathology. *Acta Neuropathologica*. (119):75–88

125. Schwerk C *et al*., (2015). The choroid plexus: a multi-role player during infectious diseases of the CNS. *Front Cell Neurosci.* 9: 80
126. Lundkvist GB., Kristensson K., Bentivoglio M., (2004) Why Trypanosomes Cause Sleeping Sickness. *Physiology*. 19(4):198-206
127. Bentivoglio M., Kristensson K., Rottenberg ME., (2018) Circumventricular Organs and Parasite Neurotropism: Neglected Gates to the Brain? *Frontiers in immunology*. 9:2877
128. Eltayeb R *et al.*, (2002) Trypanosoma brucei brucei Induces Interferon-γ Expression in Rat Dorsal Root Ganglia Cells via a Tyrosine Kinase–Dependent Pathway . *J Infect Dis*. 181(1):400-4
129. Saunders NR *et al*., (2016) The biological significance of brain barrier mechanisms: help or hindrance in drug delivery to the central nervous system? *F1000Research*. 5: F1000 Faculty Rev-313
130. Masocha W., Kristensson K., Rottenberg ME., (2014) Neurobiology of African trypanosomiasis. *Neglected Tropical Diseases and Conditions of the Nervous System*. pp 183-200
131. Laperchia C *et al.*, (2018) Neural Damage in Experimental Trypanosoma brucei gambiense Infection: Hypothalamic Peptidergic Sleep and Wake-Regulatory Neurons. *Front Neuroanat*. 12:13.
132. Eckel-Mahan K., Sassone-Corsi P., (2013) Metabolism and the Circadian Clock Converge. *Physiol Rev*. 93(1): 107–135
133. Jagannath A *et al*., (2017) The genetics of circadian rhythms, sleep and health. *Human Molecular Genetic*s. 26(R2):R128-R138
134. Mohawk JA., Green CB., Takahashi JS., (2012) Central and Peripheral Circadian Clocks in Mammals. *Annu Rev Neurosci*. 35:445-62
135. Scheiermann C., Kunisaki Y., Frenette PS., (2013) Circadian control of the immune system. *Nature Reviews Immunology*. (13):190–198
136. Tesoriero C *et al*., (2018) Neural Damage in Experimental Trypanosoma brucei gambiense Infection: The Suprachiasmatic Nucleus. *Front Neuroanat*. 12:6
137. Lundkvist GB., Hill RH., Kristensson K., (2002) Disruption of Circadian Rhythms in Synaptic Activity of the Suprachiasmatic Nuclei by African Trypanosomes and Cytokines. *Neurobiol Dis*.11(1):20–7.
138. Stehle JH., von Gall C., Korf HW., (2003) Melatonin: A clock-output, a clock-input. *Journal of Neuroendocrinology*. 15(4):383-389
139. Armstrong SM., (1989) Melatonin and circadian control in mammals. *Experientia*. 45(10):932-8
140. Claustrat B *et al*., (1998) Plasma melatonin rhythm is maintained in human African trypanosomiasis. *Neuroendocrinology*. 68(1):64-70.
141. Kristensson K *et al.*, (1998) African trypanosomiasis in the rat alters melatonin secretion and melatonin receptor binding in the suprachiasmatic nucleus. *Brain Res Bull*. 47(3):265-9.
142. Blum J., Schmid C., Burri C., (2006) Clinical aspects of 2541 patients with second stage human African trypanosomiasis. *Acta Trop*. 97(1):55-64
143. Stiles JK *et al.*, (2001) Trypanosoma brucei infection induces apoptosis and up-regulates neuroleukin expression in the cerebellum. *Ann Trop Med Parasitol*. 95(8):797-810
144. Kennedy PGE., Rodgers J., (2019) Clinical and neuropathogenetic aspects of human African trypanosomiasis. *Front Immunol*. 10(1):1–11.
145. Cardinal RN *et al*., (2002) Emotion and motivation: The role of the amygdala, ventral striatum, and prefrontal cortex. *Neuroscience and Biobehavioral*

Reviews. 26(3):321-52.
146. Kennedy PGE., (2008) The continuing problem of human African trypanosomiasis (sleeping sickness). *Ann Neurol.* 64(2):116–26.
147. Vertes RP., (2006) Interactions among the medial prefrontal cortex, hippocampus and midline thalamus in emotional and cognitive processing in the rat. *Neuroscience*. 142(1):1-20.
148. Baxter MG., (2013) Mediodorsal thalamus and cognition in non-human primates. *Front Syst Neurosci*. 7:38.
149. Femenía T *et al*., (2012) Dysfunctional hippocampal activity affects emotion and cognition in mood disorders. *Brain Research*. 1476:58-70.
150. Sokoloff L *et al*., (1977) The [14c]Deoxyglucose Method For The Measurement Of Local Cerebral Glucose Utilization: Theory, Procedure, And Normal Values In The Conscious And Anesthetized Albino Rat. *J Neurochem.* 28(5):897-916.
151. Dawson N *et al.*, (2008) Novel analysis for improved validity in semi-quantitative 2-deoxyglucose autoradiographic imaging. *J Neurosci Methods.* 175(1):25-35.
152. Dawson N *et al*., (2014) Subanesthetic ketamine treatment promotes abnormal interactions between neural subsystems and alters the properties of functional brain networks. *Neuropsychopharmacology*. 39(7):1786-98.
153. Shah-Simpson S *et al*., (2017) Modulation of host central carbon metabolism and in situ glucose uptake by intracellular Trypanosoma cruzi amastigotes. *PLoS Pathog*. (11):e1006747.
154. Balagura S., Kanner M., (1971) Hypothalamic sensitivity to 2-deoxy-D-glucose and glucose: Effects on feeding behavior. *Physiol Behav*. 7(2):251-5.
155. Villablanca JR., (2004) Counterpointing the functional role of the forebrain and of the brainstem in the control of the sleep-waking system. *J Sleep Res*. 13(3):179–208.
156. Lefèvre T., Thomas F., (2008) Behind the scene, something else is pulling the strings: Emphasizing parasitic manipulation in vector-borne diseases. *Infection, Genetics and Evolution*. 8:504–19.
157. Biron DG., Loxdale HD., (2012) Host–parasite molecular cross-talk during the manipulative process of a host by its parasite. *J Exp Biol*. 216(1).
158. Hurd H., (2003) Manipulation of medically important insect vectors by their parasites. *Annu Rev Entomol*. 48(1):141–61.
159. Molyneux DH., Jefferies D., (1986) Feeding behaviour of pathogen-infected vectors. *Parasitology*. 92(03):721.
160. Rogers ME *et al.*, (2007) Leishmania Manipulation of Sand Fly Feeding Behavior Results in Enhanced Transmission. *PLoS Pathog*. 3(6):e91.
161. Schwartz A., Koella JC., (2001) Trade-offs, conflicts of interest and manipulation in Plasmodium–mosquito interactions. *Trends Parasitol*. 17(4):189–94.
162. Van Den Abbeele J *et al.*, (2010) Trypanosoma brucei Modifies the Tsetse Salivary Composition, Altering the Fly Feeding Behavior That Favors Parasite Transmission. *PLoS Pathog*. 6(6):e1000926.
163. Moloo SK., (1983) Feeding behaviour of Glossina morsitans morsitans infected with Trypanosoma vivax, T. congolense or T. brucei. *Parasitology*. 6;86(01):51.
164. Moloo SK., Dar F., (1985) Probing by Glossina morsitans centralis infected with pathogenic Trypanosoma species. *Trans R Soc Trop Med Hyg*. 79(1):119.
165. Jenni L et al., (1980) Feeding behaviour of tsetse flies infected with salivarian trypanosomes. *Nature*. 283(5745):383–5.

166. Moryś JM., Jeżewska M., Korzeniewski K., (2015) Neuropsychiatric manifestations of some tropical diseases. *Int Marit Health*. 66(1):30-5.
167. Lambo TA., (1966) Neuro‐Psychiatric Syndromes Associated With Human Trypanosomiasis In Tropical Africa. *Acta Psychiatr Scand*. 42(4):474-84.
168. Silberberg D *et al*., (2015) Brain and other nervous system disorders across the lifespan-global challenges and opportunities. *Nature*. 527(7578):S151-4.
169. Litt E., Baker MC., Molyneux D., (2012) Neglected tropical diseases and mental health: A perspective on comorbidity. *Trends in Parasitology*. 28(5):195-201.
170. Dalman C *et al*., (2008) Infections in the CNS during childhood and the risk of subsequent psychotic illness: A cohort study of more than one million Swedish subjects. *Am J Psychiatry*. 165(1):59-65.
171. Ahmed AO *et al.*, (2018) Schizophrenia heterogeneity revisited: Clinical, cognitive, and psychosocial correlates of statistically-derived negative symptoms subgroups. *J Psychiatr Res*. 97:8-15.
172. Bornheimer LA., Jaccard J., (2017) Symptoms of Depression, Positive Symptoms of Psychosis, and Suicidal Ideation Among Adults Diagnosed With Schizophrenia Within the Clinical Antipsychotic Trials of Intervention Effectiveness. *Arch Suicide Res*. 21(4):633-45.
173. Etkin A., Gyurak A., O'Hara R., (2013) A neurobiological approach to the cognitive deficits of psychiatric disorders. *Dialogues Clin Neurosci.* 15(4):419.
174. Erhart SM., Marder SR., Carpenter WT., (2006) Treatment of schizophrenia negative symptoms: Future prospects. *Schizophrenia Bulletin.* 32(2):234-7.
175. Leask SJ., (2004) Environmental influences in schizophrenia: the known and the unknown. *Adv Psychiatr Treat*. 10(5):323-30.
176. Krabbendam L., Van Os J., (2005) Schizophrenia and urbanicity: A major environmental influence - Conditional on genetic risk. *Schizophrenia Bulletin*. 31(4):795-9.
177. Stone JL *et al*., (2008) Rare chromosomal deletions and duplications increase risk of schizophrenia. *Nature*. 455(7210):237.
178. Snyder MA., Gao WJ., (2013) NMDA hypofunction as a convergence point for progression and symptoms of schizophrenia. *Front Cell Neurosci*. 7:31.
179. Kantrowitz JT., Javitt DC., (2010) N-methyl-d-aspartate (NMDA) receptor dysfunction or dysregulation: The final common pathway on the road to schizophrenia? *Brain Res Bull*. 83(3-4):108-21.
180. Javitt DC., (2010) Glutamatergic theories of schizophrenia. *Isr J Psychiatry Relat Sci*. 47(1):4
181. Krystal JH *et al.*, (2003) NMDA receptor antagonist effects, cortical glutamatergic function, and schizophrenia: Toward a paradigm shift in medication development. *Psychopharmacology*. 169(3-4):215-33.
182. Torrey EF., Yolken RH., (2007) Schizophrenia and toxoplasmosis. *Schizophrenia Bulletin*. 33(3):727-8.
183. Yolken RH., Dickerson FB., Fuller Torrey E., (2009) Toxoplasma and schizophrenia. *Parasite Immunology*. 31(11):706-15.
184. Amole B *et al*., (1989) Neurochemical measurements in the brains of mice infected with Trypanosoma brucei brucei (TREU 667). *Ann Trop Med Parasitol*. 83(3):225-32.
185. Anderson G., Maes M., (2013) Schizophrenia: Linking prenatal infection to cytokines, the tryptophan catabolite (TRYCAT) pathway, NMDA receptor hypofunction, neurodevelopment and neuroprogression. *Prog Neuro-Psychopharmacology Biol Psychiatry*. 42:5-19.

186. Mathieu C *et al*., (2014) Trypanosoma brucei eflornithine transporter AAT6 is a low affinity, low selective transporter for neutral amino acids. *Biochem J*. 18:9–18.
187. Chaudhary K., Roos DS., (2005) Protozoan genomics for drug discovery. *Nat Biotechnol*. 23(9):1089–91.
188. Stibbs HH., Seed JR., (1975) Short-Term Metabolism of [14C]Tryptophan in Rats Infected with Trypanosoma brucei gambiense. *J Infect Dis*. 131(4):459–62.
189. Newport GR *et al*., (1977) Alteration of Free Serum Amino Acids in Voles Infected with Trypanosoma brucei gambiense. *J Parasitol*. 63(1):15.
190. McGettrick AF *et al.*, (2016) Trypanosoma brucei metabolite indolepyruvate decreases HIF-1α and glycolysis in macrophages as a mechanism of innate immune evasion. *Proc Natl Acad Sci USA*. 2016:201608221.
191. Hall JE., Seed JR., (1984) Increased urinary excretion of aromatic amino acid catabolites by Microtus montanus chronically infected with Trypanosoma brucei gambiense. *Comp Biochem Physiol Part B Comp Biochem*. 77(4):755–60.
192. Sawalhy A *et al.*, (1995) Catabolism of Tryptophan by Trypanosoma evansi. *J Eukaryot Microbiol*. 42(6):684–90.
193. Marciano D *et al*., (2008) Biochemical characterization of stage-specific isoforms of aspartate aminotransferases from Trypanosoma cruzi and Trypanosoma brucei. *Mol Biochem Parasitol*. 161(1):12–20.
194. Aranda A *et al*., (2006) The malate dehydrogenase isoforms from Trypanosoma brucei: Subcellular localization and differential expression in bloodstream and procyclic forms. *Int J Parasitol*. 36(3):295–307.
195. Marciano D *et al.*, (2009) Functional characterization of stage-specific aminotransferases from trypanosomatids. *Mol Biochem Parasitol*. 166(2):172–82.
196. Berriman M *et al*., (2005) The Genome of the African Trypanosome Trypanosoma brucei. *Science*. 309(5733).
197. Smith TK *et al*., (2017) Metabolic reprogramming during the *Trypanosoma brucei* life cycle. *F1000Research*. 2017:6.
198. Cote F *et al*., (2003) Disruption of the nonneuronal tph1 gene demonstrates the importance of peripheral serotonin in cardiac function. *Proc Natl Acad Sci*. 100(23):13525-30.
199. Walther DJ *et al*., (2003) Synthesis of serotonin by a second tryptophan hydroxylase isoform. *Science*. 299(5603):76
200. Gershon MD., (2013) 5-Hydroxytryptamine (serotonin) in the gastrointestinal tract. *Current Opinion in Endocrinology, Diabetes and Obesity*. 20(1):14.
201. Jenkins TA *et al.*, (2016) Influence of tryptophan and serotonin on mood and cognition with a possible role of the gut-brain axis. *Nutrients*. 8(1):1–15.
202. Kaufman J *et al.*, (2016) The 5-HT1A receptor in Major Depressive Disorder. *European Neuropsychopharmacology*. 26(3):397-410.
203. Rancillac A., (2016) Serotonin and sleep-promoting neurons. *Oncotarget*. 7(48):78222.
204. Siegel JM., (2004) The neurotransmitters of sleep. *Journal of Clinical Psychiatry*. 65(16):4-7.
205. Sangare A *et al.*, (2016) Serotonin differentially modulates excitatory and inhibitory synaptic inputs to putative sleep-promoting neurons of the ventrolateral preoptic nucleus. *Neuropharmacology*. 109:29-40.
206. Monti JM., Jantos H., (2008) The roles of dopamine and serotonin, and of their receptors, in regulating sleep and waking. *Progress in Brain Research*. 172:625-

46.
207. Ursin R., (2002) Serotonin and sleep. *Sleep Med Rev*. 6(1):55-67
208. Xie Z *et al.*, (2017) A review of sleep disorders and melatonin. *Neurological Research*. 39(6):559-65.
209. Chang Y Sen *et al*., (2016) Melatonin Supplementation for Children with Atopic Dermatitis and Sleep Disturbance: A Randomized Clinical Trial. *JAMA Pediatr*. 170(1):35-42.
210. Bartlett DJ *et al.*, (2013) Circadian rhythm disorders among adolescents: Assessment and treatment options. *Med J Aust*. 199:S16-20
211. Lähteenmäki R *et al.*, (2014) Melatonin for sedative withdrawal in older patients with primary insomnia: A randomized double-blind placebo-controlled trial. *British Journal of Clinical Pharmacology*. 77(6):975-85.
212. Amstrup AK *et al*., (2015) The effect of melatonin treatment on postural stability, muscle strength, and quality of life and sleep in postmenopausal women: A randomized controlled trial. *Nutr J*. 14(1):102.
213. Comai S., Ochoa-Sanchez R., Gobbi G., (2013) Sleep-wake characterization of double MT1/MT2 receptor knockout mice and comparison with MT1 and MT2 receptor knockout mice. *Behav Brain Res*. 243:231-8.
214. Pévet P *et al*., (2002) The chronobiotic properties of melatonin. *Cell and Tissue Research*. 309(1):183-91.
215. Touitou Y., Bogdan A., (2007) Promoting adjustment of the sleep-wake cycle by chronobiotics. *Physiol Behav*. 90(2-3):294-300.
216. Cardinali DP., Furio AM., Reyes MP., (2005) Clinical perspectives for the use of melatonin as a chronobiotic and cytoprotective agent. *Annals of the New York Academy of Sciences.* 1057(1):327-36.
217. Thomas B., Mohanakumar KP., (2004) Melatonin protects against oxidative stress caused by 1-methyl-4-phenyl-1, 2,3,6-tetrahydropyridine in the mouse nigrostriatum. *J Pineal Res.* 36(1):25-32.
218. Srinivasan V *et al.*, (2006) Melatonin in Alzheimer's disease and other neurodegenerative disorders. *Behavioral and Brain Functions*. 2(1):15.
219. Weil ZM *et al.*, (2006) Melatonin receptor (MT1) knockout mice display depression-like behaviors and deficits in sensorimotor gating. *Brain Res Bull*. 68(6):425-9.
220. Lee EJ *et al*., (2005) Melatonin attenuates gray and white matter damage in a mouse model of transient focal cerebral ischemia. *J Pineal Res*. 38(1):42-52.
221. Dehghan F *et al.*, (2013) Effect of melatonin on intracranial pressure and brain edema following traumatic brain injury: Role of oxidative stresses. *Arch Med Res.* 44(4):251-8.
222. Emet M *et al*., (2016) A Review of Melatonin, Its Receptors and Drugs. *Eurasian J Med.* 48(2):135.
223. Campbell BM *et al.*, (2014) Kynurenines in CNS disease: Regulation by inflammatory cytokines. *Frontiers in Neuroscience*. 8:12.
224. Amori L *et al.*, (2009) On the relationship between the two branches of the kynurenine pathway in the rat brain in vivo. *J Neurochem*. 109(2):316-25.
225. Takikawa O *et al.*, (1988) Mechanism of interferon-γ action. Characterization of indoleamine 2,3-dioxygenase in cultured human cells induced by interferon -γ and evaluation of the enzyme-mediated tryptophan degradation in its anticellular activity. *J Biol Chem*. 263(4):2041-8.
226. Shimizu T *et al*., (1978) Indoleamine 2,3 dioxygenase. Purfication and some properties. *J Biol Chem*. 253(13):4700-6.

227. Mándi Y., Vécsei L., (2012) The kynurenine system and immunoregulation. *Journal of Neural Transmission*. 119(2):197-209.
228. Lestage J *et al*., (2002) The enzyme indoleamine 2,3-dioxygenase is induced in the mouse brain in response to peripheral administration of lipopolysaccharide and superantigen. *Brain, Behavior, and Immunity*. 16(5):596-601.
229. Hunt NH *et al*., (2017) The kynurenine pathway and parasitic infections that affect CNS function. *Neuropharmacology*. 112:389–98.
230. Stone TW., Perkins MN., (1981) Quinolinic acid: a potent endogenous excitant at amino acid receptors in CNS. *European journal of pharmacology*. 72(4):411-2.
231. Stone TW., (2001) Kynurenines in the CNS : from endogenous obscurity to therapeutic importance. *Progress in neurobiology*. 64(2):185-218.
232. Swartz K *et al.*, (1990) Cerebral synthesis and release of kynurenic acid: an endogenous antagonist of excitatory amino acid receptors. *J Neurosci*. 10(9).
233. Rodgers J *et al*., (2009) Kynurenine pathway inhibition reduces central nervous system inflammation in a model of human African trypanosomiasis. *Brain*. 132(5):1259–67.
234. Clark CJ *et al.*, (2005) Prolonged survival of a murine model of cerebral malaria by kynurenine pathway inhibition. *Infect Immun*. 73(8):5249-51.
235. Sternberg JM *et al*., (2016). Kynurenine Pathway Activation in Human African Trypanosomiasis. *J Infect Dis*. 34(5):jiw623.
236. Knubel CP *et al*., (2010) Indoleamine 2,3-dioxigenase (IDO) is critical for host resistance against Trypanosoma cruzi. *FASEB J*. 24(8):2689-701
237. Hunt NH *et al*., (2017) The kynurenine pathway and parasitic infections that affect CNS function. *Neuropharmacology*. 112:389–98.
238. Pfefferkorn ER., Eckel M., Rebhun S., (1986) Interferon-γ suppresses the growth of Toxoplasma gondii in human fibroblasts through starvation for tryptophan. *Mol Biochem Parasitol.* 20(3):215-24.
239. Pfefferkorn ER., (1984) Interferon gamma blocks the growth of Toxoplasma gondii in human fibroblasts by inducing the host cells to degrade tryptophan. *Proc Natl Acad Sci*. 81(3):908-12
240. Fabiani S *et al.*, (2015) Neurobiological studies on the relationship between toxoplasmosis and neuropsychiatric diseases. *J Neurol Sci.* 351(1–2):3–8.
241. Okusaga O *et al*., (2016) Combined Toxoplasma gondii seropositivity and high blood kynurenine - Linked with nonfatal suicidal self-directed violence in patients with schizophrenia. *J Psychiatr Res*. 72:74-81.
242. Yolken RH., Torrey EF., (2008) Are some cases of psychosis caused by microbial agents? A review of the evidence. *Molecular Psychiatry*. 13(5):470-9.
243. Hunt NH *et al*., (2006) Immunopathogenesis of cerebral malaria. *International Journal for Parasitology*. 36(5):569-82.
244. Medana IM., Chan-Ling T., Hunt NH., (1996) Redistribution and degeneration of retinal astrocytes in experimental murine cerebral malaria: Relationship to disruption of the blood-retinal barrier. *Glia*. 16(1):51-64.
245. Donovan MJ *et al*., (2012) Indoleamine 2,3-dioxygenase (IDO) induced by Leishmania infection of human dendritic cells. *Parasite Immunol.* 34(10):464-72.
246. Divanovic S *et al*., (2012) Opposing biological functions of tryptophan catabolizing enzymes during intracellular infection. *J Infect Dis*. 205(1):152-61.
247. Schmid M *et al*., (2012) Apicomplexan parasite, Eimeria falciformis, co-opts host tryptophan catabolism for life cycle progression in mouse. *J Biol Chem.*

287(24):20197-207.
248. Bell LV., Else KJ., (2011) Regulation of colonic epithelial cell turnover by IDO contributes to the innate susceptibility of SCID mice to Trichuris muris infection. *Parasite Immunol*. 33(4):244-9.
249. Choudhry N *et al*., (2009) Interferon-γ-mediated activation of enterocytes in immunological control of Encephalitozoon intestinalis infection. *Parasite Immunol*. 31(1):2-9.
250. Oxenkrug GF., (2010) Tryptophan-kynurenine metabolism as a common mediator of genetic and environmental impacts in major depressive disorder: The serotonin hypothesis revisited 40 years later. *Isr J Psychiatry Relat Sci*. 47(1):56.
251. Schwarcz R *et al*., (2012) Kynurenines in the mammalian brain: When physiology meets pathology. *Nature Reviews Neuroscience*. 13(7):465-77.
252. Albuquerque EX., Schwarcz R., (2013) Kynurenic acid as an antagonist of α7 nicotinic acetylcholine receptors in the brain: Facts and challenges. *Biochemical Pharmacology*. 85(8):1027-32.
253. Coyle JT., (2012) NMDA receptor and schizophrenia: A brief history. *Schizophrenia Bulletin*. 38(5):920-6.
254. Moghaddam B., Javitt D., (2012) From revolution to evolution: The glutamate hypothesis of schizophrenia and its implication for treatment. *Neuropsychopharmacology*. 37(1):4-15.
255. Lodge D., Mercier MS., (2015) Ketamine and phencyclidine: The good, the bad and the unexpected. *British Journal of Pharmacology*. 172(17):4254-76.
256. Schwarcz R *et al*, (2001) Increased cortical kynurenate content in schizophrenia. *Biol Psychiatry*. 1;50(7):521-30.
257. Linderholm KR *et al*., (2012) Increased levels of kynurenine and kynurenic acid in the CSF of patients with schizophrenia. *Schizophr Bull*. 38(3):426-32.
258. Guidetti P., Okuno E., Schwarcz R., (1997) Characterization of rat brain kynurenine aminotransferases I and II. *J Neurosci Res*. 50(3):457-65.
259. Guidetti P *et al*., (2007) Astrocytic localization of kynurenine aminotransferase II in the rat brain visualized by immunocytochemistry. *Glia*. 55(1):78-92
260. Kiss C *et al*., (2003) Kynurenate production by cultured human astrocytes. *J Neural Transm*. 110(1):1-4.
261. Miller CL *et al*., (2006) Upregulation of the initiating step of the kynurenine pathway in postmortem anterior cingulate cortex from individuals with schizophrenia and bipolar disorder. *Brain Res*. 1073:25-37.
262. Miller CL *et al*., (2004) Expression of the kynurenine pathway enzyme tryptophan 2,3-dioxygenase is increased in the frontal cortex of individuals with schizophrenia. *Neurobiol Dis*. 15(3):618-29.
263. Sathyasaikumar KV *et al*., (2011) Impaired kynurenine pathway metabolism in the prefrontal cortex of individuals with schizophrenia. *Schizophr Bull*. 37(6):1147-56.
264. Dounay AB *et al*., (2013) PF-04859989 as a template for structure-based drug design: Identification of new pyrazole series of irreversible KAT II inhibitors with improved lipophilic efficiency. *Bioorganic Med Chem Lett*. 23(7):1961-6.
265. Fujigaki H *et al*., (2019) Linking phencyclidine intoxication to the tryptophan-kynurenine pathway: Therapeutic implications for schizophrenia. *Neurochemistry International*. 125:1-6
266. Dantzer R *et al*., (2008) From inflammation to sickness and depression: When the immune system subjugates the brain. *Nature Reviews Neuroscience*. 9(1):46-56.

267. Anisman H., Merali Z., Hayley S., (2008) Neurotransmitter, peptide and cytokine processes in relation to depressive disorder: Comorbidity between depression and neurodegenerative disorders. *Progress in Neurobiology*. 85(1):1-74.
268. Miller GE., Rohleder N., Cole SW., (2009) Chronic interpersonal stress predicts activation of pro- and anti-inflammatory signaling pathways 6 months later. *Psychosom Med*. 71(1):57.
269. Miller AH., Raison CL., (2016) The role of inflammation in depression: From evolutionary imperative to modern treatment target. *Nature Reviews Immunology*. 16(1):22.
270. Robinson CM., Shirey KA., Carlin JM., (2003) Synergistic Transcriptional Activation of Indoleamine Dioxygenase by IFN-γ and Tumor Necrosis Factor-α. *J Interf Cytokine Res*. 23(8):413-21.
271. Robinson CM., Hale PT., Carlin JM., (2006) NF-κB activation contributes to indoleamine dioxygenase transcriptional synergy induced by IFN-γ and tumor necrosis factor-α. *Cytokine*. 35(1-2):53-61.
272. Pemberton LA *et al*., (1997) Quinolinic acid production by macrophages stimulated with IFN-gamma, TNF-alpha, and IFN-alpha. *J Interferon Cytokine Res*. 17(10):589-95.
273. Mellor AL., Munn DH., (2004) IDO expression by dendritic cells: Tolerance and tryptophan catabolism. *Nature Reviews Immunology*. 4(10):762-74.
274. Mellor A., (2005) Indoleamine 2,3 dioxygenase and regulation of T cell immunity. *Biochemical and Biophysical Research Communications*. 338(1):20-4.
275. Owens MJ., Nemeroff CB., (1994) Role of serotonin in the pathophysiology of depression: Focus on the serotonin transporter. *Clinical Chemistry*. 40(2):288-95.
276. Raison CL *et al*., (2010) CSF concentrations of brain tryptophan and kynurenines during immune stimulation with IFN-α: Relationship to CNS immune responses and depression. *Mol Psychiatry*. 15(4):393-403.
277. Savitz J *et al*., (2015) Putative neuroprotective and neurotoxic kynurenine pathway metabolites are associated with hippocampal and amygdalar volumes in subjects with major depressive disorder. *Neuropsychopharmacology*. 40(2):463-71.
278. Swearengen JR., (2018) Choosing the right animal model for infectious disease research. *Anim Model Exp Med*. 1(2):100-8.
279. Jennings FW *et al*., (2002) Human African trypanosomiasis: Potential therapeutic benefits of an alternative suramin and melarsoprol regimen. *Parasitol Int*. 51(4):381-8.
280. McLatchie AP *et al*., (2013) Highly Sensitive In Vivo Imaging of Trypanosoma brucei Expressing 'Red-Shifted' Luciferase. *PLoS Negl Trop Dis*. 7(11).
281. Radwanska M *et al*., (2018) Salivarian trypanosomosis: A review of parasites involved, their global distribution and their interaction with the innate and adaptive mammalian host immune system. *Frontiers in Immunology*. 9:2253.
282. Giroud C *et al*., (2009) Murine models for Trypanosoma brucei gambiense disease progression - From silent to chronic infections and early brain tropism. *PLoS Negl Trop Dis*. 3(9).
283. Morrison LJ., (2011) Parasite-driven pathogenesis in Trypanosoma brucei infections. *Parasite Immunology*. 33(8):448-55.
284. MacLean LM *et al*., (2010) Focus-specific clinical profiles in human African

trypanosomiasis caused by trypanosoma brucei rhodesiense. *PLoS Negl Trop Dis.* 4(12).
285. Claes F *et al*., (2009) Bioluminescent imaging of Trypanosoma brucei shows preferential testis dissemination which may hamper drug efficacy in sleeping sickness. *PLoS Negl Trop Dis*. 3(7).
286. Blum JA *et al*., (2007) Sleeping hearts: The role of the heart in sleeping sickness (human African trypanosomiasis). *Trop Med Int Heal*. 12(12):1422-32.
287. Jung C., Hugot JP., Barreau F., (2010) Peyer's Patches: The Immune Sensors of the Intestine. *Int J Inflam*. 2010(823710):12
288. Costa FC *et al*., (2018) Expanding the toolbox for Trypanosoma cruzi: A parasite line incorporating a bioluminescence-fluorescence dual reporter and streamlined CRISPR/Cas9 functionality for rapid in vivo localisation and phenotyping. *PLoS Negl Trop Dis*. 12(4):e0006388.
289. Giordani F *et al*., (2016) The animal trypanosomiases and their chemotherapy: A review. *Parasitology*. 143(14):1862-89.
290. Maclean L *et al*., (2017) The relationship of endotoxaemia to peripheral and central nervous system inflammatory responses in Human African Trypanosomiasis. *Parasitology*. 144(4):557-62.
291. Coles JA *et al*., (2015) Intravital Imaging of a Massive Lymphocyte Response in the Cortical Dura of Mice after Peripheral Infection by Trypanosomes. *PLoS Negl Trop Dis*. 9(4).
292. Rodgers J., Bradley B., Kennedy PGE., (2017) Delineating neuroinflammation, parasite CNS invasion, and blood-brain barrier dysfunction in an experimental murine model of human African trypanosomiasis. *Methods*.127:79–87.
293. Frevert U *et al.*, (2012) Early Invasion of Brain Parenchyma by African Trypanosomes. *PLoS One*. 7(8).
294. Myburgh E *et al*., (2013) In vivo imaging of trypanosome-brain interactions and development of a rapid screening test for drugs against CNS stage trypanosomiasis. *PLoS Negl Trop Dis*. 7(8).
295. Bareš M *et al*., (2019) Consensus paper: Decoding the Contributions of the Cerebellum as a Time Machine: From Neurons to Clinical Applications. *Cerebellum*. 18(2):266-86.
296. Fine EJ., Ionita CC., Lohr L., (2002) The history of the development of the cerebellar examination. *Seminars in Neurology*. 22(4): 375
297. Grassi-Zucconi G *et al*., (1995) Sleep fragmentation, and changes in locomotor activity and body temperature in trypanosome-infected rats. *Brain Res Bull.* 37(2):123-9.
298. Stich A., Barrett MP., Krishna S., (2003) Waking up to sleeping sickness. *Trends in Parasitology*. 19(5):195-7
299. Duggan AJ., Hutchinson MP., (1966) Sleeping sickness in Europeans: a review of 109 cases. *J Trop Med Hyg*. 69(6):124-31
300. Murray M., Gardiner PR., (1988) Extravascular foci of Trypanosoma vivax in goats: The central nervous system and aqueous humor of the eye as potential sources of relapse infections after chemotherapy. *Parasitology*. 97(1):51-61
301. Herrera L *et al*., (2007) Cornea as a tissue reservoir of Trypanosoma cruzi. *Parasitol Res*. 100(6):1395-9.
302. Dieterich M., Brandt T., (2000) Brain activation studies on visual-vestibular and ocular motor interaction. *Current Opinion in Neurology*. 13(1):13-8.
303. Ndungu K *et al*., (2019) Route of inoculation influences Trypanosoma congolense and Trypanosoma brucei brucei virulence in Swiss white mice. *PLoS*

One.14(6):e0218441.
304. D'Archivio S *et al*., (2013) Non-Invasive In Vivo Study of the Trypanosoma vivax Infectious Process Consolidates the Brain Commitment in Late Infections. *PLoS Negl Trop Dis*. 7(1).
305. Etienne-Mesmin L., Chassaing B., Gewirtz AT., (2017) Tryptophan: A gut microbiota-derived metabolites regulating inflammation. *World J Gastrointest Pharmacol Ther*. 8(1):7.
306. Lovelace MD *et al*., (2017) Recent evidence for an expanded role of the kynurenine pathway of tryptophan metabolism in neurological diseases. *Neuropharmacology*. 112:373-88.
307. Gostner JM *et al*., (2015) Disturbed amino acid metabolism in HIV: Association with neuropsychiatric symptoms. *Frontiers in Psychiatry*. 6:97.
308. Morris GF *et al.*, (2015) The Many Neuroprogressive Actions of Tryptophan Catabolites (TRYCATs) that may be Associated with the Pathophysiology of Neuro-Immune Disorders. *Curr Pharm Des*. 22(8):963-77.
309. Quinones MP., Kaddurah-Daouk R., (2009) Metabolomics tools for identifying biomarkers for neuropsychiatric diseases. *Neurobiology of Disease*. 35(2):165-76.
310. Landfear SM., (2011) Nutrient transport and pathogenesis in selected parasitic protozoa. *Eukaryot Cell.* 10(4):483-93.
311. Badawy AAB., (2019) Tryptophan Metabolism: A Versatile Area Providing Multiple Targets for Pharmacological Intervention. *Egypt J Basic Clin Pharmacol*. 9
312. Kennedy PJ *et al.*, (2017) Kynurenine pathway metabolism and the microbiota-gut-brain axis. *Neuropharmacology*. 112:399-412.
313. Keszthelyi D., Troost FJ., Masclee AAM., (2009) Understanding the role of tryptophan and serotonin metabolism in gastrointestinal function. *Neurogastroenterology and Motility*. 21(12):1239-49.
314. Roager HM., Licht TR., (2018) Microbial tryptophan catabolites in health and disease. *Nature Communications*. 9(1):1-0.
315. Lesniak WG *et al*., (2013) Concurrent quantification of tryptophan and its major metabolites. *Anal Biochem.* 443(2):222–31.
316. Creek DJ *et al*., (2012) Metabolomic analysis of trypanosomatid protozoa. *Molecular and Biochemical Parasitology*. 181(2):73-84
317. Kloehn J., Saunders EC., McConville MJ., (2016) Using metabolomic approaches to characterize the human pathogen Leishmania in macrophages. *Microbial Metabolomics* (pp. 83-117). Springer, Cham.
318. Rijo-Ferreira F *et al*., (2017) Trypanosoma brucei metabolism is under circadian control. *Nat Microbiol*. 2:17032.
319. Plonski NM *et al*., (2018) Shedding light on lipid metabolism in Kinetoplastida: A phylogenetic analysis of phospholipase D protein homologs. *Gene*. 656:95-105.
320. Maslov DA *et al.*, (2019) Recent advances in trypanosomatid research: Genome organization, expression, metabolism, taxonomy and evolution. *Parasitology*. 146(1):1-27
321. Marchese L *et al*., (2018) The uptake and metabolism of amino acids, and their unique role in the biology of pathogenic trypanosomatids. *Pathogens*. 7(2):36
322. Rodgers J *et al*., (2015) Central Nervous System Parasitosis and Neuroinflammation Ameliorated by Systemic IL-10 Administration in Trypanosoma brucei-Infected Mice. *PLoS Negl Trop Dis*. 9(10).

323. Vancassel S., Capuron L., Castanon N., (2018) Brain Kynurenine and BH4 Pathways: Relevance to the Pathophysiology and Treatment of Inflammation-Driven Depressive Symptoms. *Front Neurosci*. 12:499.
324. Tan L., Yu JT., Tan L., (2012) The kynurenine pathway in neurodegenerative diseases: Mechanistic and therapeutic considerations. *Journal of the Neurological Sciences*. 323(1-2):1-8
325. Hurley LL., Tizabi Y., (2013) Neuroinflammation, neurodegeneration, and depression. *Neurotoxicity Research*. 23(2):131-44.
326. Davis I., Liu A., (2015) What is the tryptophan kynurenine pathway and why is it important to neurotherapeutics? *Expert Review of Neurotherapeutics*. 15(7): 719-721
327. Höglund E., Øverli Ø., Winberg S., (2019) Tryptophan metabolic pathways and brain serotonergic activity: A comparative review. *Frontiers in Endocrinology*. 10:158.
328. O'Farrell K., Harkin A., (2017) Stress-related regulation of the kynurenine pathway: Relevance to neuropsychiatric and degenerative disorders. *Neuropharmacology*. 112:307-23.
329. O'Mahony SM *et al.*, (2015) Serotonin, tryptophan metabolism and the brain-gut-microbiome axis. *Behavioural Brain Research*. 277:32-48.
330. Dunn AJ., Welch J., (1991) Stress-and Endotoxin-Induced Increases in Brain Tryptophan and Serotonin Metabolism Depend on Sympathetic Nervous System Activity. *J Neurochem*. 57(5):1615-22
331. Chaouloff F., (1993) Physiopharmacological interactions between stress hormones and central serotonergic systems. *Brain Research Reviews*. 18(1):1-32
332. Young SN., Leyton M., (2002) The role of serotonin in human mood and social interaction: Insight from altered tryptophan levels. *Pharmacology Biochemistry and Behavior*. 71(4):857-65
333. Bjork JM *et al*., (2000) Differential behavioral effects of plasma tryptophan depletion and loading in aggressive and nonaggressive men. *Neuropsychopharmacology*. 22(4):357-69
334. Pihl RO e*t al.*, (1995) Acute effect of altered tryptophan levels and alcohol on aggression in normal human males. *Psychopharmacology*. 119(4):353-60.
335. Gibbons JL *et al*., (1979) Manipulations of dietary tryptophan: Effects on mouse killing and brain serotonin in the rat. *Brain Res*. 169(1):139-53.
336. Van Hierden YM *et al.*, (2004) Chronic increase of dietary L-tryptophan decreases gentle feather pecking behaviour. *Appl Anim Behav Sci*. 89(1-2):71-84.
337. Lindseth G., Helland B., Caspers J., (2015) The effects of dietary tryptophan on affective disorders. *Arch Psychiatr Nurs*. 29(2):102-7
338. Strasser B., Gostner JM., Fuchs D., (2016) Mood, food, and cognition: Role of tryptophan and serotonin. *Current Opinion in Clinical Nutrition and Metabolic Care*. 19(1):55-61
339. Fernstrom JD., (1983) Role of precursor availability in control of monoamine biosynthesis in brain. *Physiological Reviews*. 63(2):484-546
340. Markus CR., (2008) Dietary amino acids and brain serotonin function; Implications for stress-related affective changes. *NeuroMolecular Medicine*. 10(4):247.
341. Headrick DR., (2014) Sleeping Sickness Epidemics and Colonial Responses in East and Central Africa, 1900-1940. *PLoS Negl Trop Dis*. 8(4).
342. Bukachi SA., Wandibba S., Nyamongo IK., (2017) The socio-economic burden

of human African trypanosomiasis and the coping strategies of households in the South Western Kenya foci. *PLoS Negl Trop Dis*. 11(10):e0006002.
343. Myint AM., (2012) Kynurenines: From the perspective of major psychiatric disorders. *FEBS Journal*. 279(8):1375-85.
344. Manji HK *et al.*, (2003) The underlying neurobiology of bipolar disorder. *World Psychiatry*. 2(3):136.
345. Smith KA., Fairburn CG., Cowen PJ., (1997) Relapse of depression after vapid depletion of tryptophan. *Lancet*. 349(9056):915-9.
346. Van der Leek AP., Yanishevsky Y., Kozyrskyj AL., (2017) The kynurenine pathway as a novel link between allergy and the gut microbiome. *Frontiers in Immunology*. 8:1374.
347. R. S, F.M. N, C.A. H. (2013) Kynurenine pathway metabolism reveals molecular links between immune system dysregulation and psychiatric diseases. *Schizophr Bull.*
348. Erhardt S *et al*., (2017) The kynurenine pathway in schizophrenia and bipolar disorder. *Neuropharmacology*. 112:297-306.
349. Ceresoli-Borroni G *et al*., (2006) Chronic neuroleptic treatment reduces endogenous kynurenic acid levels in rat brain. *J Neural Transm*. 113(10):1355-65.
350. Maes M *et al*., (2011) The new '5-HT' hypothesis of depression: Cell-mediated immune activation induces indoleamine 2,3-dioxygenase, which leads to lower plasma tryptophan and an increased synthesis of detrimental tryptophan catabolites (TRYCATs), both of which contribute to the onset of depression. *Progress in Neuro-Psychopharmacology and Biological Psychiatry*. 35(3):702-21
351. Van Donkelaar EL *et al*., (2011) Mechanism of acute tryptophan depletion: Is it only serotonin. *Molecular Psychiatry*. 16(7):695-713.
352. Neumeister A., (2003) Tryptophan depletion, serotonin, and depression: where do we stand? *Psychopharmacology bulletin*. 37(4):99-115.
353. Roiser JP *et al*., (2007) The effects of acute tryptophan depletion and serotonin transporter polymorphism on emotional processing in memory and attention. *Int J Neuropsychopharmacol*. 10(4):449-61.
354. Clarke HF *et al*., (2007) Cognitive inflexibility after prefrontal serotonin depletion is behaviorally and neurochemically specific. *Cereb Cortex*. 17(1):18-27.
355. Marañón C *et al.*, (2013) Benznidazole treatment reduces the induction of indoleamine 2,3-dioxygenase (IDO) enzymatic activity in Chagas disease symptomatic patients. *Parasite Immunol*. 35(5-6):180-7.
356. Murakami Y *et al*., (2012) Inhibition of increased indoleamine 2,3-dioxygenase activity attenuates Toxoplasma gondii replication in the lung during acute infection. *Cytokine*. 59(2):245-51.
357. Mbongue JC *et al*., (2015) The role of indoleamine 2, 3-dioxygenase in immune suppression and autoimmunity. *Vaccines*. 3(3):703-29.
358. Gironès N *et al*., (2014) Global Metabolomic Profiling of Acute Myocarditis Caused by Trypanosoma cruzi Infection. *PLoS Negl Trop Dis*. 8(11).
359. Munn DH *et al.*, (2005) GCN2 kinase in T cells mediates proliferative arrest and anergy induction in response to indoleamine 2,3-dioxygenase. *Immunity*. 22(5):633-42.
360. Mezrich JD *et al*., (2010) An Interaction between Kynurenine and the Aryl Hydrocarbon Receptor Can Generate Regulatory T Cells. *J Immunol*.

185(6):3190-8
361. Nguyen NT *et al*., (2010) Aryl hydrocarbon receptor negatively regulates dendritic cell immunogenicity via a kynurenine-dependent mechanism. *Proc Natl Acad Sci USA*. 107(46):19961-6.
362. Kanai M *et al.,* (2009) Tryptophan 2,3-dioxygenase is a key modulator of physiological neurogenesis and anxiety-related behavior in mice. *Mol Brain*. 2(1):8
363. Murakami Y *et al.,* (2013) Remarkable role of indoleamine 2,3-dioxygenase and tryptophan metabolites in infectious diseases: potential role in macrophage-mediated inflammatory diseases. *Mediators of inflammation*. 2013: 391984.
364. Palego L *et al*., (2016) Tryptophan biochemistry: Structural, nutritional, metabolic, and medical aspects in humans. *Journal of Amino Acids*. 2016: 8952520
365. Morgan CJ., Badawy AAB., (1989) Effects of a suppression test dose of dexamethasone on tryptophan metabolism and disposition in the rat. *Biol Psychiatry*. 25(3):359-62
366. Funakoshi H., Kanai M., Nakamura T., (2011) Modulation of tryptophan metabolism, promotion of neurogenesis and alteration of anxiety-related behavior in tryptophan 2,3-dioxygenase-deficient mice. *Int J Tryptophan Res*. 4: 7–18.
367. Badawy AAB., (2017) Tryptophan availability for kynurenine pathway metabolism across the life span: Control mechanisms and focus on aging, exercise, diet and nutritional supplements. *Neuropharmacology*. 112:248-63.
368. Munn DH., Mellor AL., (2016) IDO in the Tumor Microenvironment: Inflammation, Counter-Regulation, and Tolerance. *Trends in Immunology*. 37(3):193-207.
369. Favre D *et al*., (2010) Tryptophan catabolism by indoleamine 2, 3-dioxygenase 1 alters the balance of TH17 to regulatory T cells in HIV disease. *Sci Transl Med*. 2(32):32ra36.
370. Espey MG., Namboodiri MAA., (2000) Selective metabolism of kynurenine in the spleen in the absence of indoleamine 2,3-dioxygenase induction. *Immunol Lett*. 71(1):67-72.
371. Takikawa O *et al.,* (1986)Tryptophan degradation in mice initiated by indoleamine 2,3-dioxygenase. *J Biol Chem*. 261(8):3648-53
372. He JJ *et al.,* (2016) Transcriptomic analysis of global changes in cytokine expression in mouse spleens following acute Toxoplasma gondii infection. *Parasitol Res*. 115(2):703-12.
373. Drewes JL *et al*., (2016) Distinct patterns of tryptophan maintenance in tissues during kynurenine pathway activation in simian immunodeficiency virus-infected macaques. *Front Immunol*. 7:605
374. Fleckner J *et al.,* (1995) Differential regulation of the human, interferon inducible tryptophanyl-trna synthetase by various cytokines in cell lines. *Cytokine*. 7(1):70-7.
375. Fleckner J., Rasmussen HH., Justesen J., (1991) Human Interferon γ potently induces the synthesis of a 55-kDa protein (γ2) highly homologous to rabbit peptide chain release factor and bovine tryptophanyl-tRNA synthetase. *Proc Natl Acad Sci USA*. 88(24):11520-4.
376. Boasso A *et al*., (2005) Regulation of indoleamine 2,3-dioxygenase and tryptophanyl-tRNA-synthetase by CTLA-4-Fc in human CD4+ T cells. *Blood*. 105(4):1574-81.

377. Murray MF., (2003) Tryptophan depletion and HIV infection: A metabolic link to pathogenesis. *Lancet Infectious Diseases*. 3(10):644-52.
378. Schröcksnadel K *et al*., (2006) Monitoring tryptophan metabolism in chronic immune activation. *Clinica Chimica Acta*. 364(1-2):82-90.
379. Wu G., (2009) Amino acids: Metabolism, functions, and nutrition. *Amino Acids*. 37(1):1-7.
380. Rankin LC., Artis D., (2018) Beyond Host Defense: Emerging Functions of the Immune System in Regulating Complex Tissue Physiology. *Cell*. 173(3):554-67.
381. Le Floc'h N., Melchior D., Obled C., (2004) Modifications of protein and amino acid metabolism during inflammation and immune system activation. *Livestock Production Science*. 87(1):37-45
382. Newport GR *et al*., (1977) Alteration of Free Serum Amino Acids in Voles Infected with Trypanosoma brucei gambiense. *J Parasitol*. 1:15-24.
383. Newport GR., III CRP., (1977) Free Amino Acids in Brain, Liver, and Skeletal Muscle Tissue of Voles Infected with Trypanosoma brucei gambiense. *J Parasitol*. 1:1060-5.
384. Castell LM *et al*., (2000) The role of tryptophan in fatigue in different conditions of stress. *Adv Exp Med Biol*. (pp. 697-704). Springer, Boston, MA.
385. Brillon DJ *et al*., (1995) Effect of cortisol on energy expenditure and amino acid metabolism in humans. *Am J Physiol - Endocrinol Metab*. 268(3):E501-13.
386. Agudelo LZ *et al.*, (2014) Skeletal muscle PGC-1α1 modulates kynurenine metabolism and mediates resilience to stress-induced depression. *Cell*. 159(1):33-45.
387. Agus A., Planchais J., Sokol H., (2018) Gut Microbiota Regulation of Tryptophan Metabolism in Health and Disease. *Cell Host and Microbe*. 23(6):716-24.
388. Rieder R *et al.,* (2017) Microbes and mental health: A review. *Brain, Behavior, and Immunity.* 66:9-17.
389. Wang Y., Kasper LH., (2014) The role of microbiome in central nervous system disorders. *Brain, Behavior, and Immunity*. 38:1-2.
390. Cryan JF., Dinan TG., (2012) Mind-altering microorganisms: The impact of the gut microbiota on brain and behaviour. *Nature Reviews Neuroscience*. 13(10):701-12
391. Clarke G *et al*., (2013) The microbiome-gut-brain axis during early life regulates the hippocampal serotonergic system in a sex-dependent manner. *Mol Psychiatry*. 18(6):666-73.
392. Wikoff WR *et al*., (2009) Metabolomics analysis reveals large effects of gut microflora on mammalian blood metabolites. *Proc Natl Acad Sci USA.* 106(10):3698-703.
393. Bercik P *et al*., (2010) Chronic gastrointestinal inflammation induces anxiety-like behavior and alters central nervous system biochemistry in mice. *Gastroenterology*. 139(6):2102-12.
394. Gao J *et al*., (2018) Impact of the gut microbiota on intestinal immunity mediated by tryptophan metabolism. *Frontiers in Cellular and Infection Microbiology*. 8:13.
395. Li G., Young KD., (2013) Indole production by the tryptophanase TnaA in escherichia coli is determined by the amount of exogenous tryptophan. *Microbiol*. 159(2):402-10.
396. Lee JH., Lee J., (2010) Indole as an intercellular signal in microbial

communities. *FEMS Microbiology Reviews*. 34(4):426-44.
397. Hsiao EY., (2014) Gastrointestinal issues in autism spectrum disorder. *Harvard Review of Psychiatry.* 22(2):104-11.
398. Collins SM., Surette M., Bercik P., (2012) The interplay between the intestinal microbiota and the brain. *Nature Reviews Microbiology*. 10(11):735-42.
399. Bauer E *et al.,* (2006) Influence of the gastrointestinal microbiota on development of the immune system in young animals. *Current Issues in Intestinal Microbiology.* 7(2):35-52.
400. Stefulj J *et al.,* (2001) Serotonin and immune response: Effect of the amine on in vitro proliferation of rat lymphocytes. *Neuroimmunomodulation*. 9(2):103-8.
401. Khan WI., Ghia JE., (2010) Gut hormones: Emerging role in immune activation and inflammation. *Clinical and Experimental Immunology*. 161(1):19-27.
402. O'Hara JR *et al.,* (2006) Consequences of Citrobacter rodentium infection on enteroendocrine cells and the enteric nervous system in the mouse colon. *Cell Microbiol*. 8(4):646-60.
403. Mawe GM., Hoffman JM., (2013) Serotonin signalling in the gut-functions, dysfunctions and therapeutic targets. *Nature Reviews Gastroenterology and Hepatology.* 10(8):473.
404. Sirisinha S., (2016) The potential impact of gut microbiota on your health: Current status and future challenges. *Asian Pacific Journal of Allergy and Immunology.* 34(4):249-64.
405. Zhu W *et al*., (2011) Quantitative profiling of tryptophan metabolites in serum, urine, and cell culture supernatants by liquid chromatography-tandem mass spectrometry. *Anal Bioanal Chem*. 401(10):3249-61.
406. Seibenhener ML., Wooten MC., (2015) Use of the Open Field Maze to Measure Locomotor and Anxiety-like Behavior in Mice. *J Vis Exp*. 96:1–6.
407. Lamprea MR *et al*., (2008) Thigmotactic responses in an open-field. *Brazilian J Med Biol Res*. 41(2):135–40.
408. Antunes M., Biala G., (2012) The novel object recognition memory: Neurobiology, test procedure, and its modifications. *Cogn Process*. 13(2):93–110.
409. Ennaceur A., (2010) One-trial object recognition in rats and mice: Methodological and theoretical issues. *Behav Brain Res*. 215(2):244–54.
410. Lezak KR., Missig G., Carlezon WA., (2017) Behavioral methods to study anxiety in rodents. *Dialogues Clin Neurosci*. 19(2):181–91.
411. Vilar-Pereira G *et al.,* (2012) Trypanosoma cruzi-induced depressive-like behavior is independent of meningoencephalitis but responsive to parasiticide and TNF-targeted therapeutic interventions. *Brain Behav Immun*. 26(7):1136–49.
412. Jans LAW *et al*., (2010) The effects of acute tryptophan depletion on affective behaviour and cognition in Brown Norway and Sprague Dawley rats. *J Psychopharmacol.* 24(4):605-14.
413. Lieben CKJ *et al*., (2004) Acute tryptophan depletion induced by a gelatin-based mixture impairs object memory but not affective behavior and spatial learning in the rat. *Behav Brain Res*. 151(1-2):53-64.
414. Mace JL *et al*., (2010) Effects of acute tryptophan depletion on neuropsychological and motor function in Parkinson's disease. *J Psychopharmacol*. 24(10):1465–72.
415. Chen Y., Guillemin GJ., (2009) Kynurenine pathway metabolites in humans: disease and healthy States. *Int J Tryptophan Res*. 2:1–19.

416. Chen Y., Guillemin GJ., (2009) Kynurenine pathway metabolites in humans: Disease and healthy states. *Int J Tryptophan Res*. 2(1):1–19.
417. Parrott JM *et al*., (2016) Neurotoxic kynurenine metabolism is increased in the dorsal hippocampus and drives distinct depressive behaviors during inflammation. *Transl Psychiatry*. 6(10):e918
418. Darsaud A *et al*., (2003) Clinical Follow-Up in the Rat Experimental Model of African-Trypanosomiasis. *Exp Biol Med*. 228(11):1355-62.
419. Kalueff AV *et al*., (2007) Hypolocomotion, anxiety and serotonin syndrome-like behavior contribute to the complex phenotype of serotonin transporter knockout mice. *Genes, Brain Behav*. 6(4):389-400.
420. Canli T., Lesch KP., (2007) Long story short: The serotonin transporter in emotion regulation and social cognition. *Nature Neuroscience*. 10(9):1103-9.
421. Murphy DL *et al*., (2008) How the serotonin story is being rewritten by new gene-based discoveries principally related to SLC6A4, the serotonin transporter gene, which functions to influence all cellular serotonin systems. *Neuropharmacology*. 55(6):932-60.
422. Hillegaart V., Estival A., Ahlenius S., (1996) Evidence for specific involvement of 5-HT1A and 5-HT2A/C receptors in the expression of patterns of spontaneous motor activity of the rat. *Eur J Pharmacol*. 295(2-3):155-61.
423. Darsaud, A *et al*., (2003) Clinical Follow-Up in the Rat Experimental Model. *Exp Biol Med*. 228:1355–62.
424. Wolkmer P *et al*., (2013) Trypanosoma evansi infection impairs memory, increases anxiety behaviour and alters neurochemical parameters in rats. *Parasitology*. 140(11):1432-41.
425. Balogun-Mwangi O., (2018) The Culture of Mental Illness and Psychiatric Practice in Africa. *J Ment Heal*. 140(11):1432-41.
426. Fernandez SP *et al*., (2017) Constitutive and Acquired Serotonin Deficiency Alters Memory and Hippocampal Synaptic Plasticity. *Neuropsychopharmacology*. 42(2):512-23.
427. Riedel WJ *et al*., (1999) Tryptophan depletion in normal volunteers produces selective impairment in memory consolidation. *Psychopharmacology*. 141(4):362-9.
428. Park SB *et al*., (1994) Tryptophan depletion in normal volunteers produces selective impairments in learning and memory. *Neuropharmacology*. 33(3-4):575-88
429. Harrison BJ *et al*., (2004) Selective effects of acute serotonin and catecholamine depletion on memory in healthy women. *J Psychopharmacol*. 18(1):32-40.
430. Schmitt JAJ *et al*., (2000) Tryptophan depletion impairs memory consolidation but improves focussed attention in healthy young volunteers. *J Psychopharmacol*. 14(1):21-9.
431. Olivier JDA *et al*., (2008) Acute tryptophan depletion dose dependently impairs object memory in serotonin transporter knockout rats. *Psychopharmacology*. 200(2):243-54.
432. Olivier JDA *et al*., (2009) Serotonin transporter deficiency in rats contributes to impaired object memory. *Genes, Brain Behav*. 8(8):829-34.
433. Jenkins TA *et al*., (2010) Tryptophan depletion impairs object-recognition memory in the rat: Reversal by risperidone. *Behav Brain Res*. 208(2):479-83.
434. van Donkelaar EL *et al*., (2010) Acute tryptophan depletion in C57BL/6 mice does not induce central serotonin reduction or affective behavioural changes. *Neurochem Int*. 56(1):21–34.

435. Senut MC., Menetrey D., Lamour Y., (1989) Cholinergic and peptidergic projections from the medial septum and the nucleus of the diagonal band of broca to dorsal hippocampus, cingulate cortex and olfactory bulb: A combined wheatgerm agglutinin-apohorseradish peroxidase-gold immunohistochemical stu. *Neuroscience*. 30(2):385-403.
436. Tirosh A *et al*., (2005) Normal Fasting Plasma Glucose Levels and Type 2 Diabetes in Young Men. *N Engl J Med*. 353(14):1454-62.
437. Bowe JE *et al.*, (2014) Metabolic Phenotyping Guidelines: Assessing glucose homeostasis in rodent models. *J Endocrinol.* 222(3):G13-25.
438. van der Wal G *et al*., (2005) Neurological complications following Plasmodium falciparum infection. *Neth J Med*. 63(5):180-3.
439. Dzikowiec M., Góralska K., Błaszkowska J., (2017) Neuroinvasions caused by parasites. *Ann Parasitol*. 63:243-53.
440. Kalita J., Kumar P., Misra UK., (2013) Stimulus-sensitive myoclonus and cerebellar ataxia following chikungunya meningoencephalitis. *Infection*. 41(3):727-9.
441. Cherubini E., Miles R., (2015) The CA3 region of the hippocampus: How is it? What is it for? How does it do it? *Frontiers in Cellular Neuroscience*. 9:19.
442. Grafton ST., Hamilton AFDC., (2007) Evidence for a distributed hierarchy of action representation in the brain. *Hum Mov Sci*. 26(4):590-616.
443. D'Aiuto L *et al.*, (2015) Persistent infection by HSV-1 is associated with changes in functional architecture of iPSC-derived neurons and brain activation patterns underlying working memory performance. *Schizophr Bull*. 41(1):123-32.
444. Andrade R., Haj-Dahmane S., (2013) Serotonin neuron diversity in the dorsal raphe. *ACS Chemical Neuroscience*. 4(1): 22-25
445. Olivier B., (2015) Serotonin: A never-ending story. *European Journal of Pharmacology*. 753:2-18.
446. Etet PFS *et al*., (2012) Sleep and rhythm changes at the time of Trypanosoma brucei invasion of the brain parenchyma in the rat. *Chronobiol Int*. 29(4):469-81.
447. Yamakawa GR., Antle MC., (2010) Phenotype and function of raphe projections to the suprachiasmatic nucleus. *Eur J Neurosci*. 31(11):1974-83.
448. Stibbs HH., Curtis DA., (1987) Neurochemical changes in experimental African trypanosomiasis in voles and mice. *Ann Trop Med Parasitol.* 81(6):673-9.
449. Monti JM., (2011) Serotonin control of sleep-wake behavior. *Sleep Medicine Reviews*. 15(4):269-81.
450. LeDoux J., (2007) The amygdala. *Current Biology*. 17(20):R868-74.
451. Mitra R., Sapolsky RM., Vyas A., (2013) Toxoplasma gondii infection induces dendritic retraction in basolateral amygdala accompanied by reduced corticosterone secretion. *DMM Dis Model Mech*. 6(2):516-20.
452. Hari Dass SA., Vyas A., (2014) Toxoplasma gondii infection reduces predator aversion in rats through epigenetic modulation in the host medial amygdala. *Mol Eco*l. 23(24):6114-22.
453. Ihara F *et al.*, (2016) Toxoplasma gondii infection in mice impairs long-term fear memory consolidation through dysfunction of the cortex and amygdala. *Infect Immun*. 84(10):2861-70.
454. Narayanan NS., (2017) Laubach M. Inhibitory Control: Mapping Medial Frontal Cortex. *Current Biology*. 27(4):R148-50.
455. Weinberger DR., Berman KF., (1988) Speculation of the meaning of cerebral metabolic hypofrontality in schizophrenia. *Schizophrenia Bulletin*. 14(2):157-

68.
456. Mitelman SA *et al.*, (2018) Positron emission tomography assessment of cerebral glucose metabolic rates in autism spectrum disorder and schizophrenia. *Brain Imaging Behav*. 12(2):532-46.
457. Weinberger DR., Berman KF., Zec RF., (1986) Physiologic Dysfunction of Dorsolateral Prefrontal Cortex in Schizophrenia: I. Regional Cerebral Blood Flow Evidence. *Arch Gen Psychiatry*. 43(2):114-24.
458. Brown VJ., Bowman EM., (2002) Rodent models of prefrontal cortical function. *Trends in Neurosciences*. 25(7):340-3.
459. Drevets WC., (2000) Neuroimaging studies of mood disorders. *Biological Psychiatry*. 48(8):813-29
460. Maquet P *et al*., (1997) Functional neuroanatomy of human slow wave sleep. *J Neurosci.* 17(8):2807-12.
461. Merica H., Fortune RD., (2004) State transitions between wake and sleep, and within the ultradian cycle, with focus on the link to neuronal activity. *Sleep Medicine Reviews.* 8(6):473-85.
462. Ritchie E *et al.*, (2012) Control Of Sleep And Wakefulness. *Physiol Rev*. 92(3):1087-187.
463. Wulff K *et al*., (2010) Sleep and circadian rhythm disruption in psychiatric and neurodegenerative disease. *Nature Reviews Neuroscience*. 11(8):589-99.
464. Buguet A *et al*., (2001) The duality of sleeping sickness: Focusing on sleep. *Sleep Medicine Reviews*. 5(2):139-53.
465. Dawson N *et al*., (2011) Cerebral metabolic responses to 5-HT2A/C receptor activation in mice with genetically modified serotonin transporter (SERT) expression. *Eur Neuropsychopharmacol*. 21(1):117-28.
466. King SL., Hegadoren KM., (2002) Stress Hormones: How Do They Measure Up? *Biol Res Nurs*. 4(2):92-103.
467. Schoenfeld TJ., Gould E., (2012) Stress, stress hormones, and adult neurogenesis. *Experimental Neurology*. 233(1):12-21.
468. Sapolsky RM., (1996) Stress, glucocorticoids, and damage to the nervous system: the current state of confusion. *Stress*. 1(1):1-9.
469. Sapolsky RM., (2000) Glucocorticoids and hippocampal atrophy in neuropsychiatric disorders. *Archives of General Psychiatry.* 57(10):925-35.
470. Romano MC *et al*., (2015) Parasites and steroid hormones: Corticosteroid and sex steroid synthesis, their role in the parasite physiology and development. *Frontiers in Neuroscience*. 9:224.
471. Ezeh IO *et al.*, (2019) Reduced fasting blood glucose levels following relapse in diminazene aceturate (Dinazene®) treated Trypanosoma brucei infected albino rats. *J Parasit Dis*. 43(2):329-32.
472. Sivajothi S., Rayulu VC., Sudhakara Reddy B., (2015) Haematological and biochemical changes in experimental Trypanosoma evansi infection in rabbits. *J Parasit Dis*. 39(2):216-20.
473. Takeet M., Fagbemi B., (2010) Haematological, pathological and plasma biochemical changes in rabbits experimentally infected with *Trypanosoma congolense*. *Sci World J*. 4(2).
474. Mishra RR., Senapati SK., Sahoo SC., (2017) Trypanosomiasis induced oxidative stress and hemato-biochemical alteration in cattle. *J Entomol Zool Stud*. 5(2):721–4.
475. Saleh MA., Al-Salahy MB., Sanousi SA., (2009) Oxidative stress in blood of camels (Camelus dromedaries) naturally infected with Trypanosoma evansi. *Vet*

Parasitol. 162(3-4):192-9.
476. Paxinos G., Franklin KBJ., (2001) The Mouse Brain in Stereotaxic Coordinates, 2nd edition. *Academic Press.* 200(1):65-9.
477. Reeds PJ., (2018) Dispensable and Indispensable Amino Acids for Humans. *J Nutr*. 130(7):1835S-40S.
478. Alsford S., Horn D., (2008) Single-locus targeting constructs for reliable regulated RNAi and transgene expression in Trypanosoma brucei. *Mol Biochem Parasitol*. 161(1):76–9.
479. Alsford S., Horn D., (2008) Single-locus targeting constructs for reliable regulated RNAi and transgene expression in Trypanosoma brucei. *Mol Biochem Parasitol*. 161(1):76–9.
480. Wen J., Nowicki C., Blankenfeldt W., (2015) Structural basis for the relaxed substrate selectivity of Leishmania mexicana broad specificity aminotransferase. *Molecular and Biochemical Parasitology*. 202(2):34-7.
481. Seed JR., Hall JE., Sechelski J., (1982) Phenylalanine metabolism in Microtus montanus chronically infected with Trypanosoma brucei gambiense. *Comp Biochem Physiol -- Part B Biochem*. 71(2):209-15.
482. Voorheis HP., (1969) The effect of T. brucei (S-42) on host carbohydrate metabolism: liver production and peripheral tissue utilization of glucose. *Trans R Soc Trop Med Hyg*. 63(1):122-3
483. Li JV et al., (2011) Metabonomic investigation of single and multiple strain Trypanosoma brucei brucei infections. *Am J Trop Med Hyg*. 84(1):91-8
484. Hall JE., Seed JR., (1984) Increased urinary excretion of aromatic amino acid catabolites by Microtus montanus chronically infected with Trypanosoma brucei gambiense. *Comp Biochem Physiol B.* 77(4):755–60.
485. Sawalhy EL *et al*., (1995) Catabolism of Tryptophan by Trypanosoma evansi. *J Eukaryot Microbiol.* 42(6):684-90.
486. Sawalhy El *et al*., (1998) Increased Excretion of Aromatic Amino Acid Catabolites in Animals Infected with Trypanosoma brucei evansi. *J Parasitol.* 1:469-73.
487. Stibbs HH., Seed JR., (1973) Chromatographic evidence for the synthesis of possible sleep-mediators in Trypanosoma brucei gambiense. *Experientia*. 29(12):1563-5.
488. Creek DJ *et al*., (2015) Probing the Metabolic Network in Bloodstream-Form Trypanosoma brucei Using Untargeted Metabolomics with Stable Isotope Labelled Glucose. *PLoS Pathog*. 11(3).
489. Leija C *et al*., (2016) Pyrimidine Salvage Enzymes Are Essential for De Novo Biosynthesis of Deoxypyrimidine Nucleotides in Trypanosoma brucei. *PLoS Pathog*. 12(11).
490. De Koning HP., Bridges DJ., Burchmore RJS., (2005) Purine and pyrimidine transport in pathogenic protozoa: From biology to therapy. *FEMS Microbiology Reviews*. 29(5):987-1020.
491. Lovelace MD *et al*., (2016) Current evidence for a role of the kynurenine pathway of tryptophan metabolism in multiple sclerosis. *Frontiers in Immunology.* 7:246.
492. Baumgartner R., Forteza MJ., Ketelhuth DFJ., (2017) The interplay between cytokines and the Kynurenine pathway in inflammation and atherosclerosis. *Cytokine*. 122:154148.
493. Nemeth H., Toldi J., Vecsei L., (2005) Role of Kynurenines in the Central and Peripherial Nervous Systems. *Curr Neurovasc Res*. 2(3):249-60.

494. Cervenka I., Agudelo LZ., Ruas JL., (2017) Kynurenines: Tryptophan's metabolites in exercise, inflammation, and mental health. *Science*. 357(6349):eaaf9794.
495. Aranda A *et al*., (2006) The malate dehydrogenase isoforms from Trypanosoma brucei: Subcellular localization and differential expression in bloodstream and procyclic forms. *Int J Parasitol*. 36(3):295-307.
496. Vernal J *et al*., (2001) Sequencing and heterologous expression of a cytosolic-type malate dehydrogenase of Trypanosoma brucei. *Mol Biochem Parasitol*. 117(2):217.
497. Cazzulo Franke MC *et al*., (1999) The NAD-linked aromatic α-hydroxy acid dehydrogenase from Trypanosoma cruzi. *Eur J Biochem*. 266(3):903–10.
498. Stibbs HH., Seed JR., (1975) Further studies on the metabolism of tryptophan in Trypanosoma brucei gambiense: Cofactors, inhibitors, and end-products. *Experientia*. 31(3):274-8.
499. Gietl C., (1992) Malate dehydrogenase isoenzymes: Cellular locations and role in the flow of metabolites between the cytoplasm and cell organelles. *Biochimica et Biophysica Acta (BBA)/Protein Structure and Molecular*. 1100(3):217-34.
500. Cannata JJB *et al*., (1979) Two forms of 'malic' enzyme with different regulatory properties in Trypanosoma cruzi. *Biochem J*. 184(2):409-19.
501. Van Weelden SWH *et al*., (2005) New functions for parts of the krebs cycle in procyclic Trypanosoma brucei, a cycle not operating as a cycle. *J Biol Chem*. 280(13):12451-60.
502. Mathieu C *et al.*, (2014) Trypanosoma brucei eflornithine transporter AAT6 is a low-affinity low-selective transporter for neutral amino acids. *Biochem J*. 463(1):9-18.
503. Schumann Burkard G., Jutzi P., Roditi I., (2011) Genome-wide RNAi screens in bloodstream form trypanosomes identify drug transporters. *Molecular and Biochemical Parasitology*. 175(1):91-4.
504. Baker N., Alsford S., Horn D., (2011) Genome-wide RNAi screens in African trypanosomes identify the nifurtimox activator NTR and the eflornithine transporter AAT6. *Mol Biochem Parasitol*. 176(1):55-7.
505. Vincent IM *et al*., (2010) A molecular mechanism for eflornithine resistance in African trypanosomes. *PLoS Pathog*. 6(11).
506. Babokhov P *et al*., (2013) A current analysis of chemotherapy strategies for the treatment of human African trypanosomiasis. *Pathogens and Global Health*. 107(5):242-52.
507. Wickstead B., Ersfeld K., Gull K., (2004) The small chromosomes of Trypanosoma brucei involved in antigenic variation are constructed around repetitive palindromes. *Genome Res*. 14(6):1014–24.
508. Kim HS *et al*., (2013) Strategies to construct null and conditional null Trypanosoma brucei mutants using Cre-recombinase and loxP. *Mol Biochem Parasitol*. 191(1):16–9.
509. Wirtz E *et al*., (1999) A tightly regulated inducible expression system for conditional gene knock-outs and dominant-negative genetics in Trypanosoma brucei. *Mol Biochem Parasitol*. 99(1):89–101.
510. Schwede T *et al*., (2003) SWISS-MODEL: an automated protein homology-modeling server. *Nucleic Acids Res*. 31(13):3381–5.
511. Ikede BO., (1974) Ocular lesions in sheep infected with Trypanosoma brucei. *J Comp Pathol*. 84(2):203-13.
512. Mortelmans J., Neetens A., (1975) Ocular lesions in experimental Trypanosoma

brucei infection in cats. *Acta Zool Pathol Antverp*. (62):149-72.
513. Ŕidley H., (1945) Ocular lesions in trypanosomiasis. *Ann Trop Med Parasitol.* 39(2):66-82.
514. Goyard S *et al.*, (2014) In vivo imaging of trypanosomes for a better assessment of host-parasite relationships and drug efficacy. *Parasitol Int*. 63(1):260-8.
515. Gika HG *et al.*, (2014) Current practice of liquid chromatography-mass spectrometry in metabolomics and metabonomics. *Journal of Pharmaceutical and Biomedical Analysis*. 87:12-25.
516. Winder CL *et al*., (2008) Global metabolic profiling of Escherichia coli cultures: An evaluation of methods for quenching and extraction of intracellular metabolites. *Anal Chem*. 80(8):2939-48.
517. Faijes M., Mars AE., Smid EJ., (2007) Comparison of quenching and extraction methodologies for metabolome analysis of Lactobacillus plantarum. *Microb Cell Fact*. 6(1):27.
518. Kennedy PGE,. (2005) Sleeping sickness - human African trypanosomiasis. *Pract Neurol*. 5(5):260–7.
519. Dunne F., O'Halloran A., Kelly JP., (2007) Development of a home cage locomotor tracking system capable of detecting the stimulant and sedative properties of drugs in rats. *Prog Neuro-Psychopharmacology Biol Psychiatry*. 31(7):1456-63.
520. Rasch B., Born J., (2013) About sleep's role in memory. *Physiol Rev*. 93(2):681-766.
521. Prince TM., Abel T., (2013) The impact of sleep loss on hippocampal function. *Learning and Memory*. 20(10):558-69.
522. Urech K., Neumayr A., Blum J., (2011) Sleeping sickness in travelers - do they really sleep? *PLoS Negl Trop Dis*. 5(11).
523. Curtis CE., D'Esposito M., (2003) Persistent activity in the prefrontal cortex during working memory. *Trends Cogn Sci*. 7(9):415-23.
524. Deng W., Aimone JB., Gage FH., (2010) New neurons and new memories: How does adult hippocampal neurogenesis affect learning and memory? *Nature Reviews Neuroscience*. 11(5):339-50.
525. Rodrigues SM., Schafe GE., Ledoux JE., (2004) Molecular mechanisms underlying emotional learning and memory in the lateral amygdala. *Neuron*. 44(1):75-91.
526. Coley AF *et al*., (2011) Glycolysis in the African Trypanosome: Targeting Enzymes and Their Subcellular Compartments for Therapeutic Development. *Mol Biol Int*. 2011: 123702.
527. Chappuis F., (2007) Melarsoprol-Free Drug Combinations for Second-Stage Gambian Sleeping Sickness: The Way to Go. *Clin Infect Dis*. 45(11):1443-5
528. Rodgers J., Steiner I., Kennedy PGE., (2019) Generation of neuroinflammation in human African trypanosomiasis. Neurol-Neuroimmunol Neuroinflammation. 6(6):e610.